



<https://theses.gla.ac.uk/>

Theses Digitisation:

<https://www.gla.ac.uk/myglasgow/research/enlighten/theses/digitisation/>

This is a digitised version of the original print thesis.

Copyright and moral rights for this work are retained by the author

A copy can be downloaded for personal non-commercial research or study,
without prior permission or charge

This work cannot be reproduced or quoted extensively from without first
obtaining permission in writing from the author

The content must not be changed in any way or sold commercially in any
format or medium without the formal permission of the author

When referring to this work, full bibliographic details including the author,
title, awarding institution and date of the thesis must be given

Enlighten: Theses

<https://theses.gla.ac.uk/>
research-enlighten@glasgow.ac.uk

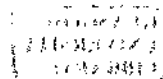
**Evaluation of telomerase control elements and
radiation-inducible WAF1 promoter for the
enhancement of targeted radiotherapy in
neuroblastoma cells**

Emilio Cosimo

A thesis submitted for the degree of Doctor of Philosophy to the Faculty of
Medicine, University of Glasgow

Targeted Therapy Group
Centre for Oncology and Applied Pharmacology
Cancer Research UK Beatson Laboratories
University of Glasgow

February 2007



ProQuest Number: 10390573

All rights reserved

INFORMATION TO ALL USERS

The quality of this reproduction is dependent upon the quality of the copy submitted.

In the unlikely event that the author did not send a complete manuscript and there are missing pages, these will be noted. Also, if material had to be removed, a note will indicate the deletion.



ProQuest 10390573

Published by ProQuest LLC (2017). Copyright of the Dissertation is held by the Author.

All rights reserved.

This work is protected against unauthorized copying under Title 17, United States Code
Microform Edition © ProQuest LLC.

ProQuest LLC.
789 East Eisenhower Parkway
P.O. Box 1346
Ann Arbor, MI 48106 – 1346

GLASGOW
UNIVERSITY
LIBRARY:

Acknowledgements

There are many people I wish to thank for making this thesis possible.

It is a pleasure to thank the Neuroblastoma Society which funded this project.

I would like to thank my supervisors Dr. Robert Mairs and Dr. Marie Boyd. With their experience, knowledge and enthusiasm, they helped me to overcome successfully all the challenges that laboratory research brings. During my writing-up period, they provided support, sound guidance and good ideas. The completion of this thesis would have been impossible without them.

I am grateful to the staff members of the Targeted Therapy Group for their help and support. In particular, I would like to thank Dr. Anthony McCluskey for introducing me to the real-time PCR "universe" and for helping me with some tricky experiments regarding the pWAF1/NAT construct.

I am indebted to Dr. Sally Pimlott and her colleagues at the Radionuclide Dispensary (Western Infirmary, Glasgow), for the synthesis of the radiopharmaceutical [^{131}I]MIBG. I wish to thank Dr. Michael Zalutsky and his valuable staff at the Department of Radiology at the Medical Center, in Duke University (Durham, North Carolina), for support and for allowing me to use his laboratory facilities, especially for providing me with the radiopharmaceutical [^{211}At]MABG.

I would like to thank my family for providing love and support every single day of my PhD project. My parents Liana Montagnani and Eugenio Cosimo, my sister Laura and my brother-in-law Andrea Polesel were particularly supportive.

Lastly, and most importantly, I wish to thank my partner Kim Appleton. I really think that her love, support and determination were crucial for the achievement of this work. I cannot count the times (not a few) she managed to encourage and motivate me, even in the most difficult moments. To her I dedicate this thesis.

Declaration

I am the sole author of this thesis. All the references have been consulted by myself in the preparation of this manuscript. All the work presented in this thesis was performed by myself, except where otherwise stated.

Emilio Cosimo

February 2007

Table of Contents

Table of Contents	2
List of Figures	5
List of Tables	9
Abbreviations.....	10
Summary	15
Chapter 1:	
Introduction: [¹³¹I]MIBG and gene therapy: A rationale for amalgamation of targeted radiotherapy with gene therapy for neuroblastoma treatment.....	17
1.1 Targeted Radiotherapy.....	18
1.1.1 Radiological bystander effect.....	18
1.2 Neuroblastoma: introduction	20
1.2.1 Molecular biology	20
1.2.2 Clinical features and conventional therapies.....	21
1.2.3 Innovative therapies	24
1.2.4 Enhancement of MIBG uptake in neuroblastoma cells.....	28
1.2.5 Promoter elements for the control of transgene expression.....	29
1.2.6 ²¹¹ At: an alternative to ¹³¹ I as conjugate for MIBG.....	32
1.2.7 Immunoliposomes as tumour-targeted gene-delivery system..	33
1.2.8 General strategy.....	34
1.3 Aims of this study	35
Chapter 2:	
Evaluation of telomerase promoters as controllers of NAT transgene transcription.....	36
2.1 Introduction	37
2.1.1 Tumour-specific promoters	38
2.1.2 Telomerase promoters	40
2.2 Materials and Methods.....	44
2.2.1 Synthesis of the radiopharmaceuticals [¹³¹ I]MIBG and [²¹¹ At]MABG	45
2.2.2 Cell culture	45
2.2.3 Plasmids	45
2.2.4 Transfections	47
2.2.5 General consideration about quantitative real-time Polymerase Chain Reaction (PCR)	48
2.2.6 TaqMan real-time PCR for hNAT and bNAT transcripts.....	48
2.2.7 SYBR Green real-time PCR for hTR and hTERT transcripts quantification	50
2.2.8 [¹³¹ I]MIBG and [²¹¹ At]MABG uptake studies in SK-N-MC and SK-N-BE(2c) cells	56
2.2.9 Spheroid clonogenic assays	56
2.2.10 Statistical analysis.....	58
2.3 Results	59

2.3.1	Real-time PCR for determination of the expression of hTR, hTERT, endogenous and transgenic NAT transcripts.....	60
2.3.2	Cellular uptake of [¹³¹ I]MIBG.....	66
2.3.3	Cellular uptake of [²¹¹ At]MABG.....	69
2.3.4	Cytotoxicity of [¹³¹ I]MIBG.....	72
2.3.5	Cytotoxicity of [²¹¹ At]MABG.....	76
2.3.6	Summary of results.....	80
2.4	Discussion.....	81

Chapter 3:

Analysis of WAF1 promoter activation after exposing neuroblastoma cells to [¹³¹I]MIBG or [²¹¹At]MABG.....		85
3.1	Introduction.....	86
3.2	Material and Methods.....	94
3.3	Results.....	101
3.3.1	Cellular uptake of [¹³¹ I]MIBG and [²¹¹ At]MABG.....	102
3.3.2	Assessment of the WAF1 promoter activation in neuroblastoma cells transfected with the pWAF1/GFP plasmid.....	105
3.3.3	Assessment of noradrenaline transporter (NAT) expression under the control of the WAF1 promoter in neuroblastoma cells: a preliminary study.....	133
3.3.4	Evaluation of the WAF1 promoter in UVW glioma cells.....	145
3.3.5	Summary of results.....	150
3.4	Discussion.....	151
3.4.1	The WAF1 promoter is inducible by both [¹³¹ I]MIBG and [²¹¹ At]MABG.....	153
3.4.2	[¹³¹ I]MIBG and [²¹¹ At]MABG dose estimation.....	154
3.4.3	Possible applications of the radio-inducible WAF1 promoter for neuroblastoma treatment.....	155
3.4.4	The endogenous NAT is overexpressed by ionising radiation, but the enhancement of the expression levels of transgenic NAT under the control of the WAF1 promoter is greater.....	157

4 Chapter 4:

Immunoliposomes: a novel gene delivery system.....		160
4.1	Introduction.....	161
4.1.1	Naked DNA.....	162
4.1.2	Viral vectors.....	163
4.1.3	Non-viral systems.....	165
4.2	Materials and Methods.....	171
4.2.1	172
4.2.2	Cell lines and culture conditions.....	172
4.2.3	FACS analysis of GD ₂ -positive and -negative neuroblastoma cells.....	173
4.2.4	Plasmid DNA preparation and radiolabelling.....	173
4.2.5	Liposome preparation and plasmid encapsulation.....	174
4.2.6	Coupling of anti-GD ₂ MAb to liposomes.....	175
4.2.7	CCLs size measurements.....	177
4.2.8	Gel retardation and DNase I protection assay.....	177
4.2.9	Binding and uptake of liposomes.....	178

4.2.10	Transfection experiments using anti-GD2-CCLs-pEGFP-N1	178
4.2.11	Uptake of plasmid by neuroblastoma cells and cell fractionation assay	179
4.3	Results	180
4.3.1	Characterisation of anti-GD2 CCLs	181
4.3.2	Binding of GD2-targeted immunoliposomes to GD2-positive and GD2-negative cells	183
4.3.3	Transfection of neuroblastoma cells with anti-GD ₂ -CCLs encapsulating plasmid DNA	187
4.3.4	Cellular internalisation of the anti-GD ₂ -CCLs	188
4.3.5	Summary of results	192
4.4	Discussion	193
4.4.1	Enhancements of endosomal escape	197
4.4.2	Nuclear translocation	198
4.4.3	Conclusions	199

Chapter 5:

Further avenues of research arising from this study, and final conclusions

		200
5.1	Telomerase promoters: enhancement of tumour specific gene therapy	201
5.1.1	Alternative tumour-specific transcriptional regulators	201
5.1.2	Enhancement of telomerase promoters' efficiency: the Cre/Lox system	202
5.2	Radiation-inducible gene therapy	204
5.2.1	Alternative radiation-inducible transcriptional regulators	206
5.2.2	Enhancement of WAF1 promoter efficiency: the Cre/Lox system	206
5.3	Choice of radionuclide: Alternatives to ¹³¹ I or ²¹¹ At as a conjugate for MIBG	207
5.3.1	[¹²³ I]MIBG and [¹²⁵ I]MIBG	207
5.4	Radiation-induced biological bystander effects (RIBBEs)	211
5.5	Alternative gene delivery systems: adenoviral vectors	213
5.6	The use of multicellular mosaic spheroids to determine transfection efficiencies	214
5.7	Conclusions	216
5.7.1	Telomerase promoter elements driving the expression of the NAT transgene	216
5.7.2	WAF1 promoter as a radio-inducible switch of the NAT transgene	216
5.7.3	Coated Cationic Immunoliposomes: a promising non-viral gene delivery system	216

References	218
------------	-----

List of Figures

Figure 1. [¹³¹ I] meta-iodobenzylguanidine ([¹³¹ I]MIBG)	26
Figure 2. The noradrenaline transporter (NAT)	27
Figure 3. Schematic representation of the telomerase enzyme complex.	43
Figure 4. Amplification plot and standard curve of the NAT sequence.	53
Figure 5. Schematic illustration of a quantitative PCR system using the SYBR Green dye.....	54
Figure 6. Melting curve analysis of fluorescence intensity vs. temperature for 100bp, 500bp, and 1000bp PCR products.	55
Figure 7. hTR and hTERT RNA quantification by qPCR in SK-N-BE(2c) cells.	61
Figure 8. hTR and hTERT RNA quantification by qPCR in SK-N-MC cells. ...	62
Figure 9. Endogenous NAT (hNAT) and transgenic (bNAT) RNA quantification by qPCR in SK-N-BE(2c) cells and three different transfectants.....	64
Figure 10. Endogenous NAT (hNAT) and transgenic (bNAT) RNA quantification by qPCR in SK-N-MC cells and three different transfectants.	65
Figure 11. [¹³¹ I]MIBG uptake in SK-N-BE(2c) parental and transfectants.....	67
Figure 12. [¹³¹ I]MIBG uptake in SK-N-MC parental and transfectants.	68
Figure 13. [²¹¹ At]MABG uptake in SK-N-BE(2c) parental and transfectants. .	70
Figure 14. [²¹¹ At]MABG uptake in SK-N-MC parental and transfectants.	71
Figure 15. Clonogenic survival curves derived by colony formation for disaggregated spheroids exposed to various doses of [¹³¹ I]MIBG.....	74
Figure 16. Clonogenic survival curves derived by colony formation for disaggregated spheroids exposed to various doses of [¹³¹ I]MIBG.....	75
Figure 17. Clonogenic survival curves derived by colony formation for disaggregated spheroids exposed to various doses of [²¹¹ At]MABG.....	78
Figure 18. Clonogenic survival curves derived by colony formation for disaggregated spheroids exposed to various doses of [²¹¹ At]MABG.....	79
Figure 19. Proposed radiation-induction scheme to increase the expression of the noradrenaline transporter (NAT) in neuroblastoma cells.	93

Figure 20. [¹³¹ I]MIBG uptake in SK-N-BE(2c) and SH-SY5Y cells parental and transfected with the pWAF1/GFP plasmid.....	103
Figure 21. [²¹¹ At]MABG uptake in SK-N-BE(2c) and SH-SY5Y cells parental and transfected with the pWAF1/GFP plasmid.....	104
Figure 22. WAF1 activity measured by the GFP fluorescence intensity determined by FACS analysis of SH-SY5Y cells (transfected with the pWAF1/GFP plasmid).	107
Figure 23. WAF1 activity measured by the GFP fluorescence intensity determined by FACS analysis in SH-SY5Y cells (transfected with the pWAF1/GFP plasmid).	108
Figure 24. WAF1 activity measured by the GFP fluorescence intensity determined by FACS analysis in SH-SY5Y cells (transfected with the pWAF1/GFP plasmid).	109
Figure 25. Effect of external beam radiation on WAF1 promoter activity in SH-SY-5YSH-SY5Y cells (transfected with the pWAF1/GFP plasmid).....	110
Figure 26. Effect of [¹³¹ I]MIBG on WAF1 promoter activity in SH-SY5Y cells (transfected with the pWAF1/GFP plasmid).	111
Figure 27. Effect of [²¹¹ At]MABG on WAF1 promoter activity in SH-SY5Y cells (transfected with the pWAF1/GFP plasmid).	112
Figure 28. WAF1 activity measured by the GFP fluorescence intensity determined by FACS analysis of SK-N-BE(2c) cells (transfected with the pWAF1/GFP plasmid).....	115
Figure 29. WAF1 activity measured by the GFP fluorescence intensity determined by FACS analysis in SK-N-BE(2c) cells (transfected with the pWAF1/GFP plasmid).....	116
Figure 30. WAF1 activity measured by the GFP fluorescence intensity determined by FACS analysis in SK-N-BE(2c) cells (transfected with the pWAF1/GFP plasmid).	117
Figure 31. Effect of external beam radiation on WAF1 promoter activity in SK-N-BE(2c) cells (transfected with the pWAF1/GFP plasmid).	118
Figure 32. Effect of [¹³¹ I]MIBG on WAF1 promoter activity in SK-N-BE(2c) cells (transfected with the pWAF1/GFP plasmid).	119
Figure 33. Effect of [²¹¹ At]MABG on WAF1 promoter activity in SK-N-BE(2c) cells (transfected with the pWAF1/GFP plasmid).	120

Figure 34. [¹³¹ I]MIBG effect on GFP protein expression in SH-SY5Y cells stably transfected with the pWAF1/GFP plasmid.....	122
Figure 35. WAF1 activity measured by the GFP fluorescence intensity determined by FACS analysis of HCT116 cells.....	124
Figure 36. Cytotoxicity of γ-rays, [¹³¹ I]MIBG or [²¹¹ At]MABG to SH-SY5Y cells (transfected with the pWAF1/GFP plasmid) determined by clonogenic assay.....	129
Figure 37. Cytotoxicity of γ-rays, [¹³¹ I]MIBG or [²¹¹ At]MABG to SK-N-BE(2c) cells (transfected with the pWAF1/GFP plasmid) determined by clonogenic assay.....	130
Figure 38. Comparison of the effect of external beam radiation, [¹³¹ I]MIBG or [²¹¹ At]MABG on WAF1 promoter activity in SH-SY5Y cells.....	131
Figure 39. Comparison of the effect of external beam radiation, [¹³¹ I]MIBG or [²¹¹ At]MABG on WAF1 promoter activity in SK-N-BE(2c) cells.....	132
Figure 40. [¹³¹ I]MIBG uptake capacity and NAT gene expression in SH-SY5Y parental cells and SH-SY5Y cells transfected with the plasmid pWAF1/NAT....	135
Figure 41. Effect of external beam radiation on [¹³¹ I]MIBG uptake capacity of SH-SY5Y transfectants.....	137
Figure 42. Effect of external beam radiation on endogenous NAT (hNAT) gene expression in SH-SY5Y cells.....	139
Figure 43. Effect of external beam radiation on endogenous NAT (hNAT) and transgenic NAT (bNAT) gene expression in SH-SY5Y cells stably transfected with the pWAF1/GFP plasmid.....	140
Figure 44. Effect of external beam radiation pre-exposure on [¹³¹ I]MIBG toxicity in SH-SY5Y cells stably transfected with the pWAF1/NAT plasmid.....	143
Figure 45. Effect of external beam radiation pre-exposure on [¹³¹ I]MIBG specific capacity of UVW parental and transfected cells with the pWAF1/NAT plasmid.....	147
Figure 46. Effect of external beam radiation pre-exposure on [¹³¹ I]MIBG toxicity in UVW cells transfected with the pWAF1/NAT plasmid.....	148
Figure 47. Schematic illustration of two types of antibody coupling on liposomes.....	169
Figure 48. Schematic representation of anti-GD2-CCL encapsulating pEFGP-N1 plasmid DNA.....	170
Figure 49. Reaction of the covalent coupling of activated monoclonal antibody (mAb) to the maleimide terminus of DSPE-PEG-MAL lipid.....	176

Figure 50. Gel retardation electrophoresis and DNase I protection assays of plasmid DNA complexed with the coated cationic liposomes (CCLs).....	182
Figure 51. Anti-GD ₂ -coated cationic liposomes (anti-GD ₂ -CCLs) binding to neuroblastoma cells.....	184
Figure 52. Fluorescence intensity distribution histogram of SK-N-BE(2c) cells or IMR-32 cells incubated for 2 hours at 37°C with anti-GD ₂ -CCLs labelled with rhoda-PE	185
Figure 53. Competition assay of immunoliposomes binding to disialoganglioside GD ₂ -positive (IMR-32) tumour cells.....	186
Figure 54. Internalisation assay of immunoliposomes binding to disialoganglioside GD ₂ -positive (IMR-32) tumour cells.....	189
Figure 55. Fluorescence intensity distribution histogram of IMR-32 cells incubated for 2 hours at 37°C with PBS, at 4°C or at 37°C with anti-GD ₂ -CCLs labelled with rhoda-PE	190
Figure 56. Cellular localisation of immunoliposomes binding to disialoganglioside GD ₂ -positive (IMR-32) tumour cells.....	191
Figure 57. Regulation of NAT gene expression by the Cre/Lox switch.....	203
Figure 58. Relationship between particle range, radiological bystander effect and linear energy transfer.....	210
Figure 59. Radiation-induced biological bystander effect (RIBBE).....	212
Figure 60. Schematic representation of mosaic spheroids.....	215

List of Tables

Table 1. International Neuroblastoma Staging System.....	23
Table 2. Effect of external beam radiation pre-exposure on [¹³¹ I]MIBG toxicity in SH-SY5Y cells stably transfected with the pWAF1/NAT plasmid.	144
Table 3. Effect of external beam radiation pre-exposure on [¹³¹ I]MIBG toxicity in UVW cells transfected with the pWAF1/NAT plasmid.....	149
Table 4. WAF1 promoter activation in neuroblastoma transfectants 48 hours after exposition to 2eGy γ -radiation, [¹³¹ I]MIBG and [²¹¹ At]MABG.	205
Table 5. Alternatives to ¹³¹ I and ²¹¹ At as conjugate for MIBG.	209

Abbreviations

[¹³¹ I]MIBG	¹³¹ Iodine-labelled meta-iodobenzylguanidine
[²¹¹ At]MABG	²¹¹ Astatine-labelled meta-astatobenzylguanidine
[³ H]CHE	³ H-labelled Cholesterol hexadecylether
[³² P]dCTP	³² P-labelled deoxycytidine-5'-triphosphate
α -MSH	α -melanocyte-stimulating hormone
μ g	Microgram
μ l	Microlitre
μ m	Micrometre
μ M	Micromole
AAV	Adeno-associated virus
AFP	α -fetoprotein promoter
asODN	Antisense oligonucleotides
ADEPT	Antibody-directed enzyme prodrug therapy
ANOVA	Analysis of variance
bNAT	Bovine noradrenaline transporter
bp	Base pair
CCD	Charge-coupled device
CCL	Coated cationic liposome
CD	Cytosine deaminase
cDNA	DNA complementary to mRNA
CE	Carboxylesterase
CEA	Carcinoembryonal antigen
CHCl ₃	Chloroform
cm	Centimetre
CMV	Cytomegalovirus
CNS	Central nervous system
CO ₂	Carbon dioxide
cpm	Counts per minute
Ct	Threshold cycle number
<i>D</i>	Dose
DMs	Double minute chromatin bodies

DNase	Deoxyribonuclease
dATP	Deoxyadenosine-5'-triphosphate
dCTP	Deoxycytidine-5'-triphosphate
dGTP	Deoxyguanosine-5'-triphosphate
DMI	Desmethylimipramine
DNA	Deoxyribonucleic acid
dNTP	2 deoxynucleotide 5 tri-phosphate
DOPE	Dioleoyl-phosphatidylethanolamine
DOTMA	Dioleoyl-trimethylammonium chloride
DSB	Double-strand DNA break
dsDNA	Double stranded DNA
DSPE	Distearoylglycero-3-phosphatidylethanolamine
DTT	Dithiothreitol
dUTP	Deoxyuracil-5'-triphosphate
ECACC	European Collection of Cell Cultures
EDTA	Ethylene-diamine-tetra-acetic acid
Egr1	Early Growth Response Protein 1
eGy	Equivalent radiation dose
Fab	mAb fragment containing one antigen-binding site
FACS	Fluorescence-activated cell sorting
FADD	Fas-associated protein with death domain
FAM	6-carboxyfluorescein
5-FC	5-fluorocytosine
FBS	Foetal bovine serum
FITC	Fluorescein isothiocyanate
g	Force of terrestrial gravity
GAPDH	Glyceraldehyde-3-phosphate dehydrogenase
GCV	Ganciclovir
GD ₂	Disialoganglioside
GDEPT	Gene-directed enzyme prodrug therapy
GFP	Green fluorescent protein
Gy	Gray
h	Hours
HA	Haemagglutinin

HCl	Hydrochloric acid
HEPES	4-(2-hydroxyethyl)-1-piperazineethanesulfonic acid
HIV	Human immunodeficiency virus
hNAT	Human noradrenaline transporter
HPLC	High Performance Liquid Chromatography
HSPC	Hydrogenated soy phosphatidylcholine
HSRs	Homogeneously staining regions
HSV	Herpes simplex virus
HSV- <i>tk</i>	Herpes simplex virus thymidine kinase
hTERT	Telomerase protein subunit
hTR	Telomerase RNA subunit
IC ₁₀	Inhibitory concentration (10%)
IC ₅₀	Inhibitory concentration (50%)
IFN	Interferon
iNOS	Inducible nitric oxide synthase
INSS	International Neuroblastoma Staging System
IUdR	Iododeoxyuridine
Kb	Kilobase
kBq	Kilobequerel
kDa	Kilodalton
keV	Kiloelectronvolt
Ig	Immunoglobulin
l	Litre
LET	Linear energy transfer
LOH	Loss of heterozygosity
mAb	Monoclonal antibody
MABG	Metaastatobenzylguanidine
MAL	Maleimide
MBq	Megabequerel
MDR	Multidrug resistance
MeV	Megaelectronvolt
mg	Milligram
MgCl ₂	Magnesium Chloride
MIBG	Metaiodobenzylguanidine

mins	Minutes
ml	Millilitre
MLV	Murine leukaemia virus
mM	Millimole
mm	Millimetre
MPS	Mononuclear phagocyte system
mRNA	Messenger ribonucleic acid
MRP	Multidrug resistance-related protein
n.c.a.	No-carrier added
NaCl	Sodium Chloride
NaOH	Sodium hydroxide
NAT	Noradrenaline transporter
Nb	Neuroblastoma
ng	Nanogram
NLS	Nuclear localisation signal
ODC	Ornithine decarboxylase
°C	Degrees centigrade
PBS	Phosphate buffered saline
PCR	Polymerase chain reaction
PEG	Polyethylene glycol
PEI	Polyethylene imine
PMSF	Phenylmethanesulphonyl fluoride
pTH	Tyrosine hydroxylase promoter
qPCR	Quantitative PCR
RIBBE	Radiation-induced biological bystander effect
RNAi	Ribonucleic acid interference
rhoda-PE	Rhodamine phosphatidylethanolamine
RPM	Revolutions per minute
RSV	Rous sarcoma virus
RT	Reverse transcription
SF	Surviving fraction
TAMRA	6-carboxytetramethylrhodamine
Taq	Thermus aquaticus
TBE	Tris-Borate-EDTA

Tris	(Hydroxymethyl)aminomethane
TSA	Tumour specific antigen
V	Volt
VDEPT	Viral vector-directed enzyme prodrug therapy
WAF1	Wild-type p53-activated fragment 1

Summary

Introduction: Neuroblastoma has a long-term survival rate of only 15%. While patients with early stage disease can be treated with surgical excision of the tumour, those with inoperable disease require intensive treatment. However, little progress has been made in the survival rates of patients with advanced neuroblastoma. Targeted radiotherapy using [^{131}I]meta-iodobenzylguanidine ([^{131}I]MIBG) has induced favourable remissions in some neuroblastoma patients when used as a single agent. However, uptake of the radiopharmaceutical in malignant sites is heterogeneous and approximately 15% of neuroblastoma patients are MIBG negative by scintigraphy and therefore do not progress to [^{131}I]MIBG therapy. Therefore, the full potential of this therapy may only be realised by improving the drug accumulation capacity of neuroblastoma cells. One way to achieve this is by the introduction of cDNA of the noradrenaline transporter (NAT) into neuroblastoma cells. NAT is responsible for the intracellular accumulation of [^{131}I]MIBG. In this strategy, the NAT transgene will be under the control of tumour specific promoter sequences such as the telomerase promoters or the radiation-inducible WAF1 promoter. Furthermore, this gene therapy approach could be improved by the use of immunoliposomes as a non-viral DNA delivery system.

Aims: The aims of this study were to determine the potency of the telomerase promoters with respect to the NAT transgene expression, and to assess whether the radiopharmaceuticals [^{131}I]MIBG and [^{211}At]MABG could induce the activity of the WAF1 promoter. Finally, the capacity of GD₂-targeted coated cationic immunoliposomes to transfer plasmid DNA specifically to GD₂-positive neuroblastoma cells was evaluated.

Results: Both telomerase promoters (hTR and hTERT) were able to drive the expression of the NAT transgene in neuroblastoma cells. Furthermore, this resulted in enhanced toxicity of the [^{131}I]MIBG and [^{211}At]MABG to the transfected cells, compared to that of untransfected cells. The hTERT promoter displayed the greatest activity for both [^{131}I]MIBG and [^{211}At]MABG treatments.

The WAF1 promoter activity was inducible not only by external beam γ -rays but also by the β -emitter radionuclide ^{131}I in the form of [^{131}I]MIBG or by the α -emitter radionuclide ^{211}At conjugated to benzylguanidine ([^{211}At]MABG). *In vitro* estimation

of the equivalent radiation dose of both radiopharmaceuticals was performed. This demonstrated that levels of WAF1 promoter activation caused by [¹³¹I]MIBG or [²¹¹At]MABG were comparable to that by γ -radiation.

Preliminary toxicity experiments showed that, after irradiation, toxicity of [¹³¹I]MIBG improved in neuroblastoma cells transfected with the construct containing the NAT cDNA downstream of the WAF1 promoter sequence.

The preparation of GD₂-targeted coated cationic immunoliposomes, used in this study, successfully encapsulated plasmid DNA, and were specifically bound to and internalised by GD₂-positive neuroblastoma cells. Unfortunately, low transfection efficiency indicated limited usefulness of this methodology.

Conclusion: Increase in [¹³¹I]MIBG or [²¹¹At]MABG toxicity was achieved in neuroblastoma cells transfected with the NAT transgene under the control of the hTR or hTERT promoter. If the overexpression of the NAT transgene and the improved toxicity of radiolabelled drugs are confirmed in pre-clinical models, there is potential for therapeutic gain.

The WAF1 promoter was activated by both radiopharmaceuticals, and preliminary experiments suggest that pre-exposure to ionising radiation could increase the cytotoxicity of [¹³¹I]MIBG, via WAF1 promoter-controlled overexpression of the NAT transgene. These results together indicate potential for immediate applications in neuroblastoma patients, such as bone marrow purging.

The technology of GD₂-targeted, coated cationic immunoliposomes has great potential for its target-specificity and internalisation capacity. The low transfection effectiveness observed in this study may be improved with advances in the current methodology.

These results suggest that further advances in promoter control and immunoliposomal technology could enable the application of NAT gene transfer in combination with [¹³¹I]MIBG targeted radiotherapy.

Chapter 1

Introduction:

**[¹³¹I]MIBG and gene therapy: A rationale for
amalgamation of targeted radiotherapy with gene therapy
for neuroblastoma treatment**

1.1 Targeted Radiotherapy

After surgery, radiotherapy is the most commonly used type of cancer treatment. Approximately 50% of all patients will require radiotherapy at some stage in their treatment regimen [1]. Conventional external beam irradiation is a very effective treatment for tumours which are confined to their site of origin. However, normal tissue intolerance is the main restriction to the use of radiotherapy. In addition, many tumours do not present well-defined margins or are spread to sites distant from the primary tumour, and cannot be treated in this manner [2].

Targeted radiotherapy, where cytotoxic radionuclides are conjugated to tumour-seeking drugs, may overcome these problems [3]. The peculiar property of this alternative form of radiotherapy is the selective irradiation of malignant areas while sparing normal tissues [3]. The use of monoclonal antibodies raised against tumour-specific antigens has been successful in lymphoma therapy [4, 5], but clinical applications of these radiolabelled macromolecules have generally been poor due to limited tumour penetration, low tumour specificity and induction of anti-mouse immunoglobulin responses [6, 7].

Therefore, the use of low-molecular-weight compounds with tumour specific properties as targeting vehicles is an alternative to antibody-based techniques. These molecules are less likely to generate an immune response and have better penetration [3, 7].

1.1.1 Radiological bystander effect

A further benefit of targeted radiotherapy is that the cytotoxic effects of radionuclides are enhanced by the radiological bystander effect.

Only a fraction of tumour cells can be successfully targeted as a result of heterogeneous uptake of the radiopharmaceutical. However, energy released by decay of the radioisotope emanates from the targeted sites of the tumour in three dimensions (cross-fire), causing damage to neighbouring cells that have not accumulated the radiopharmaceutical [2]. Thus, even if the efficacy of radio-targeting of tumour cells has a success rate less than 100%, underdosing of the tumour is circumvented by the radiological bystander effect.

Targeting strategies such as antibody-directed enzyme prodrug therapy (ADEPT) or gene-directed enzyme prodrug therapy (GDEPT) also make use of bystander effects. However, these methodologies depend on the transport of activated

cytotoxic drug through gap junctions, which frequently decreases with tumour progression [8-10]. However, toxicity due to radiation cross-fire is not dependent on biological cellular functions. Energy emissions from a wide range of radionuclides have been quantified and their path lengths are well known. It is therefore possible to use different radionuclides with different decay properties to treat tumour masses of widely varying size [11].

The contribution of radiological bystander effect to kill neighbouring, non-targeted cells is relatively well understood [11]. Recently, it has emerged that the physical radiation insult can be translated into biological signals or toxins by cellular response to the radiation damage. This phenomenon is known as the radiation-induced biological bystander effect (RIBBE) [12-14]. Although analysis of RIBBE induced toxicity is not the purpose of this present study, these effects may have an important role on the course of future research, which will be discussed in greater detail in section 5.4.

1.2 Neuroblastoma: introduction

Neuroblastoma, one of the most common solid tumours in children [15], derives from the precursor cells of the sympathetic nervous system (neural crest). It accounts for about 7% of all paediatric cancer [16], 96% of cases are diagnosed by the age of 10 years [17] and the median age at diagnosis for neuroblastoma patients is about 18 months [18].

1.2.1 Molecular biology

Analysis of the molecular biology of neuroblastoma began with the cytogenetic characterisation of tumour-derived cell lines. The majority of neuroblastoma cell lines show double minute chromatin bodies (DMs) or homogeneously staining regions (HSRs), both representing DNA amplification, and deletions of the short arm of chromosome 1 [19, 20]. These early studies clearly demonstrated that both gain and loss of genetic material are common in neuroblastoma cells.

1.2.1.1 Gain and loss of genetic material

MYCN gene amplification is seen in 25-33% of neuroblastoma patients [21], and is a powerful prognostic indicator independent of anatomic stage, age, and multiple other biologic measures [22, 23]. The MYCN gene was originally cloned in 1983 by isolating an amplified DNA portion with partial homology to the MYC proto-oncogene (*c-myc*) in neuroblastoma cell lines with DMs and/or HSRs [24, 25]. The MYCN gene is located on the distal short arm of chromosome 2 (2p24). Gain of 17q genetic material is the most common genetic abnormality in primary neuroblastomas and is strongly associated with adverse outcome [15, 26]. Deletions of the short arm of chromosome 1 (1p) are a common feature of advanced disease [27, 28]. Loss of heterozygosity (LOH) for the chromosome 1p is documented in 19% to 36% of primary tumours [29-36]. Chromosome 11q deletions have also been recorded in approximately 15% to 20% of neuroblastoma karyotypes [37]. Evidence indicates that a neuroblastoma suppressor gene could be located on 11q [38].

Deletion of the long arm of chromosome 14 is seen in 22% of primary tumours [39]. Other regions of the genome that have alterations, LOH and/or allelic imbalance are 3p [39], 4p [40], 5q [41], 9p [42, 43] and 18q [44].

1.2.1.2 Alterations in gene expression

Neuroblastoma tumours also show alterations in gene expression. mRNA expression of three members of the family of tyrosine kinase receptors for nerve growth factor and other neurotrophic factors *trk-A*, *trk-B*, and *trk-C* are correlated with neuroblastoma outcome [45-47]. *Trk-A* and *trk-C* expression is more common in infants and low-stage patients, and is related to a favourable outcome [48, 49]. In contrast, *trk-B* expression is associated with *N-myc* amplification, and related to a poor outcome [50, 51].

Multidrug resistance gene 1 (*MDR1*), the gene for multidrug resistance-related protein (*MRP*) and other members of these families are expressed and have potential clinical significance in neuroblastomas [52-54].

Alterations in telomerase expression have also been documented in neuroblastomas. In a study analysing neuroblastomas from untreated patients for telomerase activity, an inverse correlation is seen between telomerase activity and outcome of neuroblastoma patients, and a direct correlation between high expression and *MYCN* amplification [55]. In most stage 4S neuroblastomas telomerase activity is absent [55, 56].

1.2.2 Clinical features and conventional therapies

At presentation, approximately a third of patients have localised disease and two-thirds have metastatic disease [21]. Neuroblastomas are extremely heterogeneous [18], and progression of the disease varies widely according to anatomic stage and age at diagnosis [15].

The clinical factors of age and stage are the most important prognostic indicators for neuroblastoma. In infants, localised and widespread diseases are highly curable [57-61]; children from 2 to 5 years old with localised forms can be cured [22, 58, 59] but metastatic disease is an indication of lethal outcome [62, 63]; and in older patients the prognosis with both localised and metastatic forms is poor [64, 65].

The International Neuroblastoma Staging System (INSS) (Table 1) is the currently used classification for clinical staging of the disease [66].

Patients with stage 1 and stage 2A disease have localized tumours and can be treated surgically, without radiotherapy or chemotherapy [67, 68]. Treatment of patients with stage 2B and stage 3, which include lymph node involvement, is

mainly surgical [69], together with chemotherapy [70]. The efficacy of radiotherapy to patients with stage 2B and 3 tumours is still uncertain [22, 71]. Patients with advanced disease (inoperable stage 3 and stage 4) are usually treated with intensive treatments or "megatherapies", including myeloablative chemotherapy, total body irradiation followed by bone marrow rescue [63, 72, 73]. A distinct subset of patients present spontaneous disease regression without intensive intervention (stage 4S) [21, 74].

However, regardless of such aggressive therapies, the survival rates of patients with advanced disease has not substantially improved [75].

Stage 1:	Localized tumour* with complete gross excision, with or without microscopic residual disease; representative ipsilateral lymph nodes negative for tumour microscopically (nodes attached to and removed with the primary tumour may be positive).
Stage 2A:	Localized tumour with incomplete gross excision; representative ipsilateral nonadherent lymph nodes negative for tumour microscopically.
Stage 2B:	Localized tumour with or without complete gross excision, with ipsilateral nonadherent lymph nodes positive for tumour. Enlarged contralateral lymph nodes must be negative microscopically.
Stage 3:	Unresectable unilateral tumour infiltrating across the midline**, with or without regional lymph node involvement; or localized unilateral tumour with contralateral regional lymph node involvement; or midline tumour with bilateral extension by infiltration (unresectable) or by lymph node involvement.
Stage 4:	Any primary tumour with dissemination to distant lymph nodes, bone, bone marrow, liver, skin, and/or other organs, except as defined for stage 4S.
Stage 4S:	Localized primary tumour, as defined for stage 1, 2A, or 2B, with dissemination limited to skin, liver, and/or bone marrow*** (limited to infants younger than 1 year).
*	Multifocal primary tumours (e.g., bilateral adrenal primary tumours) should be staged according to the greatest extent of disease, as defined above, and followed by a subscript "M" (e.g., 3M).
**	The midline is defined as the vertebral column. Tumours originating on one side and "crossing the midline" must infiltrate to or beyond the opposite side of the vertebral column.
***	Marrow involvement in stage 4S should be minimal, i.e., less than 10% of total nucleated cells identified as malignant on bone marrow biopsy or on marrow aspirate. More extensive marrow involvement would be considered to be stage 4. The MIBG scan (if done) should be negative in the marrow.

Table 1. International Neuroblastoma Staging System [66].

1.2.3 Innovative therapies

Mechanisms involved in neuroblastoma tumorigenesis and drug resistance have been the main focus of recent studies. Such investigations have introduced new potential drugs that can target the tumour more selectively than existing agents.

For example, induction of differentiation is a promising approach for treatment of neuroblastoma. Natural retinoic-acid derivatives have been shown to induce differentiation *in vitro* [76-78] and a significant survival advantage in a randomised clinical trial [63]. A novel synthetic retinoid - N-(4-hydroxyphenyl)retinamide (fenretinide) - induces apoptosis rather than differentiation [79-81]. A phase I clinical trial, recently published, showed stable disease in 41 of 54 patients and manageable toxicity [82].

Inhibition of angiogenesis is another interesting approach for the treatment of this disease [83]. The agent TNP-470 has been used effectively in animal neuroblastoma models [84-87]. However, due to its high toxicity, the use of TNP-470 as a therapeutic drug in neuroblastoma patients is still uncertain. Recently, a new compound, A-357300, with target properties similar to TNP-470, has been proven effective in pre-clinical models with manageable toxicity [88].

Immunotherapy of neuroblastoma is a novel approach that is gaining popularity. Several antibodies have been raised against a surface antigen disialoganglioside GD₂, that is expressed at high density in the majority of human neuroblastoma tumours [89]. These antibodies have been used as therapeutic drugs alone [90-92] and might also provide a means of targeting selectively to neuroblastoma cells other anticancer agents such as radionuclides [93, 94] or liposomal encapsulated fenretinide [95], c-myc antisense oligodeoxynucleotides [96] or doxorubicin [97].

To date, the most promising novel treatment of neuroblastoma is targeted radiotherapy with the use of radioiodinated meta-iodobenzylguanidine (¹³¹I]MIBG - Figure 1). About 85% of neuroblastoma cells express the noradrenaline transporter (NAT - Figure 2) a 12-spanning membrane protein responsible for the re-uptake of the biogenic amines into presynaptic terminals [98-101].

Meta-iodobenzylguanidine (MIBG) is a structural analogue of noradrenaline, is a derivative of the adrenergic neurone-blocking drugs bretylium and guanethidine, and is selectively concentrated in neuroadrenergic tissue by noradrenaline transporter cellular uptake [99, 100]. Tracer doses of radioiodinated MIBG have

been used successfully for diagnostic scintigraphy of tumours derived from the neural crest [102, 103] such as neuroblastoma. It is expected that the ability of neural crest-derived tumours to accumulate and retain high concentration of [¹³¹I]MIBG will lead to more extensive therapeutic application of this drug [104, 105].

Targeted therapy using [¹³¹I]MIBG has induced favourable remissions in some neuroblastoma patients when used as a single agent [106-110]. However, uptake of the radiopharmaceutical in malignant sites is heterogeneous [111] and approximately 15% of neuroblastoma patients are MIBG negative by scintigraphy and therefore do not progress to [¹³¹I]MIBG therapy. These factors clearly suggest that the use of MIBG alone is unlikely to cure advanced stage disease. Therefore the full potential of this therapy may only be realised when it is combined with other agents [112] and/or by improving the drug accumulation capacity of neuroblastoma cells [98].

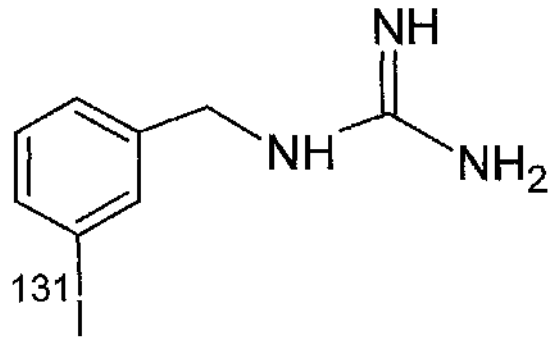


Figure 1. [¹³¹I] meta-iodobenzylguanidine ([¹³¹I]MIBG). [¹³¹I]MIBG is a structural analogue of noradrenergic neurone blockers bretylium and guanethidine. It is selectively concentrated in neuroadrenergic tissue by the noradrenaline transporter (NAT). [¹³¹I]MIBG causes favourable remissions in neuroblastoma patients when used as a single agent.

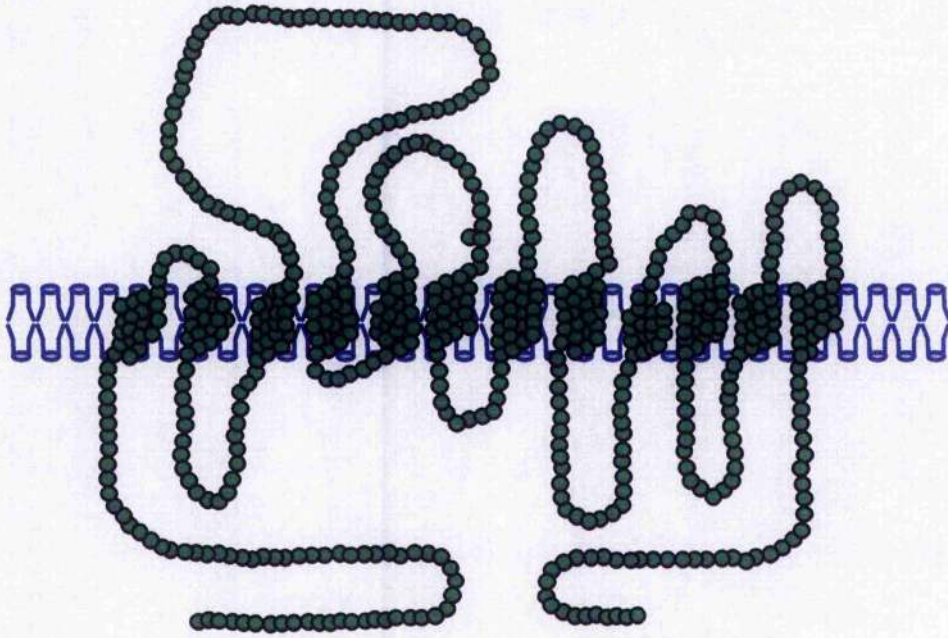


Figure 2. The noradrenaline transporter (NAT) is responsible for the active intracellular accumulation of catecholamine neurotransmitters in neuroadrenergic tissue by a process known as Uptake-1. It is expressed in 85% of neuroblastoma tumours. The NAT protein consists of 617 amino acids and has 12 transmembrane domains. This conformation is similar to that of other membrane-associated proteins that are responsible for ion and solute transport. Note that the number of circles is not an accurate representation of the number of amino acids residues.

1.2.4 Enhancement of MIBG uptake in neuroblastoma cells

Several studies have shown increase of MIBG uptake in neuroblastoma cells after treatment with anticancer agents.

For example, Smets et al. (1991) reported an enhancement factor of 1.8 in the capacity of MIBG uptake in SK-N-SH cells after exposure to 5Gy γ -rays [113]. Montaldo and his group showed an uptake-enhancement factor of 3 in SK-N-SH and SK-N-BE(2)c cells co-treated with IFN-gamma and all-trans retinoic acid [114]. In the same study, uptake enhancement was registered in all the neuroblastoma cells tested after exposure to a combination of IFN-gamma and IFN-alpha [114]. Two studies showed that the use of cisplatin increases the cell capacity to accumulate MIBG by a factor of 2.8 [115] or 1.5 [116]. In the latter study, exposure to doxorubicin caused an uptake-enhancement factor of 3 in neuroblastoma cells [116].

A novel approach to increase MIBG accumulation in malignant cells has considered means of enhancing NAT gene transcription.

The sequencing of the NAT cDNA [101] and the recent development of systems of transfer and expression of the NAT gene indicate that higher levels of tumour MIBG accumulation could be attained by gene therapy. Recently, it was shown that transfection of the NAT gene into neuroblastoma cells induced the expression of a functional transporter which improved the active uptake of [131]MIBG [98]. Particularly, this study showed a dose-dependent toxicity to the host cells and, for the first time, the potential benefits of combining gene transfer with targeted radiotherapy in neuroblastoma.

Targeting gene expression specifically to tumour cells is one of the most important goals of research in cancer gene therapy. Taking into consideration the clinical strategy, it must be ensured that the NAT transgene will operate exclusively in tumour and not in normal tissues of the body. The present study will focus on two approaches in order to address this issue: tumour-specific or radiation-inducible promoter elements for the transgene expression, and immunoliposomes as tumour-targeted gene-delivery system.

1.2.5 Promoter elements for the control of transgene expression

1.2.5.1 Telomerase promoters

As cells proliferate, DNA sequences are lost from telomeres (the cap of the ends of eukaryotic chromosomes) due to the so-called end-replication problem [117]. This progressive telomere loss can be prevented if cells have sufficiently high levels of telomerase, a cellular reverse transcriptase that adds nucleotide repeats onto pre-existing telomeres. Most normal somatic cells do not have sufficient telomerase activity and suffer shortening of chromosomes resulting in senescence [118, 119]. Approximately 90% of human cancers have active telomerase whereas normal somatic tissues have no detectable activity [120], with the exception of renewing tissues such as bone marrow and gastrointestinal tissues [121-123]. The active telomerase is formed by two components: the RNA subunit hTR and the catalytic protein component encoded by the hTERT gene [124]. There is evidence that the regulation of both telomerase genes occurs partially at the transcriptional level [125-127]. These studies indicate that hTR gene is upregulated in cancer cells, but its activity is barely detectable in some normal tissues [128, 129]. The expression of the hTERT gene is low in cancer cells and is generally undetectable in normal cells [130, 131]. There is a clear differential in the transcriptional regulation levels for both genes between malignant and normal tissue, therefore both promoters may be useful for targeting therapeutic genes to tumours [125, 132].

In a recent study, it was shown that efficient tumour cell kill was achieved by administration of [¹³¹I]MIBG, following the expression of exogenous NAT cDNA under the control of the hTR or hTERT promoters [133]. In this report, it was demonstrated that, unlike most mammalian promoters, both telomerase promoters were strong inducers of NAT gene expression [133].

This result is very encouraging for the development of tumour-directed gene therapy and the treatment of neuroblastoma. In the present study, the levels of noradrenaline transporter transgene overexpression driven by telomerase promoters will be assessed in two neuroblastoma cell lines. Furthermore, [¹³¹I]MIBG toxicity will be evaluated in neuroblastoma cells containing the NAT

transgene under the control of either the hTR or hTERT promoter, and will be compared with the [¹³¹I]MIBG toxicity to untransfected cells.

1.2.5.2 WAF1 promoter

One of the benefits of ionising radiation in gene therapy is that as well as cell killing effect, radiation can also activate therapeutic transgenes which are driven by a radiation-inducible promoter. Transcriptional regulation specific to the radiation field may be achievable by using either conformal or brachytherapy or by targeted delivery of radioisotopes.

The radiation-inducible gene called "wild-type p53-activated fragment 1" (WAF1) is a potential component of the p53 tumour growth suppression pathway [134]. In a recent study, a construct containing the WAF1 promoter driving the nitric oxide synthase (iNOS) gene expression was transfected into endothelial cells. After exposure to a dose of 4Gy external beam radiation, an impressive 9.5-fold induction of the iNOS protein expression was registered. Furthermore, this system was shown to generate significant relaxation of arterial segments, indicating the potential to induce physiological effects using an X-ray-inducible promoter in combination with ionising radiation [135].

A similar transgenic construct (containing the WAF1 promoter driving the expression of the NAT gene: pWAF1/NAT) is proposed in this study to upregulate the synthesis of the NAT in neuroblastoma cells. This strategy is discussed in details in section 3.2 (see Figure 3-1 in section 3.2).

In the present study, the WAF1 promoter activation will be evaluated in neuroblastoma cells treated with external beam radiation, [¹³¹I]MIBG or meta-[²¹¹At]astatobenzylguanidine ([²¹¹At]MABG), an astatinated analogue of MIBG(see section 1.2.6 for details).

1.2.6 ^{211}At : an alternative to ^{131}I as conjugate for MIBG

In cancer treatment, radionuclides other than ^{131}I prove to be more effective in some situations. The choice of the radionuclide should consider maximisation of the effectiveness of the radiopharmaceutical in tumours, minimising toxicity to normal tissue. Because of the relatively long path length of the β -particles of ^{131}I (800 μm), the tumour-absorbed dose fraction becomes progressively smaller as the tumour volume decreases, and more of the energy is deposited outside the target. α -particles, which exhibit high linear energy transfer (LET – the measure of energy transferred per unit length of track), have a range of 4 to 5 cell diameters [136]. For this reason α -emitting radionuclides might be ideal for the treatment of micrometastatic disease. ^{211}At , an α -emitting isotope of Astatine (At), is a radiohalogen that has potential as an alternative to radio-iodine in the treatment of neuroblastoma by noradrenaline analogues [11].

Astatine is the heaviest of the halogens found underneath iodine in group 7A of the periodic table, and has similar chemical properties to iodine. Astatine is one of the rarest naturally occurring elements, with the total amount in earth's crust estimated to be less than 29 grams. Astatine can be generated in a cyclotron by bombarding natural bismuth metal with α -particles [136].

^{211}At has a shorter particle range than ^{131}I (50 μm for ^{211}At , compared to 800 μm for ^{131}I). This means that [^{211}At]MABG therapy will affect fewer untargeted cells by the radiological bystander effect than [^{131}I]MIBG therapy.

However, ^{211}At has very high LET (99keV/ μm) compared to ^{131}I (0.24keV/ μm) [137]. Therefore, [^{211}At]MABG treatment is more likely to cause irreparable damage than [^{131}I]MIBG therapy, resulting in superior toxicity in micrometastases [11, 137].

In this study, comparison of [^{211}At]MABG toxicity with that of [^{131}I]MIBG is performed in neuroblastoma cells transfected with the noradrenaline transporter gene, controlled by either the hTR or hTERT promoters. Furthermore, the [^{211}At]MABG capacity to induce the WAF1 promoter is compared with that of [^{131}I]MIBG.

1.2.7 Immunoliposomes as tumour-targeted gene-delivery system

One of the crucial aspects for a successful gene therapy strategy is the use of an effective gene-delivery system.

The delivery of therapeutic transgenes by liposomal encapsulation is a means of overcoming hazards associated with use of viral vectors such as infectivity, oncogenicity and immunogenicity. Two recent investigations by our collaborators [138, 139] and others [140] have shown the efficacy of liposome-based delivery systems in releasing antisense oligonucleotides (asODNs), specific for oncogenic sequences, into human cancer cells, including neuroblastoma. This liposomal preparation involved neutralisation of negative charges on asODNs by a primary positive-charged lipidic coat followed by neutral lipid encapsulation. The resulting structures, called coated cationic liposomes (CCLs), have a prolonged *in vivo* circulation time [141]. This is due to stabilisation against adsorption by plasma proteins and subsequent clearance by the mononuclear phagocyte system. Several lines of evidence indicate that liposomes tend to accumulate and, consequently, release their content to regions in the body where capillary endothelium allows their extravasation, such as newly forming, immature blood vessels within primary tumours and developing metastases [142-144].

The targeting property of CCLs can be improved by coupling to their external surface a monoclonal antibody (mAb) or its Fab fragment, directed to tumour-specific antigens (see section 4.1.3.5). The mAb is generally coupled to a maleimide-derivatised polyethyleneglycol-lipid integrated in the liposomal structure. Our collaborators have successfully applied this strategy using a mAb directed against the neuroblastoma-specific antigen GD₂ [95, 97, 138, 139]. They have shown a high level of tumour-specificity of the targeting system and the improvement of the antineoplastic compounds (encapsulated in immunoliposomal complex) in terms of stability, minimal toxicity to normal tissue and selective concentration in tumour.

1.2.8 General strategy

In order to control the NAT transgene expression within neuroblastoma, we intend to transfect human neuroblastoma cells with a plasmid construct which contains the NAT gene cDNA transcriptionally controlled by specific promoter sequences (telomerase or WAF1). Once inside the cell, the promoter will facilitate the expression of the transgene, thereby causing enhanced [¹³¹I]MIBG or [²¹¹At]MBAG uptake and toxicity.

In order to ensure the transfection of the transgene specifically in neuroblastoma cells a novel delivery system based on anti-GD₂ CCLs (coated cationic liposomes) will be employed. This is expected to overcome the hazards associated with viral vector-based delivery systems, while maintaining target specificity and enabling prolonged circulation time in the body.

1.3 Aims of this study

Experimental evidence has shown that the introduction of the NAT transgene into neuroblastoma cells enhances active intracellular accumulation of [¹³¹I]MIBG leading to a dose-dependent toxicity [98]. However, to date, no attempt has been made to control the transgene expression in neuroblastoma cells, avoiding non-specific and potentially harmful NAT activity in normal tissue.

In a clinical scenario, the effectiveness of gene therapy intervention can be improved if the transgenic and therapeutic construct is delivered via a vector specifically designed to target tumour cells and to protect the DNA content from the host defence mechanisms. Coated cationic immunoliposomes have the potential to accomplish these goals, bypassing the hazards associated with viral vector-based delivery systems.

The aims of this study were:

- i. To investigate the feasibility of gene therapy for neuroblastoma using the NAT transgene under the control of either of the two telomerase promoters. The study will assess the potency of the hTERT and hTR promoters with respect to the NAT transgene expression and will assess potential enhancements of [¹³¹I]MIBG or [²¹¹At]MABG treatment in neuroblastoma cells.
- ii. To assess whether targeted radiopharmaceuticals in the form of MIBG (radiolabelled with ¹³¹I or ²¹¹At) can induce the activity of the WAF1 promoter and, if so, to compare this effect with that generated by external beam radiation.
- iii. To evaluate the capacity of GD₂-targeted immunoliposomes to transfer genetic material selectively to GD₂-positive neuroblastoma cells, thereby increasing their susceptibility to treatment with [¹³¹I]MIBG or [²¹¹At]MABG.

Chapter 2

Evaluation of telomerase promoters as controllers of NAT transgene transcription

2.1 Introduction

2.1.1 Tumour-specific promoters

Ideally, tumour-specific promoters controlling therapeutic transgenes, should have high activity in tumour cells and be silent in normal cells. Promoter elements such as the α -fetoprotein promoter (AFP) which, under non-pathological conditions, is active specifically in the foetal liver but becomes reactivated in hepatoma cells and the promoter for the gene encoding carcinoembryonal antigen (CEA) which is reactivated in several types of adenocarcinoma, have high potential and have been utilized for tumour specific expression of transgenes [145, 146].

Other promoters active in tumours have been employed for transcriptional regulation of therapeutic genes. For example, the ErbB2/HER2 gene is overexpressed at the transcriptional level in about 30% of breast and pancreatic tumours [147]. A retroviral vector containing this promoter driving the cytosine deaminase (CD) gene has been successfully used for expression of CD with subsequent 5-fluorocytosine (5-FC)-mediated cell death exclusively in ErbB2-positive cells [148, 149].

Similarly, the MUC1/DF3 gene, encoding a mucin-like glycoprotein, is transcriptionally upregulated in breast and cholangiocarcinomas. Inhibition of tumour growth was observed when a replication-defective adenovirus containing the HSV-*tk* (Herpes simplex virus thymidine kinase) gene driven by the MUC1/DF3 enhancer region was used in a metastatic breast cancer model [150].

Another interesting tumour-specific control element is the promoter of the osteocalcin gene, highly expressed in osteogenic sarcomas. A phase I trials now in progress using an adenoviral vector expressing HSV-*tk* under the control of this promoter [151] in order to target androgen-independent prostate cancer.

A recent study utilised the L-plastin promoter which is active in malignant epithelial cells, but not in normal tissue (except haemopoietic cells). The use of a replication incompetent adenovirus containing the CD gene under the control of the human L-plastin promoter caused significant size reduction of human ovarian tumour xenografts [152].

Finally, recent interest has been focused on the Midkine gene which encodes for a heparin binding growth factor highly expressed in many tumours [153] but not in liver tissue [154]. The promoter region of the Midkine gene has been inserted in an adenoviral vector to drive the expression of the HSV-*tk* gene targeting the Wilm's

tumour and neuroblastoma cell lines [154]. Similar applications have been successful for targeting ovarian cancer cells and pancreatic cells [155, 156].

2.1.2 Telomerase promoters

An attractive alternative to promoters which are active in few tumour types, are promoter elements of genes such as the human telomerase that are expressed in a wider variety of tumour cells. This is probably the only gene that can be strictly qualified as cancer specific and whose promoter is being used to control the expression of transgenes in many different tumour cell lines.

Human telomeres contain long stretches of the repetitive sequence TTAGGG [157, 158] which are bound by specific proteins. With each cell division, telomeres shorten by ~50–200bp [159], primarily because the lagging strand of DNA synthesis is unable to replicate the extreme 3' end of the chromosome (known as the end replication problem) [160]. When telomeres become sufficiently short, cells enter an irreversible growth arrest called cellular senescence. In most instances cells become senescent before they can accumulate enough mutations to become cancerous, thus the growth arrest induced by short telomeres may be a potent anti-cancer mechanism.

Telomerase [161-167] helps to stabilize telomere length in human stem cells, reproductive cells [168] and cancer cells [120, 169] by adding TTAGGG repeats onto the telomeres using its intrinsic RNA (hTR) as a template for reverse transcription (Figure 3) [170]. Telomerase is active in approximately 90% of human cancers, whereas in normal somatic tissues the activity levels are either low or undetectable [120, 121, 123]. Human telomerase activity depends on the presence of both the RNA subunit (hTR) and the catalytic protein component (hTERT). The regulation of both telomerase genes occurs partially at the transcriptional level [125-127]. There is a clear differential between tumour and normal tissue with respect to the activity of the telomerase promoters [171].

A number of studies have used these two promoters to drive therapeutic genes.

The first study using a retroviral system containing the hTERT promoter in combination with a *Cre/loxP* site-specific recombination technology was described in a system to kill specifically p53-negative tumour cells while sparing normal wild-type cells.

Either hTR or hTERT promoters were inserted in expression vectors upstream the diphtheria toxin A chain gene in order to target bladder and liver tumour cell lines [125].

Glioma cells were also targeted with the hTERT promoter driving the expression of either Fas-associated protein with death domain (FADD) or rev-caspase-6. Subcutaneous human glioma xenografts treated with this construct were significantly reduced in volume compared to control tumours [172-174].

In human tumour xenograft and syngeneic mouse UV-2237m fibrosarcomas, an adenoviral vector containing a hTERT promoter-driven Bax transgene expression system, successfully targeted the apoptotic pathway [175, 176].

Intratumoural injection of a construct containing the HSV-*tk* gene driven by the hTERT promoter avoided the liver toxicity of the CMV promoter following GCV administration [132].

A recent study [177] analysed hTR and hTERT activity in a panel of 10 cell lines and showed cancer specificity of these promoters. The hTR promoter, showing a superior activity in telomerase-positive cell lines, was used to drive the nitroreductase gene to sensitize cells to the pro-drug CB1954. In two xenograft tumour models, the hTR-driven vector produced up to 97% reduction in tumour volume, a higher antitumour effect than a CMV-driven construct [177].

Finally in the last few years, our research group reported several works in which targeted radiotherapy was improved by gene therapy. In particular, it was shown that the expression of the NAT gene (responsible for the intracellular accumulation of MIBG), driven by either hTR or hTERT promoters, resulted in enhanced toxicity of [¹³¹I]MIBG in cells derived from glioma [133, 178], bladder cancer [179] and adenocarcinoma of prostate [180]. These studies have demonstrated that NAT gene can be transcriptionally controlled by the telomerase promoters. These findings have also shown the potential of [¹³¹I]MIBG treatment of such tumours, which normally do not express the NAT gene and therefore not eligible for this type of therapy.

In this study, we show for the first time improved uptake and kill by [¹³¹I]MIBG or [²¹¹At]MABG of neuroblastoma cells transfected with the NAT gene under the control of either the hTR or hTERT promoter. This strategy may be useful for the treatment of those neuroblastomas that have little or negligible MIBG uptake capacity (15% of neuroblastomas) [2].

Interestingly, targeted radiotherapy can improve a limitation of gene therapy. Gene transfer is a highly inefficient process *in vivo*. Therefore, gene therapy must include a significant bystander effect to enable the sterilisation of untargeted

malignant cells which do not accumulate the radiopharmaceutical. A benefit of radionuclide treatment is the contribution to cell-kill conferred by the cross-fire of radioactive decay particles, bombarding adjacent non-targeted cells.

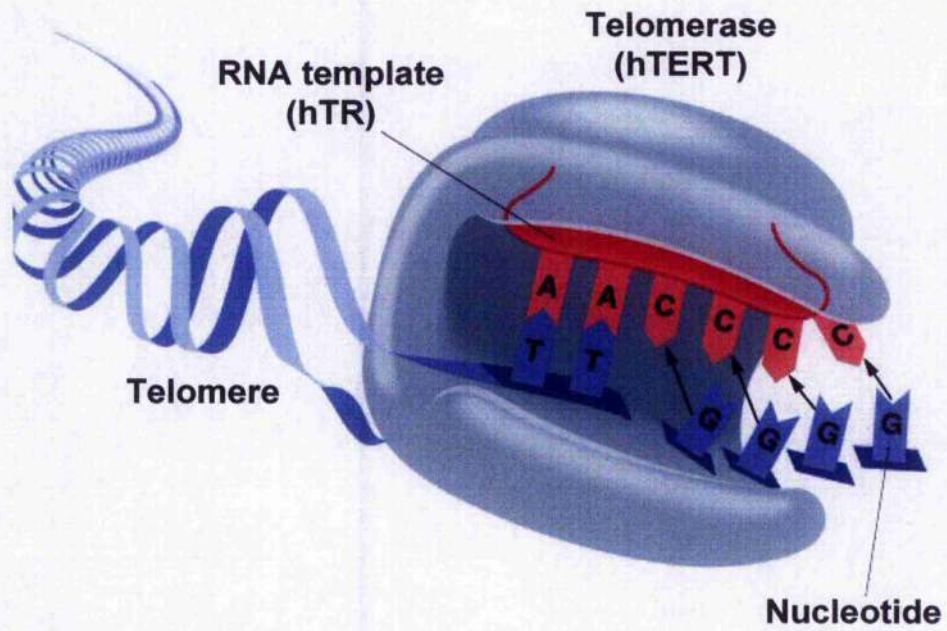


Figure 3. Schematic representation of the telomerase enzyme complex. The protein component's catalytic subunit (hTERT) acts as a reverse transcriptase, using telomerase RNA (hTR) (red) as a template for the addition of telomeric repeat sequences to the telomere DNA strand (blue).

2.2 *Materials and Methods*

2.2.1 Synthesis of the radiopharmaceuticals [¹³¹I]MIBG and [²¹¹At]MABG

No-carrier-added [¹³¹I]MIBG was prepared using a solid-phase system where the precursor of [¹³¹I]MIBG was attached to an insoluble polymer via the tin-Aryl bond [181]. The reaction conditions, HPLC purification procedure, and radiochemical yield were as described previously [182].

[²¹¹At] was produced on the Duke University Medical Center cyclotron by 27-28 MeV α -particle-beam bombardment of a natural bismuth target. The activity was distilled and trapped into chloroform (or in some cases 0.1N NaOH), as previously described [183]. For the synthesis of [²¹¹At]MABG a one-step procedure from 1-[3-(trimethylsilyl)benzyl]-guanidine was used. The reaction conditions, HPLC purification procedure, and radiochemical yield were as described previously [184].

2.2.2 Cell culture

The neuroblastoma cell line SK-N-MC was obtained from ECACC (Salisbury, Wiltshire, UK). SK-N-BE(2c) cells [185] were a gift from Dr. Montaldo (Genoa, Italy). Both neuroblastoma cell lines have the capacity for active uptake of MIBG [100, 186]. Cells were maintained in the logarithmic phase of growth at 37°C in 75cm² plastic culture flasks (Corning Inc., Corning, NY) in a 5% CO₂-95% air humidified incubator. They were subcultured in RPMI-1640 medium supplemented with 10% heat inactivated foetal bovine serum, 50IU/ml sodium penicillin G, 50mg/mL streptomycin sulphate, and 2mM L-glutamine. Medium and supplements were obtained from Invitrogen (Paisley, UK).

2.2.3 Plasmids

The bovine NAT cDNA inserted into the EcoRI site of the eukaryotic expression vector pSG-5 (Stratagene, Cambridge, UK), was kindly provided by Dr Michael Bruss and Professor Heinz Bonisch (University of Bonn, Germany). Owing to the lack of selection markers in this plasmid and the presence of a SV40 promoter, which expresses genes optimally in cells expressing the large T antigen, the 3.2kb bovine NAT cDNA (bNAT) was initially subcloned into the EcoRI site of the pIND vector (Invitrogen, Paisley, UK). As only one restriction enzyme was used for subcloning into the pIND plasmid, the bNAT cDNA was present in different clones, in both sense and antisense orientations. Restriction mapping was used to identify

the clones of pIND/bNAT recombinant plasmids with the insert in the correct orientation (results not shown). The latter plasmid has suitable restriction enzyme sites for subcloning the bNAT cDNA into the KpnI / Xho sites of the promoterless pEGFP-1 (BD Biosciences Clontech, Palo Alto, CA), from which the EGFP gene had been removed. This new construct was referred to as promoterless/bNAT. The bNAT cDNA was also subcloned into the pcDNA3 episomal expression vector (Invitrogen, Paisley, UK). This vector, referred to as pCMV/NAT, was utilized as a positive control, because of the presence of the cytomegalovirus (CMV) enhancer-promoter for high level of protein expression. By virtue of the presence in the promoterless/NAT construct of a multiple cloning site region upstream of the bNAT coding sequence, the assessment of a particular promoter was possible. The 872bp hTR promoter fragment [189] or the 536bp hTERT promoter fragment [190] were then subcloned into the multiple cloning site of the promoterless plasmid containing the bNAT cDNA.

In this study, the construct containing the hTR promoter inserted upstream of the bNAT cDNA was referred to as pHTR/NAT, and the vector with the bNAT transgene controlled by the hTERT promoter was referred to as pHTERT/NAT.

2.2.4 Transfections

Cells were plated at a density of 1×10^5 cells per well on 6-well plates and incubated in full medium at standard culture conditions, 2 days to 80% confluency. For each transfection, 2 μ g DNA in 250 μ L of Opti-MEM medium and 10 μ L Lipofectamine™ 2000 in 250 μ L of Opti-MEM medium were prepared and incubated for 5 minutes at room temperature. Opti-MEM medium and Lipofectamine™ 2000 were obtained from Invitrogen (Paisley, UK). Then, the diluted DNA and the diluted Lipofectamine™ 2000 were mixed gently and incubated for another 20 minutes at room temperature. The mixture was then added to each well and incubated with the cells at 37°C and 5% CO₂ incubator for 24 hours. Subsequently, stable transfectants were selected by growing cells in 500 μ g/ml G418, obtained from Invitrogen (Paisley, UK).

For both SK-N-BE(2c) and SK-N-MC cells, 6 different transfections of each plasmid (pCMV/NAT, pTR/NAT or pTERT/NAT) were attempted. The transfections that produced cells exhibiting the highest capacity for [¹³¹I]MIBG uptake were chosen for subsequent analyses.

2.2.5 General consideration about quantitative real-time Polymerase Chain Reaction (PCR)

Quantitative real-time PCR is based on detection of a fluorescent signal produced proportionally during the amplification of a PCR product. This allows visualization directly of the exponential part of the PCR reaction.

In brief, the detection system consisted of a thermal cycler connected to a laser and charge-coupled device (CCD) optics system. An optical fibre inserted through a lens is positioned over each well, and laser light is directed through the fibre to excite the fluorochrome in the PCR solution. Emissions are sent through the fibre to the CCD camera, where they are analyzed by the software's algorithms. Collected data are subsequently sent to the computer.

The software calculates the threshold cycle (Ct) for each reaction with which there is a linear relationship to the amount of starting DNA. Ct is the cycle number at which the reporter dye emission intensities rises above background noise. The Ct is determined at the most exponential phase of the reaction and is more reliable than end-point measurements of accumulated PCR products used by traditional PCR methods. The Ct is inversely proportional to the copy number of the target template; the higher the template concentration, the lower the Ct measured.

2.2.6 TaqMan real-time PCR for hNAT and bNAT transcripts

Isolation of total RNA was performed using RNeasy Mini Kit (Qiagen, USA), according to the manufacturer's instructions.

2.2.6.1 Primers and probes

Primer and probe sequences were designed from the published sequence for the human noradrenaline transporter (hNAT) (accession No. M65105) using the ABI prism PrimerExpress™ v1.0 software. Both primers and probe were custom synthesised (MWG-Biotech, Milton Keynes, UK). The sense primer corresponded to bases 241-260 of the hNAT sequence (5'-CGCTCCCCCTACCTCTGCTA-3'). The antisense primer was complementary to bases 372-391 of the hNAT sequence (5'-AGATTTTCCAAACGGTGGCA-3'). These primers generated a PCR product of 151 base pairs. The internal probe corresponded to bases 273-299 of the hNAT sequence (5'-CGGTGCCTTCTTGATCCCGTACACAC T-3'). The probe was labelled with the fluorescent reporter dye 6-carboxyfluorescein (FAM) at the 5'

end, and the quencher molecule 6-carboxytetramethylrhodamine (TAMRA) at the 3' end.

Similarly, the primer and probe sequences were designed from the published sequence for the bovine noradrenaline transporter (bNAT) (accession No. U09198), and custom synthesised as above (MWG-Biotech). The sense primer corresponded to bases 1583-1602 of the bNAT sequence (5'-TCAGCAACGACATCCAGCAG-3'). The antisense primer was complementary to bases 1637-1657 of the bNAT sequence (5'-GGCTGACAAACTTCCAGCAGA-3'). These primers generated a PCR product of 75 base pairs. The internal probe corresponded to bases 1612-1635 of the bNAT sequence (5'-TTCAAGCCCGGCCTGTACTIONGGAGA-3'). This probe was also labelled with the fluorescent reporter dye FAM at the 5' end, and the quencher molecule TAMRA at the 3' end.

The housekeeping gene glyceraldehyde-3-phosphate dehydrogenase (GAPDH) was used as an internal standard for all real-time PCR reactions. GAPDH PCR was carried out using the commercially available TaqMan® GAPDH control reagents (Perkin-Elmer Applied Biosystems, Cheshire, UK, P/N 402869).

2.2.6.2 Quantitative real-time RT-PCR reaction conditions

Quantitative real-time RT-PCR was carried out using the commercially available TaqMan® Reverse Transcription reagents and TaqMan® Universal PCR Master Mix (Perkin-Elmer Applied Biosystems, Warrington UK: P/N N808-0234 and 4304437 respectively).

Briefly, 1µg of total RNA was reverse transcribed in a 50µl reaction volume, containing 5.5mM MgCl₂, 5µl 10x TaqMan® RT buffer, 2mM dNTP mix (500µM each nucleotide), 20 units of RNase Inhibitor, 2.5µM oligo d(T)₁₆ and 62.5 units of MultiScribe Reverse Transcriptase.

Next, 2.5µl of the resulting solution, containing cDNA template, was added to an amplification reaction mixture of total volume 25µl consisting of 12.5µl TaqMan® Universal PCR Master Mix and 100nM each of both primers and probe.

The thermal cycling conditions consisted of an initial incubation for 2 minutes at 50°C, followed by 10 minutes at 95°C. Thermal cycling was then carried out at 95°C for 15 seconds, followed by 60°C for 1 minute, for 40 cycles.

Each assay included standard curves of hNAT, bNAT and GAPDH (10¹ to 10⁸ copies) and a no-template control, along with the unknown cDNA templates obtained from the reverse-transcription step. PCR reactions were performed using a Chromo4 Real Time PCR Instrument (MJ Research, Inc.), which measured the fluorescent signal generated by the PCR reaction.

2.2.6.3 Analysis

A range of quantities of hNAT-, bNAT- and GAPDH-specific PCR products were amplified using the real-time PCR method to establish corresponding Ct values (Figure 4A). These were plotted against the initial quantity of substrate to produce standard curves (Figure 4B).

Relative quantification determined by the ratio between the quantity of the target cDNA and the reference cDNA (GAPDH) within the same sample was performed.

2.2.7 SYBR Green real-time PCR for hTR and hTERT transcripts quantification

The methodology for quantification of hTR and hTERT RNA employs a fluorescent dye, called SYBR Green I that binds to the minor groove of the DNA double helix. In solution, the unbound dye exhibits very little fluorescence, however,

fluorescence is greatly enhanced upon double helix DNA-binding. The principle is outlined in Figure 5.

At the beginning of amplification (Figure 5A), the reaction mixture contains the denatured DNA, the primers, and the dye. The unbound dye molecules weakly fluoresce, producing a minimal background fluorescence signal which is subtracted during computer analysis. After annealing of the primers (Figure 5B), a few dye molecules can bind to the double strand. DNA binding results in a dramatic increase of the SYBR Green I molecules to emit light upon excitation. During elongation (Figure 5C), increasingly more dye molecules bind to the newly synthesised DNA. When the reaction is monitored continuously, an increase in fluorescence is recorded in real-time. At DNA denaturation for the next heating cycle, the dye molecules are released and the fluorescence signal drops. Fluorescence measurement at the end of the elongation step of every PCR cycle is performed to monitor the increasing amount of amplified DNA.

2.2.7.1 Reverse transcription reaction

In a volume of 20 μ l, a reverse transcription reaction with 1 μ g total RNA was performed using the Gene Amp RNA PCR KIT (Applied Biosystems, Roche, New Jersey USA), adding 2.5 μ M Oligo d(T)16 primer for hTERT quantification or 2.5 μ M Random Hexamers for hTR quantification, according to manufacturer's instructions.

2.2.7.2 Real-time PCR reaction conditions and primers

The qPCR reaction was carried out with 1 μ l of the RT reaction solution (containing cDNA) in a 20 μ l volume using the DyNAmo SYBR® Green qPCR kit (Finnzymes Oy, Finland).

Primers for hTERT cDNA amplification [191] were added to final concentrations of 0.2 μ M. The enzyme was activated at 94°C for 10 minutes, followed by 40 cycles of 95°C for 5 seconds, 62°C for 15 seconds and 72°C for 15 seconds.

Primers for hTR cDNA amplification were added to a final concentrations of 0.2 μ M. Primer sequences were designed from the published sequence for the hTR (accession No. U86046). The sense primer corresponded to bases 140-163 of the hTR sequence (5'-CTAACCCCTAACTGAGAAGGGCGTA-3'). The antisense primer was complementary to bases 293-269 of the hTR sequence (5'-GGCGAACGGGCCAGCAGCTGACATT-3'). The enzyme was activated at 94°C for

10 minutes, followed by 32 cycles of 95°C for 30 seconds, 59.5°C for 45 seconds and 72°C for 30 seconds.

The housekeeping gene GAPDH was used as an internal standard for all real-time PCR reactions. GAPDH PCR was carried out using specific primers (Cat. N. 5405-1, BD Biosciences Clontech, Palo Alto, CA) at a final concentration of 0.3µM. The enzyme was activated at 94°C for 10 minutes, followed by 30 cycles of 95°C for 30 seconds, 60°C for 45 seconds and 72°C for 1 minute.

Each assay included standard curves of hTR, hTERT and GAPDH (0.1 to 100ng of DNA) a no-template control, along with the unknown cDNA templates obtained from the reverse-transcription step. PCR reactions were performed using a Chromo4 Real Time PCR Instrument (MJ Research, Inc.), which measured the fluorescent signal generated by the PCR reaction.

2.2.7.3 Melting curve analysis

Melting Curve analysis (Figure 6) was automatically performed by OpticonMONITOR™ 3.1 software for each PCR reaction. It was used to check the specificity of an amplified product, in order to eliminate artefacts (such as primer-dimers) from the process of quantification. The melting point of the product depends mostly on base composition and length. When the temperature is gradually increased, a sharp decrease in SYBR green fluorescence is registered as the product undergoes denaturation. When plotted as a negative first derivative, the temperature of the peak is defined as the T_m , or melting temperature of the product.

2.2.7.4 Data analysis

Dilution series of cDNA of known concentration from SK-N-MC cells was used to generate standard curves for each reaction. The standard curve was a plot of the threshold cycle (Ct) against the log of the amount of DNA added. A linear regression analysis of the standard plot was used to calculate the amount of DNA in unknown samples (Figure 4).

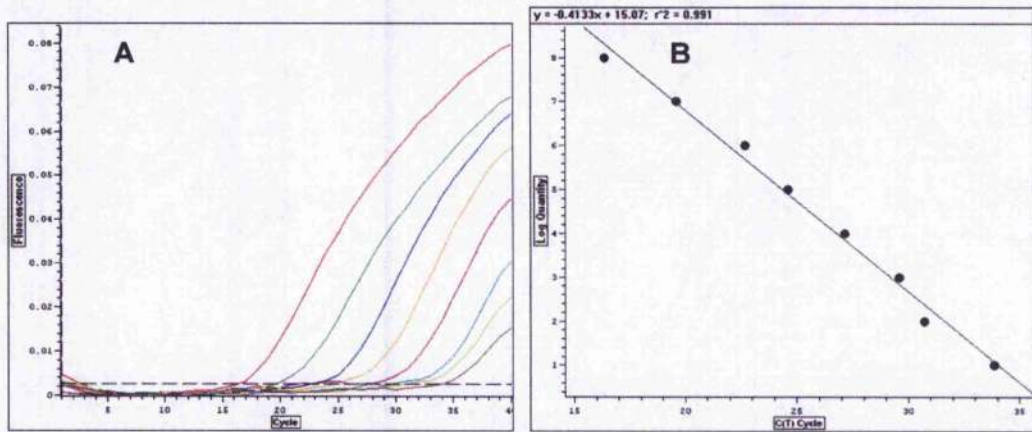


Figure 4. Amplification plot and standard curve of the NAT sequence. Human NAT standards were obtained by PCR amplification of cDNA from the cell line SK-N-BE(2c). The human NAT-specific PCR product was then quantified spectrophotometrically, serially diluted and amplified using the real-time PCR method. **A:** The plot, from left to right, correspond to 10^8 to 10^1 NAT sequence copies. **B:** The Ct values obtained were plotted against the initial quantity of substrate to produce a standard curve. The same procedure was used to quantify bovine NAT-, hTERT-, hTR-specific and the reference GAPDH sequences.

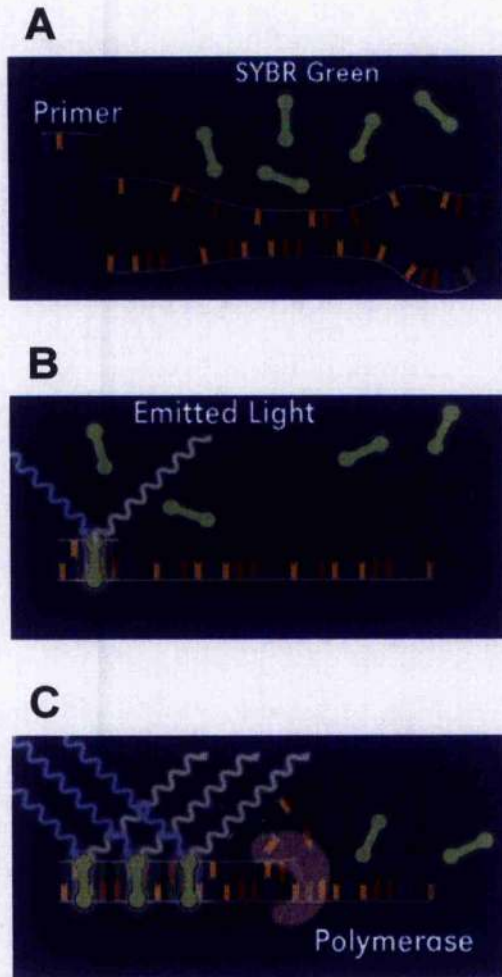


Figure 5. Schematic illustration of a quantitative PCR system using the SYBR Green dye. At high temperatures, during the DNA denaturation step, the SYBR Green dye molecules are unbound and exhibit little fluorescence (A). During the annealing step, as the temperature drops to allow the primers to bind, a few dye molecules begin to bind, resulting in a low fluorescence signal (B). As the complementary strands are synthesized (elongation), SYBR Green molecules are rapidly incorporated into the new DNA and the increase in fluorescence can be measured in real time (C). When the cycle returns to the high temperature denaturation step, the dye molecules are released and the signal returns to background levels. As the target sequence is amplified, SYBR Green binds to each new copy of double strand DNA. The fluorescent intensity measured is proportionate to the amount of PCR products produced.

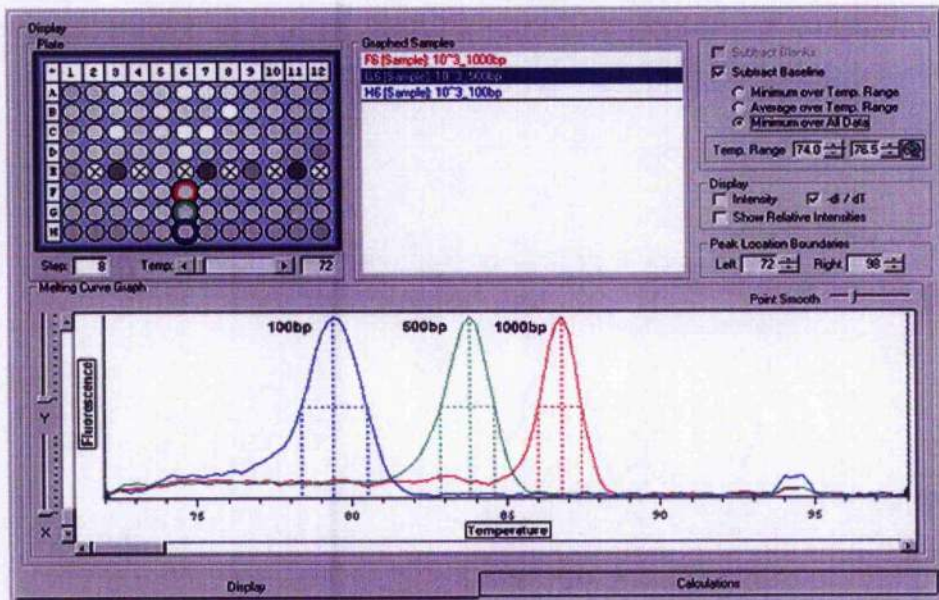


Figure 6. Melting curve analysis of fluorescence intensity vs. temperature for 100bp, 500bp, and 1000bp PCR products. The maximum $-dI/dT$ value for a peak corresponds to the melting temperature of the product. The approximate melting temperature is 79.6°C for the 100bp PCR products, 83.8°C for the 500bp PCR products, and 86.6°C for the 1000bp PCR products. As expected, the melting temperature increases as the length of the product increases.

2.2.8 [¹³¹I]MIBG and [²¹¹At]MABG uptake studies in SK-N-MC and SK-N-BE(2c) cells

Monolayers were prepared by seeding the appropriate numbers of cells in six-well plates at an initial density of 0.5×10^5 cells per well and culturing for 48 hours. MIBG and MABG incorporation was measured by incubating the cells for 2 hours with 7kBq of [¹³¹I]MIBG or [²¹¹At]MABG. Non-specific uptake was measured in the presence of 1.5mM desmethylimipramine (DMI; Sigma-Aldrich, Dorset, UK), a powerful inhibitor of the active uptake mediated by the NAT. After incubation, medium was removed, the cells were washed with phosphate-buffered saline (PBS) and radioactivity was extracted using two aliquots of 10% (w/v) trichloroacetic acid. The activities of the extracts were then measured in a gamma-well counter. Uptake was expressed as counts per minute (cpm) per 10^6 cells.

2.2.9 Spheroid clonogenic assays

SK-N-MC and SK-N-BE(2c) cells, stably transfected with plasmids containing the NAT gene under the control of the CMV, hTR or hTERT promoters (pCMV/NAT, phTR/NAT and phTERT/NAT), were grown as tumour spheroids as described previously [187, 192]. Spheroids of 200 - 300µm diameter were incubated with various activity concentrations of [¹³¹I]MIBG or [²¹¹At]MABG. After incubation for 2 hours at 37°C, the medium was removed and the spheroids washed twice with PBS to remove any free [¹³¹I]MIBG or [²¹¹At]MABG.

Fresh culture medium was added to the washed spheroids which were then incubated with agitation at 37°C for 48 hours to allow bystander effects to accumulate [178]. They were then incubated for 10 minutes at 37°C with PBS containing 0.25% (v/v) trypsin and 1mM ethylenediaminetetraacetic acid (EDTA) and mechanically disaggregated to a single cells suspension using a syringe (gauge 18). Microscopic examination confirmed that the cell preparations were free from clumps. The resulting single cell suspensions contained more than 98% viable cells according to trypan blue exclusion. Cells were counted and seeded in triplicate into 25cm² vented flasks for clonogenic assay at 1×10^3 cells / flask. The cultures were incubated at 37°C until discrete colonies had formed. The cells were then fixed and stained with Carbol Fuchin (RA Lamb, Middlesex, UK), before counting and calculation of surviving fractions. Results were expressed as a percentage of the initial concentration of cells plated, known as the plating

efficiency. The cytotoxic potency of the radiopharmaceutical was determined by comparing the number of colonies formed by treated cells to the number of colonies formed by untreated control (the surviving fraction, or SF). For each transfectant, experiments were performed three times, in triplicate.

2.2.10 Statistical analysis

Results are expressed as mean \pm standard deviation (s.d.). All data are from at least three independent experiments. Data were analysed by Student's t-test using SPSS software, version 13 (IL). A p value of less than 0.05 was considered statistically significant.

2.3 Results

2.3.1 Real-time PCR for determination of the expression of hTR, hTERT, endogenous and transgenic NAT transcripts

2.3.1.1 Quantification of hTR and hTERT transcripts

Transcriptional activity of the two telomerase components was assessed in neuroblastoma cells. The hTR and hTERT RNA levels were analysed by quantitative PCR in SK-N-BE(2c) and SK-N-MC cells (Figure 7 and Figure 8). Results are presented as nanograms (ng) of hTR or hTERT RNA per 1ng of GAPDH RNA. In both SK-N-BE(2c) and SK-N-MC cell lines, hTR and hTERT RNA is detectable, indicating expression of both transcripts. Further, in SK-N-BE(2c) cells no significant difference ($p > 0.1$) in transcript levels was observed between the two telomerase components (approx. 0.8ng / ng of GAPDH). However, in SK-N-MC cells, RNA levels of hTERT (0.8ng / ng of GAPDH) were higher than that of hTR (0.3ng / ng of GAPDH) ($p < 0.05$).

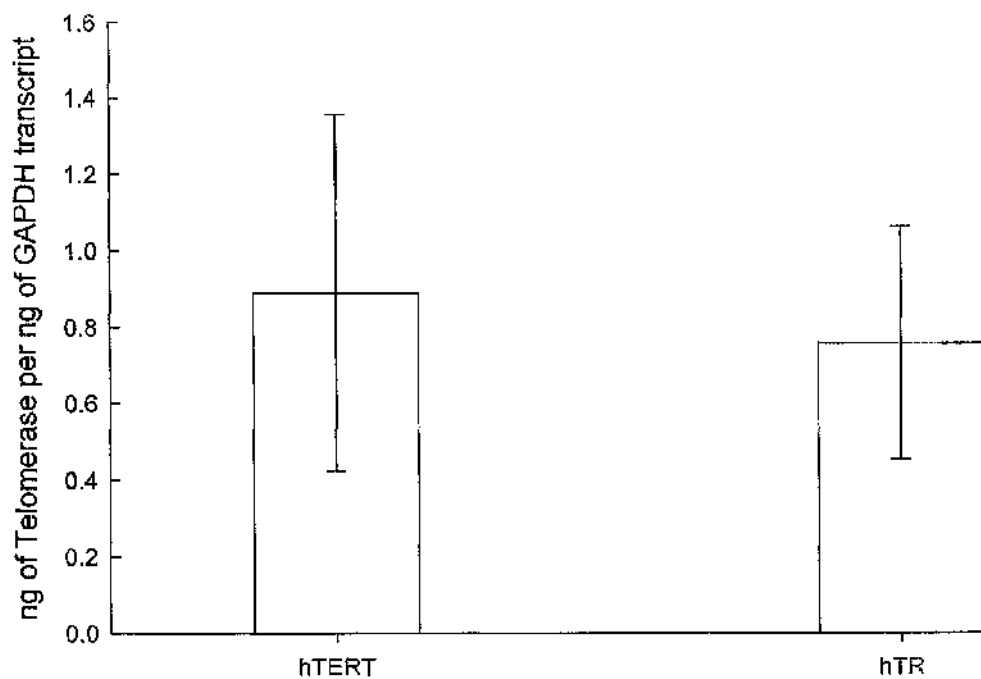


Figure 7. hTR and hTERT RNA quantification by qPCR in SK-N-BE(2c) cells. Results are expressed as a ratio of ng of either hTR or hTERT RNA transcript to ng of GAPDH transcript. Data are means and s.d. of three measurements performed in triplicate. Results were analysed by Student's t-test. The levels of hTERT RNA transcript were not significantly higher than that of hTR RNA transcript ($p > 0.1$).

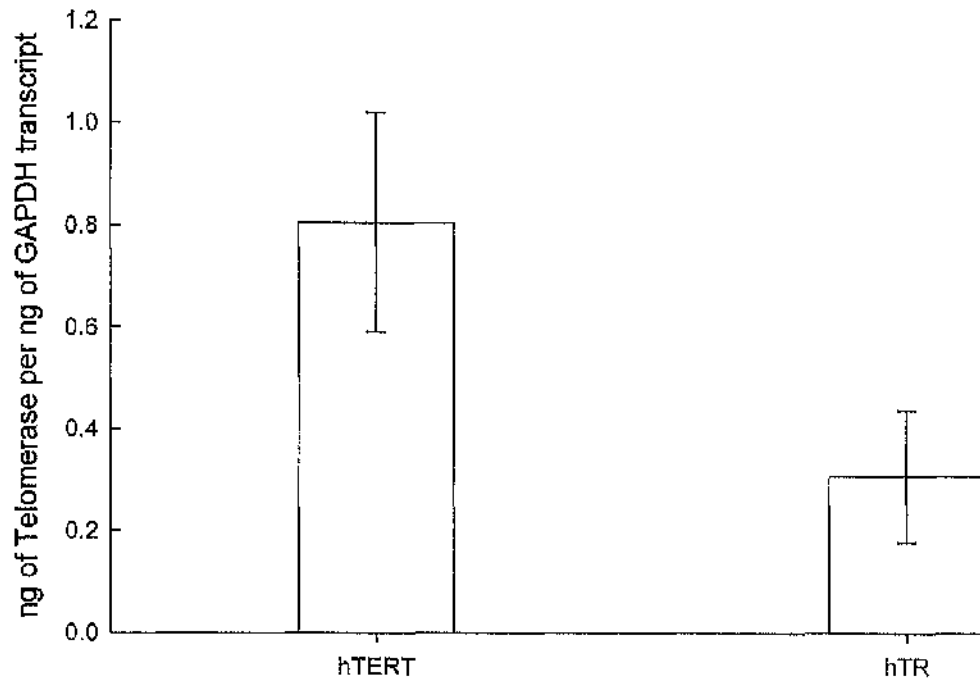


Figure 8. hTR and hTERT RNA quantification by qPCR in SK-N-MC cells. Results are expressed as a ratio of ng of either hTR or hTERT RNA transcript to ng of GAPDH transcript. Data are means and s.d. of three measurements performed in triplicate. Results were analysed by Student's *t*-test. The hTERT RNA transcript levels were significantly higher than that of hTR ($p < 0.05$).

2.3.1.2 Quantification of hNAT and bNAT mRNAs

Quantitative PCR assays specific for mRNA of the endogenous or the transgenic NAT (hNAT and bNAT respectively) were conducted using SK-N-BE(2c) and SK-N-MC cells both stably transfected with the pCMV/NAT, phTR/NAT or phTERT/NAT plasmid.

In the SK-N-BE(2c) cells the transcript copy number of the hNAT was 4 per copy of GAPDH and did not change significantly in any of the transfectants (Figure 9). The bNAT mRNA was undetectable in parental cells and pCMV/NAT transfected cells, whereas in cells transfected with phTR/NAT or phTERT/NAT plasmids, the bNAT mRNA was present: 0.2 copies or 1.64 copies per 1 copy of GAPDH in phTR/NAT or phTERT/NAT transfectants respectively (Figure 9). This result suggests that no transgenic NAT gene, when under control of the CMV promoter, was expressed in SK-N-BE(2c) cells. However, the transgenic NAT gene was transcribed when this cell line was transfected with phTR/NAT or phTERT/NAT plasmid. Further, it is shown that the hTERT promoter was more active than the hTR promoter with respect to driving the expression of the transgenic NAT gene.

In the SK-N-MC parental cells and all the transfectants hNAT mRNA was undetectable (Figure 10). The bNAT mRNA was undetectable in parental cells. These findings agree with previous reports that showed poor MIBG specific uptake and undetectable mRNA levels of endogenous NAT in SK-N-MC cells [98]. In pCMV/NAT, phTR/NAT and phTERT/NAT transfectants 0.66, 0.04 and 0.13 copies of bNAT per copy of GAPDH respectively were registered (Figure 10). Similarly to the SK-N-BE(2c) cells experiments, these data suggest that in the SK-N-MC cells the hTERT promoter displayed higher activity than the hTR promoter, resulting in higher transgenic NAT gene expression.

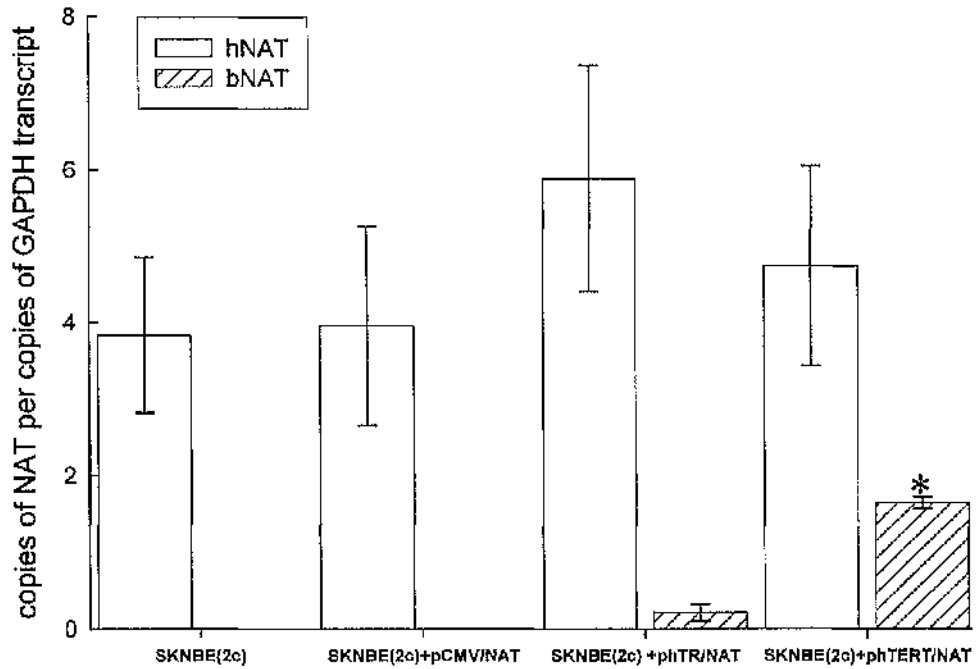


Figure 9. Endogenous NAT (hNAT) and transgenic (bNAT) RNA quantification by qPCR in SK-N-BE(2c) cells and three different transfectants.

SK-N-BE(2c) cells were transfected with the bovine NAT gene, whose expression is driven by (i) the CMV promoter (SK-N-BE(2c)+pCMV/NAT), (ii) the promoter of the RNA component of telomerase (SK-N-BE(2c)+phTR/NAT) or (iii) the promoter of the protein component of telomerase (SK-N-BE(2c)+phTERT/NAT). Results are expressed as a ratio of number of copies of hNAT (empty bars) or bNAT (shaded bars) RNA transcript to number of copies of GAPDH transcript. Data are means and s.d. of three measurements performed in triplicate. Results were analysed by Student's t-test. The hNAT RNA transcript levels in each transfectants were not significantly higher than that in the parental cells. The bNAT RNA transcript levels in cells transfected with the phTERT/NAT plasmid (highlighted with *) were significantly higher ($p < 0.05$) than that in cells transfected with the phTR/NAT plasmid.

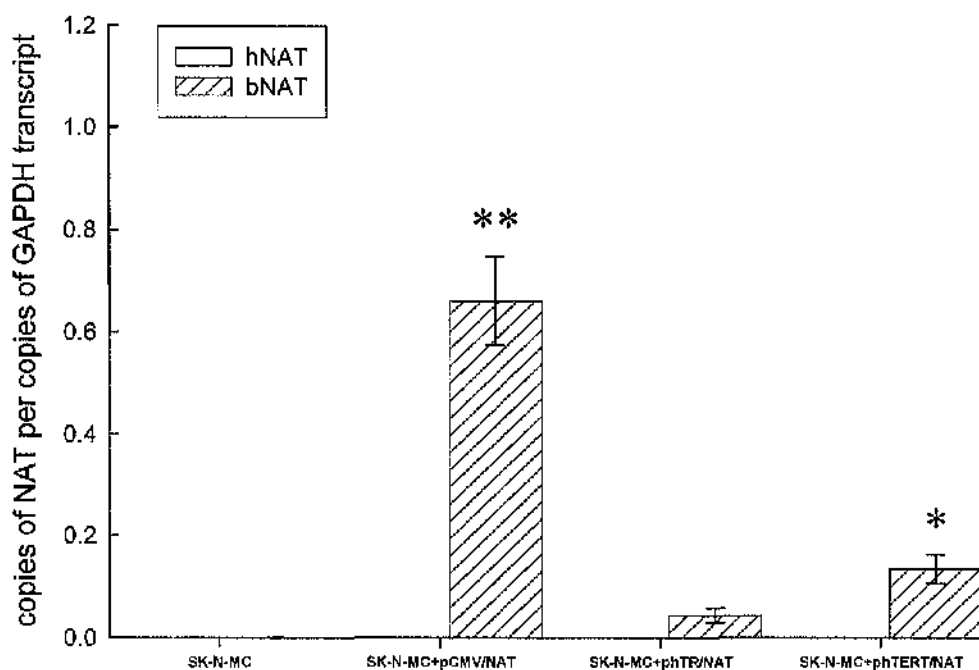


Figure 10. Endogenous NAT (hNAT) and transgenic (bNAT) RNA quantification by q PCR in SK-N-MC cells and three different transfectants.

SK-N-MC cells were transfected with the bovine NAT gene, whose expression is driven by (i) the CMV promoter (SK-N-MC+pCMV/NAT), (ii) the promoter of the RNA component of telomerase (SK-N-MC+phTR/NAT) or (iii) the promoter of the protein component of telomerase (SK-N-MC+phTERT/NAT). Results are expressed as a ratio of number of copies of hNAT (empty bars) or bNAT (shaded bars) RNA transcript to number of copies of GAPDH transcript. Data are means and s.d. of three measurements performed in triplicate. Results were analysed by Student's t-test. The bNAT RNA transcript levels in cells transfected with the phTERT/NAT plasmid (highlighted with *) were significantly higher than that in cells transfected with the phTR/NAT plasmid ($p < 0.05$). RNA transcript levels in cells transfected with the pCMV/NAT plasmid (highlighted with **) were significantly higher than that in cells transfected either with the phTR/NAT or the phTERT/NAT plasmid ($p < 0.01$).

2.3.2 Cellular uptake of [¹³¹I]MIBG

2.3.2.1 [¹³¹I]MIBG uptake in SK-N-BE(2c) cells

The activity of the noradrenaline transporter was assessed by [¹³¹I]MIBG uptake assay in each transfectant and compared with that of SK-N-BE(2c) parental cells (Figure 11). The relative uptake of MIBG in each transfectant reflected the RNA levels of NAT showed in Figure 9. In particular, the phTERT/NAT plasmid conferred to the host cells a greater ability to accumulate [¹³¹I]MIBG than the phTR/NAT construct. SK-N-BE(2c) cells transfected with the pCMV/NAT plasmid did not improve their capacity to uptake [¹³¹I]MIBG compared to the untransfected ones, confirming the NAT RNA analysis, that bNAT gene was not expressed by the CMV promoter in these cells. This could be due to the fact that, as several reports showed, in stable transfectants the CMV promoter may be silenced by methylation [193-195]. However, a statistically significant increase in MIBG uptake was registered in cells transfected with the bNAT gene under the control of either the hTR or hTERT promoters. Furthermore, it should be noted that as SK-N-BE(2c) cells have endogenous NAT expression, increase in MIBG uptake was a combination of the hNAT and the bNAT activity contributions.

2.3.2.2 [¹³¹I]MIBG uptake in SK-N-MC cells

Whereas in untransfected SK-N-MC cells, negligible levels of [¹³¹I]MIBG active uptake were registered, SK-N-MC cells transfected with the pCMV/NAT, phTR/NAT or phTERT/NAT plasmid were all able to actively concentrate [¹³¹I]MIBG (Figure 12). In contrast to the SK-N-BE(2c) cells, the highest levels of uptake were registered in cells transfected with the pCMV/NAT plasmid (189657 cpm/10⁶ cells). In cells transfected with the plasmid containing the hTERT promoter driving the expression of the NAT transgene the specific uptake was higher than that registered in cells transfected with the construct containing the hTR promoter (152728 and 54854 cpm/10⁶ cells respectively). These results reflect the NAT mRNA analysis, indicating that the hTERT promoter displayed a higher activity than the hTR promoter.

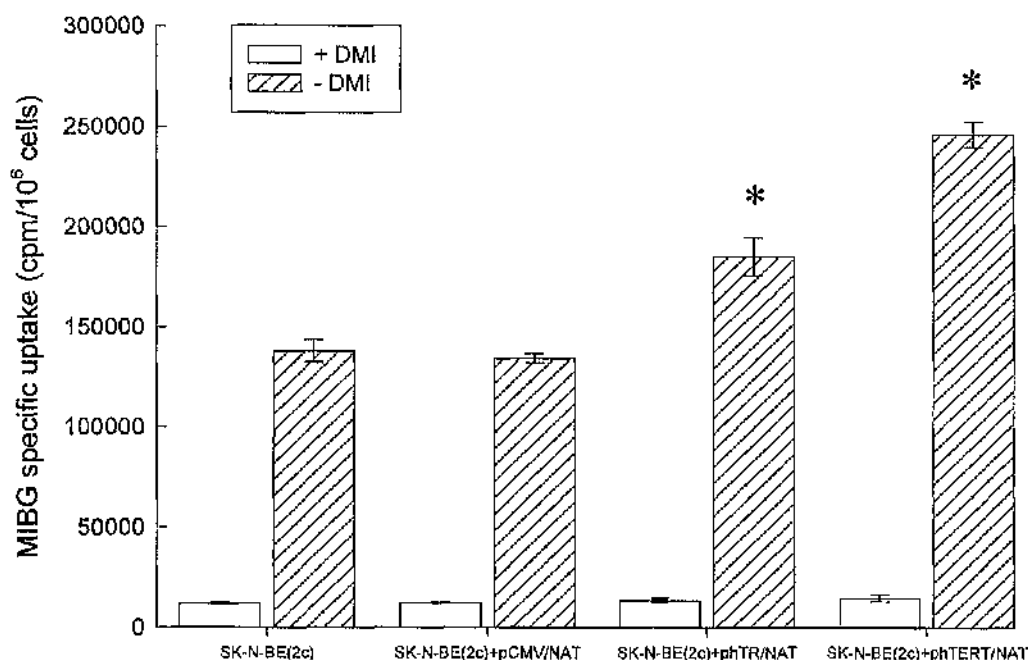


Figure 11. [¹³¹I]MIBG uptake in SK-N-BE(2c) parental and transfectants.

Cells were transfected with the NAT gene, whose expression is driven by (i) the CMV promoter (SK-N-BE(2c)+pCMV/NAT), (ii) the hTR promoter (SK-N-BE(2c)+phTR/NAT) or (iii) the hTERT promoter (SK-N-BE(2c)+phTERT/NAT). Uptake assay was performed in the presence or absence of DMI (desmethylimipramine), a powerful inhibitor of the active uptake mediated by the noradrenaline transporter. Results were expressed as counts per minute (cpm) per 10⁶ cells. Data are means \pm s.d. of three experiments. Results were analysed by Student's t-test. Results showing significant enhancement of uptake ($p < 0.05$) compared to parental SK-N-BE(2c) cells are highlighted (*).

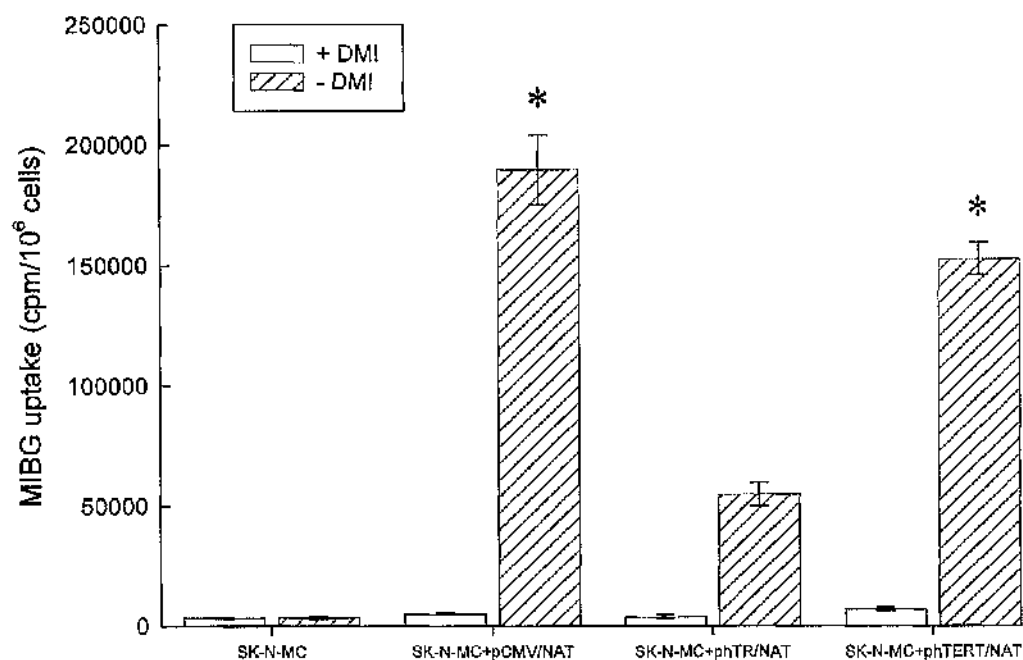


Figure 12. [¹³¹I]MIBG uptake in SK-N-MC parental and transfectants.

Cells were transfected with the NAT gene, whose expression is driven by (i) the CMV promoter (SK-N-MC+pCMV/NAT), (ii) the hTR promoter (SK-N-MC+phTR/NAT) or (iii) the hTERT promoter (SK-N-MC+phTERT/NAT). Uptake assay was performed in the presence or absence of DMI (desmethylimipramine), a powerful inhibitor of the active uptake mediated by the noradrenaline transporter. Results were expressed as counts per minute (cpm) per 10⁶ cells. Data are means ± s.d. of three experiments. Results were analysed by Student's t-test. Results showing significant enhancement of uptake ($p < 0.05$) compared to SK-N-MC+phTR/NAT transfectants are highlighted (*).

2.3.3 Cellular uptake of [²¹¹At]MABG

A comparison of the uptake of [¹³¹I]MIBG with [²¹¹At]MABG was performed in order to assess the cytotoxicity of both ¹³¹I and ²¹¹At. Specific uptake study was conducted using [²¹¹At]MABG in SK-N-BE(2c) (Figure 13), and SK-N-MC cells (Figure 14).

2.3.3.1 [²¹¹At]MABG uptake in SK-N-BE(2c) cells

As shown in Figure 13, the capacity of intracellular concentration of [²¹¹At]MABG was greater in SK-N-BE(2c) cells transfected with phTR/NAT ($p < 0.05$) or phTERT/NAT plasmid ($p < 0.05$) than that in SK-N-BE(2c) parental cells. Similarly to the [¹³¹I]MIBG uptake study (section 2.3.2.1), SK-N-BE(2c) cells transfected with the pCMV/NAT plasmid did not improve their capacity to uptake [²¹¹At]MABG compared to the untransfected ones. These findings show that, in accordance with the [¹³¹I]MIBG uptake study, the hTERT promoter activity was higher than that of the hTR promoter in SK-N-BE(2c) cells.

2.3.3.2 [²¹¹At]MABG uptake in SK-N-MC cells

Whereas in untransfected SK-N-MC cells, negligible levels of [²¹¹At]MABG active uptake were registered, SK-N-MC cells transfected with the pCMV/NAT, phTR/NAT or phTERT/NAT plasmid were all able to actively concentrate [²¹¹At]MABG. In contrast to the SK-N-BE(2c) cells, the highest levels of uptake were registered in cells transfected with the pCMV/NAT plasmid (11196 cpm/10⁶ cells). In cells transfected with the plasmid containing the hTERT promoter driving the expression of the NAT transgene, the specific uptake was higher ($p < 0.05$) than that registered in cells transfected with the construct containing the hTR promoter (5706 and 2745 cpm/10⁶ cells respectively). These results reflect the NAT mRNA analysis, indicating that the hTERT promoter displayed a higher activity than the hTR promoter. These findings indicate that in the SK-N-MC cells, and transfectants, the [²¹¹At]MABG uptake capacity was similar to the uptake of [¹³¹I]MIBG (section 2.3.2.2).

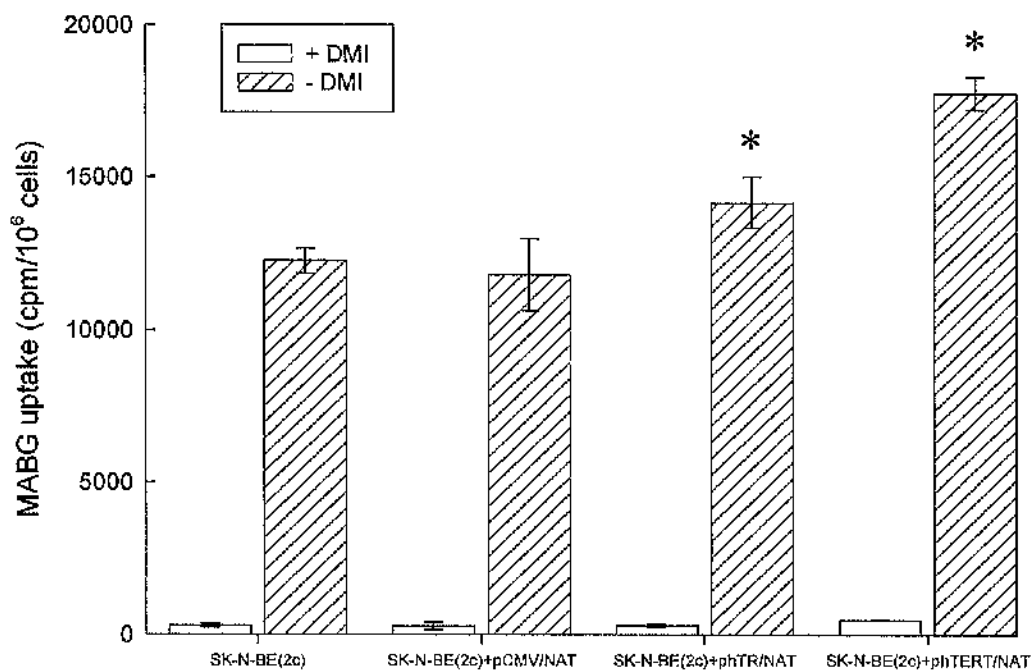


Figure 13. [²¹¹At]MABG uptake in SK-N-BE(2c) parental and transfectants.

Cells were transfected with the NAT gene, whose expression is driven by (i) the CMV promoter (SK-N-BE(2c)+pCMV/NAT), (ii) the hTR promoter (SK-N-BE(2c)+phTR/NAT) or (iii) the hTERT promoter (SK-N-BE(2c)+phTERT/NAT). Uptake assay was performed in the presence or absence of DMI (desmethylimipramine), a powerful inhibitor of the active uptake mediated by the noradrenaline transporter. Results were expressed as counts per minute (cpm) per 10⁶ cells. Data are means \pm s.d. of three experiments. Results were analysed by Student's t-test. Results showing significant enhancement of uptake ($p < 0.05$) compared to parental SK-N-BE(2c) cells are highlighted (*).

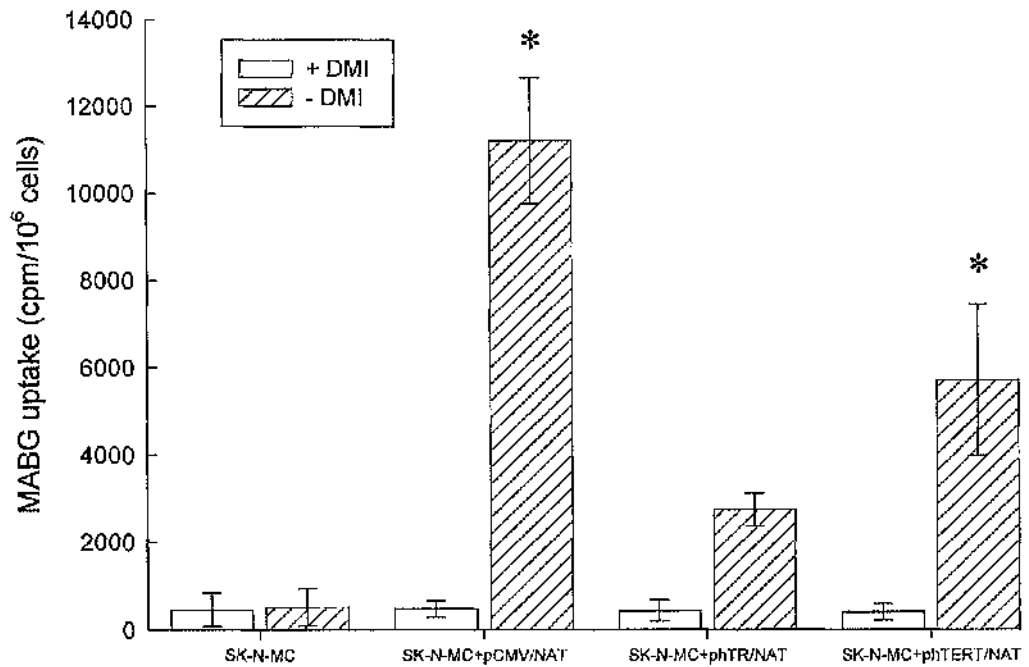


Figure 14. [²¹¹At]MABG uptake in SK-N-MC parental and transfectants. Cells were transfected with the NAT gene, whose expression is driven by (i) the CMV promoter (SK-N-MC+pCMV/NAT), (ii) the hTR promoter (SK-N-MC+phTR/NAT) or (iii) the hTERT promoter (SK-N-MC+phTERT/NAT). Uptake assay was performed in the presence or absence of DMI (desmethylimipramine), a powerful inhibitor of the active uptake mediated by the noradrenaline transporter. Results were expressed as counts per minute (cpm) per 10⁶ cells. Data are means ± s.d. of three experiments. Results showing significant enhancement of uptake ($p < 0.05$) compared to the SK-N-MC+phTR/NAT transfectants are highlighted (*).

2.3.4 Cytotoxicity of [¹³¹I]MIBG

Clonogenic assays were performed to determine whether uptake of [¹³¹I]MIBG translated into dose-dependent cell kill in three-dimensional spheroids composed of parental cells or composed of cells transfected with the transgenic NAT gene driven by the CMV, hTR or hTERT promoters.

2.3.4.1 [¹³¹I]MIBG toxicity in SK-N-BE(2c) cells

As demonstrated in Figure 15, following administration of [¹³¹I]MIBG dose-dependent toxicity was observed in SK-N-BE(2c) cells derived from spheroids and all transfectants. Greater than 98% clonogenic cell kill after treatment with [¹³¹I]MIBG was achieved regardless of the promoter driving NAT expression. Therefore, for comparison of the potency of the promoters the activity concentration required to reduce clonogenic survival to 2% was chosen. The concentrations of [¹³¹I]MIBG required to reduce to 2% the survival of clonogens derived from the spheroids were 1.12 MBq/ml (untransfected cells), 1.45 MBq/ml (cells transfected with the pCMV/NAT plasmid), 0.86 MBq/ml (cells transfected with the pHTR/NAT plasmid) and 0.64 MBq/ml (cells transfected with the pHTERT/NAT plasmid). These results indicated that in this cell line, the [¹³¹I]MIBG toxicity is enhanced by the NAT transgene under the control of the hTR or hTERT promoters, reflecting the [¹³¹I]MIBG uptake capacity (Figure 11). Furthermore, in accordance with the [¹³¹I]MIBG uptake experiments, the greatest cell kill was achieved in SK-N-BE(2c) cells transfected with the NAT transgene controlled by the hTERT promoter. Finally, transfection of SK-N-BE(2c) cells with the pCMV/NAT did not improve [¹³¹I]MIBG toxicity.

2.3.4.2 [¹³¹I]MIBG toxicity in SK-N-MC cells

Untransfected SK-N-MC cells exhibited negligible capacity for active uptake of MIBG. This resulted in absence of toxicity of [¹³¹I]MIBG even at the maximum activity concentration administered. Dose-dependent toxicity was found in SK-N-MC cells transfected with the plasmids containing the NAT transgene under the control of the CMV, hTR or hTERT promoters (Figure 16).

Greater than 60% clonogenic cell kill after treatment with [¹³¹I]MIBG was achieved regardless of the promoter driving NAT expression. Therefore, for comparison of the potency of the promoters the activity concentration required to reduce

clonogenic survival to 40% was chosen. The concentrations of [¹³¹I]MIBG required to reduce to 40% the survival of clonogens derived from the spheroids were 0.5 MBq/ml (cells transfected with the pCMV/NAT plasmid), 2 MBq/ml (cells transfected with the phTR/NAT plasmid) and 1.06 MBq/ml (cells transfected with the phTERT/NAT plasmid). These findings reflected the results generated from the [¹³¹I]MIBG uptake study, suggesting that in SK-N-MC cells the NAT transgene upregulation driven by the hTERT promoter was higher than the upregulation controlled by the hTR promoter.

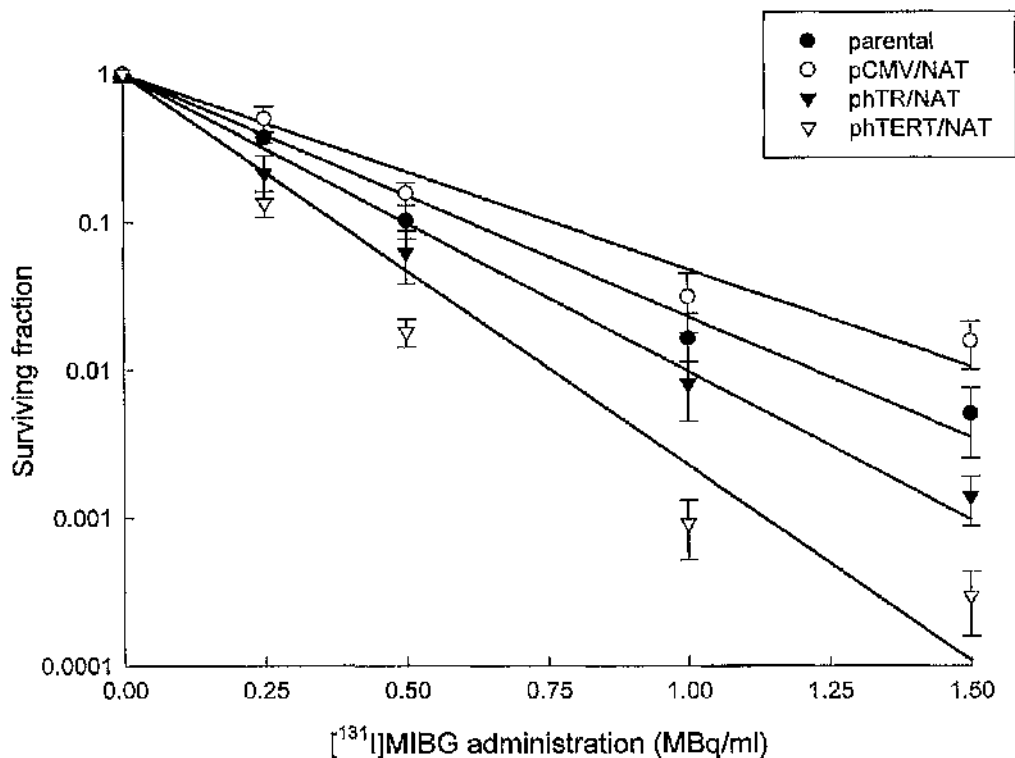


Figure 15. Clonogenic survival curves derived by colony formation for disaggregated spheroids exposed to various doses of [¹³¹I]MIBG.

To establish the [¹³¹I]MIBG dose-dependency of cell kill in spheroids derived from SK-N-BE(2c) parental cells (●) and cells transfected with pCMV/NAT (○), phTR/NAT (▼) or phTERT/NAT (▽) plasmid, 3×10^6 cells were seeded into spinner flasks. After 4 days a range of concentrations of [¹³¹I]MIBG was added (0 – 2 MBq/ml). After 2 hours the cells were washed to remove free [¹³¹I]MIBG and after addition of fresh medium the cells were left for 48 hours before creation of single cell suspensions and seeding in triplicate into 25 mm² flasks at 5×10^3 cells/flask. The cultures were incubated at 37 °C until discrete colonies had formed. The cells were then fixed and stained with Carbol Fuchin (RA Lamb, Middlesex, UK), before counting and calculation of survival fractions. The values are mean surviving fractions with error bars showing standard deviations (n=6). Because a log scale is used on the abscissa, a surviving fraction of for example 0.1 corresponds to 10% clonogenic survival.

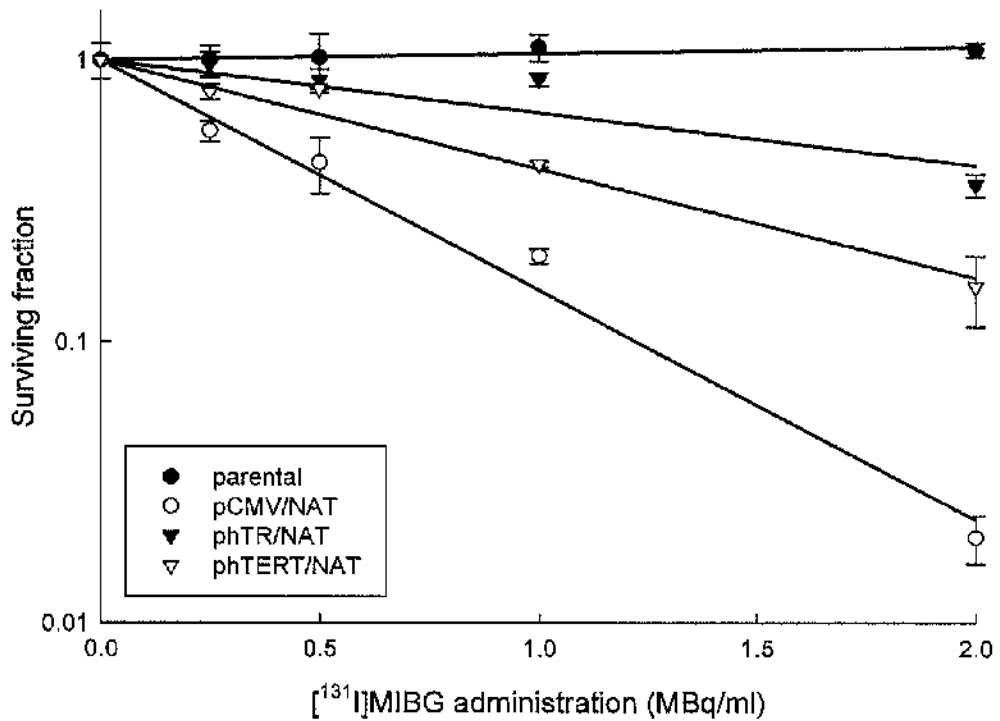


Figure 16. Clonogenic survival curves derived by colony formation for disaggregated spheroids exposed to various doses of [¹³¹I]MIBG.

To establish the [¹³¹I]MIBG dose-dependency of cell kill in spheroids derived from SK-N-MC parental cells (●) and cells transfected with CMV/NAT (○), hTR/NAT (▼) or hTERT/NAT (▽) plasmid, 3×10^6 cells were seeded into spinner flasks. After 4 days a range of concentrations of [¹³¹I]MIBG was added (0 – 2 MBq/ml). After 2 hours the cells were washed to remove free [¹³¹I]MIBG and after addition of fresh medium the cells were left for 48 hours before creation of single cell suspensions and seeding in triplicate into 25 mm² flasks at 5×10^3 cells/flask. The cultures were incubated at 37 °C until discrete colonies had formed. The cells were then fixed and stained with Carbol Fuchin (RA Lamb, Middlesex, UK), before counting and calculation of survival fractions. The values are mean surviving fractions with error bars showing standard deviations (n=6). Because a log scale is used on the abscissa, a surviving fraction of for example 0.1 corresponds to 10% clonogenic survival.

2.3.5 Cytotoxicity of [²¹¹At]MABG

Clonogenic assays were performed to determine whether uptake of [²¹¹At]MABG translated into dose-dependent cell kill in three-dimensional spheroids composed of parental cells or composed of cells transfected with the transgenic NAT gene driven by the CMV, hTR or hTERT promoters.

2.3.5.1 [²¹¹At]MIBG toxicity in SK-N-BE(2c) cells

In order to compare cell kill efficacy using a different radionuclide, spheroids derived from SK-N-BE(2c) parental cells and transfectants were exposed to [²¹¹At]MABG. Dose-dependent toxicity was also observed after treating spheroids with this radiopharmaceutical (Figure 17). Greater than 99% clonogenic cell kill after treatment with [²¹¹At]MABG was achieved regardless of the promoter driving NAT expression. Therefore, for comparison of the potency of the promoters the activity concentration required to reduce clonogenic survival to 1% was chosen. The concentrations of [²¹¹At]MABG required to reduce to 1% the survival of clonogens derived from the spheroids were 13.6 kBq/ml (untransfected cells), 15.4 kBq/ml (cells transfected with the pCMV/NAT plasmid), 10.36 kBq/ml (cells transfected with the pHTR/NAT plasmid) and 8.8 kBq/ml (cells transfected with the pHTERT/NAT plasmid).

Therefore, as observed in cytotoxicity experiments using [¹³¹I]MIBG (Figure 15), the introduction into SK-N-BE(2c) cells of the NAT transgene under the control of the CMV promoter did not improve [²¹¹At]MABG toxicity. Similarly, in SK-N-BE(2c) cells the hTERT promoter was once again more active than the hTR promoter.

2.3.5.2 [²¹¹At]MIBG toxicity in SK-N-MC cells

Untransfected SK-N-MC cells exhibited negligible capacity for active uptake of MABG. This resulted in absence of toxicity of [²¹¹At]MABG to parental cells (Figure 18). Dose-dependent toxicity was found in SK-N-MC cells transfected with the plasmids containing the NAT transgene under the control of the CMV, hTR or hTERT promoters. Greater than 90% clonogenic cell kill was achieved after treatment with [²¹¹At]MABG, regardless of the promoter driving NAT expression. Therefore, for comparison of the potency of the promoters the activity concentration required to reduce clonogenic survival to 10% was chosen. The concentrations of [²¹¹At]MABG required to reduce to 10% the survival of clonogens

derived from the spheroids were 6.2 kBq/ml (cells transfected with the pCMV/NAT plasmid), 13.9 kBq/ml (cells transfected with the phTR/NAT plasmid) and 8 kBq/ml (cells transfected with the phTERT/NAT plasmid), respectively. Therefore, the [²¹¹At]MABG toxicity is improved when SK-N-MC cells are transfected with the NAT transgene controlled by either the hTR or hTERT promoter. As seen in [¹³¹I]MIBG toxicity studies (Figure 16), the most active of the two telomerase promoters investigated in this study was the hTERT promoter. Furthermore, unlike the findings from [¹³¹I]MIBG toxicity experiments, cells transfected with the CMV promoter upstream the NAT transgene displayed sensitivity to [²¹¹At]MABG comparable to that of cells with the plasmid containing the hTERT promoter driving the NAT transgene.

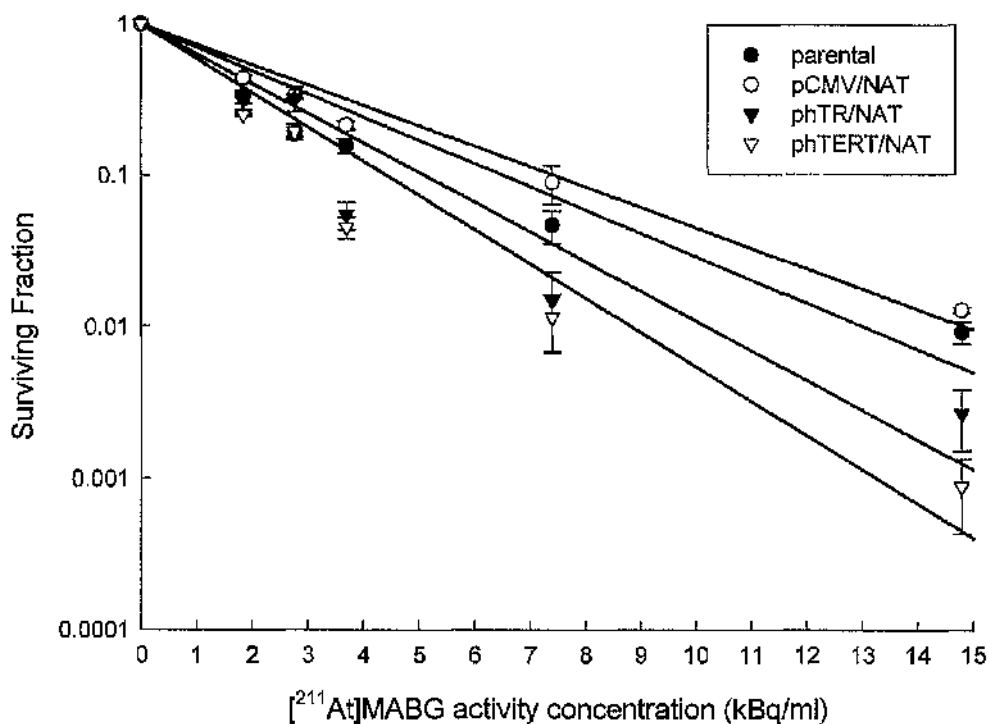


Figure 17. Clonogenic survival curves derived by colony formation for disaggregated spheroids exposed to various doses of [²¹¹At]MABG.

To establish the [²¹¹At]MABG dose-dependency of cell kill in spheroids derived from SK-N-BE(2c) parental cells (●) and cells transfected with pCMV/NAT (○), phTR/NAT (▼) or phTERT/NAT (▽) plasmid, 3×10^6 cells were seeded into spinner flasks. After 4 days a range of concentrations of [²¹¹At]MABG was added (0 – 14.8 kBq/ml). After 2 hours the cells were washed to remove free [²¹¹At]MABG and after addition of fresh medium the cells were left for 48 hours before creation of single cell suspensions and seeding in triplicate into 25 mm² flasks at 5×10^3 cells/flask. The cultures were incubated at 37 °C until discrete colonies had formed. The cells were then fixed and stained with Carboi Fuchin (RA Lamb, Middlesex, UK), before counting and calculation of survival fractions. The values are mean surviving fractions with error bars showing standard deviations (n=6). Because a log scale is used on the abscissa, a surviving fraction of for example 0.1 corresponds to 10% clonogenic survival.

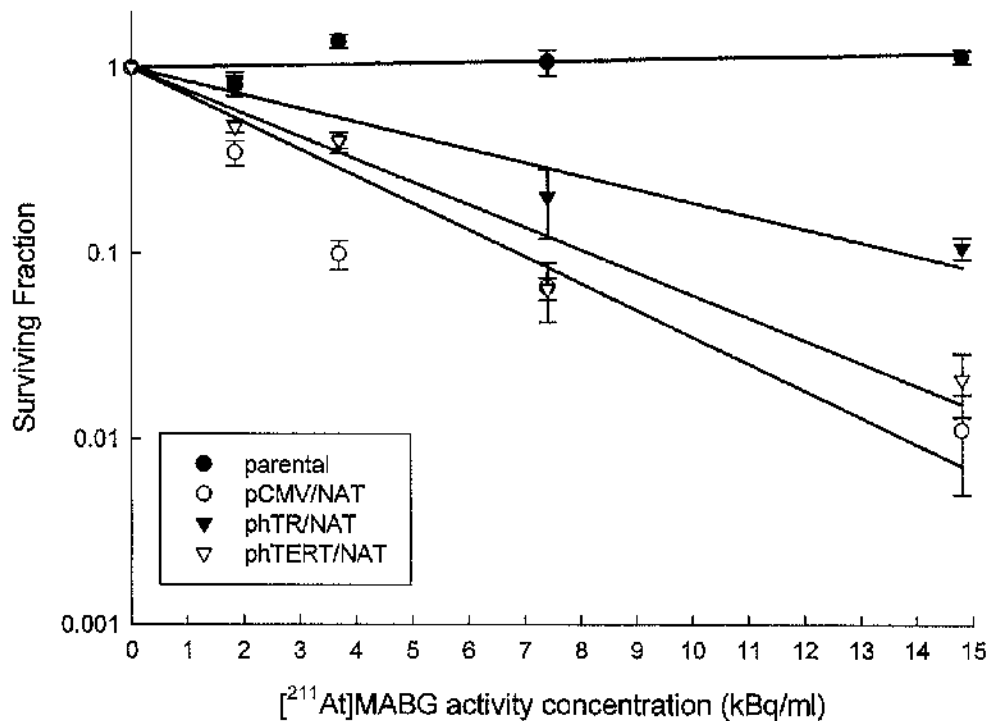


Figure 18. Clonogenic survival curves derived by colony formation for disaggregated spheroids exposed to various doses of [²¹¹At]MABG.

To establish the [²¹¹At]MABG dose-dependency of cell kill in spheroids derived from SK-N-MC parental cells (●) and cells transfected with CMV/NAT (○), hTR/NAT (▼) or hTERT/NAT (▽) plasmid, 3×10^5 cells were seeded into spinner flasks. After 4 days a range of concentrations of [²¹¹At]MABG was added (0 – 14.8 kBq/ml). After 2 hours the cells were washed to remove free [²¹¹At]MABG and after addition of fresh medium the cells were left for 48 hours before creation of single cell suspensions and seeding in triplicate into 25 mm² flasks at 5×10^3 cells/flask. The cultures were incubated at 37 °C until discrete colonies had formed. The cells were then fixed and stained with Carbol Fuchsin (RA Lamb, Middlesex, UK), before counting and calculation of survival fractions. The values are mean surviving fractions with error bars showing standard deviations (n=6). Because a log scale is used on the abscissa, a surviving fraction of for example 0.1 corresponds to 10% clonogenic survival.

2.3.6 Summary of results

Both telomerase promoters (hTR and hTERT) had the capacity to drive the expression of the NAT transgene. Further, this resulted in increase of the [¹³¹I]MIBG and [²¹¹At]MABG toxicity to the transfected cells compared to that of untransfected cells, in both SK-N-BE(2c) and SK-N-MC cell lines. The hTERT promoter demonstrated the greatest activity in both cell lines, for both [¹³¹I]MIBG and [²¹¹At]MABG treatments.

According to qPCR analysis, in SK-N-BE(2c) cells the ubiquitous CMV promoter did not drive the expression of the NAT transgene. These findings were reflected in the uptake assay (Figure 11 and Figure 13) and cell kill study (Figure 15 and Figure 17), where the SK-N-BE(2c) cells transfected with the pCMV/NAT plasmid did not display improved uptake capacity nor enhanced sensitivity to [¹³¹I]MIBG and [²¹¹At]MABG treatments.

2.4 Discussion

These in vitro results show that the amalgamation of NAT gene transfer with [¹³¹I]MIBG therapy is a promising tumour-specific approach for neuroblastoma treatment. Recent experimental data, in accordance with this study, indicate promise for cancer treatment by [¹³¹I]MIBG therapy/gene therapy combinations [133, 187, 188, 192].

For this gene transfer/targeted radiotherapy combination, a tumour-specific promoter, such as telomerase [133, 177] was chosen to drive the NAT transgene expression exclusively into tumour cells. Telomerase, a ribonucleoprotein, belongs to the reverse transcriptase class of enzymes. It stabilises the length of the 3' (lagging) end of chromosomes. Up-regulation of telomerase activity is an important factor in the immortality of cancer cells [196, 197]. Whilst some non-cancerous tissue, such as male germ cells, lymphocytes and some stem cell populations express telomerase, there is a clear differential in expression levels between neuroblastomas and normal tissue [177, 196, 198].

The present study aimed to determine the optimal conditions for the NAT gene transfer [¹³¹I]MIBG or [²¹¹At]MABG strategy with respect to promoter control of the transgene. For the first time, it was shown that the promoters of both hTR and hTERT genes are suitable for controlling the expression of the NAT transgene in neuroblastoma cells. Quantitative PCR, [¹³¹I]MIBG or [²¹¹At]MABG uptake and cell kill assays all demonstrated that telomerase promoters are able to drive the expression of the NAT transgene which is translated into active transporter and rendered the host cells more susceptible to [¹³¹I]MIBG or [²¹¹At]MABG treatment. This strategy was successful not only in SK-N-MC cells which normally do not present detectable level of NAT [98], but also in SK-N-BE(2c) cells which already express high level of endogenous NAT [98].

In the latter cell line, transfections performed with the pCMV/NAT plasmid did not produce cells expressing the transgenic bNAT (see Figure 9), probably due to the CMV promoter inactivation via DNA methylation. As mentioned in section 2.3.2.1, several lines of evidence suggest that the CMV promoter can be silenced by DNA methylation in human tumour cells [194, 195] and zebrafish embryos [193]. Interestingly, the CMV promoter can be reactivated in glioma cells U87 by administration of the 5'-aza-2'-deoxycytidine [194], a DNA methyltransferase inhibitor, shown to reverse methylation and cause reexpression of silenced genes

[199]. In order to optimise experimental settings, it would be important to further investigate this phenomenon in SK-N-BE(2) cells.

In this study it emerged that the hTERT promoter exhibited higher activity than the hTR promoter, suggesting that the hTERT promoter could be the control element of choice for the NAT expression in pre-clinical investigations.

Considering the findings regarding the SK-N-MC cell line, the introduction of the NAT transgene under the control of either the hTR or hTERT promoter dramatically improved [^{131}I]MIBG and [^{211}At]MABG toxicity. Based on these results, this approach could be applied to neuroblastomas that do not accumulate actively the radiopharmaceutical and therefore are not eligible for targeted radiotherapy. Further, it is likely that this approach is also beneficial to tumours that display heterogeneous MIBG uptake within the mass, where targeted radiotherapy alone is unlikely to cure disease [3].

In the present study, an alternative radionuclide, ^{211}At , was used in the benzylguanidine preparation ([^{211}At]MABG) and its toxicity was evaluated in comparison with the ^{131}I preparation. For the MIBG targeted radiotherapy of neuroectodermal tumours, the radionuclide conventionally used is ^{131}I . However, tumours of under millimetre dimensions are suboptimal targets for treatment with ^{131}I β -particles whose mean range is about 800 μm [200]. In addition to underdosing of small tumour deposits, long range β -emissions may damage surrounding normal tissues [11, 201, 202]. Due to their short path length, radionuclides that decay by the emission of α -particles, such as the heavy halogen ^{211}At , offer the possibility of combining cell-specific molecular targeting with radiation having a range in tissue of only 50 to 80 μm [203, 204]. Moreover, α -particles are much more radiotoxic than β -emitting radionuclides, as demonstrated in this study (Figure 13 and Figure 14), and their cytotoxic efficiency is independent of cell cycle status and oxygen concentration. Recently, clinical trials involving anti-tumour antibodies labelled with α -particle-emitting radionuclides have commenced [204, 205].

The combination of β - and α -emitters, in the form of [^{131}I]MIBG and [^{211}At]metastatobenzylguanidine ([^{211}At]MABG), could be an option for the treatment of neuroblastomas, further increasing the efficiency and specificity of this targeted radiotherapy strategy.

Clonogenic assays were performed in three-dimensional spheroids rather than monolayers. Previously it has been shown that greater cell kill was achieved, for the same dose of [¹³¹I]MIBG, in three-dimensional spheroids compared to monolayers, demonstrating the existence of collateral cell kill [179, 187]. This is fundamental for the success of gene therapy, since gene transfer is an inefficient process. In particular, gene transfer cannot reach 100% efficiency using existing techniques [3, 188, 192]. Therefore the mechanism of induction of radiation-induced bystander effects must be delineated in order to maximise the efficacy of gene therapy combined with targeted radionuclide treatment [2, 192, 206]. Two types of bystander effect have been identified (see sections 1.1.1 and 5.4 for details): namely a physical effect in the form of decay particle, crossfire irradiation from targeted cells to neighbouring, untargeted cells, observed mainly in conjunction with low linear energy transfer (LET) β - and γ -emitters; and transmissible biological effects resulting from the radiation insult. The latter phenomenon is more pronounced following high LET radiation [13, 207, 208]. This new treatment strategy, using a novel gene therapy approach in combination with a well-established treatment option for neuroblastoma (targeted radiotherapy) might render radiation treatment more effective and more readily tolerated. The large differential in telomerase expression between normal tissue and tumour, and the radiosensitivity of neuroblastoma make this type of cancer an attractive candidate for the therapeutic scheme proposed in the present study.

Chapter 3

Analysis of WAF1 promoter activation after exposing neuroblastoma cells to [¹³¹I]MIBG or [²¹¹At]MABG

3.1 Introduction

The combination of targeted radiotherapy with gene therapy appears to be a promising approach to improve the therapeutic ratio of cancer therapy. However, the main limitation of gene therapy strategies is lack of target specificity. Novel approaches to circumvent this issue have been devised. In chapter 2, both telomerase promoters (hTR and hTERT) were studied as tumour-specific driving elements of the noradrenaline transporter gene expression in neuroblastoma cells. Alternatively, inducible promoters can be employed to control gene expression transcriptionally.

3.1.1 Radiation-inducible promoters

Genes that are activated in response to ionising radiation, have recently attracted interest in cancer gene therapy. This is because their promoter regions can be utilised to drive transcription of transgenes in response to radiation. This allows the regulation of the expression of the therapeutic gene spatially and temporally by ionising radiation [209]. The use of such a control element to drive the expression of noradrenaline transporter (NAT) transgene would be of great benefit for targeted radiotherapy of neuroblastoma. It would be possible to enhance NAT transgene expression specifically in cells targeted by radiopharmaceuticals, such as [¹³¹I]MIBG or [²¹¹At]MABG. This would then lead to a higher capacity of targeted neuroblastoma cells to accumulate [¹³¹I]MIBG or [²¹¹At]MABG, resulting in a greater toxicity of the radiopharmaceuticals. Thanks to this radionuclide-inducible system, it would be possible to minimise expression of the NAT transgene in normal cells, which are not targeted by the drug.

Several studies have investigated the potential of radio-inducible promoters such as the early growth response gene 1 (Egr-1) [210]. The promoter region contains a consensus sequence CC(A/T)₆GG, called "CArG" box, the radiation-inducible element [211], targeted by reactive oxygen intermediates [212]. The Egr-1 promoter has been used successfully in several suicide gene therapy strategies [213-217]. However, all these studies were based on the use of external beam ionising radiation rather than radiopharmaceuticals. To date, only one report [218] showed Egr-1 promoter activation in rat intracerebral glioma, after treatment with the thymidine analogue 5-iodo-2'-deoxyuridine radiolabelled with the Auger electron emitter iodine-125 ([¹²⁵I]IdUrd). However, no further investigation

concerning clinically relevant radioactivity concentrations or therapeutic effect of the radiopharmaceutical in this system has followed this study.

In this approach, the reporter gene expression was detectable in non-irradiated cells, which might limit the use of the Egr-1 promoter in combination with cytotoxic agents [219]. Non-controlled expression of the therapeutic gene could generate unwanted damage to non-target cells, therefore it is essential that the non-specific promoter activity is minimised.

An interesting gene therapy approach employed the radiation-induced promoter of the bacterial RecA gene. Significant increase in TNF α secretion was seen after a radiation dose of 2Gy in the anaerobic apathogenic bacterium, *Clostridium*, containing the RecA promoter upstream the TNF α gene [220].

Finally, significant cell kill resulted after 2Gy irradiation of A549 cells, transfected with four tandem repeats of the NF- κ B binding site of the c-IAP2 gene driving the expression of the suicide gene BAX [221].

Although promising, the studies regarding the RecA and c-IAP2 promoters did not involve targeted radiotherapy.

3.1.2 Radiation-inducible WAF1 promoter

Our study has focused on the evaluation of the promoter for the gene p21 or "wild-type p53-activated fragment 1" (WAF1). WAF1 is a well-characterised cyclin-dependent kinase (CDK) inhibitor that belongs to the Cip/Kip family of CDK inhibitors [222]. Its main activity is inhibition of the cyclin/cdk2 complexes and cell cycle progression [223]. The gene WAF1 was first cloned and characterised as an important mediator, acting as inhibitor of the cyclin-dependent kinase activity in p53-dependent cell cycle arrest induced by DNA damaging agents doxorubicin [224] and γ -rays [134].

3.1.2.1 WAF1 promoter induction by external beam radiotherapy

Many studies show that the WAF1 promoter is radiation-inducible and its activation is also increased in tumour cells [225-232]. In addition, activity appears to be independent of p53 status in a wide range of tumour types [230, 233, 234]. Furthermore, there is evidence indicating that the WAF1 promoter is activated *in vitro* in cells exposed to hypoxia [235]. This promoter therefore displays three potential levels of specificity: tumour, radiation and hypoxia specificity. These characteristics make the WAF1 promoter an attractive tool for radiation-controlled expression of transgenes such as the NAT gene.

In the attempt to combine gene therapy with radiotherapy, the potential of the use of the WAF1 promoter, as a radio-inducible control element of therapeutic transgenes, was recently investigated [135, 235, 236]. Worthington and colleagues [135] initially evaluated the induction of the WAF1 promoter activity by γ -radiation treatment of endothelial cells or rat tail artery, transfected with the WAF1 promoter controlling the green fluorescent protein (GFP) expression. In endothelial cells exposed to 4Gy ionising radiation, the levels of the GFP protein were 9.6 times higher than that in unirradiated cells. Subsequently, in the rat-tail vein exposed to 4 and 6Gy ionising radiation a 4.5- and 8-fold induction of the GFP protein was shown, respectively.

These findings indicate that γ -rays application, via the radiation-inducible WAF1 promoter, can control the expression of a transgene in endothelial cells.

Furthermore, in the same report, a construct containing the nitric oxide synthase (iNOS) gene downstream of the WAF1 promoter was transfected into endothelial cells. After exposure to a dose of 4Gy external beam radiation, an impressive 9.5-

fold induction of the iNOS protein expression was achieved [135]. Interestingly, this system was shown to generate significant relaxation of arterial segments, indicating the potential to induce physiological effects using an γ -ray-inducible promoter in combination with ionising radiation [135]. Additional studies showed that WAF1 promoter-controlled expression of iNOS resulted in an increase in sensitivity to subsequent radiation therapy in both a murine fibrosarcoma and the human colon HT29 xenograft [235, 236].

It is clear, from the aforementioned studies, that the induction of the WAF1 promoter activity by conventional γ -radiation is feasible and well documented in both endothelial cells and tumour cells.

3.1.2.2 WAF1 promoter induction by targeted radiotherapy

To date, there is no report regarding the use of targeted radiotherapy agents to activate the WAF1 promoter in cancer cell lines. Furthermore, the use of such promoters to drive therapeutically relevant transgenes would be of great advantage in cancer treatment regimes, where the use of radiopharmaceuticals is an important tool of therapy and / or tumour imaging. It could then be possible to induce the expression of a therapeutic transgene, via WAF1 promoter control, exclusively in cells that are targeted by the radiopharmaceutical. In this way, the use of targeted radiotherapy agents could achieve activation of the WAF1 promoter, and in turn overexpression of the transgene, exclusively in targeted cells, without affecting non-targeted cells. This level of specificity can not be achieved with conventional external beam radiotherapy.

Based on this hypothesis, the present study will investigate the feasibility of using the radiolabelled agents [^{131}I]MIBG and [^{211}At]MABG in order to enhance the expression of GFP marker gene controlled by the radiation-inducible WAF1 promoter.

Two radiation types, specifically β -particle emissions (generated by [^{131}I]MIBG) and α -particles emissions (generated by [^{211}At]MABG), will be assessed for their efficacy in WAF1 promoter activation, and they will be compared with external beam radiation, in the form of γ -rays.

3.1.2.2.1 Estimation of radiation dose delivered by radiopharmaceuticals

Radiation dose estimation is required to determine the effectiveness of targeted radionuclide therapy. Dosimetry is generally performed to establish a correlation

between the quantity of radiation delivered to a target and the biological damage observed, or that can be reliably predicted [237]. This information is also needed to optimise the choice of treatment modalities and predict the resulting biological effect determining the degree of therapeutic efficacy. Moreover, an objective dosimetry is required in order to compare different radiotherapy regimes (i.e. targeted radiotherapy) and relate them to classical treatments (conventional external beam radiation), for which radiobiological knowledge is well-established and clinical experience extensive.

Therefore, estimation of the radiation dose of radioactivity delivered by a radiopharmaceutical that generates a quantifiable biological effect is necessary.

In this study, the radiation doses corresponding to the [^{131}I]MIBG and [^{211}At]MABG activity concentrations that activate the WAF1 promoter will be estimated in neuroblastoma cells. The levels of WAF1 promoter activation will be quantified by measuring the fluorescence intensity of the GFP, the DNA of which is inserted downstream of the WAF1 promoter.

3.1.2.2.2 WAF1 promoter driving the noradrenaline transporter transgene expression

The use of a transgenic construct containing the WAF1 promoter upstream of the NAT transgene could upregulate the synthesis of NAT in neuroblastoma cells in response to ionising radiation. Based on previous reports [98, 187, 188], it is expected that this will lead to a greater capacity of cellular uptake of [^{131}I]MIBG or [^{211}At]MABG and therefore to a higher toxicity of the radiolabelled compounds.

Assessment of the WAF1 promoter activation and dosimetry of each radiolabelled agent will produce valuable information. This could optimise experimental parameters and procedures that will be used to better investigate the NAT transgene overexpression controlled by the WAF1 promoter in neuroblastoma cells. This strategy involves introduction of the NAT transgene (driven by the WAF1 promoter) into neuroblastoma cells, followed by an initial dose of radiation in the form of [^{131}I]MIBG or [^{211}At]MABG (which is concentrated preferentially by neuroblastoma cells) (Figure 19). As mentioned above, this will facilitate the tumour-specific overexpression of transgenic NAT. A second administration of [^{131}I]MIBG or [^{211}At]MABG, should be more avidly concentrated by target tumour cells, leading to their sterilisation. The use of radioisotopes conjugated to a

tumour-seeking agent such as benzylguanidine is an attractive option for the induction of the WAF1 promoter. If the WAF1 promoter activation via [^{131}I]MIBG or [^{211}At]MABG radiation is confirmed in neuroblastoma cells, the application of this strategy in the clinic could circumvent the limitations of external beam radiotherapy minimising toxicity to normal tissue.

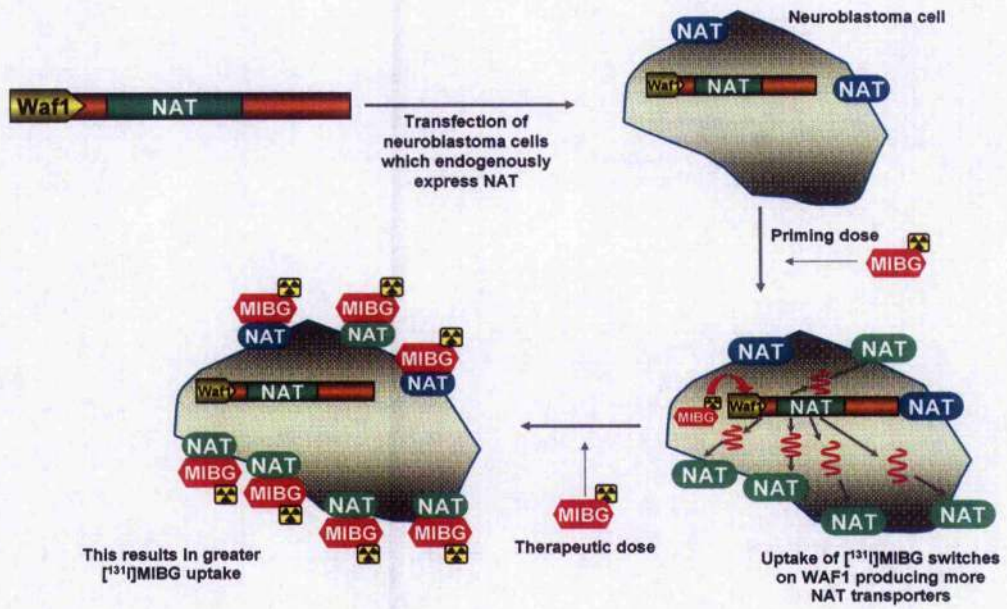


Figure 19. Proposed radiation-induction scheme to increase the expression of the noradrenaline transporter (NAT) in neuroblastoma cells. By placing the NAT transgene under the control of the radiation-inducible WAF1 promoter, administration of radioactivity in the form of $[^{131}\text{I}]\text{MIBG}$ (priming dose) (concentrated preferentially by neuroblastoma cells) will potentially facilitate the tumour-specific overexpression of NAT, thereby enabling increased uptake of a second dose of $[^{131}\text{I}]\text{MIBG}$ (therapeutic dose).

3.2 *Material and Methods*

3.2.1 Cell culture

The neuroblastoma cell line SH-SY5Y [185, 238] was obtained from ECACC (Salisbury, Wiltshire, UK). SK-N-BE(2c) cells were also employed (see section 2.2.2). Both neuroblastoma cell lines have the capacity for uptake of MIBG [100, 186]. The colon tumour cell line HCT116 were obtained from American Type Culture Collection (Rockville, MD) and HCT116 cells carrying a targeted knock out for the genes p53 (HCT116 p53 -/-) [239] were kindly donated by Dr. Jane Plumb (Centre of Oncology and Applied Pharmacology, Glasgow, UK). The non-NAT expressing human glioma cell line UVW [187, 188] was chosen for comparative studies. Cells were maintained in the logarithmic phase of growth at 37°C in 75cm² plastic culture flasks (Corning Inc., Corning, NY) in a 5% CO₂ - 95% air humidified incubator. Cells were subcultured in RPMI-1640 medium supplemented with 10% heat inactivated foetal bovine serum (FBS), 50IU/ml sodium penicillin G, 50mg/ml streptomycin sulphate, and 2mM L-glutamine. Medium and supplements were purchased from Gibco (Paisley, UK).

3.2.2 Synthesis of [¹³¹I]meta-iodobenzylguanidine and [²¹¹At]meta-astatobenzylguanidine

No-carrier-added [¹³¹I]MIBG and [²¹¹At]MABG were prepared as described in section 2.2.1.

3.2.3 Plasmids

The WAF1 promoter, inserted into the XhoI site of the pEGFP-1 reporter vector (BD Biosciences Clontech, Palo Alto, CA), was kindly provided by J Worthington (School of Biomedical Sciences, University of Ulster, UK). For the present study, the plasmid containing the WAF1 promoter controlling the transcription of the GFP marker gene will be referred to as pWAF1/GFP plasmid.

In a second vector, based on pEGFP-1 (BD Biosciences Clontech, Palo Alto, CA), the GFP cDNA was removed, and bNAT cDNA inserted into Hind III/Not I sites. The WAF-1 promoter DNA fragment was then inserted into Eco47 III / Kpn I site.

The construct containing the WAF1 promoter controlling the transcription of the NAT transgene will be referred to as pWAF1/NAT plasmid.

Plasmid purifications were carried out using Plasmid Maxi Kit (Qiagen, Germany), according to the manufacturer instructions.

3.2.4 In vitro transfections

SH-SY5Y, SK-N-BE(2c), HCT116 and U2OS cells were transfected with the pWAF1/GFP or the pWAF1/NAT plasmids using Lipofectamine™ 2000 (Invitrogen, Paisley, UK), as described in section 2.2.4.

3.2.5 TaqMan® Real Time-Polymerase Chain Reaction (PCR) for hNAT and bNAT transcripts

Isolation of total RNA was performed using RNeasy Mini Kit (Qiagen, Germany) according to manufacturer's instructions. See Section 2.2.4 for details on real-time PCR conditions specific for hNAT and bNAT mRNAs.

3.2.6 FACS analysis of GFP expression in neuroblastoma cells

Cells stably transfected with the pWAF1/GFP plasmid were seeded at a concentration of 1.5×10^5 cells / well in six-well plates. Two days later the cells received treatment (0 – 10Gy external beam, 0 – 2MBq/ml [131 I]MIBG or 0 – 29.6kBq/ml [211 At]MABG). At each time point cells were washed twice with PBS, harvested and resuspended in 500 μ l of PBS-1%FBS. Each sample was thereafter analysed on a Becton Dickinson FACScan flow cytometer with an excitation wavelength of 488nm and FITC collection wavelength using a band-pass filter at 530 ± 15 nm, which registers the fluorescence intensity of the GFP protein in each event (cell). Dead cells were gated out of the analysed cohort by forward and side scatter. The level of GFP fluorescence in live cells was determined using the Becton Dickinson CellQuest program. Briefly, the distribution of GFP fluorescence in the cell population was plotted against the cell number on a 4-log linear scale. For each sample, 10,000 events (cells) were analysed. Data were expressed as the ratio of mean fluorescence intensity of treated cells compared to the basal level of control (untreated cells stably transfected with the pWAF1/GFP plasmid).

3.2.7 Western Blotting analysis

Cells stably transfected with the pWAF1/GFP plasmid were seeded at a concentration of 1.5×10^5 cells / well in six-well plates. Two days later the cells received treatment (0 – 10Gy external beam, 0 – 2MBq/ml [131 I]MIBG or 0 – 29.6kBq/ml [211 At]MABG). At each time point, samples for protein analysis were extracted by lysing cells with Laemmli buffer (Sigma). Protein concentration was quantified with the use of the BioRad protein assay (BioRad, Munich, Germany), according to the manufacturer instructions. A total protein quantity of 15 μ g of each sample was electrophoresed through a polyacrylamide gel (NuPAGE BIS-TRIS gel, Invitrogen, UK), and then transferred to polyvinylidene fluoride (PVDF) membrane at 125mA for 45min. (Immobilon-P, Millipore, UK). The PVDF

membranes were incubated for 2 hours at room temperature in blocking solution (5% non-fat milk in TBS-Tween buffer (25mM Tris-HCl, pH 7.5, 0.8% NaCl, 0.02% KCl, 0.05% Tween-20). The nitrocellulose membranes were then probed in blocking solution for 2 hours with a mouse monoclonal anti-GFP antibody (diluted 1:10000) (BD Biosciences Clontech, Palo Alto, CA) and a rabbit polyclonal anti-GAPDH (diluted 1:2000) (abcam, Cambridge, UK), for loading control. Peroxidase-conjugated goat anti-mouse (diluted 1:2000) and anti-rabbit (diluted 1:5000) antibodies (DAKO, Denmark) were used as secondary antibodies. Immune complexes (i.e., proteins of interest) were visualized with the use of an enhanced chemiluminescence system (ECL Detection Reagent Amersham Pharmacia Biotech, UK), following the instructions provided by the manufacturer. The relative amount of transferable GFP protein in a given sample was quantified by densitometry of X-ray films and normalised by the intensity of each band corresponding to the GAPDH protein. Results presented are from two independent experiments each performed in triplicate wells. The band intensity level determination was performed by TotalLab software (Nonlinear Dynamics, Newcastle upon Tyne, UK).

3.2.8 [¹³¹I]MIBG uptake studies

SK-N-BE(2c) parental and transfected cells (with the plasmid pWAF1/GFP), SH-SY5Y parental cells and transfectants (with the plasmids pWAF1/GFP or pWAF1/NAT) and UVW parental and transfected cells (with the plasmid pWAF1/NAT) were seeded in six-well plates at initial density of 5×10^4 cells per well and cultured for 48 hours. MIBG incorporation was measured by incubating the cells for 2 hours with 7kBq/ml of [¹³¹I]MIBG of specific activity 45-65MBq/mg, (Dupont Radiopharmaceuticals, Hertfordshire, UK). Non-specific uptake was measured in the presence of 1.5mM desmethylimipramine (DMI) (Sigma, UK). After incubation, medium was removed and the cells were washed with PBS. Radioactivity was extracted using two aliquots of 10% (w/v) trichloroacetic acid. The activities of the extracts were then measured in a gamma-well counter (Cobra II, PerkinElmer, MA). Uptake was expressed as cpm (counts per minute) per 10^6 cells.

For experiments using the pWAF1/NAT plasmid, SH-SY5Y and UVW cells were pre-exposed to 0 - 8Gy from a ⁶⁰Co source. After 2 days (time necessary for optimal WAF1 promoter activation, determined in the experiments regarding pWAF1/GFP transfectants, see section 3.3.2), [¹³¹I]MIBG uptake assay was performed as described above.

3.2.9 Clonogenic assay for neuroblastoma cells treated with external beam ionising radiation, [¹³¹I]MIBG or [²¹¹At]MABG

SK-N-BE(2c) cells transfected with the plasmid pWAF1/GFP, SH-SY5Y transfectants (with the plasmid pWAF1/GFP or pWAF1/NAT), and UVW cells transfected with the pWAF1/NAT construct were seeded in 25cm² flasks at 0.5×10^5 per flask. After 2 days, when the cultures were 70% confluent, medium was removed and replaced with fresh medium.

Cells transfected with the pWAF1/GFP construct were exposed to 0 - 2MBq/ml [¹³¹I]MIBG, 0 - 29.4kBq/ml [²¹¹At]MABG or to 0 - 10Gy external beam radiation from a ⁶⁰Co source.

For experiments using the pWAF1/NAT plasmid, SH-SY5Y cells were pre-exposed to 0 - 8Gy and UVW cells to 0 - 6Gy ionising radiation, from a ⁶⁰Co source. After 2 days (time necessary for optimal WAF1 promoter activation, determined in the experiments regarding pWAF1/GFP transfectants, see section 3.3.2), cells were

treated with 0 – 1MBq/ml (SH-SY5Y cells) or 0 – 8MBq/ml (UVW cells) [¹³¹I]MIBG. Cells were incubated with [¹³¹I]MIBG for 2 hours, after which uptake is maximal [240]. After treatment, medium was removed and the cells were washed thrice with PBS, suspended by treatment with trypsin and counted using a haemocytometer. For every treatment, 1×10^3 cells were seeded, in triplicate, in 25cm² flasks (Nunclon Plastics, Roskilde, Denmark) in 10ml fresh medium. The cultures were then incubated at 37°C in 5% CO₂. After 10 to 14 days, medium was removed and the colonies were fixed and stained with carbol fuchsin (R.A. Lamb, Middlesex, United Kingdom), before counting and calculation of surviving fractions. Results were expressed as a percentage of the initial concentration of cells plated, known as the plating efficiency. The cytotoxic potency of the radiopharmaceutical was determined by comparing the number of colonies formed by treated cells to the number of colonies formed by untreated control (the surviving fraction, or SF). For each transfectant, experiments were performed three times, in triplicate.

3.2.10 Statistical analysis

Results are expressed as mean \pm standard deviation (s.d.). All data are from at least three independent experiments. Data were analysed by Student's *t*-test or ANOVA test (with Bonferroni correction) using SPSS software, version 13 (IL). A *p* value of less than 0.05 was considered statistically significant.

3.3 Results

3.3.1 Cellular uptake of [¹³¹I]MIBG and [²¹¹At]MABG

The activity of the noradrenaline transporter was assessed by [¹³¹I]MIBG (Figure 20) and [²¹¹At]MABG (Figure 21) uptake assay in SK-N-BE(2c) and SH-SY5Y cells transfected with the pWAF1/GFP plasmid, and was compared with that in parental SK-N-BE(2c) and SH-SY5Y cells. No difference in [¹³¹I]MIBG uptake capacity was detected between the parental and the transfected (with the pWAF1/GFP plasmid) SK-N-BE(2c) cells. Similarly, SH-SY5Y cells showed a capacity to accumulate [¹³¹I]MIBG comparable to that showed by SH-SY5Y cells transfected with the pWAF1/GFP plasmid.

These results indicates that the transfection of the pWAF1/GFP plasmid in SK-N-BE(2c) and SH-SY5Y cells did not alter the activity of the noradrenaline transporter.

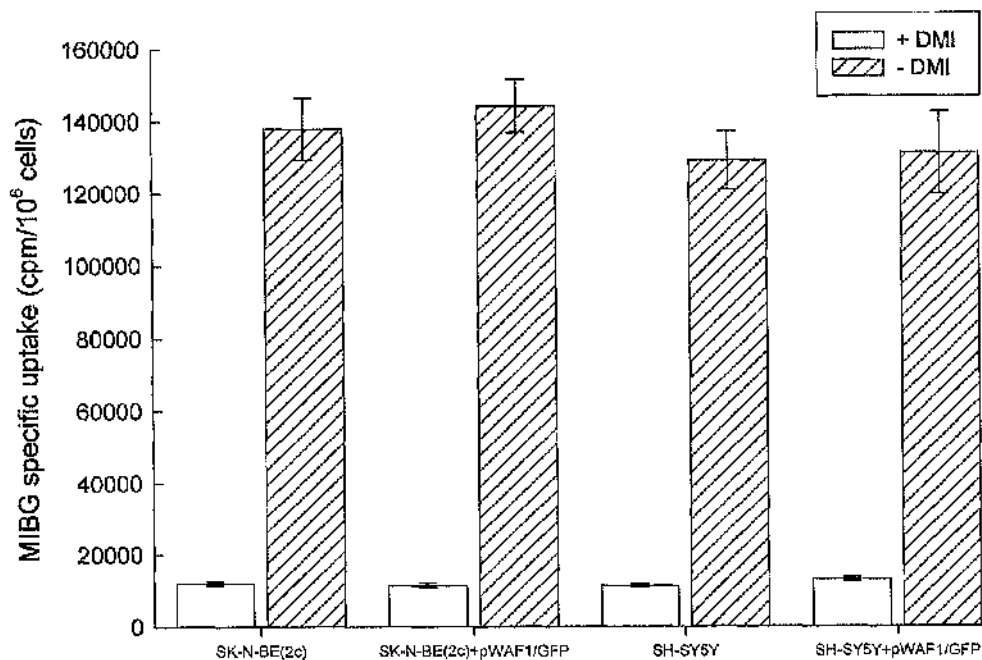


Figure 20. [¹³¹I]MIBG uptake in SK-N-BE(2c) and SH-SY5Y cells parental and transfected with the pWAF1/GFP plasmid.

Uptake assay was performed in the presence or absence of DMI (desmethylimipramine), a powerful inhibitor of the active uptake mediated by the noradrenaline transporter. Results were expressed as counts per minute (cpm) per 10⁶ cells. Data are means ± s.d. of three experiments.

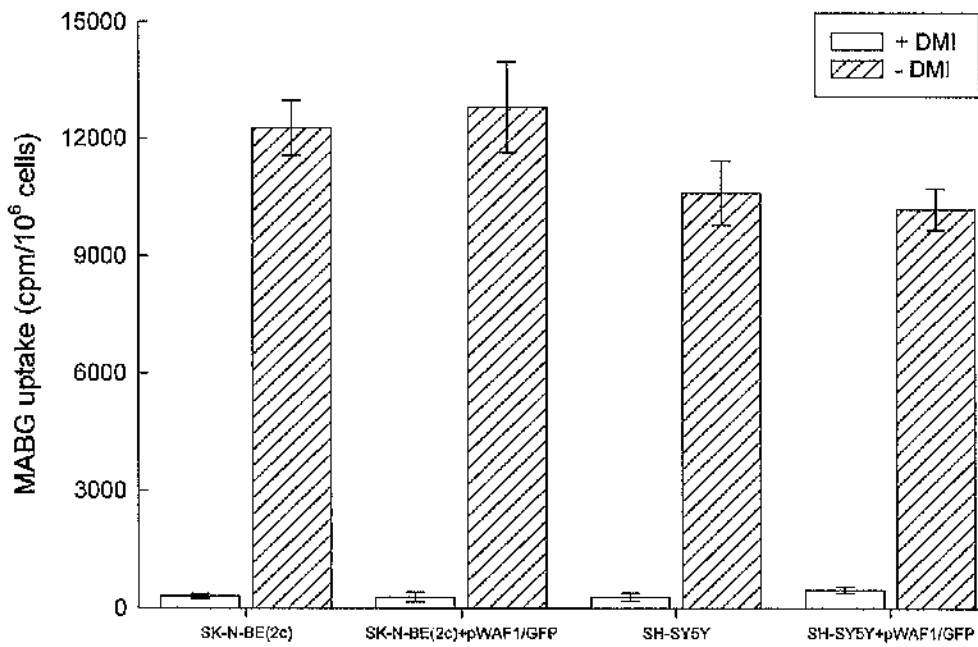


Figure 21. [²¹¹At]MABG uptake in SK-N-BE(2c) and SH-SY5Y cells parental and transfected with the pWAF1/GFP plasmid. Uptake assay was performed in the presence or absence of DMI (desmethylimipramine), a powerful inhibitor of the active uptake mediated by the noradrenaline transporter. Results were expressed as counts per minute (cpm) per 10⁶ cells. Data are means ± s.d. of three experiments.

3.3.2 Assessment of the WAF1 promoter activation in neuroblastoma cells transfected with the pWAF1/GFP plasmid

3.3.2.1 WAF1 promoter activation in SH-SY5Y cells

The fluorescence intensity ratios increased in a time- and dose-dependent fashion after exposing SH-SY5Y cells stably transfected with the pWAF1/GFP plasmid to γ -rays (Figure 22). The maximum ratio of the fluorescence intensity levels of irradiated cells to that of control cells (about 4.4) was registered 48 hours after 10Gy radiation. After 72 and 96 hours there was no significant change in the fluorescence intensity.

There was also a time- and dose-dependent increase in fluorescence levels when SH-SY5Y cells (stably transfected with the pWAF1/GFP plasmid) were treated with 0.2 to 2MBq/ml of [131 I]MIBG (Figure 23). At 72 hours after incubation with 0.1, 0.2 or 0.5MBq/ml of radiopharmaceutical, no further increase in fluorescence intensity was observed. However, unlike activation by external beam ionising radiation, cells treated with the highest activity concentrations (1 or 2MBq/ml) exhibited no plateau with respect to fluorescence intensity to the final data point analysed, 96 hours after treatment (3.28 and 3.45 fold increase respectively).

In the case of SH-SY5Y cells (stably transfected with the pWAF1/GFP plasmid) treated with 1.85 to 29.6kBq/ml of [211 At]MABG, fluorescence intensity increased in a dose- and time-dependent manner (Figure 24). Treatment with 1.85, 3.7 or 7.4kBq/ml of radiopharmaceutical resulted in maximal fluorescence after 96 hours. In contrast, no plateau in fluorescence was observed 96 hours after treatment with 14.8 or 29.6kBq/ml of [211 At]MABG, at which time fluorescence output was greater than that of the control by factors of 4.64 and 5.33 respectively.

The data generated from experiments involving SH-SY5Y cells transfected with the GFP gene controlled by the WAF1 promoter suggested that after the first radiation administration at least 48 hours were needed to cause more than 2-fold increase of the fluorescence levels, and therefore activation of the WAF1 promoter. This was observed regardless of the radiation type used. These observations were more obvious when the fluorescence intensity data were re-plotted against dose of external beam radiation (Figure 25) or administered activity concentrations of [131 I]MIBG (Figure 26) and [211 At]MABG (Figure 27).

In the case of external beam radiation treatment (Figure 25), 24 hours after each radiation dose the fluorescence intensity levels in cells were significantly lower ($p < 0.05$) than that registered at 48, 72 or 96 hours after radiation.

Similarly, 24 hours after exposure to 0.5 to 2MBq/ml of [¹³¹I]MIBG (Figure 26) cells were significantly less fluorescent ($p < 0.05$) than cells analysed 48, 72 or 96 hours after radiation.

The cellular fluorescence intensity 24 hours after treatment with 3.7 to 29.6kBq/ml of [²¹¹At]MABG (Figure 27) was also significantly lower ($p < 0.05$) than that registered at 48, 72 or 96 hours after radiation. Notably, fluorescence intensity levels registered 96 hours after treatment with 14.8 or 29.6kBq/ml of [²¹¹At]MABG were higher ($p < 0.05$) than that measured at 48 and 72 hours.

These findings suggest that perhaps, regardless of the radiation type used to activate the WAF1 promoter, the second administration of ionising radiation would be given 48 hours after the first activating administration. This is the time required for maximum activation levels of the WAF1 promoter.

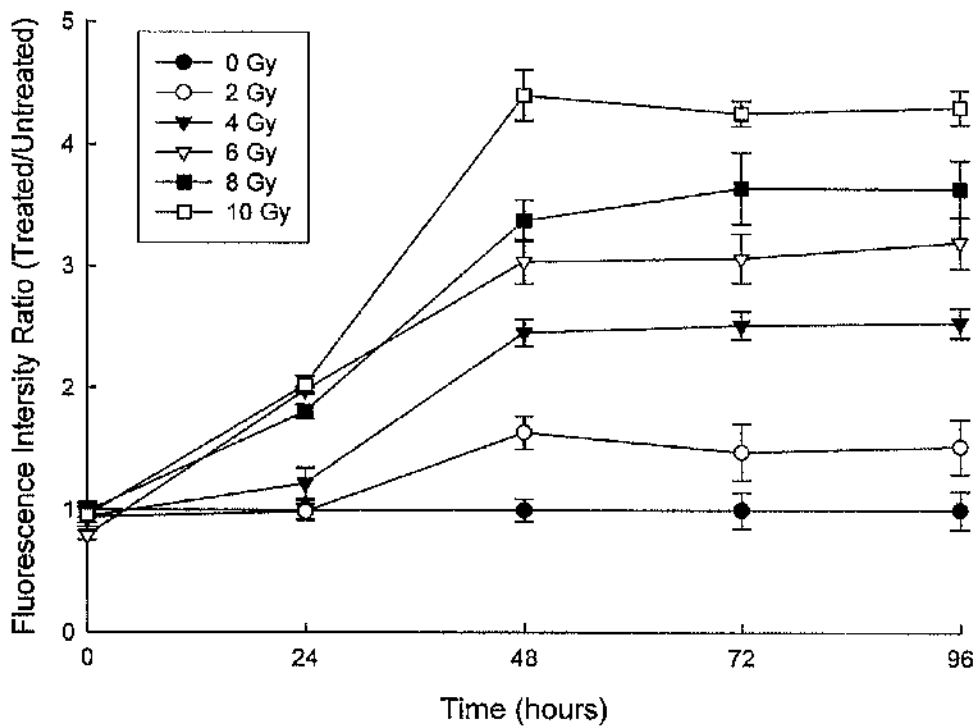


Figure 22. WAF1 activity measured by the GFP fluorescence intensity determined by FACS analysis of SH-SY5Y cells (transfected with the pWAF1/GFP plasmid). Cells were exposed to 0, 2, 4, 6, 8 or 10Gy of γ -rays. Cells were seeded 2 days before the treatment at a concentration of 2.5×10^5 cells/well in six-well plates. At 0, 24, 48 and 72h after irradiation samples were resuspended and analysed at a FACScan (Becton Dickinson UK Ltd). Data are presented as fluorescence intensity ratio of irradiated cells to unirradiated cells (control), means \pm s.d. of measurements from three independent experiments.

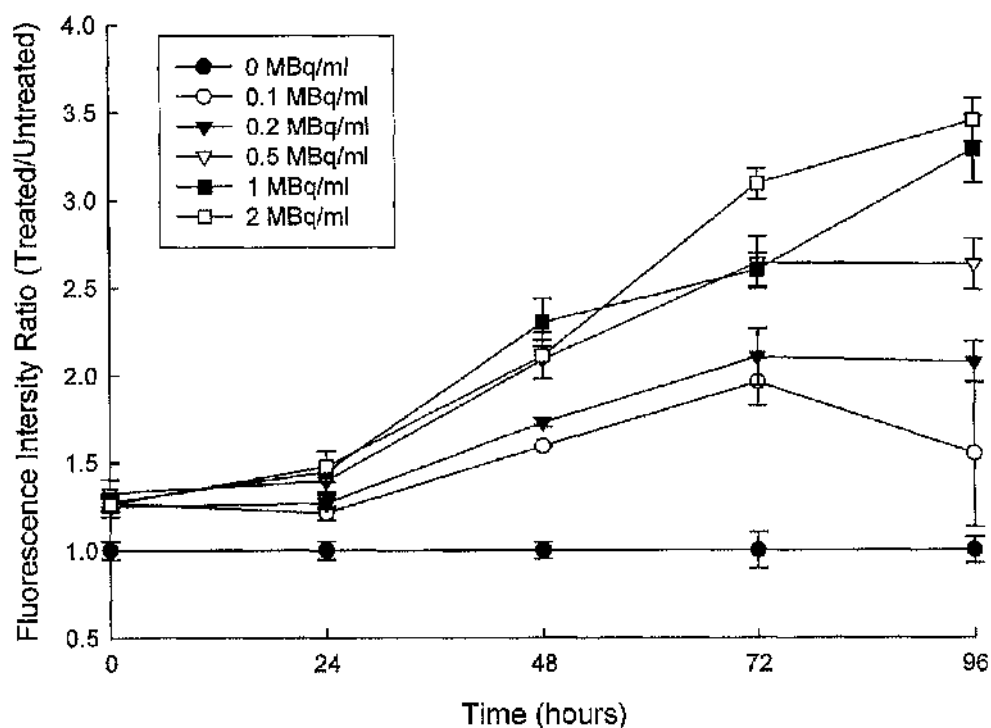


Figure 23. WAF1 activity measured by the GFP fluorescence intensity determined by FACS analysis in SH-SY5Y cells (transfected with the pWAF1/GFP plasmid). Cells were exposed for 2 hours to 0.2, 0.5, 1, 1.5 or 2MBq/ml n.c.a. [¹³¹I]MIBG. Cells were seeded 2 days before the treatment at a concentration of 2.5×10^5 cells/well in six-well plates. At 0, 24, 48, 72 and 96h after irradiation samples were resuspended and analysed at a FACScan (Becton Dickinson UK Ltd). Data are presented as fluorescence intensity ratio of irradiated to unirradiated cells (control), means \pm s.d. of measurements from three independent experiments.

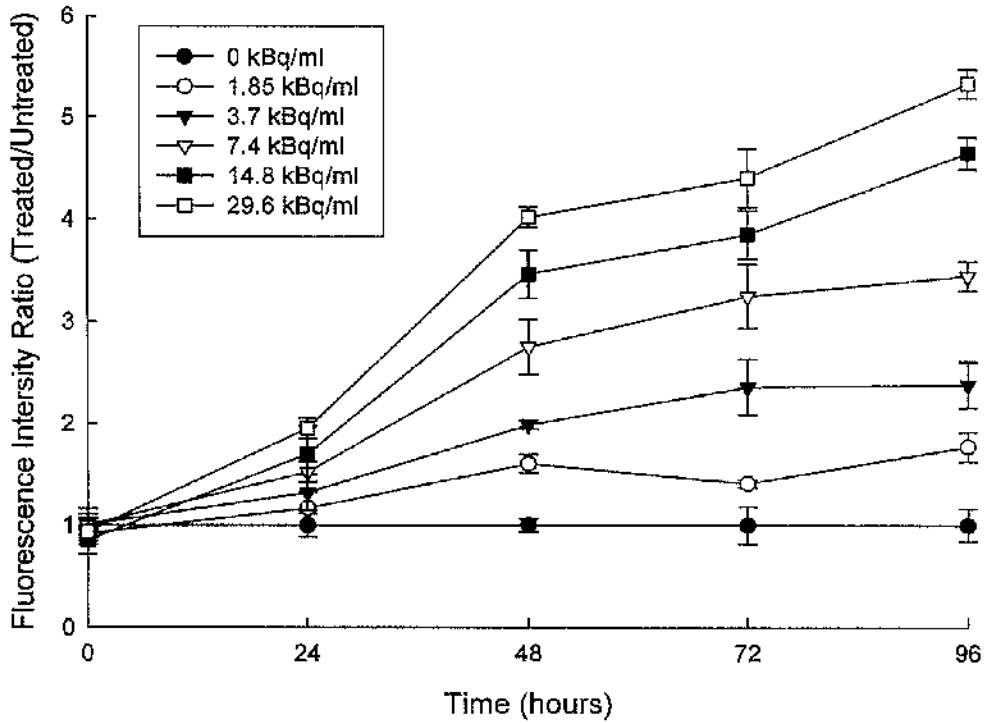


Figure 24. WAF1 activity measured by the GFP fluorescence intensity determined by FACS analysis in SH-SY5Y cells (transfected with the pWAF1/GFP plasmid). Cells were exposed for 2 hours to 1.85, 3.7, 7.4, 14.8 or 29.6 kBq/ml $[^{211}\text{At}]\text{MABG}$. Cells were seeded 2 days before the treatment at a concentration of 2.5×10^5 cells/well in six-well plates. At 0, 24, 48, 72 and 96h after irradiation samples were resuspended and analysed at a FACScan (Becton Dickinson UK Ltd). Data are presented as fluorescence intensity ratio of irradiated to unirradiated cells (control), means \pm s.d. of measurements from three independent experiments.

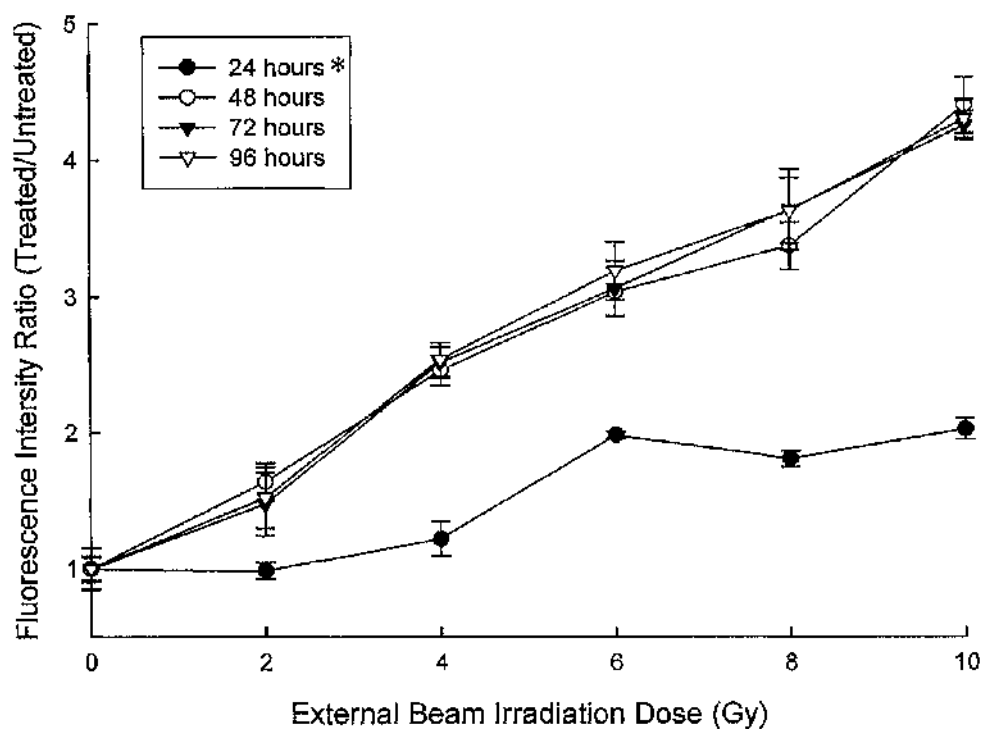


Figure 25. Effect of external beam radiation on WAF1 promoter activity in SH-SY-5YSH-SY5Y cells (transfected with the pWAF1/GFP plasmid) Comparing the dose-response of cells 24, 48, 72 or 96 hours after external beam irradiation. Data are presented as fluorescence intensity ratio of irradiated to unirradiated cells (control), means \pm s.d. of measurements from three independent experiments treatment (* significantly lower, ANOVA test performed for each radiation dose: $p < 0.05$).

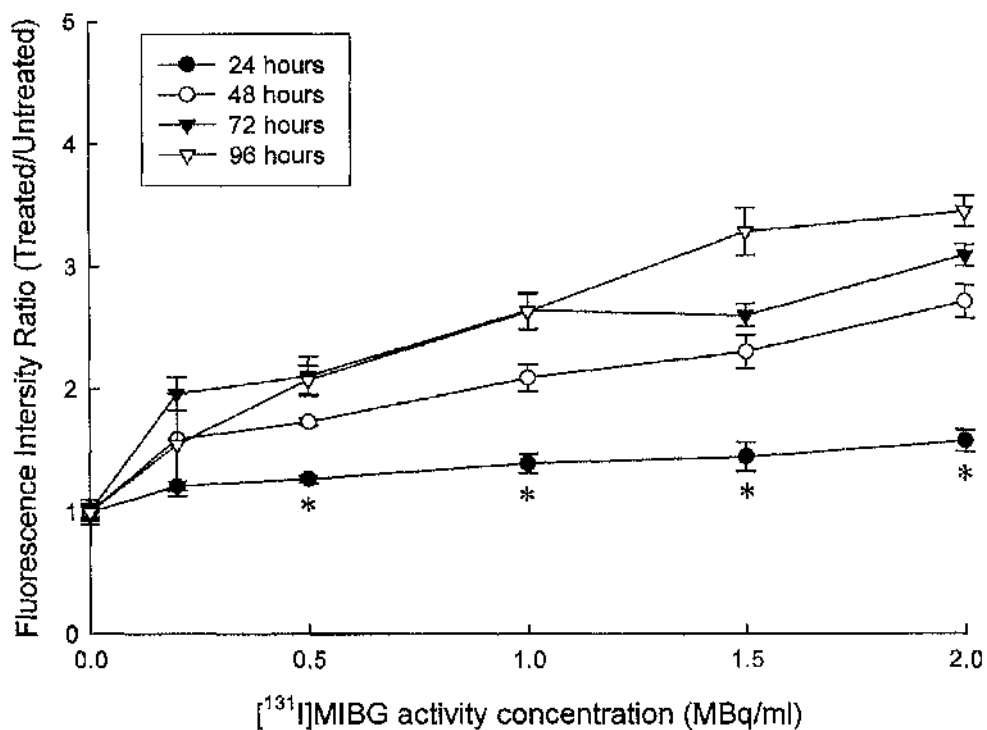


Figure 26. Effect of [¹³¹I]MIBG on WAF1 promoter activity in SH-SY5Y cells (transfected with the pWAF1/GFP plasmid). Comparing the dose-response of cells 24, 48, 72 or 96 hours after [¹³¹I]MIBG treatment. Data are presented as fluorescence intensity ratio of irradiated to unirradiated cells (control), means \pm s.d. of measurements from three independent experiments (* significantly lower, ANOVA test performed for each activity concentration: $p < 0.05$).

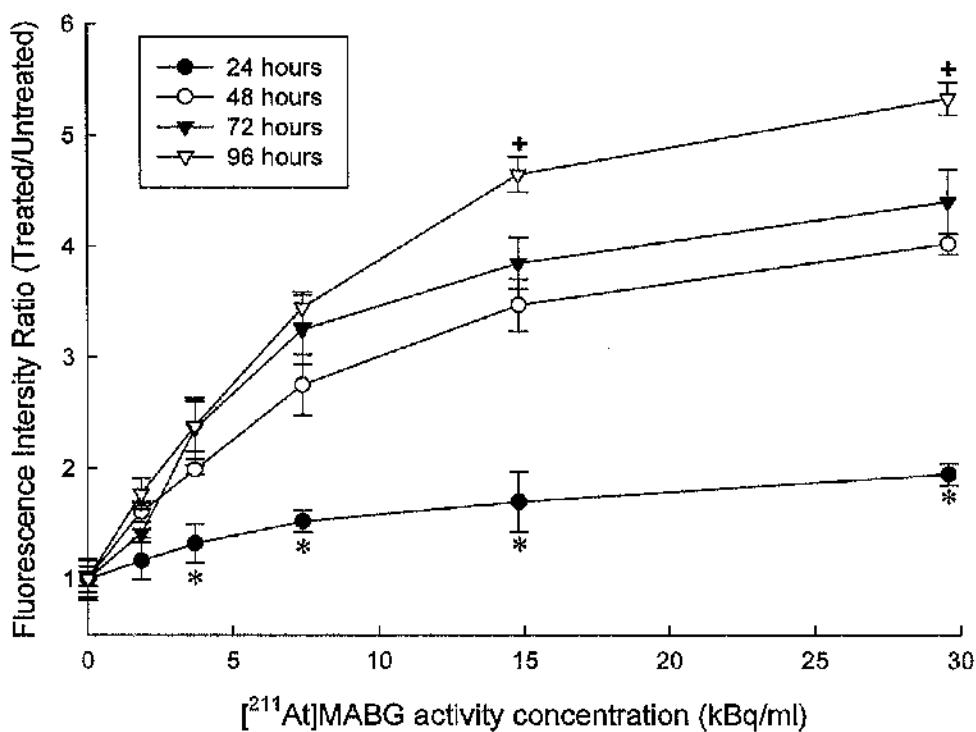


Figure 27. Effect of [²¹¹At]MABG on WAF1 promoter activity in SH-SY5Y cells (transfected with the pWAF1/GFP plasmid). Comparing the dose-response of cells 24, 48, 72 or 96 hours after [²¹¹At]MABG treatment. Data are presented as fluorescence intensity ratio of irradiated to unirradiated cells (control), means \pm s.d. of measurements from three independent experiments (* significantly lower, + significantly higher, ANOVA test performed for each activity concentration: $p < 0.05$).

3.3.2.2 WAF1 promoter activation in SK-N-BE(2c) cells

In order to investigate the universality of the phenomenon, activation of the WAF1 promoter by external beam radiation, [^{131}I]MIBG and [^{211}At]MABG was assessed in a second neuroblastoma cell line, SK-N-BE(2c).

Similarly to SH-SY5Y cells, SK-N-BE(2c) transfectants exposed to γ -rays (Figure 28) showed a dose-dependent increase in fluorescence intensity with the highest ratio value of 2.05 in fluorescence levels 96 hours after the highest dose (10Gy) was administered.

The use of the radiopharmaceutical [^{131}I]MIBG (Figure 29) also caused a dose- and time-dependent increase in fluorescence levels. The maximum fluorescence intensity ratio (2.40) was recorded at 72 hours, reaching a plateau at 96 hours.

After exposure to [^{211}At]MABG (Figure 30), a pattern similar to that observed in transfectants treated with [^{131}I]MIBG (Figure 29) was observed. The maximum fluorescence intensity ratio (2.14) was recorded at 72 hours. At 96 hours the fluorescence intensity ratio levels dropped not significantly in cells treated with 3.7, 7.4, 14.8 and 29.6kBq/ml [^{211}At]MABG, and significantly ($p < 0.05$) in cells exposed to 1.85kBq/ml [^{211}At]MABG).

The data generated from experiments involving SH-SY5Y cells transfected with the GFP gene controlled by the WAF1 promoter suggested that after the first radiation administration at least 48 hours were needed to cause a substantial increase of the fluorescence levels, and therefore activation of the WAF1 promoter. These observations were clearer when the fluorescence intensity data were re-plotted against radiation doses of external beam radiation (Figure 31) or administered activity concentrations of [^{131}I]MIBG (Figure 32) and [^{211}At]MABG (Figure 33).

In the case of external beam radiation treatment (Figure 31), 24 hours after each radiation dose the fluorescence intensity levels in cells were significantly lower ($p < 0.05$) than that registered at 48, 72 or 96 hours after radiation.

Similarly, 24 hours after exposure to 1 to 2MBq/ml of [^{131}I]MIBG (Figure 32) cells were significantly less fluorescent ($p < 0.05$) than cells analysed 48, 72 or 96 hours after radiation.

The cellular fluorescence intensity 24 hours after treatment with 3.7 to 29.6kBq/ml of [²¹¹At]MABG (Figure 33) was also significantly lower ($p < 0.05$) than that registered at 48, 72 or 96 hours after radiation.

As seen in SH-SY5Y cells, these results suggests that the second administration of ionising radiation should be given 48 hours after the first activating administration, time required for maximum activation levels of the WAF1 promoter.

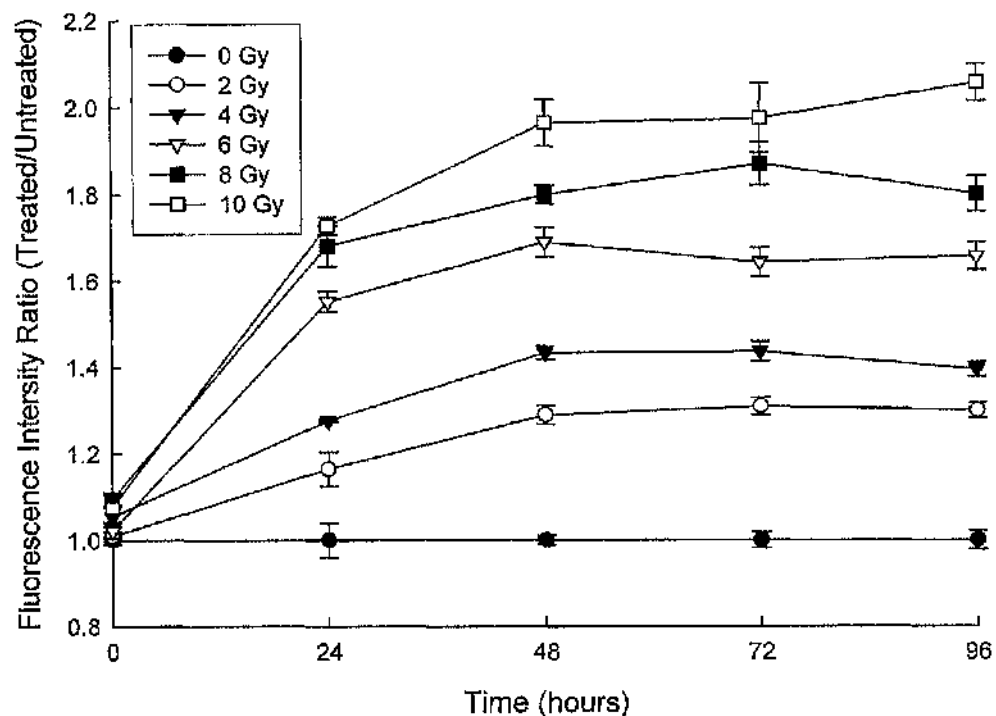


Figure 28. WAF1 activity measured by the GFP fluorescence intensity determined by FACS analysis of SK-N-BE(2c) cells (transfected with the pWAF1/GFP plasmid). Cells were exposed to 0, 2, 4, 6, 8 10Gy of γ -rays. Cells were seeded 2 days before the treatment at a concentration of 2.5×10^5 cells/well in six-well plates. At 0, 24, 48 and 72h after irradiation samples were resuspended and analysed at a FACScan (Becton Dickinson UK Ltd). Data are presented as fluorescence intensity ratio of irradiated cells to unirradiated cells (control), means \pm s.d. of measurements from three independent experiments.

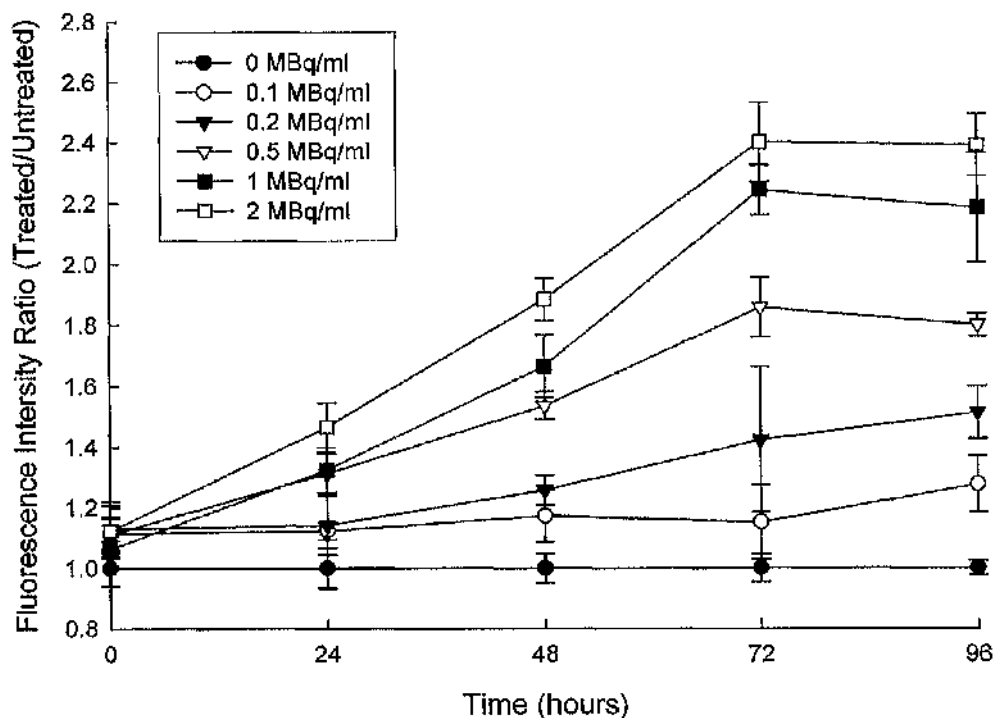


Figure 29. WAF1 activity measured by the GFP fluorescence intensity determined by FACS analysis in SK-N-BE(2c) cells (transfected with the pWAF1/GFP plasmid). Cells were exposed for 2 hours to 0.2, 0.5, 1, 1.5 and 2 MBq/ml n.c.a. ^{131}I MIBG. Cells were seeded 2 days before the treatment at a concentration of 2.5×10^5 cells/well in six-well plates. At 0, 24, 48, 72 and 96h after irradiation samples were resuspended and analysed at a FACScan (Becton Dickinson UK Ltd). Data are presented as fluorescence intensity ratio of irradiated to unirradiated cells (control), means \pm s.d. of measurements from three independent experiments.

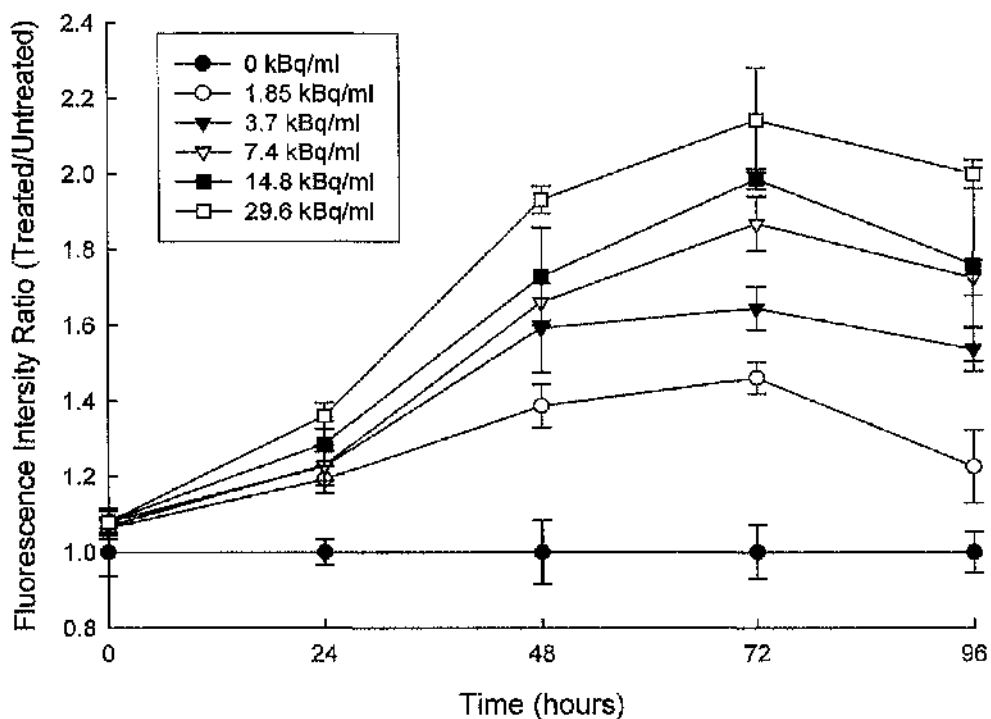


Figure 30. WAF1 activity measured by the GFP fluorescence intensity determined by FACS analysis in SK-N-BE(2c) cells (transfected with the pWAF1/GFP plasmid). Cells were exposed for 2 hours to 1.85, 3.7, 7.4, 14.8 or 29.6 kBq/ml [^{211}At]MABG. Cells were seeded 2 days before the treatment at a concentration of 2.5×10^5 cells/well in six-well plates. At 0, 24, 48, 72 and 96h after irradiation samples were resuspended and analysed at a FACScan (Becton Dickinson UK Ltd). Data are presented as fluorescence intensity ratio of irradiated to unirradiated cells (control), means \pm s.d. of measurements from three independent experiments.

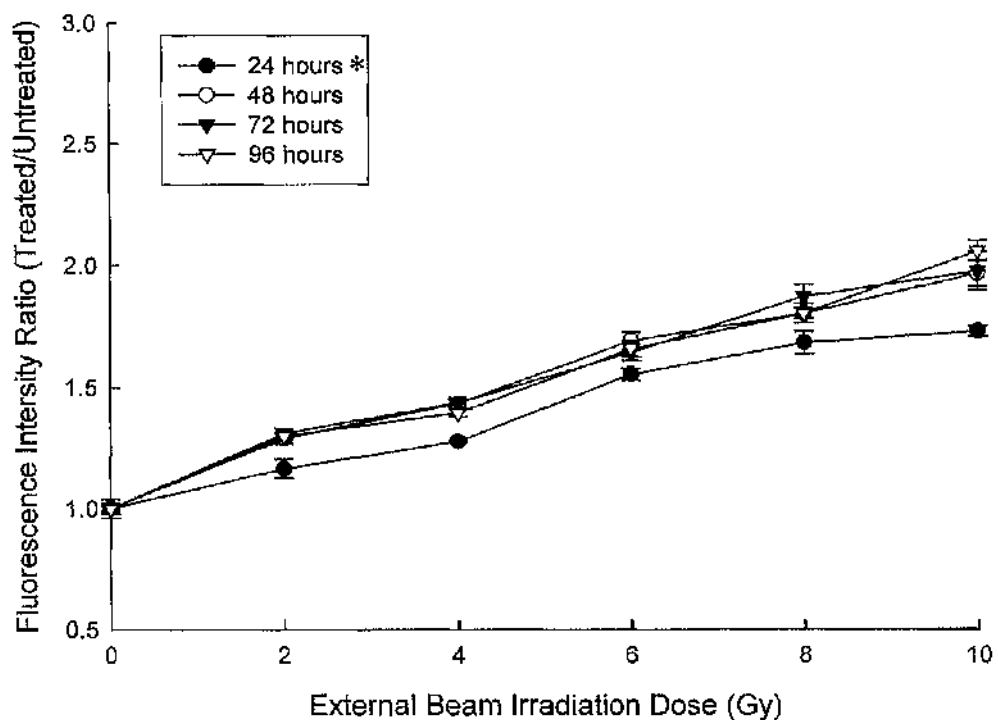


Figure 31. Effect of external beam radiation on WAF1 promoter activity in SK-N-BE(2c) cells (transfected with the pWAF1/GFP plasmid). Comparing the dose-response of cells 24, 48, 72 or 96 hours after external beam irradiation. Data are presented as fluorescence intensity ratio of irradiated to unirradiated cells (control), means \pm s.d. of measurements from three independent experiments (* significantly lower, ANOVA test: $p < 0.05$).

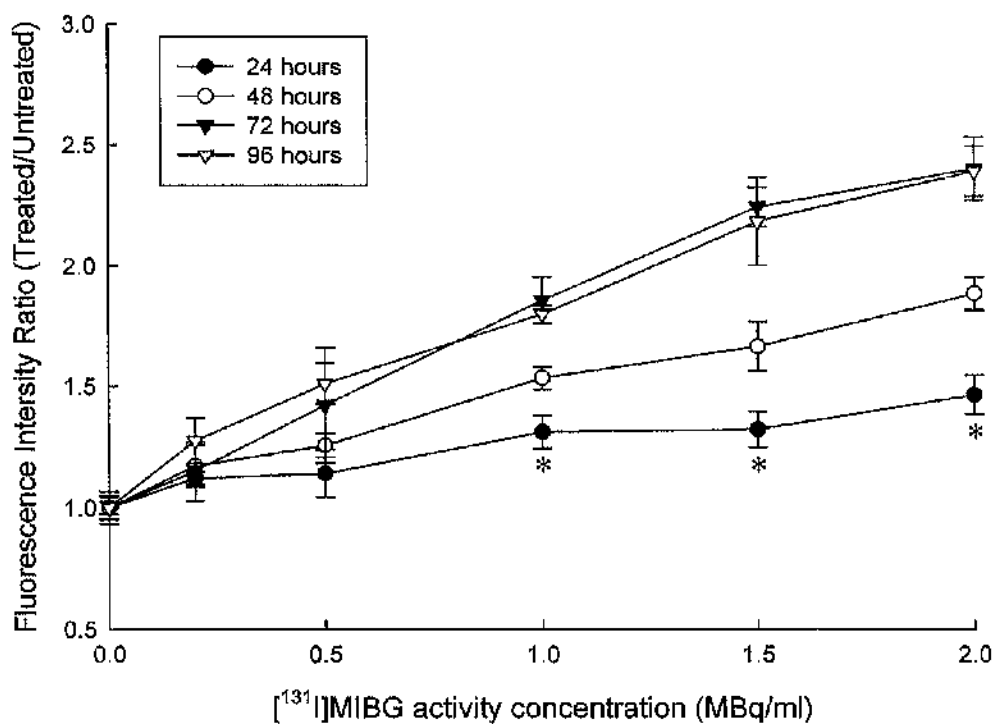


Figure 32. Effect of [¹³¹I]MIBG on WAF1 promoter activity in SK-N-BE(2c) cells (transfected with the pWAF1/GFP plasmid).

Comparing the dose-response of cells 24, 48, 72 or 96 hours after [¹³¹I]MIBG treatment. Data are presented as fluorescence intensity ratio of irradiated to unirradiated cells (control), means \pm s.d. of measurements from three independent experiments (* significantly lower, ANOVA test: $p < 0.05$).

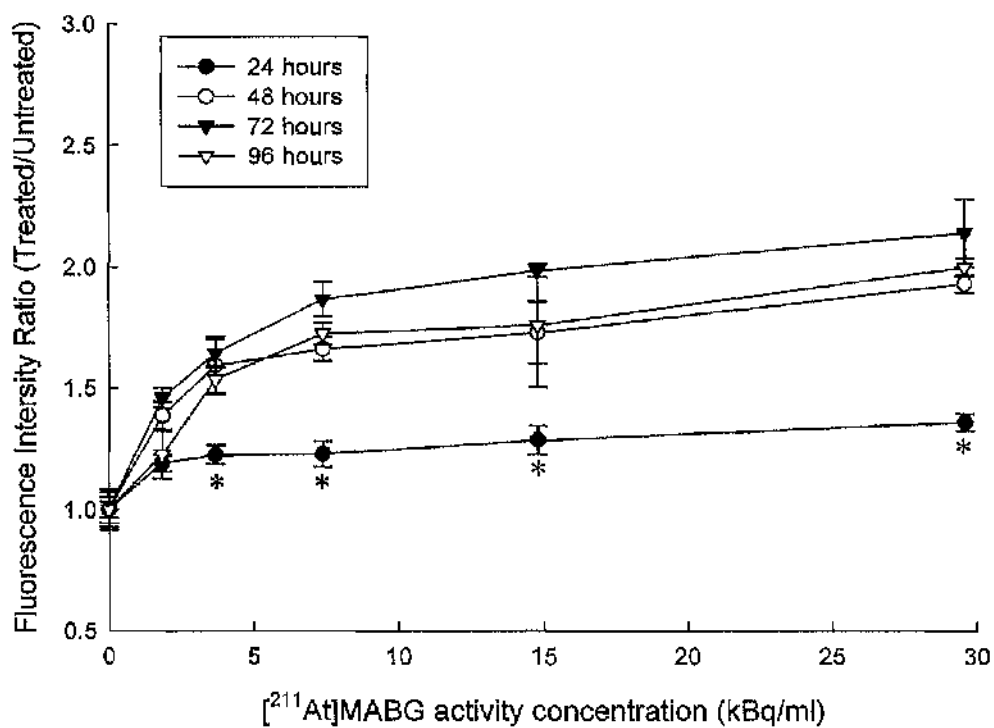


Figure 33. Effect of [²¹¹At]MABG on WAF1 promoter activity in SK-N-BE(2c) cells (transfected with the pWAF1/GFP plasmid).

Comparing the dose-response of cells 24, 48, 72 or 96 hours after [²¹¹At]MABG treatment. Data are presented as fluorescence intensity ratio of irradiated to unirradiated cells (control), means \pm s.d. of measurements from three independent experiments (* significantly lower, ANOVA test: $p < 0.05$).

3.3.2.3 Western blot analysis of GFP protein for evaluation of WAF1 promoter activation in SH-SY5Y cells

Western blot analysis of GFP and GAPDH proteins was performed for comparison with the FACs analysis findings. The evaluation of GFP levels was performed using SH-SY5Y cells transfected with the pWAF1/GFP plasmid and then incubated with [¹²⁵I]MIBG (Figure 34). This set of experiments was performed following the same conditions used in the FACs analysis experiments.

The intensity of the GFP band of each sample was quantified by densitometry and normalised to the intensity of the corresponding GAPDH loading control band. The ratios of the normalised GFP band intensity of the treated cells to that of the untreated cells were then calculated for each sample (Figure 34B).

The pattern of GFP protein expression reflected the fluorescence levels recorded by FACS analysis. In particular, the increase in GFP ratio levels was time-dependent up to 72 hours after treatment, with a plateau at 96 hours. At this time point, no significant difference between protein levels following treatment with the various activity concentrations was detected between 72 and 96 hours ($p > 0.1$).

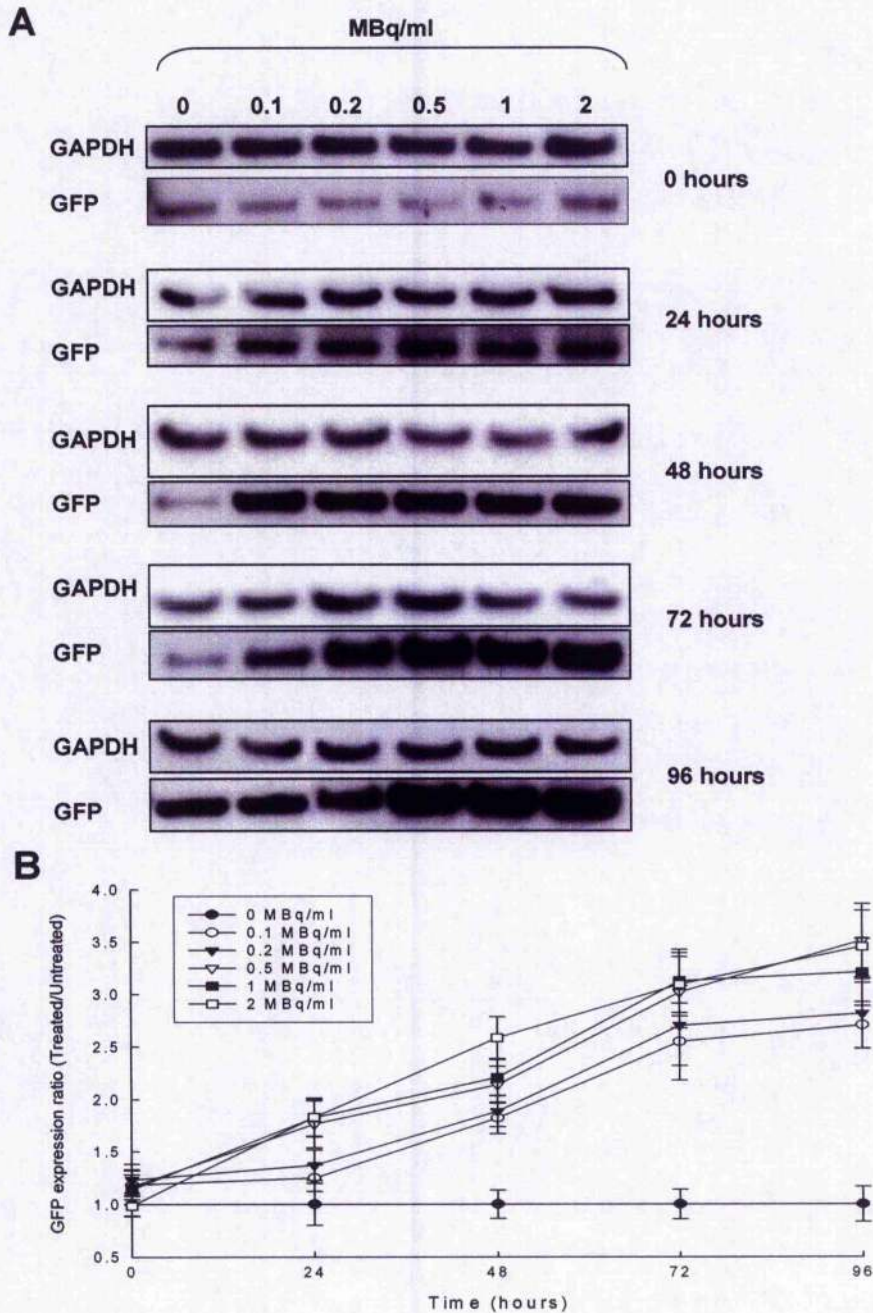


Figure 34. [^{131}I]MIBG effect on GFP protein expression in SH-SY5Y cells stably transfected with the pWAF1/GFP plasmid.

A) Western blot analysis of GFP expression in SH-SY5Y cells.

B) WAF1 activity measured by the GFP expression levels determined by Western blot analysis in SH-SY5Y cells (transfected with the pWAF1/GFP plasmid).

Cells were exposed for 2 hours to 0.1, 0.2, 0.5, 1 or 2MBq/ml [^{131}I]MIBG. Cells were seeded 2 days before the treatment at a concentration of 2.5×10^5 cells/well in six-well plates. At 0, 24, 48, 72 and 96 hours after irradiation protein were extracted and Western blot analysis was performed as described in material and methods section. Data are presented as GFP expression (normalised by the GAPDH) ratio of irradiated to unirradiated cells (control), means \pm s.d. of measurements from three independent experiments.

3.3.2.4 WAF1 promoter activation in p53-wild type or p53-null HCT116 cells

It was noticeable that overall the SH-SY5Y transfectants (Figure 22 to Figure 24) were more "responsive" to all radiation types than the SK-N-BE(2c) transfectants (Figure 28 to Figure 30) with respect to fluorescence intensity increase. This suggests that WAF1 promoter activation is greater in SH-SY5Y cell. It has been reported that SH-SY5Y cells express the wild type form of p53 [241], whereas in SK-N-BE(2c) cells p53 is mutated [242]. As a possible explanation, the role of p53 status for the lower responsiveness of SK-N-BE(2c) cells with respect to WAF1 promoter activation was investigated. Therefore, isogenic p53-null (p53 $-/-$) and wild-type (p53 $+/+$) cells of the colorectal tumour cell line HCT116 were stably transfected with the pWAF1/GFP plasmid, treated with external beam radiation and their fluorescence intensity ratios were compared. In both p53 $-/-$ and p53 $+/+$ cells the fluorescence levels increased in a dose- and time-dependent manner (Figure 35). Interestingly, the ratio values of fluorescence intensity in cells with p53 knockout were higher than that in cells expressing wild type p53 48 hours after 4 or 8Gy radiation ($p = 0.0397$ and 0.0173 respectively), and 72 hours after 8Gy radiation ($p = 0.0476$). This phenomenon should be further investigated in order to elucidate potential mechanisms involved in the regulation of the WAF1 promoter. However, it is unlikely that expression of p53 could negatively affect the WAF1 promoter activation in tumour cells, as the inducing effect that p53 has on the WAF1 gene expression in response to DNA damage is well established [243]. These findings suggest, in accordance with a previous report [235], that the absence of p53 expression in HCT116 cells did not affect the WAF1 promoter activity following external beam ionising irradiation.

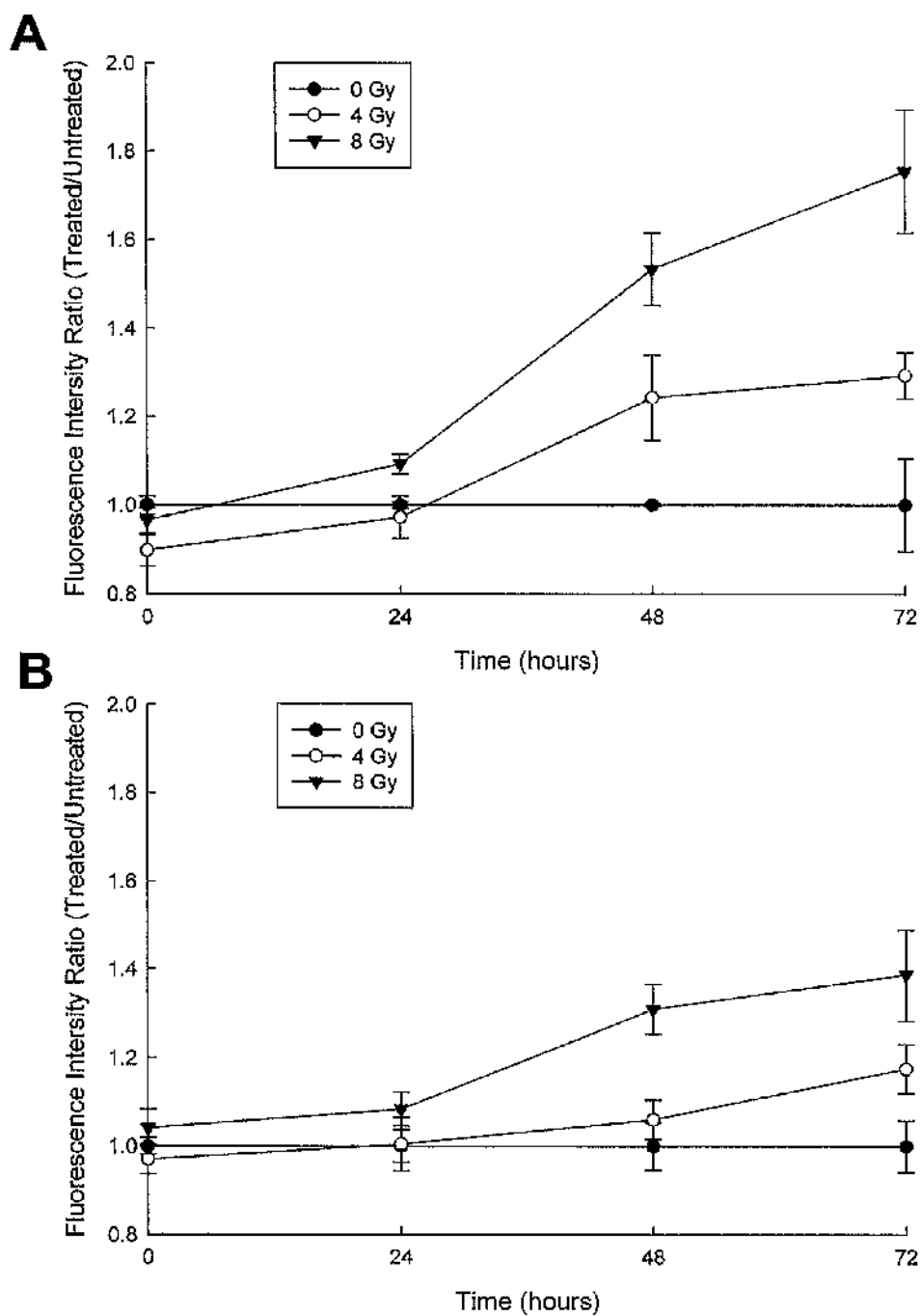


Figure 35. WAF1 activity measured by the GFP fluorescence intensity determined by FACS analysis of HCT116 cells.

HCT116 p53^{-/-} cells (A) and HCT116 p53^{+/+} cells (B) stably transfected with the pWAF1/GFP plasmid were analysed. Cells were seeded 2 days before the treatment at a concentration of 2.5×10^5 cells/well in six-well plates. Cells were then exposed to 0, 4 or 8Gy of γ -ray. At 0, 24, 48 and 72 hours after irradiation samples were resuspended and analysed at a FACScan (Becton Dickinson UK Ltd). Data are presented as fluorescence intensity ratio of irradiated cells to unirradiated cells (control), means \pm s.d. of measurements from three independent experiments.

3.3.2.5 Estimation of the radiation dose of radiopharmaceuticals required for the WAF1 promoter activation in neuroblastoma cells

3.3.2.5.1 Curve-fitting to cell kill plots and equivalent radiation dose estimation

To determine the influence of radiation dose and quality on the activation of the WAF1 promoter, we compared in both cell lines (SH-SY5Y cells in Figure 36; SK-N-BE(2c) cells in Figure 37) the toxicity of external beam radiation (Figure 36A and Figure 37A) with that of [¹³¹I]MIBG (Figure 36B and Figure 37B) and [²¹¹At]MABG (Figure 36C and Figure 37C).

Curves were fitted to each cell kill plot. In the case of cell kill generated by low-LET (linear energy transfer) radiation (external beam radiation and [¹³¹I]MIBG), the linear-quadratic model with the expression $S = e^{-\alpha D - \beta D^2}$ was used. S was the fraction of cells surviving a dose D and α was a constant describing the initial slope of the cell survival curve and β was a constant describing the quadratic component of cell killing. The linear-quadratic model was applied as it is generally assumed that low-LET radiation can kill a cell in two ways: single lethal event or two sublethal events [244]. In the expression $S = e^{-\alpha D - \beta D^2}$, the single event killing is represented by $e^{-\alpha D}$ and the two event killing by $e^{-\beta D^2}$.

The linear model was used for the cell kill generated by high-LET radiation ([²¹¹At]MABG) with the relationship $S = e^{-\alpha D}$. It is assumed that high-LET radiation can kill a cell in a single lethal event [244].

In this way, it was possible to calculate the activity concentration (of [¹³¹I]MIBG or [²¹¹At]MABG) or the dose (of external beam radiation) expected to generate a given survival fraction. For example, 0.45MBq/ml [¹³¹I]MIBG was expected to generate a survival fraction of 0.4 in SH-SY5Y transfectants.

In accordance with previous studies [245], the SH-SY5Y transfectants were more radiosensitive than the SK-N-BE(2c) transfectants (SF2 = 0.20 and 0.66 respectively).

The equivalent radiation dose value (eGy) was subsequently estimated for any activity concentration of [¹³¹I]MIBG or [²¹¹At]MABG expected to cause a given level of toxicity, measured as survival fraction. For example, in order to generate a survival fraction of 0.4 in SH-SY5Y transfectants, 1.28Gy of external beam radiation (Figure 36A), 0.45MBq/ml [¹³¹I]MIBG (Figure 36B) or 1.56kBq/ml

[²¹¹At]MABG (Figure 36C) was required. Therefore with respect to radiotoxicity, we can assume that 0.45MBq/ml [¹³¹I]MIBG or 1.56kBq/ml [²¹¹At]MABG is equivalent to 1.28Gy of external beam radiation.

The equivalent radiation doses were calculated from the radioactivity concentrations expected to generate survival fractions ranging from 1 to 0.05. As a result, an equivalent radiation dose was estimated for any expected activity concentration of radiopharmaceutical.

3.3.2.5.2 Calculation of fluorescence intensity ratios by any given radiation activity concentration

Curve-fitting was then performed in the plots corresponding to Figure 25, Figure 26 and Figure 27 (for SH-SY5Y cells), and Figure 31, Figure 32 and Figure 33 (for SK-N-BE(2c) cells). These plots reported the fluorescence intensity ratios as a function of dose or activity concentration of each radiation type. The linear quadratic relationship $FIR = y_0 + ax + bx^2$ was used, because it best reflected the dose-response (with respect to fluorescence intensity ratio) of both SH-SY5Y and SK-N-BE(2c) transfectants to the three radiation types (correlation coefficient $r^2 > 0.9$). *FIR* was the fluorescence intensity ratio that resulted after treatment with a radiation dose or activity concentration of x ; y_0 was the fluorescence intensity ratio after no treatment, a and b were equation constants. By doing so, it was possible to calculate the fluorescence intensity ratio expected by any dose (of external beam radiation) or activity concentration (of [¹³¹I]MIBG or [²¹¹At]MABG). For example, a fluorescence intensity ratio of 1.23 was expected in SH-SY5Y transfectants exposed to 0.45MBq/ml [¹³¹I]MIBG.

Consequently, the fluorescence intensity ratios, expected in cells exposed to specific radiation doses or radioactivity concentrations, were plotted against the equivalent radiation doses (eGy) calculated. For example, in the case of SH-SY5Y transfectants, a fluorescence intensity ratio of 1.23 (expected to be found in SH-SY5Y transfectants exposed to 0.45MBq/ml [¹³¹I]MIBG) was plotted against 1.28eGy, which was estimated to be equivalent to 0.45MBq/ml (section 3.3.2.5.1). This analysis was conducted for both cell lines (SH-SY5Y cells in Figure 38 and SK-N-BE(2c) cells in Figure 39) at each time point.

In this way, it was possible to estimate the radiation dose needed to generate a specific increase of fluorescence, thus WAF1 promoter activation. In addition, it

allowed us to compare the WAF1 promoter activation by three radiation types. This comparison was conducted throughout the dose range using the ANOVA test. In SH-SY5Y transfectants, 24 hours after treatment, [¹³¹I]MIBG and [²¹¹At]MABG were significantly superior ($p < 0.01$, ANOVA test with Bonferroni correction) to external beam irradiation with respect to WAF1 activation (Figure 38A). For example, at 24 hours after 3.32eGy of external beam radiation, [¹³¹I]MIBG or [²¹¹At]MABG treatments the fluorescence intensity ratio were 1.16, 1.45 or 1.35 respectively.

No significant difference of WAF1 promoter activation was found in cells 48 (Figure 38B), 72 (Figure 38C) or 96 (Figure 38D) hours after exposure to external beam radiation, [¹³¹I]MIBG or [²¹¹At]MABG ($p > 0.1$ for each time point). These findings indicate that the WAF1 promoter activation occurs primarily during the first 48 hours after treatment.

In the case of SK-N-BE(2c) transfectants, a survival fraction of 0.4 was registered when cells were exposed to 0.52MBq/ml [¹³¹I]MIBG, 1.33KBq/ml [²¹¹At]MABG or 3.71Gy of external beam radiation. The same analysis of the dose-dependency (eGy) of expression of the marker gene used for the SH-SY5Y transfectants data, was applied to the SK-N-BE(2c) transfectants data.

The most efficient means to activate the WAF1 promoter at 24 hours after treatment was external beam radiation ($p < 0.01$, Figure 39A).

At 48 (Figure 39B), 72 (Figure 39C) or 96 (Figure 39D) hours after radiation exposure, both external beam and [¹³¹I]MIBG treatments were superior to that of [²¹¹At]MABG with respect to WAF1 promoter activation ($p < 0.01$). For example the fluorescence intensity ratio at 48 hours after 3.52eGy of external beam radiation, [¹³¹I]MIBG or [²¹¹At]MABG treatment were 1.31, 1.28 or 1.14 respectively.

These data suggest that for optimal WAF1 promoter activation in the SH-SY5Y or SK-N-BE(2c) transfectants [¹³¹I]MIBG is a suitable radiopharmaceutical. It was shown that in both cell lines, [¹³¹I]MIBG was as effective in inducing the WAF1 promoter activity as external beam radiation (Figure 38 and Figure 39).

The [²¹¹At]MABG treatment was as effective as that of external beam radiation or [¹³¹I]MIBG in SH-SY5Y but not in SK-N-BE(2c) transfectants, in which the WAF1 promoter activation levels following [²¹¹At]MABG treatment were significantly lower ($p < 0.01$) than that following either external beam radiation or [¹³¹I]MIBG (Figure 39).

The most opportune time for the administration of the second (therapeutic) dose of radiopharmaceutical is 48 hours after the first dose for the SH-SY5Y and SK-N-BE(2c) transfectants.

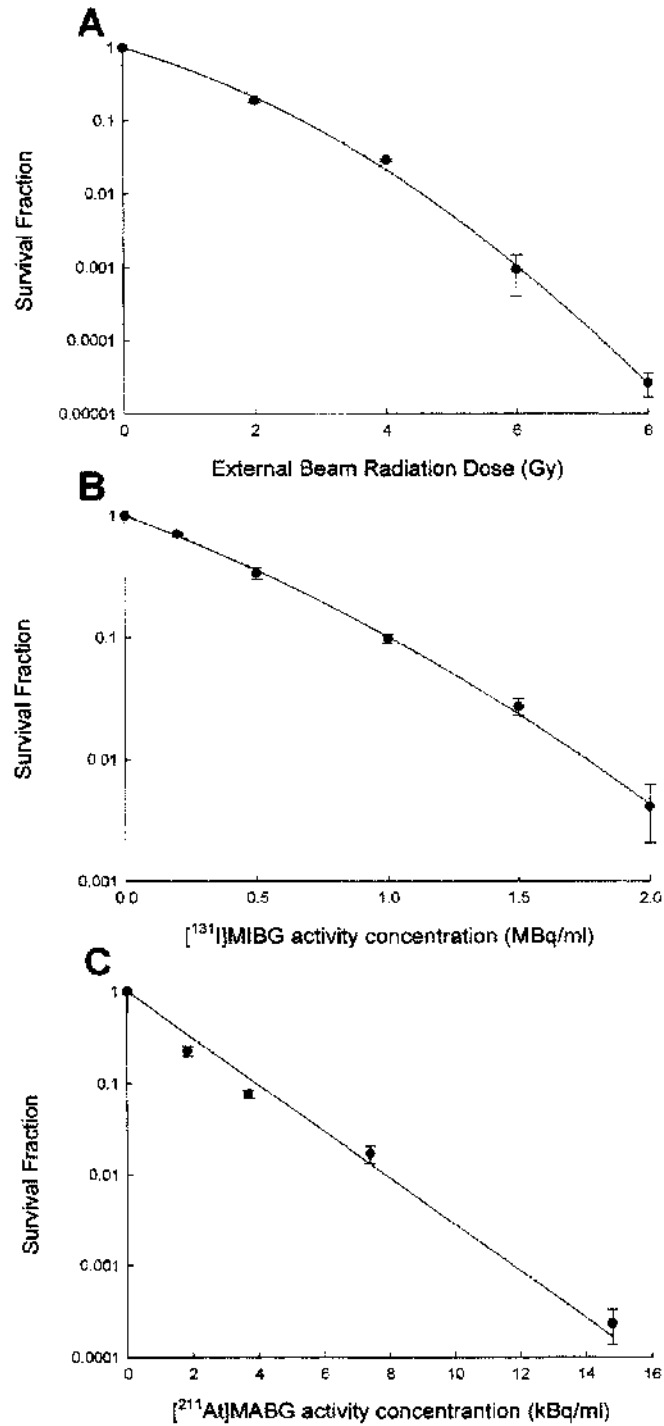


Figure 36. Cytotoxicity of γ -rays (A), [¹³¹I]MIBG (B) or [²¹¹At]MABG (C) to SH-SY5Y cells (transfected with the pWAF1/GFP plasmid) determined by clonogenic assay. Cells were treated as described in Material and methods. Means \pm s.d. of measurements from three independent experiments.

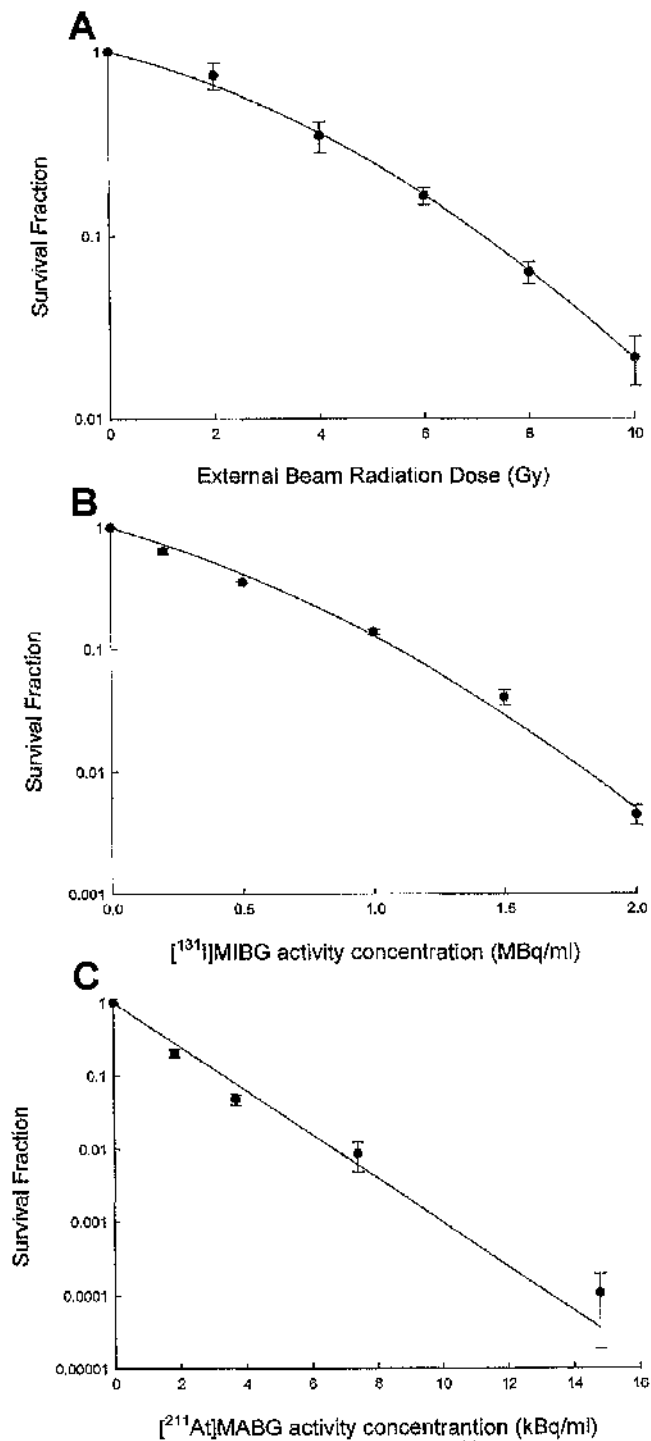


Figure 37. Cytotoxicity of γ -rays (A), [¹³¹I]MIBG (B) or [²¹¹At]MABG (C) to SK-N-BE(2c) cells (transfected with the pWAF1/GFP plasmid) determined by clonogenic assay. Cells were treated as described in Material and methods. Means \pm s.d. of measurements from three independent experiments.

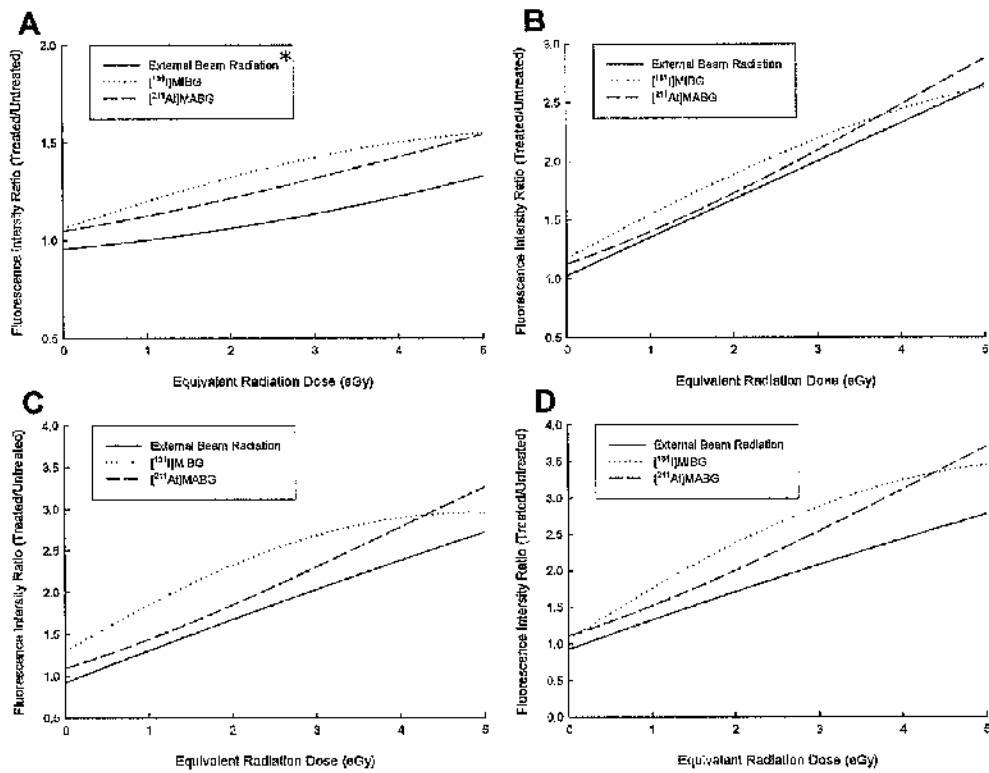


Figure 38. Comparison of the effect of external beam radiation, ^{131}I MIBG or ^{211}At MABG on WAF1 promoter activity in SH-SY5Y cells. Cells were stably transfected with the pWAF1/GFP plasmid and fluorescence intensity ratio levels were calculated 24 (A), 48 (B), 72 (C) or 96 (D) hours after treatment (* significantly lower, ANOVA test with Bonferroni correction: $p < 0.01$).

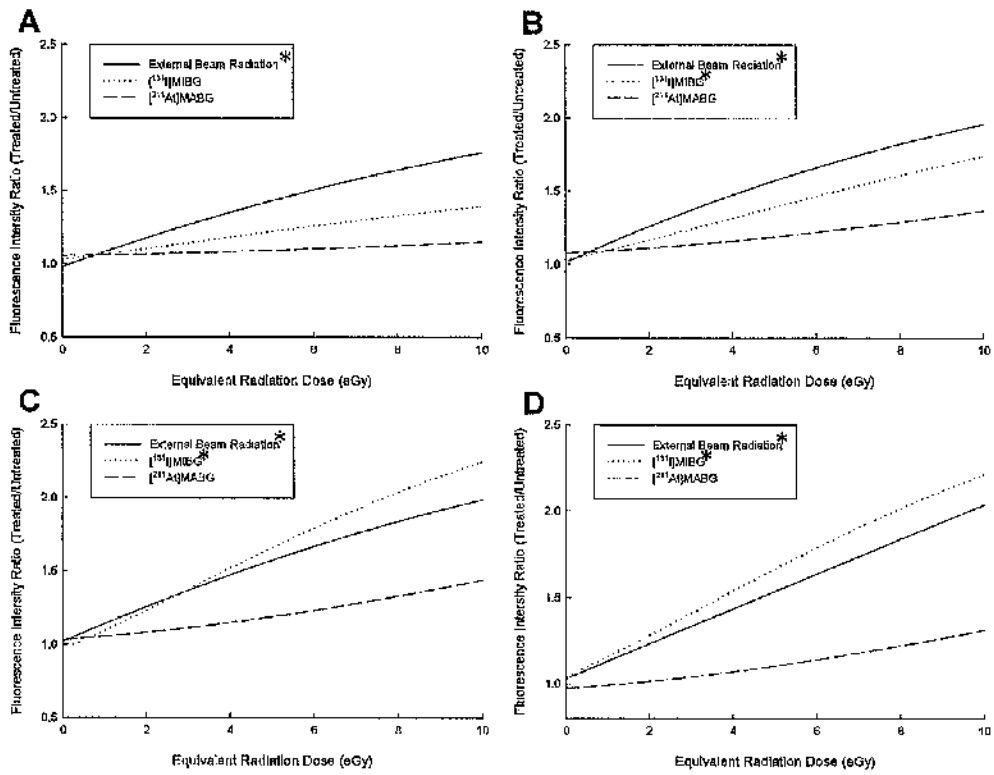


Figure 39. Comparison of the effect of external beam radiation, [^{131}I]MIBG or [^{211}At]MABG on WAF1 promoter activity in SK-N-BE(2c) cells. Cells were stably transfected with the pWAF1/GFP plasmid and fluorescence intensity ratio levels were calculated 24 (A), 48 (B), 72 (C) or 96 (D) hours after treatment (* significantly higher, ANOVA test with Bonferroni correction: $p < 0.01$).

3.3.3 Assessment of noradrenaline transporter (NAT) expression under the control of the WAF1 promoter in neuroblastoma cells: a preliminary study

The human neuroblastoma SH-SY5Y cells already express the noradrenaline transporter [246]. The transcription and activity levels of the endogenous (human) NAT (hNAT) were examined in SH-SY5Y cells in order to compare these levels with that of the cells transfected with a plasmid containing the NAT cDNA of bovine origin (bNAT), under the control of the WAF1 promoter. This comparison allowed us to assess whether the transfection process affected the expression of the endogenous NAT (hNAT).

In addition, a plasmid containing the NAT cDNA of bovine origin (bNAT), under the control of the WAF1 promoter (plasmid named pWAF1/NAT), was stably transfected in SH-SY5Y cells. In these transfectants, [¹³¹I]MIBG uptake assay and real-time PCR assay specific for mRNA of both endogenous (hNAT) and transgenic NAT (bNAT) gene were also performed.

3.3.3.1 Comparison of [¹³¹I]MIBG uptake capacity and NAT mRNA levels in untransfected SH-SY5Y cells with that in cells transfected with the pWAF1/NAT plasmid

As shown in Figure 40A, unirradiated SH-SY5Y cells transfected with the pWAF1/NAT plasmid displayed a higher capacity to accumulate [¹³¹I]MIBG than untransfected SH-SY5Y cells ($p = 0.003$). This suggests that the increase in [¹³¹I]MIBG accumulation capacity of SH-SY5Y cells, transfected with the pWAF1/NAT plasmid, is due to the transgenic NAT (bNAT) expression promoted by the WAF1 promoter activity in absence of radiation.

In order to further investigate this possibility, quantitative PCR specific for messenger RNA (mRNA) of both endogenous and transgenic NAT (hNAT and bNAT respectively) was performed.

Results were expressed as number of mRNA copies of NAT (either hNAT or bNAT) per one copy of GAPDH (Figure 40B). The mRNA levels of endogenous NAT (hNAT) did not change after the transfection of the pWAF1/NAT plasmid in SH-SY5Y cells. Furthermore, in transfected cells mRNA levels of the NAT transgene (bNAT) were detectable, indicating that the WAF1 promoter is already active in unirradiated tumour cells, in accordance with previous studies [135, 235, 236].

These findings indicate that the transfection of the transgenic NAT gene (bNAT) under the control of the WAF1 promoter rendered unirradiated SH-SY5Y cells able to accumulate the radiopharmaceutical more efficiently. Furthermore, results generated from quantitative PCR assay suggest that the increase in uptake capacity of SH-SY5Y cells was due to the expression and the activity of the transgenic NAT gene (bNAT) controlled by the WAF1 promoter and that transfection had no effect on the expression of the endogenous NAT gene (hNAT).

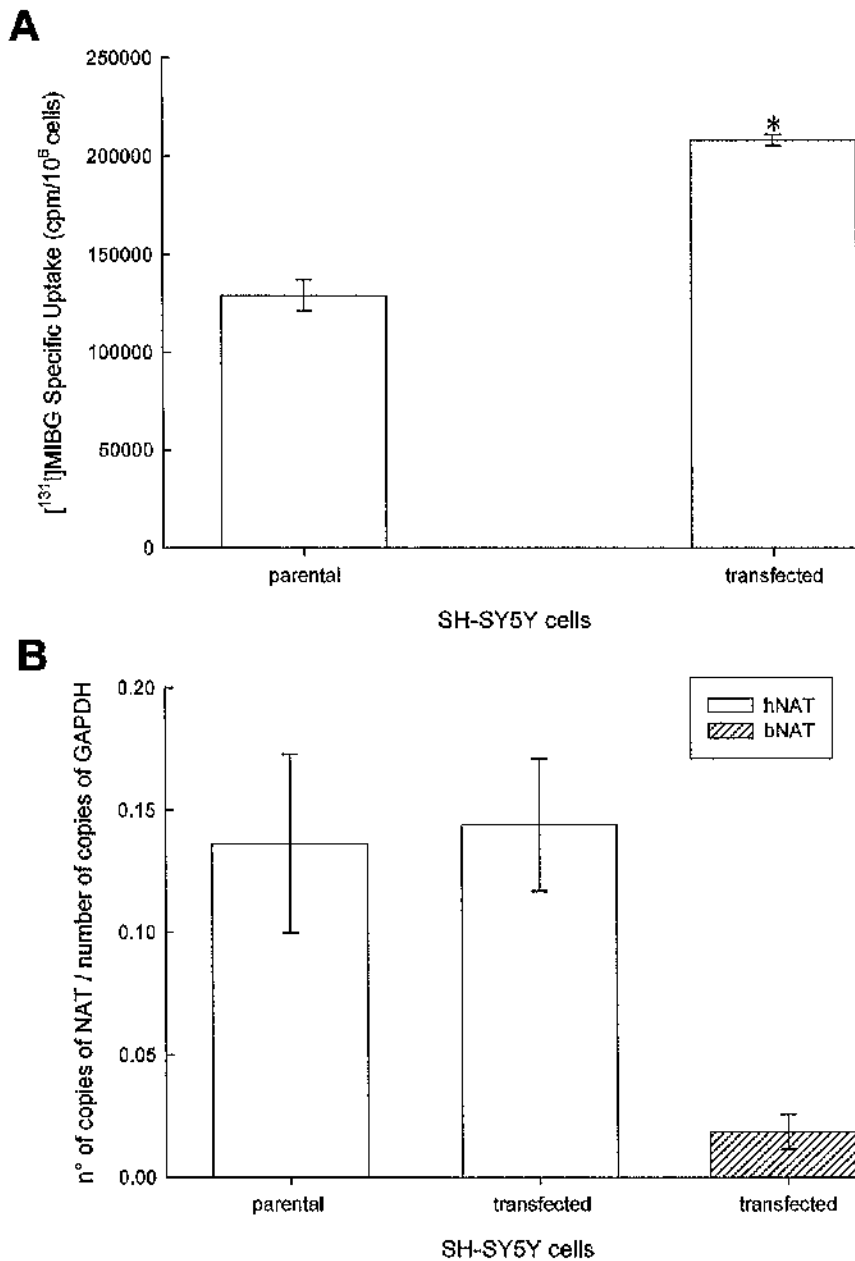


Figure 40. [¹³¹I]MIBG uptake capacity and NAT gene expression in SH-SY5Y parental cells and SH-SY5Y cells transfected with the plasmid pWAF1/NAT.

A) [¹³¹I]MIBG specific uptake in SH-SY5Y parental cells and cells stably transfected with the pWAF1/NAT plasmid. Cells were treated as described in Material and methods. Uptake was expressed as counts per minute (cpm) per 10⁶ cells. Means ± s.d. of measurements from three independent experiments (* significantly higher than parental cells, *t*-test: < 0.05).

B) Levels of mRNA of endogenous NAT (hNAT) in SH-SY5Y cells parental (1) or stably transfected with the pWAF1/NAT plasmid (2). Levels of mRNA of transgenic NAT (bNAT) (3). Using the RNA obtained from the neuroblastoma cell line, endogenous NAT (hNAT), transgenic NAT (bNAT) and GAPDH expression was assessed by reverse transcription and real-time PCR amplification. The results are means ± s.d. of three separate determinations in triplicate.

3.3.3.2 Changes in [¹³¹I]MIBG uptake capacity in SH-SY5Y cells transfected with pWAF1/NAT plasmid after exposure to external beam radiation

Uptake assay was performed 48 hours after external beam radiation treatment to allow activation of the WAF1 promoter (see section 3.3.2.1). However, the [¹³¹I]MIBG uptake capacity changes with variations in cell density [114, 115]. Therefore, uptake assay was conducted taking into consideration cell death occurring after ionising radiation treatment. In particular, a range of cell densities was used for each dose of external beam radiation. [¹³¹I]MIBG uptake assay was performed only with cells with a density comparable to that of unirradiated cells. SH-SY5Y cells stably transfected with pWAF1/NAT plasmid concentrated [¹³¹I]MIBG more efficiently than the unirradiated cells 48 hours after exposure to 4 ($p = 0.004$) or 8Gy ($p = 0.023$) of γ -rays (Figure 41). In particular, SH-SY5Y cells stably transfected with pWAF1/NAT plasmid and treated with 4 and 8Gy of γ -rays were able to accumulate the radiopharmaceutical 1.5 and 1.65 times more efficiently than unirradiated transfectants respectively. However, there was no significant difference in uptake capacity between SH-SY5Y transfectants that received 4Gy of γ -rays and those that were exposed to 8Gy ($p > 0.1$). These findings indicate that irradiating SH-SY5Y cells transfected with the pWAF1/NAT plasmid, results in [¹³¹I]MIBG uptake enhancement.

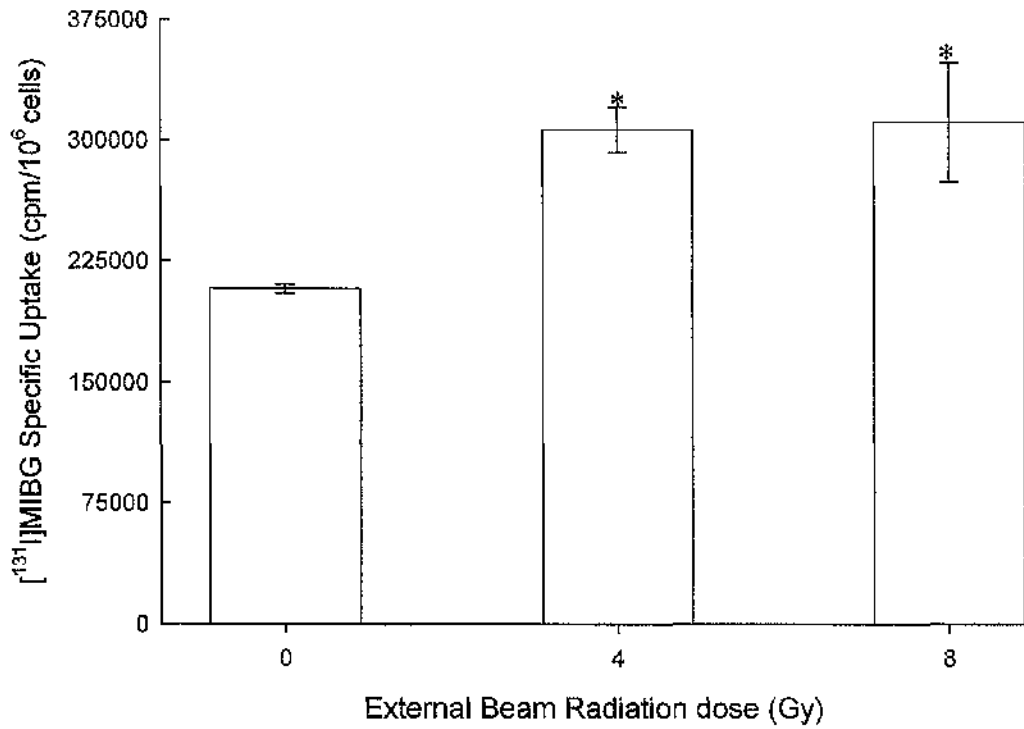


Figure 41. Effect of external beam radiation on [¹³¹I]MIBG uptake capacity of SH-SY5Y transfectants.

Cells were stably transfected with the pWAF1/NAT plasmid and 48 hours after exposure to external beam radiation [¹³¹I]MIBG specific uptake capacity was measured. Cells were treated as described in Material and methods. Uptake was expressed as counts per minute (cpm) per 10⁶ cells. Means ± s.d. of measurements from three independent experiments (* significantly higher than unirradiated control, t-test: < 0.05).

3.3.3.3 Changes in NAT mRNA levels in SH-SY5Y cells transfected with the pWAF1/NAT plasmid after exposure to external beam radiation

As shown in Figure 40A, the untransfected SH-SY5Y cells already possess a capacity for accumulating [¹³¹I]MIBG. In order to determine the contribution of both hNAT and bNAT to concentration of radiopharmaceutical, real-time PCR specific for both mRNAs was performed.

Untransfected SH-SY5Y cells irradiated with 4 or 8Gy of γ -rays expressed higher mRNA levels of NAT gene than unirradiated cells ($p < 0.05$, Figure 42). However, there was no significant difference in transcription levels of endogenous NAT between SH-SY5Y cells irradiated with 4Gy and cells exposed to 8Gy of γ -rays ($p > 0.1$).

Transcript levels of both variants of the NAT gene (hNAT and bNAT) significantly increased ($p < 0.05$) in cells transfected with the pWAF1/NAT plasmid and exposed to γ -rays (Figure 43). The transcript levels of the endogenous NAT gene (hNAT) in transfected cells were not significantly different from that found in untransfected cells ($p > 0.1$, Figure 40B).

Interestingly, mRNA levels of the endogenous NAT (hNAT) were 2.7 (after 8Gy-radiation), 4.1 (after 4Gy-radiation) and 7.8 (no radiation) times higher than the transgenic NAT (bNAT) levels (Figure 43). However, the radiation-induced enhancement of expression relative to the unstimulated level was greater for the transgene NAT (bNAT) than for the endogenous NAT (hNAT) gene. In particular, the transgene (bNAT) mRNA levels increased 3-fold or 6-fold when cells were exposed to 4 or 8Gy respectively, whereas the mRNA levels of the endogenous NAT (hNAT) increased 1.7-fold or 2.1-fold in cells exposed to 4 or 8Gy radiation respectively.

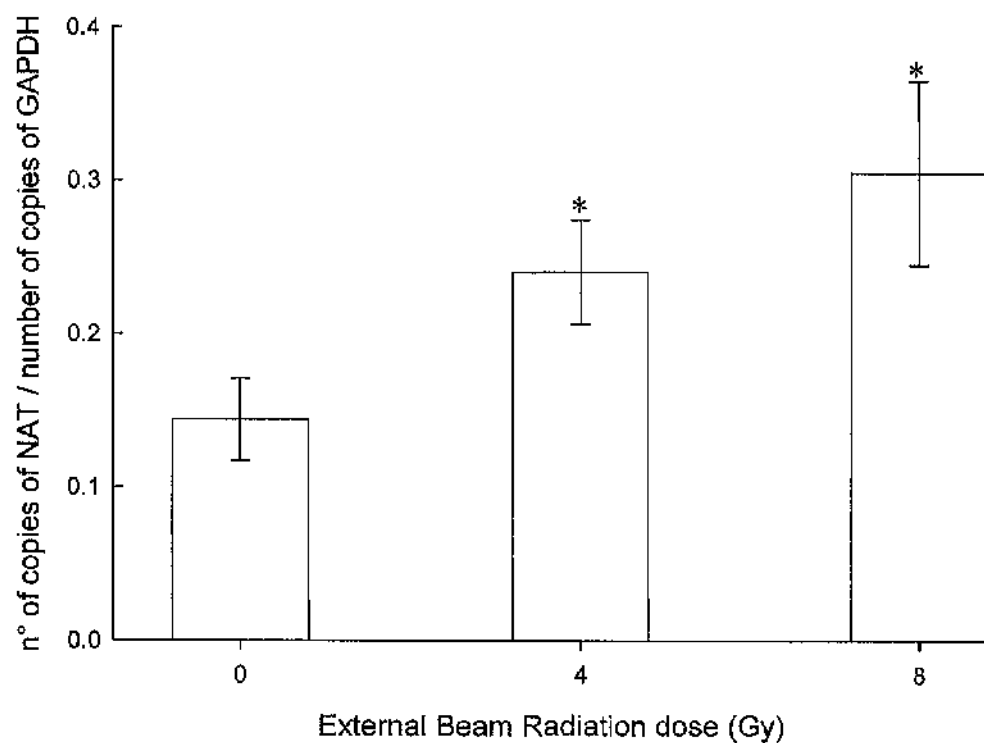


Figure 42. Effect of external beam radiation on endogenous NAT (hNAT) gene expression in SH-SY5Y cells. Using the RNA obtained from the neuroblastoma cell line, hNAT and GAPDH expression was assessed by reverse transcription and real-time PCR amplification. The results are means \pm s.d. of three separate determinations in triplicate (* significantly higher than unirradiated control, *t*-test: $p < 0.05$).

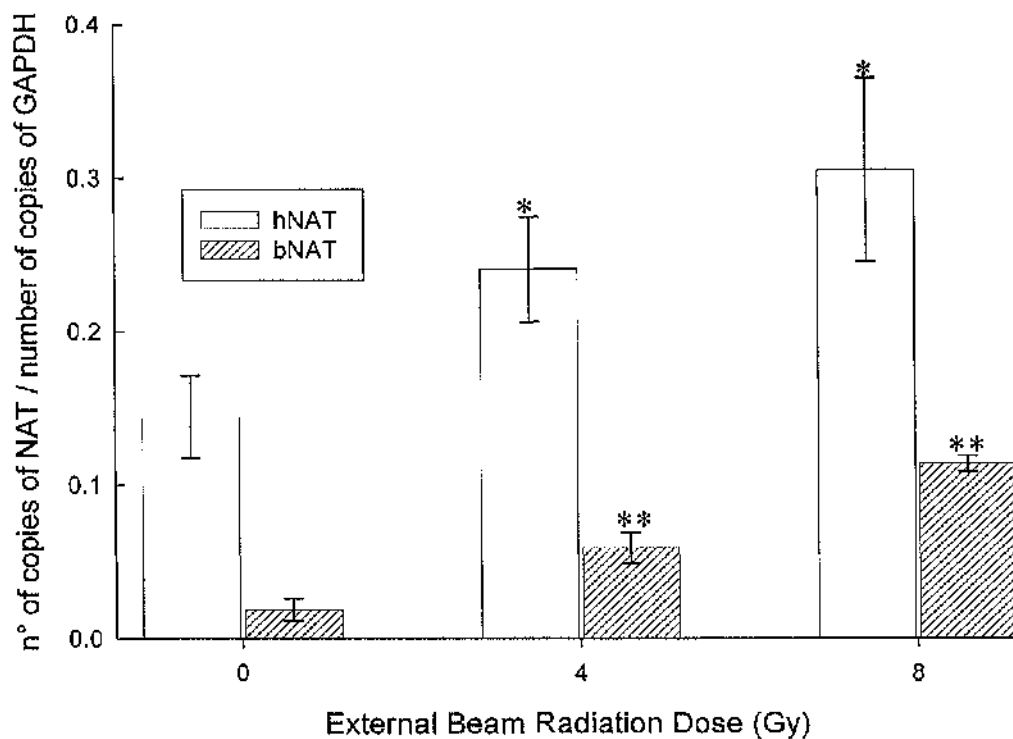


Figure 43. Effect of external beam radiation on endogenous NAT (hNAT) and transgenic NAT (bNAT) gene expression in SH-SY5Y cells stably transfected with the pWAF1/GFP plasmid. Using the RNA obtained from the neuroblastoma cell line, endogenous NAT (hNAT), transgenic NAT (bNAT) and GAPDH expression was assessed by reverse transcription and real-time PCR amplification. The results are means \pm s.d. of three separate determinations in triplicate (* [for hNAT] or ** [for bNAT] significantly higher than unirradiated control, *t*-test: $p < 0.05$).

3.3.3.4 [¹³¹I]MIBG toxicity assay in SH-SY5Y cells transfected with the pWAF1/NAT plasmid

An assessment of the effect of γ -radiation on [¹³¹I]MIBG toxicity was conducted in SH-SY5Y cells stably transfected with the pWAF1/NAT plasmid. Cells were exposed to 0-8Gy of γ -rays and 48 hours later (time required for an optimal WAF1 promoter activation) were incubated for two hours with 0.2-1MBq/ml [¹³¹I]MIBG. Clonogenic assay was performed 24 hours after radiopharmaceutical incubation. [¹³¹I]MIBG toxicity to the cells was dependent on the activity concentration used. Exposure to γ -rays resulted in a higher [¹³¹I]MIBG toxicity to the cells in a dose-dependent manner (Figure 44). For example, 1MBq/ml radiopharmaceutical caused a survival fraction of 0.09 in cells that did not receive any external beam radiation, whereas the same activity concentration generated a survival fraction of 0.0005 in cells exposed to 8Gy 48 hours earlier.

Curve fitting was performed using the clonogenic data shown in Figure 44 in order to quantify the effect of γ -radiation on the increase of NAT expression controlled by the WAF1 promoter. The linear-quadratic model with the expression $S = e^{-\alpha D - \beta D^2}$ was used to fit cell kill data generated by the low-LET radiation of [¹³¹I]MIBG. S was the fraction of cells surviving a dose D and α and β were constants (for details see section 3.3.2.5).

Greater than 90% clonogenic cell kill after treatment with [¹³¹I]MIBG was achieved regardless of the pre-exposure dose of external beam radiation. Therefore, for comparison of the effect of external beam radiation on [¹³¹I]MIBG toxicity the activity concentration required to reduce clonogenic survival to 10% was chosen. The inhibitory concentration (10%) (IC₁₀) values (which represent the [¹³¹I]MIBG activity concentration required to generate 10% surviving fraction) of the radiopharmaceutical were then calculated (Table 2). The [¹³¹I]MIBG toxicity increased in cells that received at least 2Gy pre-irradiation compare to non pre-irradiated cells. Specifically, the [¹³¹I]MIBG IC₁₀ at 0Gy was 1.3, 2.3, 3.4 and 5.4 times the IC₁₀ at 2, 4, 6 and 8Gy respectively. Considering the cells that have received a radiation dose (2 to 8Gy) of γ -rays, the [¹³¹I]MIBG IC₁₀ decreased in a dose-dependent manner.

These findings show that in SH-SY5Y cells stably transfected with the pWAF1/NAT plasmid, the effectiveness of [¹³¹I]MIBG treatment increased when cells were pre-exposed to γ -radiation.

On the basis of the [¹³¹I]MIBG uptake results (shown in section 3.3.3.2) and mRNA levels of both endogenous and transgenic NAT genes (shown in section 3.3.3.3) collected in SH-SY5Y cells (stably transfected with the pWAF1/NAT plasmid), it is likely that the enhanced [¹³¹I]MIBG toxicity, achieved by γ -rays exposure, could be the result of upregulation of both endogenous and transgenic NAT genes.

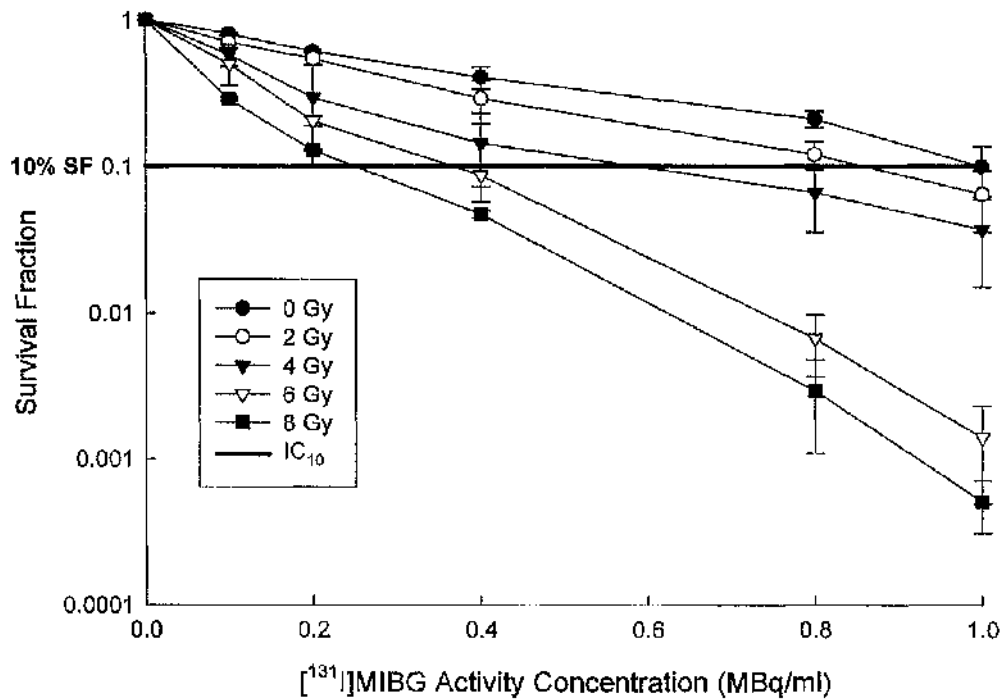


Figure 44. Effect of external beam radiation pre-exposure on [¹³¹I]MIBG toxicity in SH-SY5Y cells stably transfected with the pWAF1/NAT plasmid. Cells were treated as described in Material and methods. In particular, cells were exposed to 0, 2, 4, 6 or 8Gy external beam radiation. After 48 hours cells were treated with 0-1 MBq/ml [¹³¹I]MIBG. Means ± s.d. of measurements from three independent experiments.

E.B. dose (Gy)	[¹³¹ I]MIBG IC ₁₀ activity concentration (MBq/ml)
0	1.13
2	0.85
4	0.49
6	0.33
8	0.21

Table 2. Effect of external beam radiation pre-exposure on [¹³¹I]MIBG toxicity in SH-SY5Y cells stably transfected with the pWAF1/NAT plasmid. The [¹³¹I]MIBG activity concentrations needed to generate IC₁₀s for each external beam dose were calculated after applying the linear-quadratic model with the expression $S = e^{-\alpha D - \beta D^2}$. S was the fraction of cells surviving a dose D , α and β were constants, and e is the mathematical constant equal to approximately 2.71828183.

3.3.4 Evaluation of the WAF1 promoter in UVW glioma cells

UVW glioma cells, which normally do not express the NAT gene, were also transfected with the pWAF1/NAT plasmid. This cell line was chosen because it does not express endogenous NAT (hNAT) and does not possess any capacity of active accumulation of [¹³¹I]MIBG. Therefore, this characteristic simplifies the analysis of the transgenic NAT (bNAT) expression controlled by the WAF1 promoter. Therefore, any change in [¹³¹I]MIBG uptake capacity of UVW glioma cells is attributable exclusively to the transgenic NAT (bNAT) activity.

External beam pre-irradiation effects on [¹³¹I]MIBG uptake (Figure 45) and toxicity (Figure 46) were performed as described above.

3.3.4.1 [¹³¹I]MIBG uptake assay in UVW cells containing the plasmid pWAF1/NAT

Untransfected UVW cells (filled circle, Figure 45) had a negligible capacity to actively uptake [¹³¹I]MIBG. This condition did not change after exposing untransfected UVW cells to 4 or 8Gy-radiation (open circle and filled triangle respectively, Figure 45).

After transfection with the pWAF1/NAT construct, the cells acquired a significant uptake capacity (about 20000 cpm / 10⁶ cells; open triangle, Figure 45), displaying 20-fold increase. This indicates that in tumour cells the WAF1 promoter is active ("leaky") also in absence of ionising radiation, confirming experimental data discussed in section 3.3.2.1 and previous reports [135, 235, 236].

After γ -irradiation, UVW cells, stably transfected with the pWAF1/NAT construct, exhibited greater ability to accumulate the radiopharmaceutical in a dose-dependent manner (Figure 45). The highest uptake value in transfected cells treated with 4Gy radiation (filled square) was registered at 48 hours (33-fold increase) and with 8Gy (open square) it was recorded at 24 hours (39-fold increase). A decline in uptake ability was observed 72 hours after the irradiation. It is likely that this decrease seen 3 days after the radiation treatment depended on cellular mechanisms responding to the radiation insult. This in turn could have resulted in a progressive decrease of any transcription activity of genes that are not essential for survival.

These results indicate that also in UVW glioma cells, transfected with the pWAF1/NAT construct, the WAF1 promoter is inducible by ionising radiation. Its

induction led to upregulation of the transgenic NAT (bNAT) gene, and in turn in enhanced capacity for cellular [¹³¹I]MIBG accumulation.

3.3.4.2 [¹³¹I]MIBG Toxicity assay in UVW cells containing the plasmid pWAF1/NAT

In cell kill experiments, exposure to increasing γ -ray doses enhanced the toxicity of [¹³¹I]MIBG to the transfected cells in a dose-dependent manner (Figure 46).

Greater than 50% clonogenic cell kill after treatment with [¹³¹I]MIBG was achieved regardless of the pre-exposure dose of external beam radiation. Therefore, for comparison of the effect of external beam radiation on [¹³¹I]MIBG toxicity the activity concentration required to reduce clonogenic survival to 50% was chosen. The IC₅₀ values of the radiopharmaceutical were calculated as described in the experiments regarding the SH-SY5Y cells (section 3.3.3.4). The [¹³¹I]MIBG IC₅₀ values decreased in a dose-dependent manner (Table 3). For example, in order to kill 50% of the unirradiated cell population 6.55MBq/ml [¹³¹I]MIBG was needed. Slightly more than a half of this radiopharmaceutical concentration (3.55MBq/ml) was sufficient to cause the same toxic effect in cells exposed to 6Gy γ -rays.

These findings indicate that in UVW glioma cells, stably transfected with the pWAF1/NAT plasmid, the effectiveness of [¹³¹I]MIBG treatment increased when cells were pre-exposed to γ -rays. In this case, the WAF1 promoter-driven upregulation of the transgenic NAT (bNAT) gene is responsible for this effect.

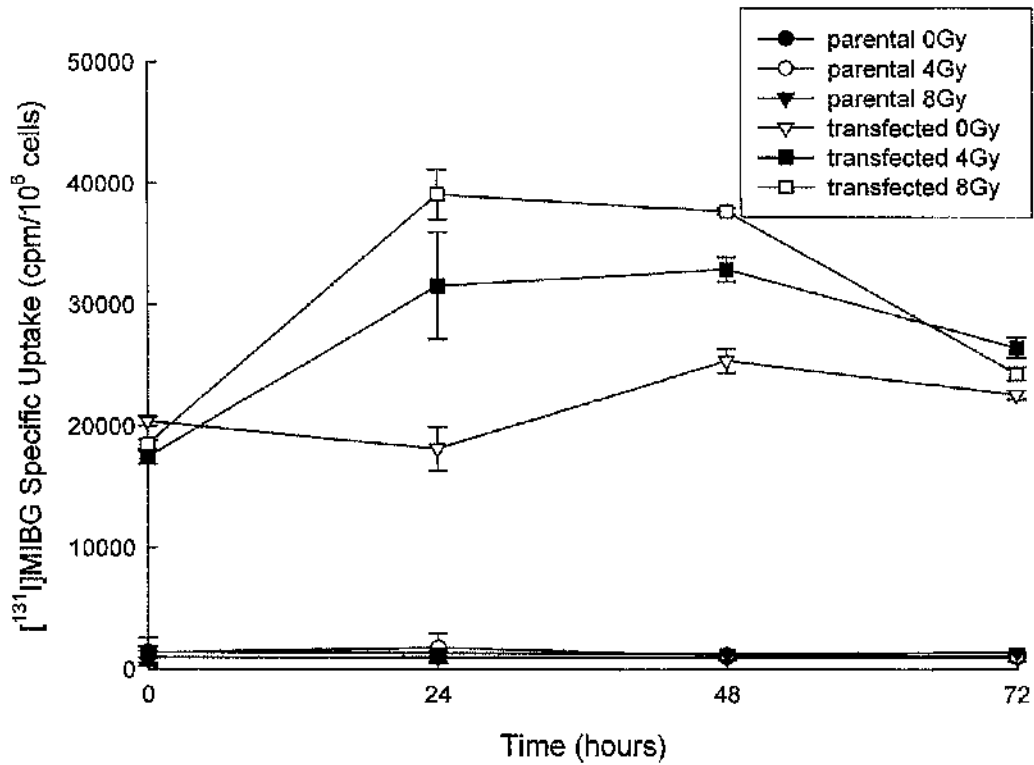


Figure 45. Effect of external beam radiation pre-exposure on [^{131}I]MIBG specific capacity of UWW parental and transfected cells with the pWAF1/NAT plasmid. Cells were treated as described in Material and methods. Uptake was expressed as counts per minute (cpm) per 10^6 cells. Means \pm s.d. of measurements from three independent experiments.

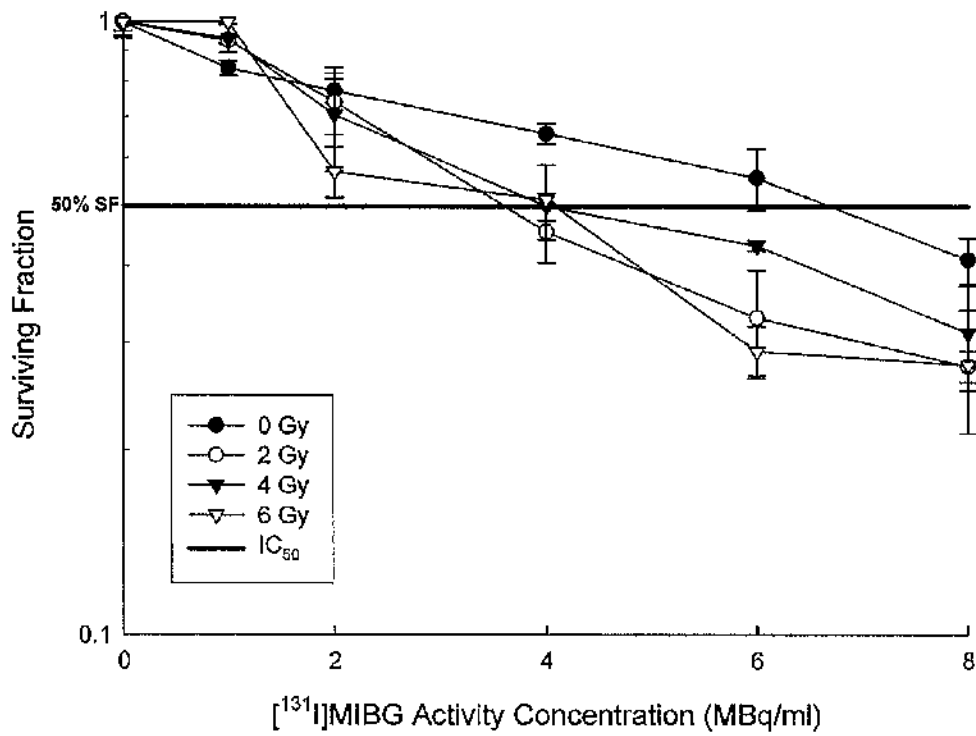


Figure 46. Effect of external beam radiation pre-exposure on [¹³¹I]MIBG toxicity in UVW cells transfected with the pWAF1/NAT plasmid.

Cells were treated as described in Material and methods. In particular, cells were exposed to 0, 2, 4 or 6 Gy external beam radiation. After 48 hours cells were treated with 0-8 MBq/ml [¹³¹I]MIBG. Means ± s.d. of measurements from three independent experiments.

External Beam. Dose (Gy)	[¹³¹ I]MIBG IC ₆₀ activity concentration (MBq/ml)
0	6.55
2	5.20
4	4.45
6	3.55

Table 3. Effect of external beam radiation pre-exposure on [¹³¹I]MIBG toxicity in UVW cells transfected with the pWAF1/NAT plasmid.

The [¹³¹I]MIBG activity concentrations needed to generate IC₆₀s for each external beam dose were calculated after applying the linear-quadratic model with the expression $S = e^{-\alpha D - \beta D^2}$. S was the fraction of cells surviving a dose D , α and β were constants, and e is the mathematical constant equal to approximately 2.71828183.

3.3.5 Summary of results

In the present study, it was shown that in two neuroblastoma cell lines (SH-SY5Y and SK-N-BE(2c), stably transfected with a plasmid containing the WAF1 promoter upstream of the GFP cDNA), the WAF1 promoter activity was inducible not only by external beam γ -rays but also by the β -emitter radionuclide ^{131}I , in the form of [^{131}I]MIBG, or by the α -emitter radionuclide ^{211}At , conjugated to benzylguanidine ([^{211}At]MABG). Furthermore, the minimum amount of time required for a substantial WAF1 promoter activation was observed to be 48 hours after treatment.

In vitro estimation of the equivalent radiation dose, corresponding to the administered activity of both radiopharmaceuticals, was performed. This demonstrated that, in SK-N-BE(2c) transfectants, the levels of WAF1 promoter activation caused by [^{131}I]MIBG or [^{211}At]MABG were comparable to that by γ -radiation. In SH-SY5Y transfectants, the levels of WAF1 promoter activation caused by [^{131}I]MIBG (but not by [^{211}At]MABG) were comparable to that by γ -radiation.

Finally, preliminary toxicity experiments showed that, after pre-exposure to γ -radiation, toxicity of [^{131}I]MIBG improved not only in neuroblastoma cells, but also in glioma cells (which normally do not express the NAT gene). In these experiments, both cell lines were transfected with the construct containing the NAT cDNA downstream of the WAF1 promoter sequence.

3.4 Discussion

Our results suggest that the radio-inducible WAF1 promoter is a promising tool for therapeutic gene expression controlled by targeted radiotherapy agents. In particular, we showed that the WAF1 promoter is inducible not only by γ -radiation as previously reported [135] but also by the β -particle emitter ^{131}I , in the form of [^{131}I]MIBG, and the α -particle emitter [^{211}At], in the form of [^{211}At]MABG. We also found that the WAF1 promoter is active in malignant cells that were not exposed to radiation. Moreover, recent studies showed that the "leakiness" of this promoter is not present in normal cells [235].

The use of the radiopharmaceutical [^{131}I]MIBG has achieved favourable remissions and manageable toxicity in neuroblastoma treatment [107-110, 247]. However, improvement is needed to achieve long-term cure. The combination of gene therapy with targeted radiotherapy is a promising approach to address this issue [2]. Recently, it has been shown that improvement of MIBG accumulation in neuroblastoma cells was possible after transfection with cDNA of the bovine NAT gene [98, 187]. In our strategy, the WAF1 promoter was chosen as a driving element of transgene expression. Recent studies showed that this promoter is inducible by X-rays in tumour cells *in vitro* [135, 236] and *in vivo* [235]. The latter article indicated also that the WAF1 promoter is "leaky" only in malignant cells not in normal tissue, introducing a second level of specificity. Furthermore, hypoxic conditions induce WAF1 promoter activity [235], adding a further layer of regulation specificity. Hypoxic conditions are often present in areas of solid tumour where blood circulation is compromised because of disorganised blood vessels and tumour cells that grow at a rate higher than the developing capillary network of the mass [248]. Therefore, WAF1 promoter activation enhanced by hypoxic conditions, together with ionising radiation, could be highly beneficial to achieve overexpression of the NAT transgene specifically in neuroblastoma tumours.

3.4.1 The WAF1 promoter is inducible by both [¹³¹I]MIBG and [²¹¹At]MABG

Our data using the WAF1 promoter driving the reporter gene GFP suggest that both benzylguanidine preparations ([¹³¹I]MIBG and [²¹¹At]MABG) are suitable for WAF1 promoter activation. The optimal time interval between the first (priming) and the second (therapeutic) radiopharmaceutical administration is 48 hours.

In terms of radiation dose (determined by clonogenic survival), [¹³¹I]MIBG is a more potent activator of the WAF1 promoter than [²¹¹At]MABG. The optimal combination of the analogues of the radiopharmaceutical, with respect to priming and therapy, must now be investigated *in vivo*. In this way it will be possible to determine tumour versus normal tissue damage.

In particular, [¹³¹I]MIBG treatment generated a better compromise between radiotoxicity and WAF1 promoter activation than [²¹¹At]MABG treatment in neuroblastoma cells. It is important to spare the tumour cells receiving the activating administration because in an *in vivo* scenario, where transfection efficiency is very low, the cells successfully transfected and targeted by [¹³¹I]MIBG will overexpress the NAT gene. This will enhance the effects of the therapeutic administration in at least two ways. First, the greater accumulation of radiopharmaceutical will result in a greater toxicity to the targeted cells. Second, the greater radiation crossfire to neighbouring untargeted cells will be more efficacious. Very low concentrations of radioactivity (1.85 – 29.6kBq/ml) given in the form of [²¹¹At]MABG (Figure 24 for SH-SY5Y cells and Figure 30 for SK-N-BE(2c) cells) caused a greater increase of fluorescence intensity levels compare to that generated by higher concentrations (0.2 – 2MBq/ml) of [¹³¹I]MIBG (Figure 23 for SH-SY5Y cells and Figure 29 for SK-N-BE(2c) cells). However, in accordance with previous findings [178], in our experiments the radiotoxicity of [²¹¹At]MABG to the cells (Figure 36C and Figure 37C) is approximately three orders of magnitude greater than that of the iodinated version of the radiopharmaceutical (Figure 36B and Figure 37B). Therefore, at low equivalent radiation doses (reflecting the toxicity of the radiopharmaceutical), [¹³¹I]MIBG treatment activates the WAF1 promoter to a level higher than [²¹¹At]MABG. Based on this observation, the use of beta-particle emitter ¹³¹I, in the form of [¹³¹I]MIBG, is more suitable for the first activating administration.

3.4.2 $[^{131}\text{I}]$ MIBG and $[^{211}\text{At}]$ MABG dose estimation

In this study, radiation dose estimation was performed by comparison of toxicity of external beam radiation with that of $[^{131}\text{I}]$ MIBG or $[^{211}\text{At}]$ MABG to neuroblastoma cells. Curve fitting was applied at the cell kill data of each radiation type and subsequently dose estimation was performed (for more details see section 3.3.2).

This estimation allowed the comparison of the three radiation types in inducing the WAF1 promoter. In our experiments, the most effective way to induce the activation of this promoter resulted from the use of $[^{131}\text{I}]$ MIBG with 48 hours required for significant WAF1 promoter activation ($p < 0.01$).

These findings will be used for future investigations on the use of a plasmid containing the NAT transgene (bNAT) under the control of the WAF1 promoter to enhance $[^{131}\text{I}]$ MIBG toxicity in neuroblastoma cells.

The methodology applied will serve as a foundation for future studies of the activating properties of alternative radiopharmaceuticals which are capable of targeting malignant cells. Examples include analogues of DNA precursors (e.g. radiolabelled IUdR) and tumour-specific radiolabelled antibodies.

Therefore, the dosimetry could be used as a reference to predict specific activation levels of the WAF1 promoter in response to specific radiation doses.

3.4.3 Possible applications of the radio-inducible WAF1 promoter for neuroblastoma treatment

It is possible to envisage a therapeutic strategy in which [¹³¹I]MIBG is used to trigger the WAF1 promoter, which controls the NAT transgene expression in transfected neuroblastoma cells. At least 48 hours after the first radiopharmaceutical administration (time necessary for an optimal noradrenaline transporter overexpression), treatment would be performed with a specific benzylguanidine preparation. The choice of the radiopharmaceutical would be based upon the size of the tumour. For instance, short-range emitters such as [¹²³I]MIBG or [¹²⁵I]MIBG would be suited to the treatment of circulating tumour cells, whereas mid-range α -emitters as [²¹¹At]MIBG would be more effective for treating small clumps of tumour cells. Finally, long-range β -emitters such as [¹³¹I]MIBG would be superior in the treatment of subclinical metastases or macroscopic tumours (see section 5.3 for more details).

Rescue of autologous haemopoietic stem cell after the use of high-dose chemotherapy or radiotherapy is central in improving outcome of patients older than 1 year who have metastatic disease [63, 249, 250]. Effective purging of tumour cells from haematopoietic cells may help minimize treatment-associated causes of relapse. Current bone marrow purging techniques for neuroblastoma use monoclonal antibodies directed against cell surface markers to isolate either tumour cells [251] or haematopoietic stem cells [252, 253]. These methods appear to be effective only if the tumour burden is less than 1%, and contaminating tumour cells have been detected after purging [249, 251-256]. Bone marrow purging in neuroblastoma patients could be the most practical application of the present gene therapy strategy. The harvested bone marrow tissue (containing neuroblastoma cells) would be transfected with the pWAF1/NAT construct. The targeted radiolabelled agent [¹³¹I]MIBG then would be administered and actively accumulated specifically by neuroblastoma cells. This should enhance the expression of the NAT transgene via WAF1 promoter activation and, therefore, generate a greater toxicity of a second administration of [¹³¹I]MIBG to neuroblastoma cells, resulting in sterilisation of contaminating tumour cells, with minimal toxicity to the bone marrow cells. However, a recent study reported that peripheral blood lymphocytes express the NAT gene [257]. With this in mind, it

would be interesting to investigate haemopoietic cells contained in normal bone marrow for NAT gene expression. This information is necessary prior to pursuing the envisaged system for bone marrow purging motioned above.

It would be also interesting to investigate the capability of using [^{123}I]MIBG or [^{125}I]MIBG to induce WAF1 promoter activation. In particular, [^{123}I]MIBG is currently employed as an imaging tool for neuroblastoma patients [103, 258]. If the use of this radiolabelled agent would activate the WAF1 promoter, this gene therapy strategy could be therefore applied to neuroblastoma patients undergoing a [^{123}I]MIBG scintigraphy. For instance, after inoculating into patients the pWAF1/NAT construct followed by [^{123}I]MIBG scintigraphy, the neuroblastoma cells should overexpress the NAT transgene, as controlled by the WAF1 promoter, and the patients therefore should be more sensitive to the targeted radiotherapy in the form [^{131}I]MIBG. It would therefore allow the use of [^{123}I]MIBG for a twofold aim: scintigraphy and sensitisation to [^{131}I]MIBG.

3.4.4 The endogenous NAT is overexpressed by ionising radiation, but the enhancement of the expression levels of transgenic NAT under the control of the WAF1 promoter is greater

We have shown that cell transfection with the pWAF1/NAT construct increased toxicity of [¹³¹I]MIBG treatment to neuroblastoma cells following prior exposure to γ -rays (Figure 44), because of NAT overexpression driven by the WAF1 promoter (Figure 43). The cells used in those toxicity experiments already expressed the endogenous noradrenaline transporter. The results from quantitative PCR specific for either the endogenous or the transgenic NAT mRNA, showed that the cellular expression levels of both transporters increased after exposure to γ -rays. Furthermore, the endogenous transporter levels were much higher than the transgenic transporter expression regardless of the pre-irradiation dose. However, the enhancement of expression levels compared to that of unirradiated cells was greater for exogenous NAT. This indicates the potential of pWAF1/NAT construct transfer to facilitate radiation-specific expression.

Interestingly, our results suggest that ionising radiation enhances the expression of the endogenous noradrenaline transporter. By comparing mRNA levels, it is apparent that the human transporter plays a bigger role than the transgenic transporter in both [¹³¹I]MIBG uptake-capacity and toxicity increase after pre-irradiation. Our findings are in line with a previous study, which showed that treatment with ionising radiation enhanced uptake of MIBG by neuroblastoma cells in culture [113]. Considering our real-time PCR results, it is possible to state that the previously reported enhancement of the cellular accumulation of MIBG could result from transcriptional activation of the noradrenaline transporter gene. Other molecules, such as cisplatin, doxorubicin, interferon- γ and phorbol esters, can also induce MIBG uptake in neuroblastoma cells [114, 115, 259]. In common with these agents, ionising radiation causes damage to the DNA, which enhances p53 expression. Ionising radiation can induce the expression of p53-dependent genes, such as the CIP1 gene, which encodes the cell cycle kinase inhibitor p21 [260]. It is possible that ionising radiation up-regulates the transcription of the noradrenaline transporter gene via a putative p53 consensus sequence in the promoter. Unfortunately, little is known about the promoter region upstream the NAT gene. A recent study characterized potential bindings sites for transcription

factors within 4 kb of the 5' untranslated region of the human NAT gene, including Sp1, AP-2, MRE-BP, SDR_RS, UCE.2, IRF-2, TFE-S and a cAMP response element (CRE) [261].

Additionally, several lines of evidence indicate that phosphorylation is involved in the regulation of NAT activity. In particular, Protein Kinase C (PKC) can downregulate NAT function by transporter phosphorylation, inducing the sequestration of the transporters from the plasma membrane [262-265]. Protein phosphatase also plays a significant role in the modulation of the NAT activity [265, 266]. Inhibition of phosphatase activity results in limited recycling of the transporter to the plasma membrane by increasing phosphorylation status of NAT [265].

In order to improve strategies that aim to induce the expression and function of NAT, elucidation of the mechanisms and cellular pathways of NAT regulation will be essential.

It is clear from our findings that ionising radiation up-regulates the transgenic NAT gene in neuroblastoma cells in culture. In order to determine the potential for the enhancement of MIBG uptake of the transgenic construct in the absence of endogenous NAT expression, we transfected a glioblastoma cell line (UWV) which normally does not express the NAT gene with the pWAF1/NAT vector. We then performed a cell kill study after administering [¹³¹I]MIBG to pre-irradiated transfected cells. Pre-incubation with radiopharmaceutical resulted in an increase in MIBG uptake and toxicity. These findings suggest that the transgenic NAT is upregulated through WAF1 promoter activation in glioma cells that normally do not express the noradrenaline transporter.

In vivo studies demonstrated that the WAF1 promoter is specifically active in the tumour mass that did not receive any dose of radiation, whereas it remains silent in normal tissue [235]. Moreover, it was reported that hypoxic conditions enhanced the promoter activation in malignant cells in absence of radiation. Thus, the WAF1 promoter may display several levels of specificity, such as radiation, hypoxia and tumour. These features render the WAF1 promoter a strong candidate for control of transgene expression in a tumour- and radiation-specific manner.

Bearing in mind these observations, with our novel approach it will also be possible to treat with [¹³¹I]MIBG therapy tumours, such as glioma, which normally are not eligible for targeted radiotherapy. In our laboratory it was observed that

after transfection of the NAT gene into a human glioma cell line, [131 I]MIBG was actively concentrated, resulting in increased toxicity [187, 188]. This demonstrated the potential of gene therapy in combination with MIBG-targeted radiotherapy for the treatment of tumours of non-neuroectodermal origin [187].

4 Chapter 4

Immunoliposomes: a novel gene delivery system

4.1 Introduction

For an effective gene therapy strategy the delivery of DNA to the target-cells must be efficient and at the same time safe for the patient.

4.1.1 Naked DNA

The simplest approach to gene delivery is direct gene transfer with naked plasmid DNA. Since the demonstration of the possibility of gene expression by naked plasmid injected intramuscularly [267], there has been increasing interest in this form of gene delivery. Recent studies have shown that other tissues such as skin, liver, kidney and some tumours are also amenable to naked DNA-mediated gene transfer [268, 269]. However, because of clearance by the mononuclear phagocyte system and degradation by serum nucleases, the expression level and extension of injected naked DNA are generally limited. Thus, systemic administration of naked plasmid DNA generally results in little and localised gene expression in major organs for short periods of time.

Systemic targeted gene delivery therefore requires the use of vector technology. A vector which will deliver more efficiently and safely the therapeutic DNA to the target-cells, with a limited toxicity sparing surrounding tissue, is necessary for a successful gene therapy strategy. The ideal vector must have a high specificity for target-cells, low toxicity, and long systemic circulation. It also must provide protection for the transgenes working as a shield reducing the DNA degradation.

In the field of gene delivery, two main types of vector system are currently investigated: viral and non-viral vectors.

4.1.2 Viral vectors

In general, vectors derived from viruses are more efficient gene-delivery systems *in vivo*, but are associated with a few limitations such as toxicity and strong antiviral host immune responses [270, 271].

4.1.2.1 Retrovirus

The first class of vector to be developed for gene therapy was based on retrovirus [272], specifically on the simple Moloney murine leukaemia virus (MLV) - a C-type oncoretrovirus. To date, retroviral vectors are the second most utilised system in gene therapy clinical trials after adenoviruses [273]. A limitation to the efficacy of C-type retrovirus vectors is that they can only access the cell nucleus in the case of nuclear membrane breakage. Therefore, they can only transduce proliferating cells.

4.1.2.2 Lentivirus

Great interest has focused on the development of lentivirus vectors mostly based on human immunodeficiency virus (HIV), which can naturally penetrate an intact nuclear membrane and transduce non-dividing cells. Therapeutic efficacy has been shown in animal models of Parkinson disease [274], sickle cell disease [275] and haemophilia A [276].

4.1.2.3 Adenovirus

Adenoviral vectors are currently the most popular technology used in gene therapy clinical trials [273]. They are efficient vectors with respect to delivery of their genetic pool to the cell nucleus [277]. Further, adenoviral vectors have been employed in several clinical trials in cancer patients with encouraging results [278-288].

4.1.2.4 Adeno-associated virus

Adeno-associated virus (AAV)-based vectors have recently gained popularity as potential vectors for gene therapy. The major advantages of using AAV are non-pathogenicity [289], long-term expression of transgenes [290], relatively low immunogenicity [291-293] and high infectivity of both dividing and non-dividing cells [293-295]. A clinical trial involving haemophilia B patients reported successful transfection and expression of human blood coagulation factor IX after muscle-

directed gene transfer of an AAV vector [296]. Other trials for cystic fibrosis, prostate cancer and several CNS disorders are also ongoing [273].

4.1.2.5 Herpes simplex virus

Herpes simplex virus-1 is the largest of all viruses that are being developed for gene therapy and replication-defective HSV-1 vectors can accommodate up to 40 kb of foreign DNA [297], allowing the delivery of several separate expression cassettes, or large single genes [298]. HSV-1 vectors have been used in gene delivery approaches to central nervous system diseases [299-301], cancer [302, 303], peripheral neuropathy [304, 305] and chronic pain [306, 307]. An alternative approach to cancer gene therapy has been to exploit the natural ability of viruses to replicate and lyse cells [308]. In cancer gene therapy HSV-1 thymidine kinase-depleted vector had promising oncolytic properties in glioma animal models [309], but the thymidine kinase mutation rendered the virus insensitive to antiherpetic drugs. A safer generation of vectors with a mutation at the γ -34.5 gene (encoding the ICP34.5 product, which inhibits apoptosis by infected cells) are currently used in a phase II trial for head and neck cancer and a phase I for high grade glioma [273] (trial ID UK-66 and UK-50).

4.1.3 Non-viral systems

Viral vectors are highly efficient at transducing cells. However, safety issues such as immunogenicity, integration into the host chromosome and toxicity make non-viral delivery systems an attractive alternative. Lipid-based delivery systems bring several advantages: *in vivo* safety, lack of immunogenicity, protection against degradation, ease of preparation and up-scaling, and relatively unlimited size of nucleic acids that can be encapsulated.

The first studies involving DNA or RNA encapsulation into large, mostly negatively charged liposomes were conducted more than two decades ago [310-312]. DNA cellular uptake and transfection were reported using these liposomes [313-316], however the nucleic acid encapsulation efficiency was very limited. Furthermore, the presence of negative charges also induces opsonisation (interaction with plasma proteins) causing them to be rapidly cleared from the blood stream and to accumulate in the mononuclear phagocyte system (MPS). *In vivo* transfection efficiency of targeted tissues other than liver or spleen is therefore limited [317, 318].

4.1.3.1 Gene delivery via cationic liposomes

A significant improvement to DNA transfection efficiency was made when Felgner published for the first time a study showing that complexes of plasmid DNA and the cationic lipid dioleyl-trimethylammonium chloride (DOTMA) with dioleoyl-phosphatidylethanolamine (DOPE), were avidly internalised by cells resulting in high expression of the plasmid DNA [319, 320]. Subsequently many applications of alternative cationic lipids and helper lipids were reported by others, bringing to the development of generations of lipid-based vectors with increasing *in vitro* transfection efficiencies [321-324]. Improved variants including fusogenic [325], pH- [326, 327] or thermo-sensitive [328, 329] liposomes have been successfully employed.

4.1.3.2 Drug delivery via pegylated liposomes

High serum concentrations, scavenging mechanisms like the mononuclear phagocyte system (MPS) and biological target-cell accessibility are some of the main obstacles that effective *in vivo* delivery systems have to overcome. The first generation of cationic liposomes tended to form aggregates *in vivo* resulting in

rapid clearance by macrophages, most likely because of their positive surface charge [330, 331]. The introduction of a Polyethylene glycol (PEG) to liposome formulations dramatically decreased the uptake of liposomes by the MPS and prolonged the circulation time in blood [332-334]. Even though the functional mechanism of PEG in the MPS recognition process is uncertain, Papahadjopoulos et al. (1991) proposed a model where stabilization results from local surface concentration of highly hydrated groups of PEG that sterically inhibit both electrostatic and hydrophobic interactions of a variety of blood components at the liposome surface [333]. The use of this type of liposome formulation (stealth liposomes) has led to a significant improvement in liposomal drug delivery to solid tumours via the systemic route. There has been strong evidence suggesting that given a long circulation time, liposomes encapsulating anticancer drugs accumulate preferentially in the tumour site due to the leaky immature vasculature in the tumour, exhibiting enhanced therapeutic efficacy [333, 335, 336]. This can be considered as a passive tumour-targeting and has produced a clinical-approved anticancer drug called Doxil [337].

4.1.3.3 Immunoliposomes

Many studies have tried to develop ways to enhance the specificity of liposomal delivery systems, generally by conjugating ligands to the liposome surface that will initiate a specific interaction with the target cells. Ligands include vitamins [338], glycoproteins [339], peptides [340], oligonucleotides aptamers [341] and the most widely used ligands in the form of antibodies or antibody fragments. The first study using monoclonal antibodies (mAbs) conjugated to liposomes was reported by Torchilin et al. [342], who showed that anti-myosin immunoliposomes maintained their capacity to specifically bind to the receptor on the target cells. Subsequently, other groups also reported covalent coupling of mAbs to liposomes for successful specific cell targeting *in vitro* [343-348]. However, the *in vivo* application of immunoliposomes has been restrained by poor stability in the circulation [349-351] and rapid clearance by the MPS [352-356].

Based on the numerous reports of the advantages of PEG-coated liposomes in reducing uptake by organs of the MPS, as mentioned earlier, attempts have also been made to use PEG to form sterically stabilised immunoliposomes. For the attachment of antibodies to the surface of PEG-liposomes, two main strategies

have been employed: coupling of the antibody directly to the liposome bilayer (type A, Figure 47) and attachment of the antibody to the terminal end of PEG molecule (type B, Figure 47) [357-359]. The latter strategy seems to be preferred, as it should minimise interference of the PEG with the antibody-antigen interaction (steric hindrance) and with coupling of the antibody to the liposome [359].

4.1.3.4 Coated Cationic Liposomes (CCLs)

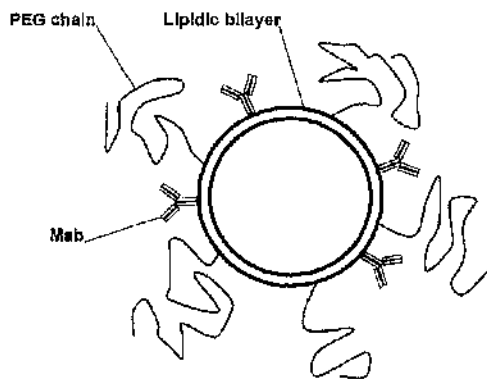
Pegylated lipids and covalently bound mAbs to the terminal end of the PEG molecule have also been employed for the formulation of liposomes for DNA delivery. In the present study a novel method of preparation of DNA encapsulating liposomes, first introduced by Allen and co-workers [360], was assessed. Briefly, these particles consist of a core made up of DNA in the form of oligonucleotides complexed to cationic lipid, which is coated by a layer of neutral lipids, including a lipid-anchored PEG polymer. This type of liposome formulation, called coated cationic liposomes (CCLs), presents high stability in serum and long circulation properties in mice and rats [141]. Successful applications *in vitro* and *in vivo* have been reported. Pagnan et al. [138] and Brignole et al [361], using CCLs targeted by antibodies directed against the disialoganglioside GD₂, showed inhibition of the proto-oncogene c-myc expression and growth inhibition of the GD₂-positive human neuroblastoma cell lines GI-LI-N and HTLA-230. Further, antitumour activity in mice bearing metastatic neuroblastoma xenografts was reported by Brignole et al. [96] using c-myc oligonucleotide encapsulated in CCLs directed against GD₂-positive cells. In a xenograft melanoma model, Pastorino et al. [362] showed significant tumour growth delay and increased average life span in mice treated with c-myc oligonucleotide encapsulated in anti-GD₂ CCLs compared with that of the control mice.

4.1.3.5 Anti-GD2 Coated Cationic Liposomes as gene delivery vectors in neuroblastoma

Based on these promising findings, we decided to take advantage of the anti-GD₂-CCLs technique to deliver plasmid DNA to the tumour site (Figure 48). In this study, for the first time, the anti-GD₂-CCLs technology will be used to encapsulate and deliver plasmid DNA (rather than oligonucleotides) to neuroblastoma cells, comparing transfection efficiency with that of conventional transfection reagents, such as Lipofectamine 2000 (Invitrogen, Paisley, UK).

Considering the properties of this delivery system such as long blood circulation and stability, low toxicity and preferential targeting of tumour sites, anti-GD₂ CCLs encapsulating plasmid DNA is a promising approach for gene therapy in neuroblastoma.

Type A



Type B

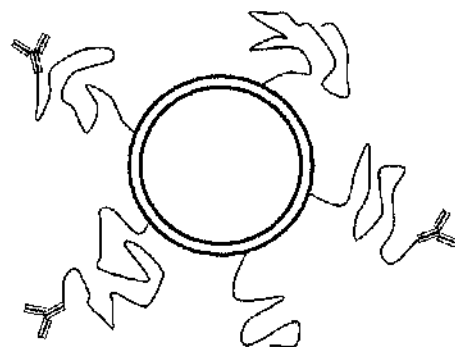


Figure 47. Schematic illustration of two types of antibody coupling on liposomes. Type A: PEG-immunoliposomes with antibody (mAb) directly attached to the lipidic bilayer; Type B: new type of PEG-immunoliposomes with antibody covalently linked to the distal terminal of DSPE-PEG-COOH.

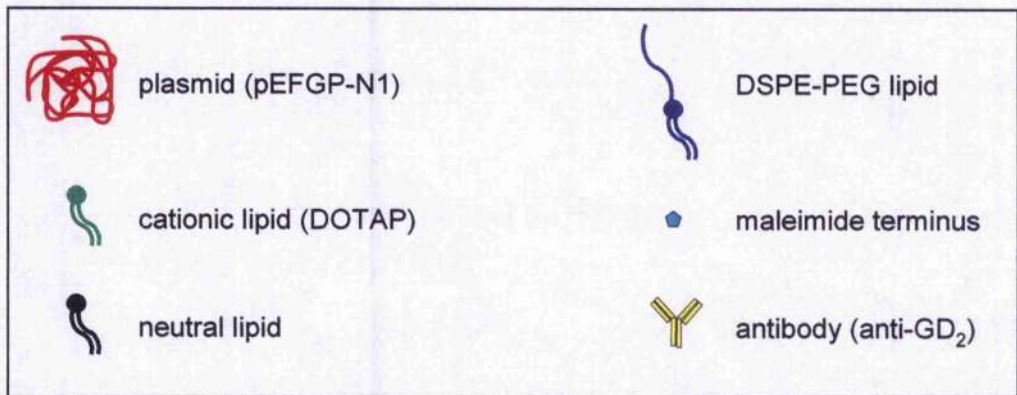
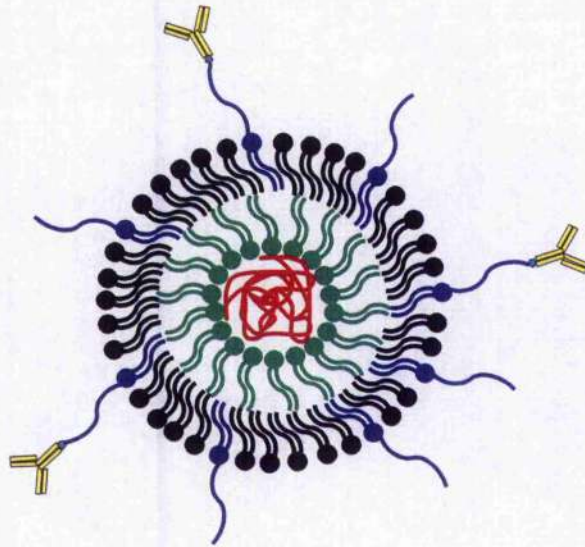


Figure 48. Schematic representation of anti-GD2-CCL encapsulating pEFGP-N1 plasmid DNA

4.2 *Materials and Methods*

4.2.1 Reagents and monoclonal antibody

Hydrogenated soy phosphatidylcholine (HSPC), cholesterol, 1,2-distearoylglycerol-3-phosphatidylethanolamine-N-polyethylene glycol-2000 (DSPE-PEG), a derivative of DSPE-PEG with a maleimide group at the distal terminus of the polyethylene glycol chain (DSPE-PEG-MAL), 1,2-dioleoyl-3-trimethylammonium propane (DOTAP) and rhodamine phosphatidylethanolamine (rhoda-PE) were purchased from Avanti Polar Lipids, Inc. (Alabaster, AL, USA). [³H]Cholesterol hexadecylether ([³H]CHE) was purchased from PerkinElmer LAS (UK) (Beaconsfield, Bucks, UK).

All the other reagents of biochemical and molecular biology grade were obtained from Sigma-Aldrich Co. (Gillingham, Dorset, UK).

The monoclonal antibody (mAb), an immunoglobulin (Ig) G2a isotype subclass, directed against disialoganglioside GD₂ (anti-GD₂) was purified from the supernatant of the 14.G2a murine hybridoma provided by R. A. Reisfeld (The Scripps Institute, La Jolla, CA) [363].

4.2.2 Cell lines and culture conditions

The neuroblastoma cell lines IMR-32 [364, 365] and GI-LI-N [365] were obtained from ECACC (Salisbury, Wiltshire, UK). SK-N-BE(2c) cells [185] were a gift from Dr. Montaldo (Genoa, Italy). Cells were maintained in the logarithmic phase of growth at 37°C in 75cm² plastic culture flasks (Corning Inc., Corning, NY) in a 5% CO₂-95% air humidified incubator. They were subcultured in RPMI-1640 medium supplemented with 10% heat inactivated foetal bovine serum, 50IU/ml sodium penicillin G, 50mg/ml streptomycin sulphate, and 2mM L-glutamine. Medium and supplements were obtained from Gibco (Paisley, UK).

4.2.3 FACS analysis of GD₂-positive and -negative neuroblastoma cells

The level of GD₂ expression was measured by fluorescence intensity detected by FACScan analysis. The GD₂-positive IMR-32 and GI-LI-N cells, and GD₂-negative SK-N-BE(2c) cells were seeded in 25mm² flasks at 37°C in a 5% CO₂-95% air humidified incubator. 48 hours later, 5 x 10⁵ cells were counted and resuspended for 30 minutes at 4°C in 100µl of purified anti-GD₂ 14G2a antibody (gift of Dr. M. Ponzoni, Gaslini Hospital, Genoa, Italy), diluted in PBS-1%FBS or in 100µl of PBS-1%FBS alone. After two washes in PBS-1%FBS, cells were incubated for 30 minutes at 4°C with 100µl of secondary fluorescent antibody FITC-anti-Mouse (IgG) (DAKO, Denmark). After two washes in PBS-FBS 1%, cell were resuspended in 500µl of PBS-1%FBS and analysed by the FACScan (BD Biosciences, Oxford, UK). The fluorescence intensity is proportional to the amount of the secondary antibody molecules (bound on the surface of each cell) specific for the Fc of the anti-GD₂ antibodies. Therefore the intensity of the fluorescence signal registered by the FACScan is proportional to the amount of anti-GD₂ antibody molecules bound to the antigen GD₂ expressed on the surface of the cells.

4.2.4 Plasmid DNA preparation and radiolabelling

The 7.164 kb pCMV-βgal plasmid contained the β-galactosidase reporter gene sequence under the control of the cytomegalovirus promoter (pCMV) (Clontech, Palo Alto, CA). The plasmid coding for enhanced green fluorescent protein (pEGFP-N1) was purchased from Clontech (Palo Alto, CA). Plasmids were purified from Escherichia coli DH5α with the maxiprep procedure by using the Qiagen Endofree Plasmid Giga Kit (Qiagen Ltd., West Sussex, UK), according to the manufacturer instructions. The size of the DNA was confirmed by 1% agarose gel electrophoresis. DNA was radio-labelled with [³²P]dCTP (370 MBq/ml) (GE Healthcare UK Ltd, Buckinghamshire, UK) using Rediprime™ II Random Prime Labelling System (GE Healthcare UK Ltd), according to the manufacturer instructions.

4.2.5 Liposome preparation and plasmid encapsulation

Coated cationic liposomes (CCLs) were synthesized as previously described [138, 360] with some modifications. 100µg of pEGFP-N1 plasmid with a trace of ³²P-labelled plasmid (to allow us to estimate the percentage of plasmid present at various stages of the procedure) was dissolved in 0.25ml distilled deionised water. Next, 0.51ml methanol and 0.25ml CHCl₃ containing 400nmol DOTAP (approximately 40 nanomoles of DOTAP / 10 micrograms of plasmid) were added, and the mixture was gently vortex mixed to form a monophasic mixture. After 30-minute incubation at room temperature, 0.25ml distilled deionised water and 0.25ml CHCl₃ were added. After mixing and centrifugation (800g for 7 minutes at room temperature), the aqueous methanol layer was removed. Under these conditions, which were developed in pilot studies using 10µg plasmid and various amounts of DOTAP, 90%-95% of the plasmid DNA was recovered in the organic phase. The resulting plasmid-to-lipid molar ratio was 1 : 1227, and a positive-to-negative charge ratio of 1 : 1.32 was obtained. Following this extraction, neutral lipids were added at the following molar ratios with respect to the amount of DOTAP used above: HSPC 15x, Cholesterol 3x, DSPE-PEG 0.24x or DSPE-PEG-MAL 0.06x. In some experiments, trace amounts of [³H]CHE and/or rhodamine phosphatidylethanolamine (rhoda-PE) were added as lipid labels. Next, 0.9ml distilled deionised water was added, and the mixture was vortex mixed and then emulsified by sonication in water bath 8 times for 1 minute. The organic phase was evaporated with the use of a rotary evaporator under a gentle stream of nitrogen (Buchi, Flawil, Switzerland). During this procedure the sample appeared first as a gel, then, upon complete CHCl₃ evaporation, as a clear aqueous solution. The liposomes were then reduced in size to approximately 100nm by extrusion six times through 400-nm, six times through 200-nm and six times through 100-nm polycarbonate membranes (Avestin, Inc., Ottawa, ON, Canada) in a Liposofast extruder (Avestin, Inc.).

External buffer exchange of the liposomes was performed by passing them through a G-50 column, equilibrated and eluted with 25mM HEPES buffered saline, pH 7.4.

4.2.6 Coupling of anti-GD₂ MAb to liposomes

A previously described method [366], slightly modified by Pagnan et al. [367], was used to covalently link mAbs to the maleimide terminus of DSPE-PEG-MAL (Figure 49). To activate the anti-GD₂s for reactivity toward the maleimide, we utilized 2-iminothiolane (Traut's reagent) to convert exposed amino groups on the antibody into free sulfhydryl groups. A 20 : 1 mole ratio of 2-iminothiolane to mAb and 1 hour of incubation at room temperature with occasional mixing gave optimal mAb activation. After separation of thiolated mAb from iminothiolane, with the use of Sephadex G-25 column chromatography, the mAb was slowly added to a 5-ml test tube containing the liposomes (with encapsulated plasmid DNA) and a small magnetic stirring bar. Optimal coupling was obtained with the use of a phospholipid-to-mAb mole ratio of 1500–2000 : 1. Oxygen was displaced by running a slow stream of nitrogen over the reaction mixture. The tube was capped and sealed with Teflon tape, and the reaction mixture was incubated overnight at room temperature with continuous slow stirring. The resulting immunoliposomes were separated from un-reacted mAb by chromatography with the use of Sepharose CL-4B, sterilised by filtration through 0.2- μ m pore cellulose membranes (Millipore Corp., Bedford, MA), and stored at 4 °C. Coupling of MAb to liposomes was quantified by adding trace amounts of ¹²⁵I-labelled MAb to the coupling reaction with liposomes, followed by γ -counting (Cobra 5002; Canberra Packard, Meriden, CT). The amount of mAb coupled to the liposomes was 45–60 μ g/ μ mole of phospholipid. Coated cationic liposomes with covalently attached anti-GD₂ MAb and encapsulated pEGFP-N1 are referred to as GD₂-targeted liposomes and abbreviated anti-GD₂-CCL-pEGFP-N1 throughout this section (Figure 48).

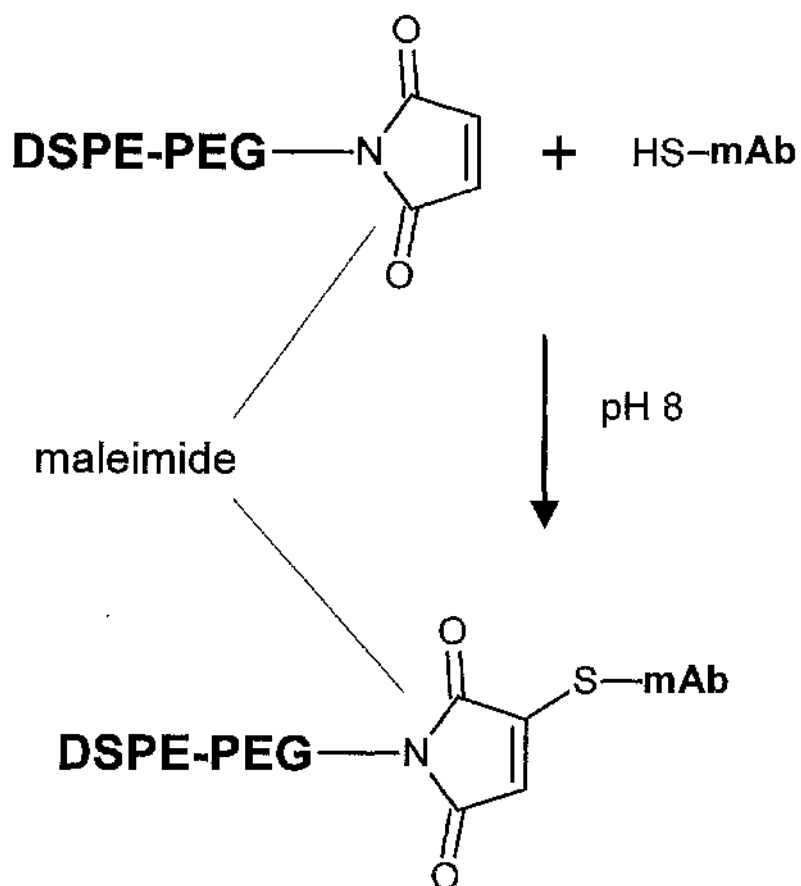


Figure 49. Reaction of the covalent coupling of activated monoclonal antibody (mAb) to the maleimide terminus of DSPE-PEG-MAL lipid.

4.2.7 CCLs size measurements

The sizes (in PBS, pH 7.4) were measured using a Malvern Zetasizer 4 (Malvern Instruments, UK). All measurements were performed at 25°C. Before the start of each measurement, standards (polystyrene latex beads, 300 nm, Sigma Co., UK, and Malvern Zetasizer standard, Malvern Instruments) were analyzed.

4.2.8 Gel retardation and DNase I protection assay

In order to assess the charge status of the liposome/DNA complex, gel retardation assay was performed. Briefly, an aliquot of the anti-GD₂-CCLs-pEGFP-N1 preparation was electrophoresed on 1% agarose gel containing ethidium bromide (0.5 µg/ml) in 1x TBE. DNA was visualised by UV illumination.

DNase I protection assay was employed to assess whether the plasmid DNA was encapsulated and therefore protected by the lipid layers from DNase I digestion. Briefly, 400nmoles of phospholipids of anti-GD₂-CCLs-pEGFP-N1 containing 2µg of DNA were incubated with 5 units of DNase I (Sigma) at 37°C for 1 hour and 30 minutes in 50mM Tris-HCl (pH 8.0), 0.1mM MgSO₄, and 0.1mM dithiothreitol in a final volume of 120 µl. To stop the enzymatic reaction, 7mM EDTA (pH 8.0) was added. Subsequently for some samples, 40mM of sodium deoxycholate was added for 1 hour at room temperature to dissociate the lipid/DNA complexes, and the DNA was purified with QIAquick PCR Purification Kit (Qiagen Ltd., West Sussex, UK).

4.2.9 Binding and uptake of liposomes

Neuroblastoma IMR-32 cells or control GD₂-negative SK-N-BE(2c) cells were incubated in complete medium for 2 hours at 37°C with 400nmoles of phospholipids of [³H]CHE-labelled liposomes with encapsulated pEGFP-N1. Cells were washed twice in PBS, treated with trypsin for 1 minute, and lysed with 1N NaOH prior to measurement of radioactivity. In competition experiments, a 50-fold excess of free MAb was added 30 minutes before addition of the liposomes. The non-specific isotype-matched antibody, code X 0943 (Dako Corp., Glostrup, Denmark), was used in competition experiments.

In internalisation experiments, GD₂-positive IMR-32 cells were incubated in complete medium 2 hours at 4°C or at 37°C with 400nmoles of phospholipids of [³H]CHE-labelled liposomes with encapsulated pEGFPN-1 plasmid. Sample preparation for radioactivity measurement was performed as described above. Similar experiments were conducted with liposomes as described above with the addition of rhodamine phosphatidylethanolamine (rhoda-PE) at 1 mol% of total phospholipids. Cells were washed twice in PBS, treated with trypsin for 1 minute, resuspended in PBS-1%FBS. Cells were thereafter analysed on a Becton Dickinson FACScan flow cytometer with an excitation wavelength of 488 nm and a collection wavelength of 585 ± 21 nm, which registers the fluorescence intensity of the rhodamine in each event (cell). Dead cells were gated out of the analysed cohort by forward and side scatter. The level of rhodamine fluorescence in live cells was determined using the Becton Dickinson CellQuest program. Briefly, the distribution of rhodamine fluorescence in the cell population was plotted against the cell number on a 4-log linear scale. For each sample, 10000 events (cells) were analysed.

4.2.10 Transfection experiments using anti-GD₂-CCLs-pEGFP-N1

For transfection of cells in adhesion, IMR-32 and GI-LI-N cells were plated at 5 x 10⁴ cells/well in 6-well plates containing complete medium and incubated for 48 hours at 37°C in standard conditions.

At the time of transfection, IMR-32, GI-LI-N and SK-N-BE(2c) cells in suspension or in adhesion were incubated for 2 hours at 37°C with a range of concentrations (0 – 3µg/ml) of pEGFP-N1 or pCMV-βgal plasmid encapsulated in anti-GD₂-CCLs.

Cells were then washed with PBS and left for 12, 24, 48 or 72 hours at 37°C with fresh medium. Cells in suspension were plated into small flasks first and incubated 24 hours at 37°C. At the same time a control set of cells were transfected with pEGFP-N1 or pCMV- β gal plasmid using Lipofectamine 2000 in accordance with the manufacturer's instructions (Invitrogen, Paisley, UK). For the cells transfected with pEGFP-N1, fluorescence intensity levels were analysed microscopically and by FACScan. For the cells transfected with pCMV- β gal, X-gal staining of β -galactosidase activity in fixed cells was performed using a lacZ reporter cell staining kit (InvivoGen, CA, USA), according to manufacturer's instructions.

4.2.11 Uptake of plasmid by neuroblastoma cells and cell fractionation assay

IMR-32 and GI-LI-N cells were incubated for 2 hours with 3 μ g of 32 P-labelled pEGFPN-1 plasmid encapsulated in 3 H-labelled liposomes. Cells were washed twice with PBS and were incubated in fresh complete medium at 37°C in standard condition for 0, 24 or 48 hours. At each time point, cells were washed twice with ice-cold PBS. After adding PBS-1mM EDTA cells were harvested and centrifuged at 3000 revolutions per minute (rpm) for 5 minutes. The cell pellet was suspended in 0.5M NaCl in 0.2M acetic acid (pH 2.5) and held at 4°C for 10 minutes to elute surface-bound plasmid DNA. Samples were centrifuged at 300g for 5 minutes at 4°C. Cells were then resuspended and incubated for 5 minutes on ice with the harvest buffer containing 10mM Hepes (pH 7.9), 50mM NaCl, 0.5M Sucrose, 0.1mM EDTA, 0.5% Triton-x-100, 1mM DTT, 10 mM tetrasodium, 100mM NaF, 17.5mM β -glycerophosphate and 1mM PMSF (Sigma-Aldrich Co., Gillingham, Dorset, UK). The suspension was then centrifuged at 1000 rpm for 10 minutes and the supernatant, containing the cytosol/membrane fraction, was separated from the precipitated nuclei fraction. Both fractions were lysed with 1N NaOH prior to measurement of radioactivity.

4.3 Results

4.3.1 Characterisation of anti-GD2 CCLs

4.3.1.1 Determination of particle size of CCLs

The CCLs measured diameter was consistent in all of the preparations, 120 ± 20 nm (mean \pm standard deviation).

4.3.1.2 Gel retardation

DNA encapsulation in CCLs and overall charge of the complexes were monitored by gel retardation electrophoresis (Figure 50A, lane 1). Migration of pEGFP-N1 was completely abolished by DNA encapsulation in the cationic lipids (upper band in lane 1, Figure 50A). Non-encapsulated plasmid migrated accordingly to its size and charge (arrow in lane 1, Figure 50A). Therefore, this result clearly indicated that DNA-CCL complex was formed, and maintained close to neutrality when the pEGFP-N1 plasmid was complexed with the DOTAP lipid at the DNA/DOTAP molar ratio used (1 : 1227).

4.3.1.3 DNase I protection

To assess the role of our complexes in protecting the DNA from attack by degrading enzymes *in vivo*, an *in vitro* DNase I protection assay was performed with anti-GD₂-CCLs encapsulating pEGFP-N1 plasmid. The gel electrophoresis data are shown in Figure 50A (lane 2) and Figure 50B. In lane 2 (Figure 50A), and in lanes 4 and 6 (Figure 50B) the complexes lipid/DNA were present and did not migrate, showing DNase I protection. The samples loaded in lanes 3 and 5 were obtained from purified plasmid DNA after DNase I exposure followed by lipid/DNA dissociation (lane 3) or after lipid/DNA dissociation only (lane 5). The presence of a migrated band in lane 3 (arrow) comparable to that in lane 5 indicated protection of the p-EGFP-N1 plasmid from the degrading enzyme.

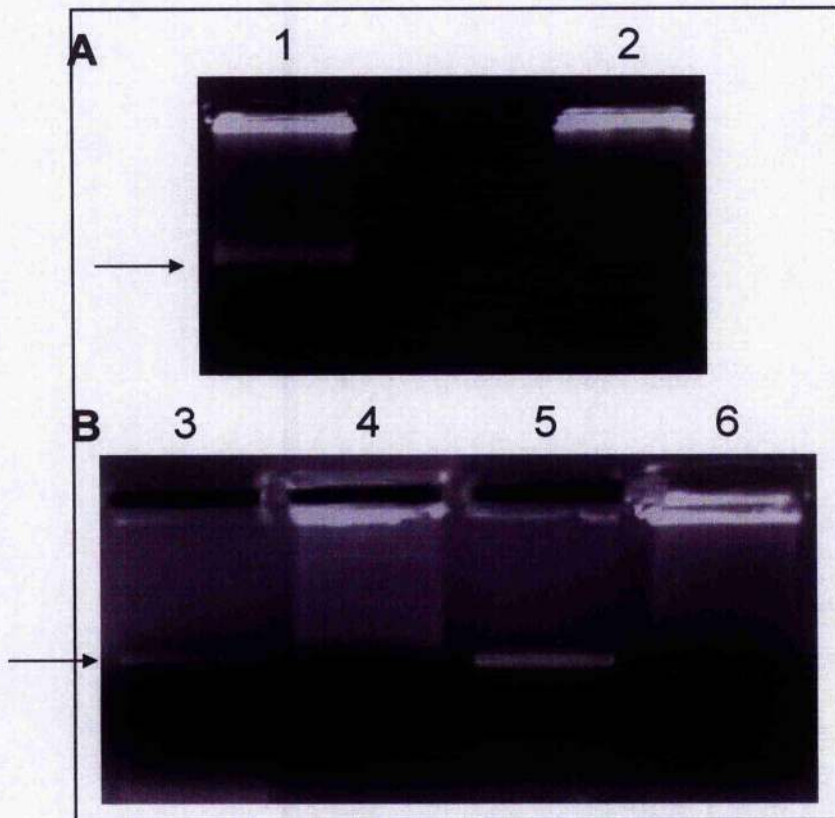


Figure 50. Gel retardation electrophoresis and DNase I protection assays of plasmid DNA complexed with the coated cationic liposomes (CCLs). **A)** Gel retardation electrophoresis assay of DNA complexed with CCLs before (1) and after (2) incubation with DNase I. **B)** DNase I protection assay (3 - 6): DNA complexed with immunoliposomes incubated with DNase I before 40mM deoxycholate (3), with 40mM deoxycholate only (5) or liposomes incubated with DNase I only (4 and 6). Electrophoresis conditions: 1% agarose gel, 80 Volts.

4.3.2 Binding of GD2-targeted immunoliposomes to GD2-positive and GD2-negative cells

In order to establish the capacity of the anti-GD₂-CCLs to bind to GD₂-positive cells a binding assay was performed. Phospholipid uptake by the GD₂-positive IMR-32 cell line was significantly higher than that by GD₂-negative SK-N-BE(2c) cells ($p < 0.001$, Figure 51). Phospholipid (i.e., liposome) concentration of 400 nmoles phospholipid/ml was shown to generate uptake of 28.4 nmoles of phospholipids per 10⁶ cells, this was 4.5 times the uptake levels recorded in GD₂-negative cells (1.37 nmoles of phospholipids per 10⁶ cells) (Figure 51).

Similarly, binding experiments conducted with liposomes labelled with rhoda-PE and analysed at FACScan, showed that liposomes labelled with rhoda-PE were able to bind to GD₂-positive IMR-32 cells resulting in increase of the fluorescence levels compared to that of SK-N-BE(2c) cells, which are GD₂-negative (Figure 52). Preincubation of cells for 30 minutes with soluble anti-GD₂ MAb significantly inhibited phospholipid uptake by IMR-32 cells ($p < 0.01$, Figure 53). Preincubation of cells for 30 minutes with soluble non-specific isotype-matched antibody did not inhibited phospholipid uptake by IMR-32 cells ($p > 0.1$, Figure 53). These results indicated that anti-GD₂-CCLs binding occurred through specific antigen-antibody recognition.

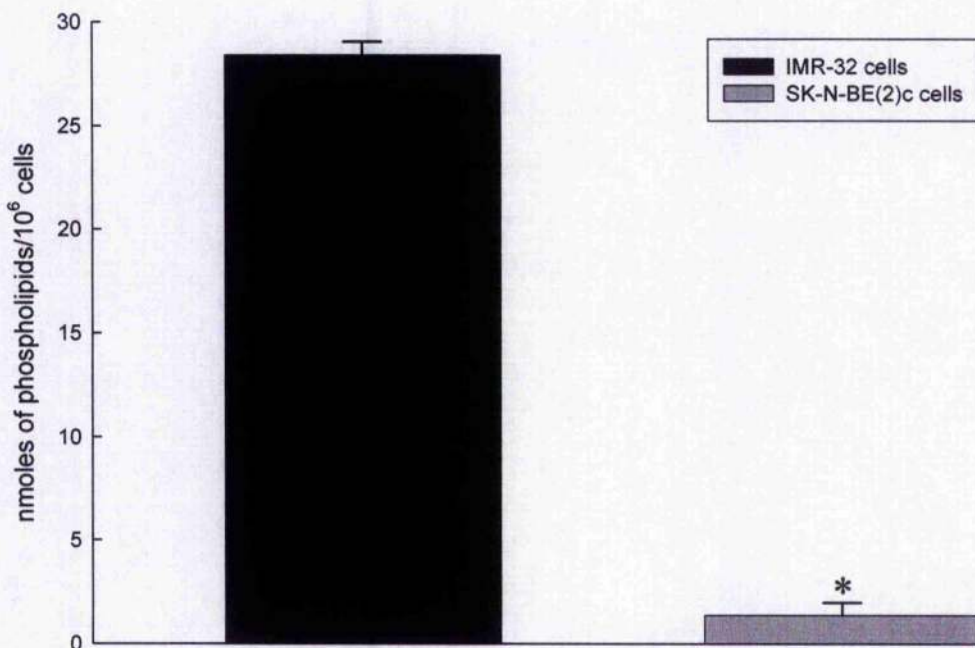


Figure 51. Anti-GD₂-coated cationic liposomes (anti-GD₂-CCLs) binding to neuroblastoma cells. Cells used: disialoganglioside GD₂-positive IMR-32 cells (black bar) and GD₂-negative SK-N-BE(2c) cells (grey bar). Cells were incubated for 2 hours with 400 nmoles phospholipids/ml of ³H-labelled anti-GD₂-liposomes with encapsulated pEGFP-N1 plasmid. Values are shown as the mean ± standard deviation (s.d.) of three repeats from two independent experiments (* significantly lower, t-test: $p < 0.01$).

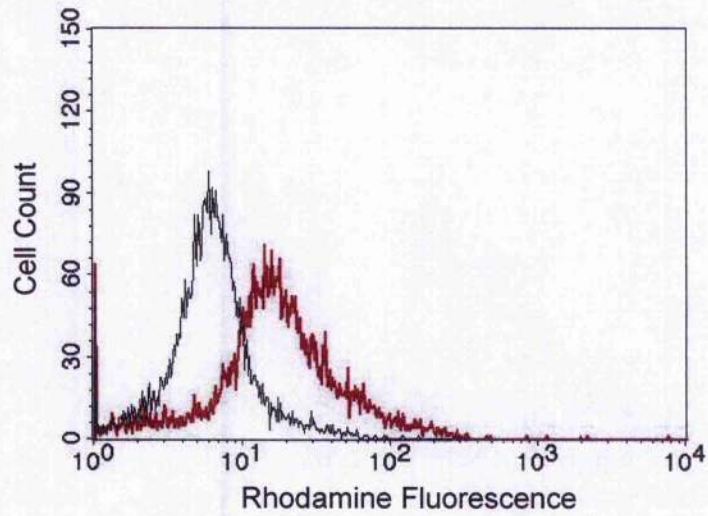


Figure 52. Fluorescence intensity distribution histogram of SK-N-BE(2c) cells (black line) or IMR-32 cells (red line) incubated for 2 hours at 37°C with anti-GD₂-CCLs labelled with rhoda-PE (red line), obtained by flow cytometry. The Y-axis represents the number of fluorescent events (cell counts), and the X-axis represents the mean channel fluorescence intensity. Experiments were independently performed two times.

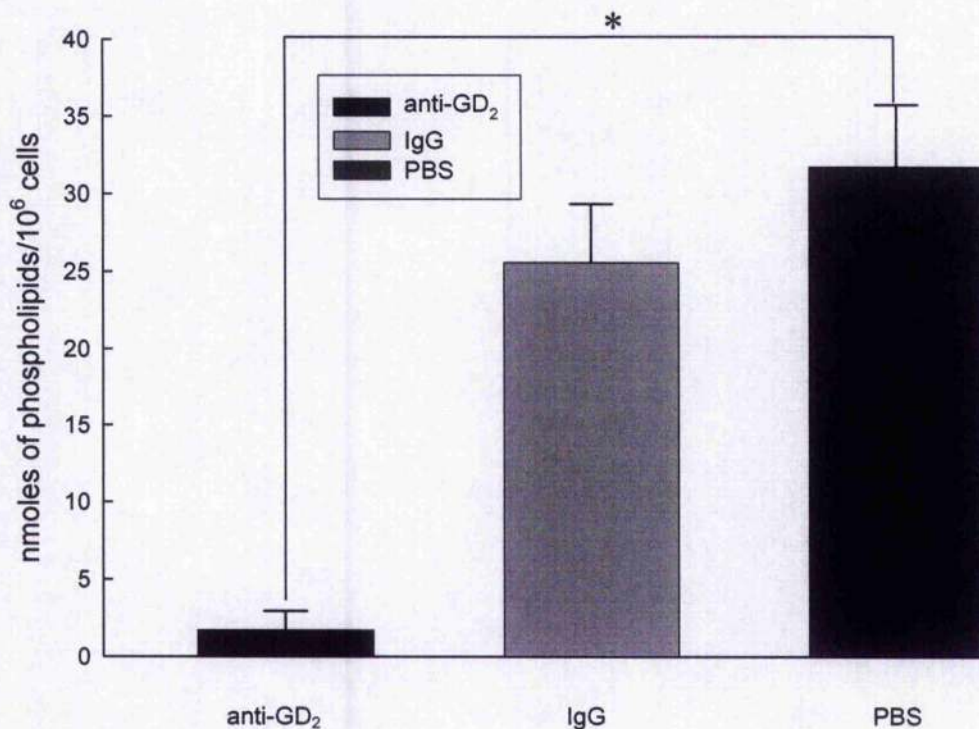


Figure 53. Competition assay of immunoliposomes binding to disialoganglioside GD₂-positive (IMR-32) tumour cells.

Cells were pre-incubated for 30 minutes with 50-times excess of free anti-GD₂ MAb (black bar), with non-specific isotype-matched antibody (light grey bar) or with PBS (dark bar). After PBS washes cells were incubated for 2 hours at 37°C with 400 nmoles phospholipids/ml of ³H-labelled anti-GD₂-liposomes with encapsulated pEGFP-N1 plasmid. Values are shown as the mean ± standard deviation (s.d.) of three repeats from two independent experiments (* significant difference, t-test: $p < 0.01$).

4.3.3 Transfection of neuroblastoma cells with anti-GD₂-CCLs encapsulating plasmid DNA

In order to assess whether these immunoliposomes were capable of gene delivery, transfection experiments were carried out. GD₂-positive cell lines IMR-32 and GI-LI-N, and GD₂-negative cell line SK-N-BE(2c) were incubated with anti-GD₂-CCLs encapsulating the pEGFP-N1 plasmid or pCMV- β gal plasmid. However, neither microscopic nor FACScan analysis registered detectable levels of fluorescence in cells incubated with anti-GD₂-CCLs encapsulating pEGFP-N1 plasmid. Further, no staining of fixed cells treated with anti-GD₂-CCLs encapsulating pCMV- β gal plasmid was observed.

As positive control, GFP or LacZ expression in IMR-32 and SK-N-BE(2c) cells was monitored 24 hours after transfection with Lipofectamine 2000 complexed to the pEGFP-N1 or pCMV- β gal plasmid.

4.3.4 Cellular internalisation of the anti-GD₂-CCLs

With the intent to explain the reasons for the absence of gene expression in neuroblastoma cells via anti-GD₂-CCLs, we attempted to examine whether the immunoliposomes were internalised and if so, in which cellular compartment they resided. Internalisation (Figure 54 and Figure 55) and fractionation (Figure 56) studies were performed. FACS analysis and radioactive counts indicated that phospholipid uptake by IMR-32 cells when incubated with liposomes at 37°C was higher than that resulting from incubation at 4°C (temperature at which internalisation is inhibited [368], Figure 54 and Figure 55). These findings indicate that the uptake process is temperature dependent and that temperature-dependent mechanisms such as endocytosis could be involved in immunoliposome uptake [318].

IMR-32 cells were incubated with anti-GD₂-CCLs containing the plasmid pEGFP-N1 traced with [³²P]dCTP. After incubation, separation of the cytoplasm/membrane fraction from the nuclear fraction was performed. Undetectable levels of plasmid were registered in the nuclei fraction 0, 24 and 48 hours after incubation (Figure 56). In the cytoplasm/membrane fraction the quantity of plasmid (expressed as percentage of ng of DNA administered per mg of protein) present was 3.88, 1.53 and 0.69, at 0, 24 and 48 hours after incubation respectively (Figure 56). The results indicate that plasmid DNA does not reach the nucleus, suggesting a possible cause for the lack of EGFP (and LacZ) gene expression.

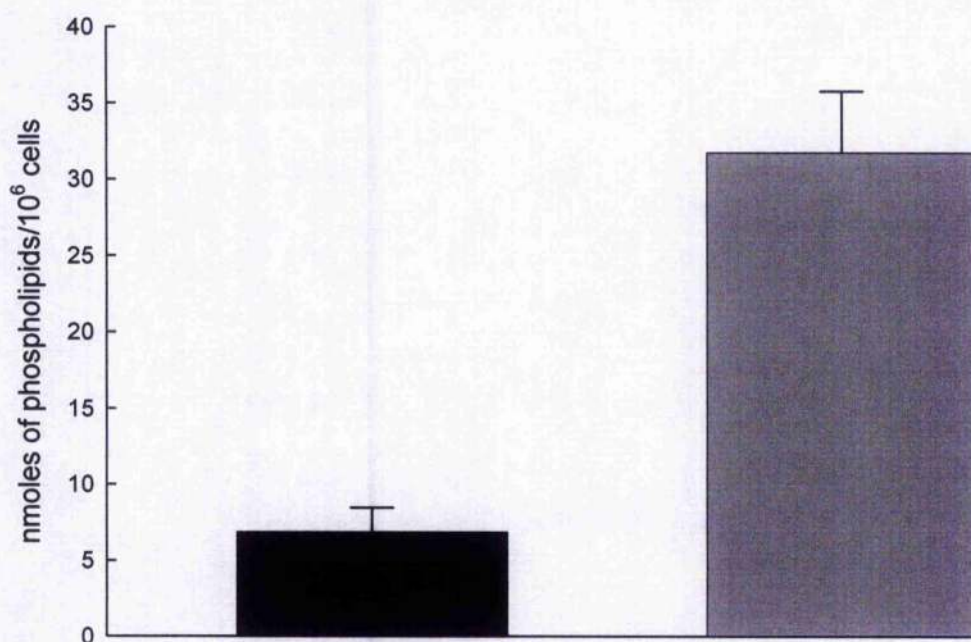


Figure 54. Internalisation assay of immunoliposomes binding to disialoganglioside GD₂-positive (IMR-32) tumour cells.

Cells were incubated for 2 hours at 4°C (black bar) or at 37°C (grey bar) with 400 nmoles phospholipids/ml of ³H-labelled anti-GD₂-liposomes with encapsulated pEGFP-N1 plasmid. Values are shown as the mean ± standard deviation (s.d.) of three repeats from two independent experiments.

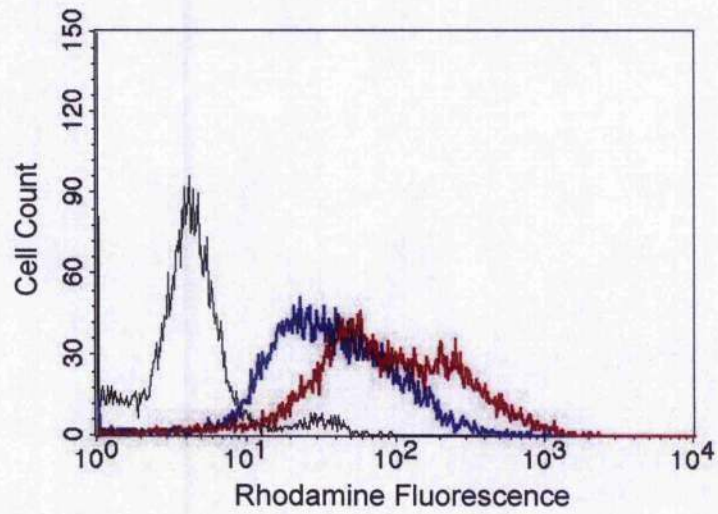


Figure 55. Fluorescence intensity distribution histogram of IMR-32 cells incubated for 2 hours at 37°C with PBS (black line), at 4°C (blue line) or at 37°C (red line) with anti-GD₂-CCLs labelled with rhoda-PE, obtained by flow cytometry. The Y-axis represents the number of fluorescent events (cell counts), and the X-axis represents the mean channel fluorescence intensity.

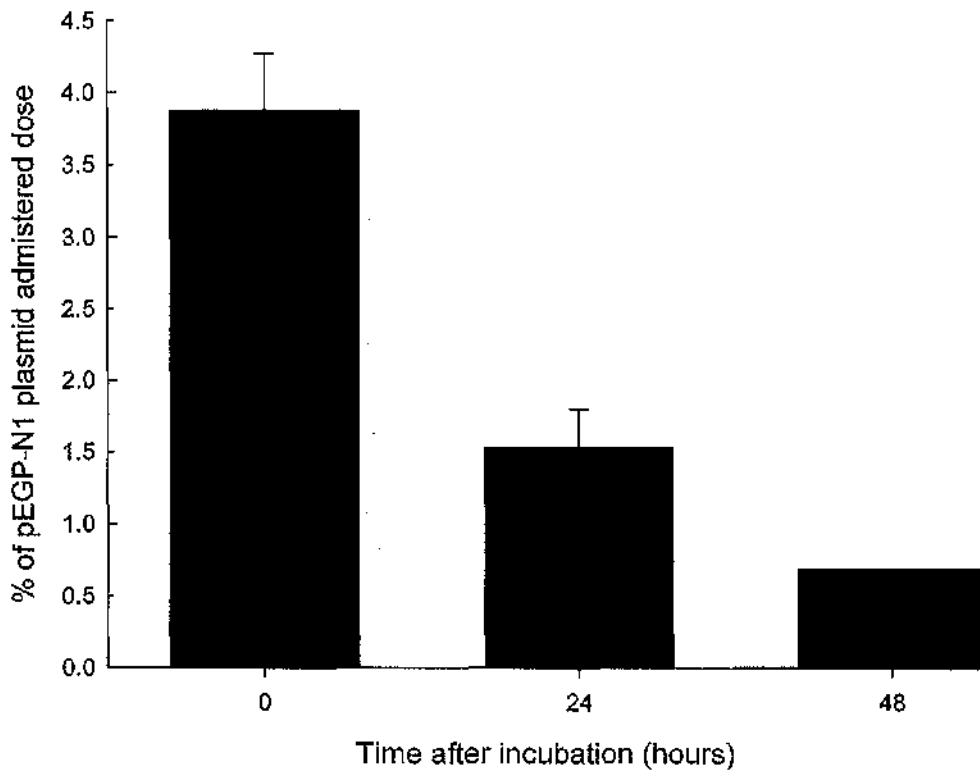


Figure 56. Cellular localisation of immunoliposomes binding to disialoganglioside GD2-positive (IMR-32) tumour cells.

Cells were incubated for 2 hours at 37°C with 400 nmoles phospholipids/ml of ^3H -labelled anti-GD₂-liposomes with encapsulated ^{32}P -labelled pEGFP-N1 plasmid (2-3 $\mu\text{g}/\text{ml}$). Cells were washed immediately, 24 or 48 hours after the incubation. The nuclei were then separated from the cytosol/membrane fraction (black bars). Both fractions were lysed with 1N NaOH prior to radioactivity measurement. Levels of the pEGFP-N1 plasmid in the nuclei fraction were undetectable. Values are shown as the mean \pm standard deviation (s.d.) of three repeats from two independent experiments.

4.3.5 Summary of results

In this study, the feasibility of producing anti-GD₂ coated cationic liposomes (anti-GD₂-CCLs), which encapsulate plasmid DNA, was shown. The resulting liposomal/plasmid complex protected the plasmid from the deoxyribonuclease I activity. This liposomal preparation displayed binding specific to GD₂-positive neuroblastoma cells. Furthermore, the binding was shown to be based on specific antibody-antigen recognition. In addition, binding experiments conducted at 4°C showed a substantial decrease in phospholipid uptake, compared to that observed in experiments performed at 37°C. These findings suggest that cellular internalisation of immunoliposomes occurred at 37°C, but not at 4°C, a temperature at which endocytosis does not occur. However, in transfection experiments, using anti-GD₂-CCLs encapsulating the pEGFP-N1 or the pCMV-βgal plasmid, it was not possible to detect GD₂-positive neuroblastoma cells expressing the EGFP gene or the LacZ gene.

In order to investigate this, GD₂-positive neuroblastoma cells were incubated with anti-GD₂-CCLs encapsulating the radiolabelled pEGFP-N1 plasmid. After performing cellular fractionation, detectable levels of pEGFP-N1 plasmid were registered in the cytoplasm/membrane fraction, but not in the nuclear fraction. The results indicate that plasmid DNA does not reach the nuclear compartment, suggesting a possible cause for the lack of EGFP and LacZ gene expression.

4.4 Discussion

In this study a novel tumour-targeting gene delivery system was investigated. The coated cationic liposomes (CCLs) have been successfully used for encapsulation and in vivo tumour delivery of DNA in the form of oligonucleotides directed against oncogenes c-myc (in neuroblastoma) and c-myc (in melanoma). Long systemic circulation and tumour targeting made the CCLs an attractive technology for plasmid DNA delivery.

In this study, for the first time, anti-GD₂-CCLs were employed for delivery of plasmid DNA. Encapsulation and DNase I protection of plasmid DNA were shown (section 4.3.1), indicating that the majority of the DNA extracted in the organic phase was inside the liposomes. The size of the anti-GD₂-CCLs containing plasmid DNA (120nm in diameter) was within the range (100 to 200nm) critical for a prolonged blood circulation and optimal extravasation into the tumour tissue [142, 369].

The binding capacity of the anti-GD₂-CCLs used in this study (section 4.3.2) was comparable with that of the liposomal formulation (on which our liposome technology is based), successfully used for encapsulation and cellular delivery of antisense oligodeoxynucleotides by Pagnan et al, 2003 [138]. In particular, in our study the liposome uptake in IMR-32 cells was 3 times higher than that observed in the report, in which neuroblastoma GI-LI-N cells were used. This difference could be due to variation in expression levels of the antigen GD₂ on the cellular surface between the two cell lines [370] and / or to differences in the structure and conformation between liposomes encapsulating plasmid DNA and liposomes containing oligodeoxynucleotides.

Binding studies demonstrated the capacity of anti-GD₂-CCLs to specifically bind to GD₂-positive cells. Furthermore, the binding was the result of a specific recognition between the anti-GD₂ antibody and the antigen. This is particularly important because one of the major issues of a safe and efficient strategy for cancer gene therapy is the targeting of tumour cells avoiding non specific transfection of normal cells. Cellular internalisation of the immunoliposomes was suggested by FACS analysis and radioactive counts of cells incubated with anti-GD₂-CCLs, whose lipidic proportion was radiolabelled with [³H]Cholesterol. The incubation temperature of 4°C dramatically reduced phospholipid uptake, indicating inhibition of immunoliposomes internalisation. In accordance with previous reports, these findings suggest that immunoliposomes are internalised through a temperature

dependent process such as endocytosis [371]. Moreover, since it has been shown that 14.G2a MAb was internalised by melanoma cells [372], the findings of the present study suggest that liposomes bind to the cell surface and are then internalised via a receptor-dependent endocytic pathway.

The fractionation study showed that 3.88% of the administered dose of plasmid pEGFP-N1 per mg of protein (corresponding to 7.77×10^6 copies of plasmid per cell) was found in the cytoplasm/membrane fraction of IMR-32 cells after 2 hours of incubation, using anti-GD₂-CCLs as vector (section 4.3.4). This percentage is comparable to that observed by a recent study [368], showing a plasmid DNA uptake of 10% of the administered dose, using an adenoviral vector. In another report where different poly(ethylenimine) (PEI) formulations were compared for intracellular delivery properties [373], 7×10^6 copies of plasmid DNA per cell were detected in C3A hepatocarcinoma cells after 2 hours incubation with 5µg of plasmid complexed with 25kDa (PEI). This value is similar to that registered in our study using anti-GD₂-CCLs as vector (7.77×10^6 copies of plasmid per cell). Both published studies showed successful plasmid transfection with detectable expression levels of the luciferase [368] and β-Galactosidase [373] transgenes. Taking into consideration these reports, from our findings it is therefore possible to assume that levels of cellular uptake of the pEGFP-N1 plasmid encapsulated in anti-GD₂-CCLs are sufficient for a successful transfection.

However, despite these encouraging results demonstrating specific DNA protection, cellular binding and internalisation, the delivery of plasmid DNA did not translate to expression of the transgene. This could be because, after endocytosis, the encapsulated DNA does not reach the nucleus. Once inside the cell before the ultimate localisation into the nucleus, the plasmid DNA has to be released from the endosomal-lysosomal pathway. Next it has to reach the nuclear target and, ultimately, cross the nuclear envelope. Although cells can internalise effectively lipid-based vehicles, plasmid DNA translocation to the nucleus is an inefficient process [371]. Therefore, improvements are needed in the field of lipid-based DNA vectors in order to increase the efficiency of nuclear translocation of plasmid DNA. To date, intracellular trafficking studies of lipid-based DNA carriers have not led to the design of vehicles that have high transfection efficiency with target-specificity, suitable for systemic administrations for *in vivo* applications. Nevertheless, in the

recent years interesting strategies have been developed with the intention to overcome the endosomal and nuclear barriers.

4.4.1 Enhancements of endosomal escape

One reason for the lack of gene expression showed in this chapter could be the presence of an intracellular barrier, to be passed by the plasmid DNA in the endocytosis pathway, the endosomal membrane. In order to enhance transfection efficiency and avoid intra-lysosomal degradation, it could be useful to facilitate the endosomal escape of DNA encapsulating CCLs before the late endosomes fuse with lysosomal compartments [374].

A possible future direction to assess this, regards the fusion of lipidic carrier with endosomal membrane [375]. From previous studies it appears that successful transfection by liposomal formulations requires membrane destabilisation in the endosomal compartment, leading to membrane fusion and release of DNA from the endosome. This process can be achieved by cationic lipids [375], acid-labile lipids [376, 377] or exchangeable or acid-labile PEG-lipids [378, 379].

Another improvement for the delivery system investigated in the present study, employs osmotic disruption of the endosome by proton capturing polycations (proton sponge mechanism) [380, 381]. The amino groups of the polycation become protonated as the proton pump in the endosomal membrane carries protons inside the endosome compartment. For the maintenance of electro-neutrality, proton binding is followed by passive influx of chloride ions. Consequently the endosome swells due to osmosis and disruption of its membrane occurs. The transfection efficiency of lipid-based DNA carriers is enhanced by polycations [382] and it could be a potential improvement for the CCLs.

Incorporation into immunoliposomes of fusogenic peptides that facilitate fusion between the liposomal and endosomal membranes could generate a further improvement of this technique. In general, the peptides are based on viral proteins which induce membrane destabilisation promoting fusion with endosomal membranes of host cells [383-385]. A well documented fusogenic protein is haemagglutinin (HA) from the influenza virus. A 23 amino acid fusogenic peptide resembling the N-terminal domain of HA has been shown to be a promising peptide in promoting the endosomal escape of liposomal contents including DNA [386, 387]. Another peptide with promising fusogenic properties is the 30 amino acid synthetic peptide GALA [388-390]. Two peptides of non-viral origin with

fusogenic capacities are the chemically modified α -melanocyte-stimulating hormone (α -MSH) [391] and the lactoferricin (a 25 amino acid peptide derived from N-terminal side of lactoferrin) [392, 393]. It will be therefore interesting in future studies to investigate the potential of fusogenic peptides for the enhancement DNA delivery via CCLs.

4.4.2 Nuclear translocation

Another problem in the complete transfection process is the presence of the nuclear envelope. It has been documented that nuclear translocation of plasmid DNA is an inefficient process [371]. Further, injection of plasmid DNA into the nuclei of mouse fibroblasts leads to gene expression in 50–100% of cells, but when the same amount of plasmid is injected into the cytoplasm, no expression is detected in any of the injected cells [394]. Several other similar experiments have confirmed these findings [371, 395–398]. However in all of these experiments the cells studied were non-dividing and in recent studies it has been reported that transfection is more successful in actively proliferating cells than in quiescent cells [399, 400]. But regardless of whether the cells undergo mitosis or not, the nuclear import of DNA is a relatively inefficient process, even when the nuclear envelope is broken [398, 401]. DNA degradation by cytosolic nucleases is another issue that hampers the nuclear translocation efficiency of plasmid DNA [402, 403].

Almost all of the effort to enhance nuclear translocation of exogenous DNA has been focused on the use of proteins or peptides containing nuclear localisation signals (NLS) as the means to guide the DNA into the nucleus. Several of these peptides have been associated to plasmid DNA by electrostatic interactions [404–409], non-specific covalent binding [410–412] or by site-specific attachment to the DNA [413–417]. The majority of these studies have reported improvements of nuclear translocation using NLS-peptides and therefore it could be worthwhile to evaluate their potential in the anti-GD₂ CCLs system.

4.4.3 Conclusions

In conclusion, the present study demonstrated the feasibility of encapsulating plasmid DNA into anti-GD₂-CCLs, so far used as vectors for oligodeoxynucleotides [96, 138, 361]. Furthermore, it was shown that GD₂-specific cellular binding, internalisation and plasmid DNA uptake were achieved by the use of this immunoliposome technology.

It is likely that transfection efficiency of the lipid-based DNA delivery system used in the present study so far is limited by all or part of the factors such as limited endosomal escape, and the low nuclear translocation. Studies on the development of plasmid DNA encapsulating immunoliposomes with improved endosomal escape properties, better protection from DNA degradation by cytosolic nucleases and enhanced nuclear transport are necessary and will be the main focus of future studies. However, lipid-based gene delivery systems are one of the most attractive and promising non-viral vector approaches in gene therapy. It is possible to envisage that the non-viral vector field of research will benefit from the studies conducted on virus-mediated gene delivery which thus could pose as model for the engineering of effective lipid-based DNA vectors.

Chapter 5

Further avenues of research arising from this study, and final conclusions

5.1 Telomerase promoters: enhancement of tumour specific gene therapy

The results of this study indicate that both telomerase promoters are suitable control elements of tumour-specific expression of the NAT transgene in neuroblastoma cells. Furthermore, the over-expression of the NAT transgene (via telomerase promoters) resulted in a higher capacity of neuroblastoma cells to accumulate [^{131}I]MIBG or [^{211}At]MABG, and enhanced sensitivity to both radiopharmaceuticals.

This section will describe the possibility of improving the expression of the NAT transgene by control elements other than hTR or hTERT promoters. The use of strategies such as the Cre/Lox system for enhancing the efficiency of telomerase promoters will also be discussed.

5.1.1 Alternative tumour-specific transcriptional regulators

Midkine (MK) is a newly identified heparin-binding growth factor that is transiently expressed in the early stages of retinoic acid-induced differentiation of embryonal carcinoma cells and is implicated in neuronal survival and differentiation [418]. It has been reported that advanced neuroblastomas express high levels of MK mRNA or protein [419]. However, no MK expression is detected in human or mouse liver [418, 420]. An adenoviral vector has been constructed to express the herpes simplex virus thymidine kinase (HSV-*tk*) under the control of the MK promoter to target Wilm's tumour and neuroblastoma cell lines [154, 421].

A recent report identified a modified ornithine decarboxylase (ODC) promoter that up-regulates the expression of carboxylesterase (CE) which in turn activates the prodrug Irinotecan in neuroblastoma cells [422, 423].

A 1.7-kbp fragment upstream of the NCX gene shows preferential promoter activity in neuroblastoma cells and when linked to the HSV-*tk* gene causes increased sensitivity to gancyclovir [424].

Tyrosine hydroxylase promoter (pTH) [425] is an interesting neuroblastoma-specific control element successfully used for HSV-*tk* mediated suicide gene therapy *in vitro* [426]. This study showed a 1.5-fold difference in gancyclovir pTH-mediated toxicity between neuroblastoma cells and tumour cells of not neuroectodermic origin.

5.1.2 Enhancement of telomerase promoters' efficiency: the Cre/Lox system

The telomerase promoters show relatively weak activity (compared to that of the CMV promoter) in the neuroblastoma cell line SK-N-MC and in some other target cells [177, 427, 428]. In a clinical scenario, this could limit therapeutic targeting in applications such as [¹³¹I]MIBG / NAT transgene strategy, where there is good correlation between NAT gene expression levels and capacity of active cellular accumulation of [¹³¹I]MIBG [100]. Therefore, strategies to improve the efficacy of telomerase gene therapy are of interest [428, 429]. One approach to enhance the expression levels of therapeutic transgenes uses the Cre/Lox switch. Cre recombinase, derived from the P1 bacteriophage [430], catalyzes site-specific recombination of DNA between LoxP site [431]. The LoxP recognition element is a 34 base pair sequence comprised of two 13 base pair inverted repeats flanking an 8 base pair spacer region which confers directionality [431]. Thus, Cre/Lox technology is a valuable tool for gene function studies [432, 433]. The therapeutic transgene (NAT gene) will be separated from a strong constitutive promoter (for example CMV promoter) by a LoxP flanked transcriptional termination signal. A weak tissues/cancer-specific promoter of interest (hTR or hTERT promoters) will drive the expression of Cre from a second vector, resulting in deletion of the stuffer and derepression of transgene expression (Figure 57). Therefore, specificity is selectively associated with a constitutively high transcription rate. This strategy has been applied in several studies of cancer gene therapy [434-438]. Because the hTR and hTERT promoters show weak activity in some cancer cells, it is reasoned that the Cre/Lox switch could be adapted not only to extend the effective target cell range, but also to enhance the transgene expression levels for telomerase-specific NAT gene therapy.

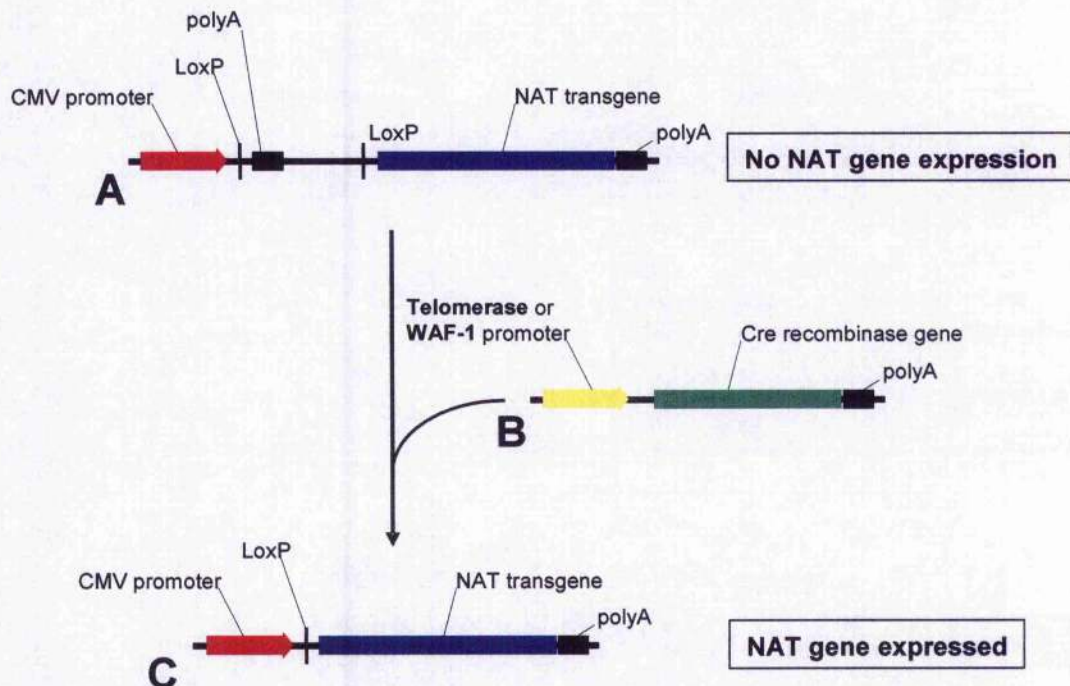


Figure 57. Regulation of NAT gene expression by the Cre/Lox switch. Transcription of the NAT gene in vector A is repressed by the presence of a LoxP-flanked stuffer fragment harbouring the SV40 late polyadenylation signal upstream of the NAT gene. In the presence of Cre protein expression, in this case directed by the telomerase or WAF-1 promoter (vector B), the stuffer and polyadenylation signal are excised, leading to the derepression of CMV dependent NAT gene expression (vector C).

5.2 Radiation-inducible gene therapy

This study showed that radioactivity can activate the WAF1 promoter, which could be a control element for therapeutic gene expression in neuroblastoma cells. Furthermore, it was also demonstrated that the promoter is inducible not only by external beam radiation (such as X-rays or γ -rays) but also by radionuclides (^{131}I or ^{211}At) bound to a tumour seeking drug, benzylguanidine. However, evidence from a previous study [135] indicates that the WAF1 promoter is a weak promoter, providing no induction at the most clinically relevant radiation dose of 2Gy. However, in our study, we observed WAF1 promoter activation in neuroblastoma cells at this radiation dose. Furthermore, an estimated radiation dose of 2eGy [^{131}I]MIBG or [^{211}At]MABG, generated a level of WAF1 promoter activation comparable to that induced by 2Gy γ -radiation in neuroblastoma cells, transfected with a plasmid containing the WAF1 promoter upstream of the GFP cDNA (pWAF1/GFP) (values of the fluorescence fold increase 48 hours after treatment are summarised in Table 4). As shown in Table 4, in SK-N-BE(2c) transfectants, the level of WAF1 promoter activation at 2eGy was modest. These findings suggest that the use of the WAF1 promoter could be limited by its low activation at the clinically relevant radiation dose of 2Gy. Therefore, a stronger promoter or an enhancement system would be desirable for pre-clinical application. In this section the use of alternative promoters as well as enhancement strategies for WAF1 promoter activation, will be discussed.

	γ-radiation	[¹³¹I]MIBG	[²¹¹At]MABG
SH-SY5Y+pWAF1/GFP	1.68	1.90	1.74
SK-N-BE(2c)+pWAF1/GFP	1.26	1.17	1.11

Table 4. WAF1 promoter activation in neuroblastoma transfectants 48 hours after exposition to 2eGy γ-radiation, [¹³¹I]MIBG and [²¹¹At]MABG. The equivalent radiation dose, referred to as eGy, was estimated as explained in section 3.3.2.5. The values are expressed as fluorescence fold increase (fluorescence increase is calculated with respect to unirradiated control).

5.2.1 Alternative radiation-inducible transcriptional regulators

The native Egr1 gene promoter [212] in combination with the herpes simplex virus thymidine kinase gene has been used to sensitise glioma cells to gancyclovir after exposure to [⁶⁷Ga]citrate [439] and to demonstrate a dose-dependent expression of reporter gene activity of up to 28 fold following radiation exposure (0 – 20Gy) [214].

Radiation-inducible bacterial promoters have also been used such as RecA, using the anaerobic apathogenic clostridia as a gene transfer system. Significant increases in β -galactosidase activity and TNF- α secretion was seen after a single dose of 2Gy [220, 440].

The use of a plasmid with four tandem repeats of the NF κ B binding site (from the radio-inducible c-IAP2 gene) driving the expression of the apoptotic suicide gene BAX, resulted in significant cell kill following a therapeutically relevant dose of 2-Gy X-rays [221].

A synthetic construct E9, incorporating nine radiosensitive CArG elements from the Egr1 promoter, has recently been developed [441]. Transfection of tumour cells with plasmids containing a reporter gene downstream of the synthetic construct resulted in improvement of the induction response to low doses of radiation and reduction of "leakiness" under non-irradiated conditions compared to that of the native Egr1 enhancer [441].

5.2.2 Enhancement of WAF1 promoter efficiency: the Cre/Lox system

The use of the Cre/Lox switch system could also be useful for the enhancement of the transcription efficiency of the WAF1 promoter (Figure 57). A recent study has applied the Cre/Lox switch to the Egr1 promoter / HSV-*tk* gene system [442]. The switch system generated a three-fold increase in cell growth inhibition compare to that using the Egr1 promoter alone to drive HSV-*tk* expression.

The radiation responsive promoter controls the expression of Cre recombinase. After radiation exposure, this then activates the transcriptionally silenced HSV-*tk* gene via the CMV promoter, by LoxP site mediated recombination. This approach could be particularly beneficial in our strategy where specific, but relatively weak radiation-responsive WAF1 promoter is employed to target NAT gene expression to neuroblastomas.

5.3 Choice of radionuclide: Alternatives to ^{131}I or ^{211}At as a conjugate for MIBG

Radionuclides other than ^{131}I may be more efficacious in some circumstances. The aim of targeted radiotherapy is delivery of radiation to tumour sites, minimising normal tissue toxicity. Nevertheless, choosing the appropriate radionuclide is pivotal to maximise the therapeutic efficacy of the radiopharmaceutical, controlling normal cellular toxicity. The path length of the emitted particles, the linear energy transfer (LET), size of tumour mass and subcellular localisation of the targeting agent are all factors that should be taken into consideration [443].

The focus of this study has been the β -emitter [^{131}I]MIBG and the α -emitter [^{211}At]MABG. While ^{131}I has a long path length and relatively low LET, ^{211}At has a shorter path length and a much higher LET than ^{131}I . In the case of ^{131}I , in very small tumours (such as micrometastases) with diameter shorter than particle path length, absorption of radiation energy is ineffective, since a proportion of the energy is deposited outside the target [443]. In the case of ^{211}At , as tumour diameter is greater than the particle range, the absorption efficiency progressively reaches a plateau, whereas increasing cell number decreases therapeutic efficacy [443].

For these reasons, ^{131}I or ^{211}At may not be the most advantageous choice of radionuclide in all therapeutic scenarios. The determination of the most suitable radionuclides with different particle range and LET could improve the therapeutic effectiveness of MIBG (Table 5 and Figure 58).

5.3.1 [^{123}I]MIBG and [^{125}I]MIBG

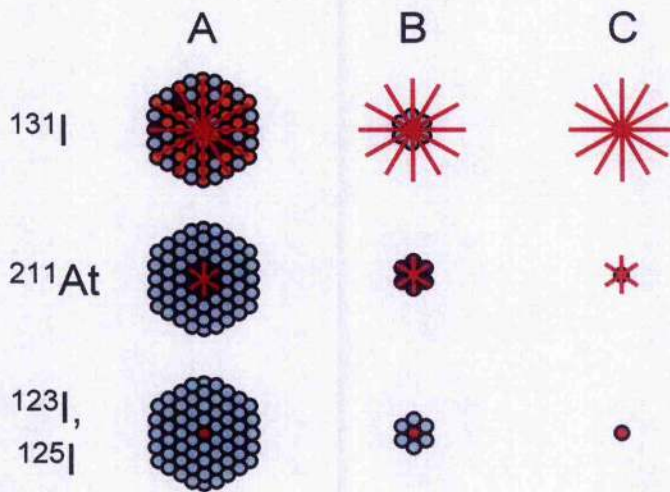
The efficacy of Auger electron emitters such as ^{123}I and ^{125}I would be confined to molecules within the nucleus [444, 445]. These radioisotopes decay by electron capture and internal conversion, which generate emission of extremely densely ionising radiation of very short range (1-10nm). Thus, Auger electron emitters would not be as effective as β -emitters when bound to targeting agents which remain in the cytoplasm or in the membrane compartment [444, 445].

However, a recent report showed that [^{123}I]MIBG and [^{125}I]MIBG were more toxic to neuroblastoma cells than expected by cytoplasmic MIBG localisation [11]. These findings suggest that short range emitters would be suitable for the treatment of circulating tumour cells (Table 5 and Figure 58). The "extra" toxicity of

^{123}I and ^{125}I labelled MIBG could be explained by the recently identified radiation-induced biological bystander effects [446-453]. It is expected that tumour-seeking drugs radiolabelled to short-range Auger emitters may be more therapeutically beneficial than was previously believed.

Radionuclide	Decay particle	Particle range	Half life	Current use
¹³¹ I	β	0.8 mm	8 days	therapy
²¹¹ At	α	0.05 mm	7 hours	therapy
¹²³ I	Auger electron	~1-10 nm	13.2 hours	imaging
¹²⁵ I	Auger electron	~1-10 nm	60.1 days	imaging

Table 5. Alternatives to ¹³¹I and ²¹¹At as conjugate for MIBG. Different radionuclides have different properties which may be more beneficial than ¹³¹I and ²¹¹At in certain circumstances. See Figure 58.



● Tumour cell	● Successfully targeted tumour cell
● Untargeted tumour cell: <u>sub-lethally</u> damaged by radiological bystander effect	● Untargeted tumour cell: <u>irreparably</u> damaged by radiological bystander effect

Figure 58. Relationship between particle range, radiological bystander effect and linear energy transfer.

A) Large tumour masses: As ^{131}I has longer particle length than ^{211}At , ^{123}I or ^{125}I , the radiological bystander effect will cause damage to a greater number of cells. **B)** Micrometastases: In smaller tumours, ^{131}I will be less effective as the majority of the energy will be deposited outside the tumour mass. ^{211}At has far greater LET, therefore, damage caused by ^{211}At to adjacent cells is more likely to be irreparable, leading to far greater toxicity in micrometastases. **C)** Circulating tumour cells: ^{123}I and ^{125}I have very short range, but very high LET, and therefore only toxic to individual cells. They will be most effective against circulating tumour cells. The longer path lengths of ^{131}I and ^{211}At are more likely to cause damage to normal tissue.

5.4 Radiation-induced biological bystander effects (RIBBEs)

Although the implications of radiological bystander effects (toxicity to non-targeted cells by radioactive decay particle emanating from targeted cells) are relatively well defined [182, 192], the importance of radiation-induced biological bystander effects (RIBBEs) has only recently been indicated [450]. RIBBEs derive from cellular processing of the radiation insult into biological factors or toxins that cause damage to unirradiated neighbouring cells. High and low LET radiations, delivered by focused microbeam or by transfer of media from irradiated to unirradiated cells, are capable of inducing RIBBEs [446-449, 451-453] (Figure 59).

RIBBEs contribute significantly to the overall effect in cells exposed to low dose and low dose rate irradiation [12, 446], characteristic of targeted radiotherapy of cancer. Thus, the importance of these bystander effects could have a strong impact on therapeutic efficacy of targeted radionuclide treatments and it should be considered in the design of radiotherapy protocols. The potency and the mechanisms of RIBBEs remain, as yet, unclear.

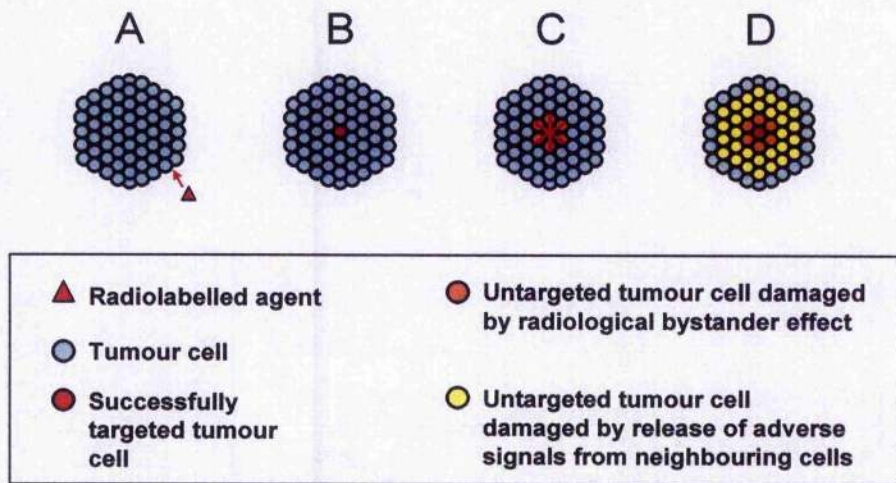


Figure 59. Radiation-induced biological bystander effect (RIBBE).

RIBBE involves the cellular processing of the radiation insult into toxic metabolites: **A)** Tumour cells are targeted by a radiopharmaceutical. **B)** Only a fraction of the tumour is successfully targeted. The majority of cells remain unaffected. **C)** Radiological bystander effect: energy released by decay of the radioisotope emanates from the targeted sites of the mass in three dimensions, damaging untargeted neighbouring cells. **D)** Radiation-damaged cells release biological signals which damage neighbouring cells.

5.5 Alternative gene delivery systems: adenoviral vectors

In the present study, we demonstrated that the anti-GD₂ coated cationic immunoliposomes (previously used for the delivery of antisense oligodeoxynucleotides [96, 361]) successfully encapsulated the pEGFP-N1 plasmid and specifically targeted neuroblastoma cells expressing the antigen GD₂. However, the transfection efficiency of this type of immunoliposome preparation was limited. For this reason, as well as taking into consideration improvements aimed to facilitate endosomal escape or nuclear translocation (discussed in sections 4.4.1 and 4.4.2), the usefulness of virus-based gene delivery systems should be investigated. Furthermore, the problem of low transfection efficiency and short term transgene expression *in vivo* are issues that can be circumvented with the use of viral vectors [318]. In 25% of all clinical trials, adenoviruses are the first utilised viral vector [273]. This type of vector is an attractive candidate for gene delivery mainly because of its capacity for carrying large DNA loads together with high transduction efficiency [454]. Engineering of recombinant adenoviral vectors could allow delivery of telomerase promoter- or WAF1 promoter-NAT transgene constructs.

5.6 The use of multicellular mosaic spheroids to determine transfection efficiencies

In [¹³¹I]MIBG and [²¹¹At]MABG toxicity assays performed for the evaluation of the potency of the hTR and hTERT promoters (see sections 2.3.4 and 2.3.5), we used cellular spheroids derived from neuroblastoma cells transfected with the phTR/NAT, phTERT/NAT or pCMV/NAT plasmids. In this way, 100% of the cells composing a single spheroid were transfected with the plasmids. This level of transfection efficiency would be highly unlikely to achieve *in vivo*. Therefore, it was not possible to evaluate the potency of the telomerase promoters in a model closer to the *in vivo* scenario, where the transfection efficiency is less than 100%.

The use of multicellular mosaic spheroids could circumvent this limitation. Multicellular mosaic spheroids are composed of variable percentages of two cells populations with different characteristics [192]. In this case, one of the cell populations does not contain any plasmid and displays no expression of the NAT gene, while the other possesses the plasmid containing the NAT transgene and is positive for NAT transgene expression.

This model could be adopted using SK-N-MC cells (which normally do not express detectable levels of NAT) and the plasmids containing the NAT transgene downstream of the hTR or the hTERT promoter (phTR/NAT and phTERT/NAT respectively). The use of mosaic spheroids generated, for example, from a mixed population, of parental cells and cells transfected with the phTERT/NAT plasmid, could be used to predict the minimum requirement for NAT transgene transfection to allow tumour sterilisation by the administration of targeted radiotherapy (for example [¹³¹I]MIBG and [²¹¹At]MABG, used in the present study, or [¹²³I]MIBG and [¹²⁵I]MIBG, described in section 5.3 (See Figure 60).

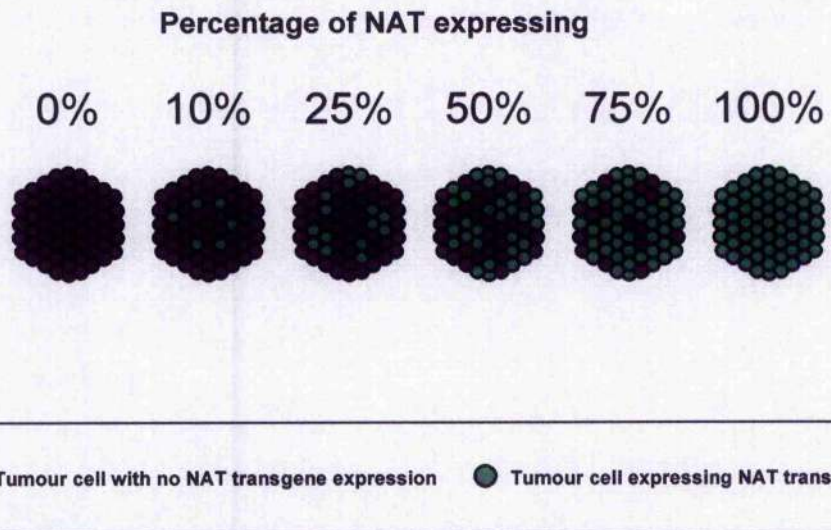


Figure 60. Schematic representation of mosaic spheroids. Multicellular mosaic spheroids are composed of variable percentage of two cell types. In this figure, one of the cell types display no expression of the NAT transgene, while the other is positive for NAT transgene expression. A mosaic spheroid model would allow estimation of minimum requirement for NAT transgene transfection to allow sterilisation by targeted radiotherapy.

5.7 Conclusions

5.7.1 Telomerase promoter elements driving the expression of the NAT transgene

The results of this study indicate that NAT transgene overexpression by control of the telomerase promoters may be achieved in neuroblastoma cells. Furthermore, the toxicity of radiopharmaceuticals [^{131}I]MIBG and [^{211}At]MABG to cells transfected with the NAT transgene under the control of either hTR or hTERT promoter is improved. If the overexpression of the NAT transgene and the improved toxicity of radiolabelled drugs are confirmed in pre-clinical models, there is potential for therapeutic gain.

5.7.2 WAF1 promoter as a radio-inducible switch of the NAT transgene

It was shown that WAF1 activity was inducible not only by external beam γ -rays but also by the β -emitter radionuclide ^{131}I in the form of [^{131}I]MIBG or by the α -emitter radionuclide ^{211}At conjugated to benzylguanidine ([^{211}At]MABG). Additionally, preliminary toxicity experiments showed that, after irradiation, toxicity of [^{131}I]MIBG improved in neuroblastoma cells transfected with the construct containing the NAT cDNA downstream of the WAF1 promoter sequence. These results together indicate potential for immediate applications in neuroblastoma patients such as bone marrow purging discussed in section 3.4.3.

5.7.3 Coated Cationic Immunoliposomes: a promising non-viral gene delivery system

The present study has introduced the method of coated cationic immunoliposomes as a non-virus based gene delivery system in neuroblastoma. This technology has great potential for its target-specificity and internalisation efficiency described in this study, and has attractive features for gene therapy strategy, for example long circulation and negligible toxicity in pre-clinical models [139, 361, 455]. Unfortunately, low transfection efficiency indicated limited usefulness of this methodology.

However, technology advances, such as introduction of nuclear localisation signals or utilisation of pH sensitive lipids to facilitate endosomal escape,

discussed in section 4.4.1, could be taken into consideration in order to overcome transfection problems.

References

1. Porter, A., A. Aref, Z. Chodounsky, A. Elzawawy, N. Manatrakul, T. Ngoma, C. Orton, E. Van't Hooft, and K. Sikora, *A global strategy for radiotherapy: a WHO consultation*. Clin Oncol (R Coll Radiol), 1999. **11**(6): p. 368-70.
2. Mairs, R.J. and M. Boyd, *Targeting Radiotherapy to Cancer by Gene Transfer*. J Biomed Biotechnol, 2003. **2003**(2): p. 102-109.
3. Mairs, R.J., S.H. Cunningham, M. Boyd, and S. Carlin, *Applications of gene transfer to targeted radiotherapy*. Curr Pharm Des, 2000. **6**(14): p. 1419-32.
4. Kaminski, M.S., J. Estes, K.R. Zasadny, I.R. Francis, C.W. Ross, M. Tuck, D. Regan, S. Fisher, J. Gutierrez, S. Kroll, R. Stagg, G. Tidmarsh, and R.L. Wahl, *Radioimmunotherapy with iodine (131)I tositumomab for relapsed or refractory B-cell non-Hodgkin lymphoma: updated results and long-term follow-up of the University of Michigan experience*. Blood, 2000. **96**(4): p. 1259-66.
5. Kaminski, M.S., A.D. Zelenetz, O.W. Press, M. Saleh, J. Leonard, L. Fehrenbacher, T.A. Lister, R.J. Stagg, G.F. Tidmarsh, S. Kroll, R.L. Wahl, S.J. Knox, and J.M. Vose, *Pivotal study of iodine I 131 tositumomab for chemotherapy-refractory low-grade or transformed low-grade B-cell non-Hodgkin's lymphomas*. J Clin Oncol, 2001. **19**(19): p. 3918-28.
6. Vaughan, A.T., P. Anderson, P.W. Dykes, C.E. Chapman, and A.R. Bradwell, *Limitations to the killing of tumours using radiolabelled antibodies*. Br J Radiol, 1987. **60**(714): p. 567-72.
7. Gaze, M.N., *The current status of targeted radiotherapy in clinical practice*. Phys Med Biol, 1996. **41**(10): p. 1895-903.
8. Denning, C. and J.D. Pitts, *Bystander effects of different enzyme-prodrug systems for cancer gene therapy depend on different pathways for intercellular transfer of toxic metabolites, a factor that will govern clinical choice of appropriate regimes*. Hum Gene Ther, 1997. **8**(15): p. 1825-35.
9. Denny, W.A. and W.R. Wilson, *The design of selectively-activated anti-cancer prodrugs for use in antibody-directed and gene-directed enzyme-prodrug therapies*. J Pharm Pharmacol, 1998. **50**(4): p. 387-94.
10. Mesnil, M. and H. Yamasaki, *Bystander effect in herpes simplex virus-thymidine kinase/ganciclovir cancer gene therapy: role of gap-junctional intercellular communication*. Cancer Res, 2000. **60**(15): p. 3989-99.
11. Cunningham, S.H., R.J. Mairs, T.E. Wheldon, P.C. Welsh, G. Vaidyanathan, and M.R. Zalutsky, *Toxicity to neuroblastoma cells and spheroids of benzylguanidine conjugated to radionuclides with short-range emissions*. Br J Cancer, 1998. **77**(12): p. 2061-8.
12. Seymour, C.B. and C. Mothersill, *Relative contribution of bystander and targeted cell killing to the low-dose region of the radiation dose-response curve*. Radiat Res, 2000. **153**(5 Pt 1): p. 508-11.
13. Hall, E.J., *The bystander effect*. Health Phys, 2003. **85**(1): p. 31-5.
14. Boyd, M., S.C. Ross, J. Dorrens, N.E. Fullerton, K.W. Tan, M.R. Zalutsky, and R.J. Mairs, *Radiation-induced biologic bystander effect elicited in vitro by targeted radiopharmaceuticals labeled with alpha-, beta-, and auger electron-emitting radionuclides*. J Nucl Med, 2006. **47**(6): p. 1007-15.
15. Maris, J.M. and K.K. Matthay, *Molecular biology of neuroblastoma*. J Clin Oncol, 1999. **17**(7): p. 2264-79.
16. Gurney, J.G., S. Davis, R.K. Severson, J.Y. Fang, J.A. Ross, and L.L. Robison, *Trends in cancer incidence among children in the U.S.* Cancer, 1996. **78**(3): p. 532-41.

17. Grovas, A., A. Fremgen, A. Rauck, F.B. Ruymann, C.L. Hutchinson, D.P. Winchester, and H.R. Menck, *The National Cancer Data Base report on patterns of childhood cancers in the United States*. *Cancer*, 1997. **80**(12): p. 2321-32.
18. Brodeur, G.M., *Neuroblastoma: biological insights into a clinical enigma*. *Nat Rev Cancer*, 2003. **3**(3): p. 203-16.
19. Biedler, J.L., L. Helson, and B.A. Spengler, *Morphology and growth, tumorigenicity, and cytogenetics of human neuroblastoma cells in continuous culture*. *Cancer Res*, 1973. **33**(11): p. 2643-52.
20. Brodeur, G.M., G. Sekhon, and M.N. Goldstein, *Chromosomal aberrations in human neuroblastomas*. *Cancer*, 1977. **40**(5): p. 2256-63.
21. Simpson, J.K. and M.N. Gaze, *Current Management of Neuroblastoma*. *Oncologist*, 1998. **3**(4): p. 253-262.
22. Matthay, K.K., C. Perez, R.C. Seeger, G.M. Brodeur, H. Shimada, J.B. Atkinson, C.T. Black, R. Gerbing, G.M. Haase, D.O. Stram, P. Swift, and J.N. Lukens, *Successful treatment of stage III neuroblastoma based on prospective biologic staging: a Children's Cancer Group study*. *J Clin Oncol*, 1998. **16**(4): p. 1256-64.
23. Seeger, R.C., G.M. Brodeur, H. Sather, A. Dalton, S.E. Siegel, K.Y. Wong, and D. Hammond, *Association of multiple copies of the N-myc oncogene with rapid progression of neuroblastomas*. *N Engl J Med*, 1985. **313**(18): p. 1111-6.
24. Kohl, N.E., N. Kanda, R.R. Schreck, G. Bruns, S.A. Latt, F. Gilbert, and F.W. Alt, *Transposition and amplification of oncogene-related sequences in human neuroblastomas*. *Cell*, 1983. **35**(2 Pt 1): p. 359-67.
25. Schwab, M., K. Alitalo, K.H. Klempnauer, H.E. Varmus, J.M. Bishop, F. Gilbert, G. Brodeur, M. Goldstein, and J. Trent, *Amplified DNA with limited homology to myc cellular oncogene is shared by human neuroblastoma cell lines and a neuroblastoma tumour*. *Nature*, 1983. **305**(5931): p. 245-8.
26. Bown, N., S. Cotterill, M. Lastowska, S. O'Neill, A.D. Pearson, D. Plantaz, M. Meddeb, G. Danglot, C. Brinkschmidt, H. Christiansen, G. Laureys, F. Speleman, J. Nicholson, A. Bernheim, D.R. Betts, J. Vandesompele, and N. Van Roy, *Gain of chromosome arm 17q and adverse outcome in patients with neuroblastoma*. *N Engl J Med*, 1999. **340**(25): p. 1954-61.
27. Brodeur, G.M., A.A. Green, F.A. Hayes, K.J. Williams, D.L. Williams, and A.A. Tsiatis, *Cytogenetic features of human neuroblastomas and cell lines*. *Cancer Res*, 1981. **41**(11 Pt 1): p. 4678-86.
28. Brodeur, G.M., J.M. Maris, D.J. Yamashiro, M.D. Hogarty, and P.S. White, *Biology and genetics of human neuroblastomas*. *J Pediatr Hematol Oncol*, 1997. **19**(2): p. 93-101.
29. Caron, H., P. van Sluis, J. de Kraker, J. Bokkerink, M. Egeler, G. Laureys, R. Slater, A. Westerveld, P.A. Voute, and R. Versteeg, *Allelic loss of chromosome 1p as a predictor of unfavorable outcome in patients with neuroblastoma*. *N Engl J Med*, 1996. **334**(4): p. 225-30.
30. Fong, C.T., N.C. Dracopoli, P.S. White, P.T. Merrill, R.C. Griffith, D.E. Housman, and G.M. Brodeur, *Loss of heterozygosity for the short arm of chromosome 1 in human neuroblastomas: correlation with N-myc amplification*. *Proc Natl Acad Sci U S A*, 1989. **86**(10): p. 3753-7.
31. Fong, C.T., P.S. White, K. Peterson, C. Sapienza, W.K. Cavenee, S.E. Kern, B. Vogelstein, A.B. Cantor, A.T. Look, and G.M. Brodeur, *Loss of*

- heterozygosity for chromosomes 1 or 14 defines subsets of advanced neuroblastomas. Cancer Res, 1992. 52(7): p. 1780-5.*
32. Gehring, M., F. Berthold, L. Edler, M. Schwab, and L.C. Amler, *The 1p deletion is not a reliable marker for the prognosis of patients with neuroblastoma. Cancer Res, 1995. 55(22): p. 5366-9.*
 33. Maris, J.M., P.S. White, C.P. Beltinger, E.P. Sulman, R.P. Castleberry, J.J. Shuster, A.T. Look, and G.M. Brodeur, *Significance of chromosome 1p loss of heterozygosity in neuroblastoma. Cancer Res, 1995. 55(20): p. 4664-9.*
 34. Martinsson, T., R.M. Sjoberg, F. Hedborg, and P. Kogner, *Deletion of chromosome 1p loci and microsatellite instability in neuroblastomas analyzed with short-tandem repeat polymorphisms. Cancer Res, 1995. 55(23): p. 5681-6.*
 35. Takita, J., Y. Hayashi, T. Kohno, M. Shiseki, N. Yamaguchi, R. Hanada, K. Yamamoto, and J. Yokota, *Allelotype of neuroblastoma. Oncogene, 1995. 11(9): p. 1829-34.*
 36. White, P.S., J.M. Maris, C. Beltinger, E. Sulman, H.N. Marshall, M. Fujimori, B.A. Kaufman, J.A. Biegel, C. Allen, C. Hilliard, and et al., *A region of consistent deletion in neuroblastoma maps within human chromosome 1p36.2-36.3. Proc Natl Acad Sci U S A, 1995. 92(12): p. 5520-4.*
 37. Mertens, F., B. Johansson, M. Hoglund, and F. Mitelman, *Chromosomal imbalance maps of malignant solid tumors: a cytogenetic survey of 3185 neoplasms. Cancer Res, 1997. 57(13): p. 2765-80.*
 38. Guo, C., P.S. White, M.J. Weiss, M.D. Hogarty, P.M. Thompson, D.O. Stram, R. Gerbing, K.K. Matthay, R.C. Seeger, G.M. Brodeur, and J.M. Maris, *Allelic deletion at 11q23 is common in MYCN single copy neuroblastomas. Oncogene, 1999. 18(35): p. 4948-57.*
 39. Thompson, P.M., B.A. Seifried, S.K. Kyemba, S.J. Jensen, C. Guo, J.M. Maris, G.M. Brodeur, D.O. Stram, R.C. Seeger, R. Gerbing, K.K. Matthay, T.C. Matise, and P.S. White, *Loss of heterozygosity for chromosome 14q in neuroblastoma. Med Pediatr Oncol, 2001. 36(1): p. 28-31.*
 40. Caron, H., P. van Sluis, R. Buschman, R. Pereira do Tanque, P. Maes, L. Beks, J. de Kraker, P.A. Voute, G. Vergnaud, A. Westerveld, R. Slater, and R. Versteeg, *Allelic loss of the short arm of chromosome 4 in neuroblastoma suggests a novel tumour suppressor gene locus. Hum Genet, 1996. 97(6): p. 834-7.*
 41. Meltzer, S.J., S.P. O'Doherty, C.N. Frantz, K. Smolinski, J. Yin, A.B. Cantor, J. Liu, M. Valentine, G.M. Brodeur, and P.E. Berg, *Allelic imbalance on chromosome 5q predicts long-term survival in neuroblastoma. Br J Cancer, 1996. 74(12): p. 1855-61.*
 42. Takita, J., Y. Hayashi, T. Kohno, N. Yamaguchi, R. Hanada, K. Yamamoto, and J. Yokota, *Deletion map of chromosome 9 and p16 (CDKN2A) gene alterations in neuroblastoma. Cancer Res, 1997. 57(5): p. 907-12.*
 43. Marshall, B., G. Isidro, A.G. Martins, and M.G. Boavida, *Loss of heterozygosity at chromosome 9p21 in primary neuroblastomas: evidence for two deleted regions. Cancer Genet Cytogenet, 1997. 96(2): p. 134-9.*
 44. Reale, M.A., M. Reyes-Mugica, W.E. Pierceall, M.C. Rubinstein, L. Hedrick, S.L. Cohn, A. Nakagawara, G.M. Brodeur, and E.R. Fearon, *Loss of DCC expression in neuroblastoma is associated with disease dissemination. Clin Cancer Res, 1996. 2(7): p. 1097-102.*

45. Nakagawara, A., M. Arima-Nakagawara, C.G. Azar, N.J. Scavarda, and G.M. Brodeur, *Clinical significance of expression of neurotrophic factors and their receptors in neuroblastoma*. Prog Clin Biol Res, 1994. **385**: p. 155-61.
46. Nakagawara, A. and G.M. Brodeur, *Role of neurotrophins and their receptors in human neuroblastomas: a primary culture study*. Eur J Cancer, 1997. **33**(12): p. 2050-3.
47. Yamashiro, D.J., X.G. Liu, C.P. Lee, A. Nakagawara, N. Ikegaki, L.M. McGregor, S.B. Baylin, and G.M. Brodeur, *Expression and function of TrkC in favourable human neuroblastomas*. Eur J Cancer, 1997. **33**(12): p. 2054-7.
48. Yamashiro, D.J., A. Nakagawara, N. Ikegaki, X.G. Liu, and G.M. Brodeur, *Expression of TrkC in favorable human neuroblastomas*. Oncogene, 1996. **12**(1): p. 37-41.
49. Ryden, M., R. Sehgal, C. Dominici, F.H. Schilling, C.F. Ibanez, and P. Kogner, *Expression of mRNA for the neurotrophin receptor trkC in neuroblastomas with favourable tumour stage and good prognosis*. Br J Cancer, 1996. **74**(5): p. 773-9.
50. Eggert, A., M.A. Grotzer, N. Ikegaki, X.G. Liu, A.E. Evans, and G.M. Brodeur, *Expression of neurotrophin receptor TrkA inhibits angiogenesis in neuroblastoma*. Med Pediatr Oncol, 2000. **35**(6): p. 569-72.
51. Ho, R., A. Eggert, T. Hishiki, J.E. Minturn, N. Ikegaki, P. Foster, A.M. Camoratto, A.E. Evans, and G.M. Brodeur, *Resistance to chemotherapy mediated by TrkB in neuroblastomas*. Cancer Res, 2002. **62**(22): p. 6462-6.
52. Goldstein, L.J., A.T. Fojo, K. Ueda, W. Crist, A. Green, G. Brodeur, I. Pastan, and M.M. Gottesman, *Expression of the multidrug resistance, MDR1, gene in neuroblastomas*. J Clin Oncol, 1990. **8**(1): p. 128-36.
53. Chan, H.S., G. Haddad, P.S. Thorner, G. DeBoer, Y.P. Lin, N. Ondrusek, H. Yeger, and V. Ling, *P-glycoprotein expression as a predictor of the outcome of therapy for neuroblastoma*. N Engl J Med, 1991. **325**(23): p. 1608-14.
54. Norris, M.D., S.B. Bordow, G.M. Marshall, P.S. Haber, S.L. Cohn, and M. Haber, *Expression of the gene for multidrug-resistance-associated protein and outcome in patients with neuroblastoma*. N Engl J Med, 1996. **334**(4): p. 231-8.
55. Hiyama, E., K. Hiyama, T. Yokoyama, Y. Matsuura, M.A. Piatyszek, and J.W. Shay, *Correlating telomerase activity levels with human neuroblastoma outcomes*. Nat Med, 1995. **1**(3): p. 249-55.
56. Poremba, C., H. Willenbring, B. Hero, H. Christiansen, K.L. Schafer, C. Brinkschmidt, H. Jurgens, W. Bocker, and B. Dockhorn-Dworniczak, *Telomerase activity distinguishes between neuroblastomas with good and poor prognosis*. Ann Oncol, 1999. **10**(6): p. 715-21.
57. Guglielmi, M., B. De Bernardi, A. Rizzo, S. Federici, C. Boglino, F. Siracusa, A. Leggio, F. Cozzi, G. Cecchetto, L. Musi, T. Bardini, A.M. Fagnani, G.C. Bartoli, A. Pampaloni, D. Rogers, M. Conte, C. Milanaccio, and P. Bruzzi, *Resection of primary tumor at diagnosis in stage IV-S neuroblastoma: does it affect the clinical course?* J Clin Oncol, 1996. **14**(5): p. 1537-44.
58. Kushner, B.H., N.K. Cheung, M.P. LaQuaglia, P.F. Ambros, I.M. Ambros, M.A. Bonilla, W.L. Gerald, M. Ladanyi, F. Gilbert, N.S. Rosenfield, and S.D.

- Yeh, *Survival from locally invasive or widespread neuroblastoma without cytotoxic therapy*. *J Clin Oncol*, 1996. **14**(2): p. 373-81.
59. Perez, C.A., K.K. Matthay, J.B. Atkinson, R.C. Seeger, H. Shimada, G.M. Haase, D.O. Stram, R.B. Gerbing, and J.N. Lukens, *Biologic variables in the outcome of stages I and II neuroblastoma treated with surgery as primary therapy: a children's cancer group study*. *J Clin Oncol*, 2000. **18**(1): p. 18-26.
60. Nickerson, H.J., K.K. Matthay, R.C. Seeger, G.M. Brodeur, H. Shimada, C. Perez, J.B. Atkinson, M. Selch, R.B. Gerbing, D.O. Stram, and J. Lukens, *Favorable biology and outcome of stage IV-S neuroblastoma with supportive care or minimal therapy: a Children's Cancer Group study*. *J Clin Oncol*, 2000. **18**(3): p. 477-86.
61. Schmidt, M.L., J.N. Lukens, R.C. Seeger, G.M. Brodeur, H. Shimada, R.B. Gerbing, D.O. Stram, C. Perez, G.M. Haase, and K.K. Matthay, *Biologic factors determine prognosis in infants with stage IV neuroblastoma: A prospective Children's Cancer Group study*. *J Clin Oncol*, 2000. **18**(6): p. 1260-8.
62. De Bernardi, B., B. Nicolas, L. Boni, P. Indolfi, M. Carli, L. Cordero Di Montezemolo, A. Donfrancesco, A. Pession, M. Provenzi, A. di Cataldo, A. Rizzo, G.P. Tonini, S. Dallorso, M. Conte, C. Gambini, A. Garaventa, F. Bonetti, A. Zanazzo, P. D'Angelo, and P. Bruzzi, *Disseminated neuroblastoma in children older than one year at diagnosis: comparable results with three consecutive high-dose protocols adopted by the Italian Co-Operative Group for Neuroblastoma*. *J Clin Oncol*, 2003. **21**(8): p. 1592-601.
63. Matthay, K.K., J.G. Villablanca, R.C. Seeger, D.O. Stram, R.E. Harris, N.K. Ramsay, P. Swift, H. Shimada, C.T. Black, G.M. Brodeur, R.B. Gerbing, and C.P. Reynolds, *Treatment of high-risk neuroblastoma with intensive chemotherapy, radiotherapy, autologous bone marrow transplantation, and 13-cis-retinoic acid. Children's Cancer Group*. *N Engl J Med*, 1999. **341**(16): p. 1165-73.
64. Gaspar, N., O. Hartmann, C. Munzer, C. Bergeron, F. Millot, L. Cousin-Lafay, A. Babin-Boilletot, P. Blouin, C. Pajot, and C. Coze, *Neuroblastoma in adolescents*. *Cancer*, 2003. **98**(2): p. 349-55.
65. Kushner, B.H., K. Kramer, M.P. LaQuaglia, S. Modak, and N.K. Cheung, *Neuroblastoma in adolescents and adults: the Memorial Sloan-Kettering experience*. *Med Pediatr Oncol*, 2003. **41**(6): p. 508-15.
66. Brodeur, G.M., J. Pritchard, F. Berthold, N.L. Carlsen, V. Castel, R.P. Castelberry, B. De Bernardi, A.E. Evans, M. Favrot, F. Hedborg, and et al., *Revisions of the international criteria for neuroblastoma diagnosis, staging, and response to treatment*. *J Clin Oncol*, 1993. **11**(8): p. 1466-77.
67. Ninane, J., J. Pritchard, P.H. Morris Jones, J.R. Mann, and J.S. Malpas, *Stage II neuroblastoma. Adverse prognostic significance of lymph node involvement*. *Arch Dis Child*, 1982. **57**(6): p. 438-42.
68. Hayes, F.A., A. Green, H.O. Hustu, and M. Kumar, *Surgicopathologic staging of neuroblastoma: prognostic significance of regional lymph node metastases*. *J Pediatr*, 1983. **102**(1): p. 59-62.
69. Oppenheimer, O., M. Alaminos, and W.L. Gerald, *Genomic medicine and neuroblastoma*. *Expert Rev Mol Diagn*, 2003. **3**(1): p. 39-54.

70. Shafford, E.A., D.W. Rogers, and J. Pritchard, *Advanced neuroblastoma: improved response rate using a multiagent regimen (OPEC) including sequential cisplatin and VM-26*. *J Clin Oncol*, 1984. **2**(7): p. 742-7.
71. Matthay, K.K., H.N. Sather, R.C. Seeger, G.M. Haase, and G.D. Hammond, *Excellent outcome of stage II neuroblastoma is independent of residual disease and radiation therapy*. *J Clin Oncol*, 1989. **7**(2): p. 236-44.
72. Frappaz, D., J. Michon, C. Coze, C. Berger, E. Plouvier, C. Lasset, J.L. Bernard, J.L. Stephan, E. Bouffet, M. Buclon, V. Combaret, A. Fourquet, T. Philip, and J.M. Zucker, *LMCE3 treatment strategy: results in 99 consecutively diagnosed stage 4 neuroblastomas in children older than 1 year at diagnosis*. *J Clin Oncol*, 2000. **18**(3): p. 468-76.
73. Philip, T., R. Ladenstein, C. Lasset, O. Hartmann, J.M. Zucker, R. Pinkerton, A.D. Pearson, T. Klingebiel, A. Garaventa, B. Kremens, J.L. Bernard, G. Rosti, and F. Chauvin, *1070 myeloablative megatherapy procedures followed by stem cell rescue for neuroblastoma: 17 years of European experience and conclusions*. *European Group for Blood and Marrow Transplant Registry Solid Tumour Working Party*. *Eur J Cancer*, 1997. **33**(12): p. 2130-5.
74. D'Angio, G.J., A.E. Evans, and C.E. Koop, *Special pattern of widespread neuroblastoma with a favourable prognosis*. *Lancet*, 1971. **1**(7708): p. 1046-9.
75. Mastrangelo, S., A. Tornesello, L. Diociaiuti, A. Pession, A. Prete, V. Rufini, L. Troncone, and R. Mastrangelo, *Treatment of advanced neuroblastoma: feasibility and therapeutic potential of a novel approach combining 131-I-MIBG and multiple drug chemotherapy*. *Br J Cancer*, 2001. **84**(4): p. 460-4.
76. Reynolds, C.P., P.F. Schindler, D.M. Jones, J.L. Gentile, R.T. Proffitt, and P.A. Einhorn, *Comparison of 13-cis-retinoic acid to trans-retinoic acid using human neuroblastoma cell lines*. *Prog Clin Biol Res*, 1994. **385**: p. 237-44.
77. Sidell, N., A. Altman, M.R. Haussler, and R.C. Seeger, *Effects of retinoic acid (RA) on the growth and phenotypic expression of several human neuroblastoma cell lines*. *Exp Cell Res*, 1983. **148**(1): p. 21-30.
78. Thiele, C.J., C.P. Reynolds, and M.A. Israel, *Decreased expression of N-myc precedes retinoic acid-induced morphological differentiation of human neuroblastoma*. *Nature*, 1985. **313**(6001): p. 404-6.
79. Lovat, P.E., M. Ranalli, M. Annichiarico-Petruzzelli, F. Bernassola, M. Piacentini, A.J. Malcolm, A.D. Pearson, G. Melino, and C.P. Redfern, *Effector mechanisms of fenretinide-induced apoptosis in neuroblastoma*. *Exp Cell Res*, 2000. **260**(1): p. 50-60.
80. Ponzoni, M., P. Bocca, V. Chiesa, A. Decensi, V. Pistoia, L. Raffaghello, C. Rozzo, and P.G. Montaldo, *Differential effects of N-(4-hydroxyphenyl)retinamide and retinoic acid on neuroblastoma cells: apoptosis versus differentiation*. *Cancer Res*, 1995. **55**(4): p. 853-61.
81. Reynolds, C.P., *Differentiating agents in pediatric malignancies: retinoids in neuroblastoma*. *Curr Oncol Rep*, 2000. **2**(6): p. 511-8.
82. Garaventa, A., R. Luksch, M.S. Lo Piccolo, E. Cavadini, P.G. Montaldo, M.R. Pizzitola, L. Boni, M. Ponzoni, A. Decensi, B. De Bernardi, F.F. Bellani, and F. Formelli, *Phase I trial and pharmacokinetics of fenretinide in children with neuroblastoma*. *Clin Cancer Res*, 2003. **9**(6): p. 2032-9.

83. Meitar, D., *Tumor Angiogenesis Correlates With Metastatic Disease, N-myc Amplification, and Poor Outcome in Human Neuroblastoma*. Journal of Clinical Oncology, 1996. **14**(2): p. 405-414.
84. Katzenstein, H.M., A.W. Rademaker, C. Senger, H.R. Salwen, N.N. Nguyen, P.S. Thorner, L. Litsas, and S.L. Cohn, *Effectiveness of the angiogenesis inhibitor TNP-470 in reducing the growth of human neuroblastoma in nude mice inversely correlates with tumor burden*. Clin Cancer Res, 1999. **5**(12): p. 4273-8.
85. Shusterman, S., S.A. Grupp, and J.M. Maris, *Inhibition of tumor growth in a human neuroblastoma xenograft model with TNP-470*. Med Pediatr Oncol, 2000. **35**(6): p. 673-6.
86. Wassberg, E., S. Pahlman, J.E. Westlin, and R. Christofferson, *The angiogenesis inhibitor TNP-470 reduces the growth rate of human neuroblastoma in nude rats*. Pediatr Res, 1997. **41**(3): p. 327-33.
87. Shusterman, S., S.A. Grupp, R. Barr, D. Carpentieri, H. Zhao, and J.M. Maris, *The angiogenesis inhibitor tnp-470 effectively inhibits human neuroblastoma xenograft growth, especially in the setting of subclinical disease*. Clin Cancer Res, 2001. **7**(4): p. 977-84.
88. Wang, J., G.S. Sheppard, P. Lou, M. Kawai, N. BaMaung, S.A. Erickson, L. Tucker-Garcia, C. Park, J. Bouska, Y.C. Wang, D. Frost, P. Tapang, D.H. Albert, S.J. Morgan, M. Morowitz, S. Shusterman, J.M. Maris, R. Lesniewski, and J. Henkin, *Tumor suppression by a rationally designed reversible inhibitor of methionine aminopeptidase-2*. Cancer Res, 2003. **63**(22): p. 7861-9.
89. Wu, Z.L., E. Schwartz, R. Seeger, and S. Ladisch, *Expression of GD2 ganglioside by untreated primary human neuroblastomas*. Cancer Res, 1986. **46**(1): p. 440-3.
90. Cheung, N.K., B.H. Kushner, S.D. Yeh, and S.M. Larson, *3F8 monoclonal antibody treatment of patients with stage 4 neuroblastoma: a phase II study*. Int J Oncol, 1998. **12**(6): p. 1299-306.
91. Frost, J.D., J.A. Hank, G.H. Reaman, S. Frierdich, R.C. Seeger, J. Gan, P.M. Anderson, L.J. Ettinger, M.S. Cairo, B.R. Blazar, M.D. Krailo, K.K. Matthay, R.A. Reisfeld, and P.M. Sondel, *A phase I/II trial of murine monoclonal anti-GD2 antibody 14.G2a plus interleukin-2 in children with refractory neuroblastoma: a report of the Children's Cancer Group*. Cancer, 1997. **80**(2): p. 317-33.
92. Yu, A.L., M.M. Uttenreuther-Fischer, C.S. Huang, C.C. Tsui, S.D. Gillies, R.A. Reisfeld, and F.H. Kung, *Phase I trial of a human-mouse chimeric anti-disialoganglioside monoclonal antibody ch14.18 in patients with refractory neuroblastoma and osteosarcoma*. J Clin Oncol, 1998. **16**(6): p. 2169-80.
93. Miederer, M., M.R. McDevitt, P. Borchardt, I. Bergman, K. Kramer, N.K. Cheung, and D.A. Scheinberg, *Treatment of neuroblastoma meningeal carcinomatosis with intrathecal application of alpha-emitting atomic nanogenerators targeting disialo-ganglioside GD2*. Clin Cancer Res, 2004. **10**(20): p. 6985-92.
94. Modak, S. and N.K. Cheung, *Antibody-based targeted radiation to pediatric tumors*. J Nucl Med, 2005. **46** Suppl 1: p. 157S-63S.
95. Raffaghello, L., G. Pagnan, F. Pastorino, E. Cosimo, C. Brignole, D. Marimpietri, P.G. Montaldo, C. Gambini, T.M. Allen, E. Bogenmann, and M.

- Ponzoni, *In vitro and in vivo antitumor activity of liposomal Fenretinide targeted to human neuroblastoma*. Int J Cancer, 2003. **104**(5): p. 559-67.
96. Brignole, C., F. Pastorino, D. Marimpietri, G. Pagnan, A. Pistorio, T.M. Allen, V. Pistoia, and M. Ponzoni, *Immune cell-mediated antitumor activities of GD2-targeted liposomal c-myc antisense oligonucleotides containing CpG motifs*. J Natl Cancer Inst, 2004. **96**(15): p. 1171-80.
 97. Pastorino, F., C. Brignole, D. Marimpietri, P. Sapra, E.H. Moase, T.M. Allen, and M. Ponzoni, *Doxorubicin-loaded Fab' fragments of anti-disialoganglioside immunoliposomes selectively inhibit the growth and dissemination of human neuroblastoma in nude mice*. Cancer Res, 2003. **63**(1): p. 86-92.
 98. Cunningham, S., M. Boyd, M.M. Brown, S. Carlin, A. McCluskey, A. Livingstone, R.J. Mairs, and T.E. Wheldon, *A gene therapy approach to enhance the targeted radiotherapy of neuroblastoma*. Med Pediatr Oncol, 2000. **35**(6): p. 708-11.
 99. Jaques, S., Jr., M.C. Tobes, J.C. Sisson, J.A. Baker, and D.M. Wieland, *Comparison of the sodium dependency of uptake of meta-iodobenzylguanidine and norepinephrine into cultured bovine adrenomedullary cells*. Mol Pharmacol, 1984. **26**(3): p. 539-46.
 100. Mairs, R.J., A. Livingstone, M.N. Gaze, T.E. Wheldon, and A. Barrett, *Prediction of accumulation of 131I-labelled meta-iodobenzylguanidine in neuroblastoma cell lines by means of reverse transcription and polymerase chain reaction*. Br J Cancer, 1994. **70**(1): p. 97-101.
 101. Pacholczyk, T., R.D. Blakely, and S.G. Amara, *Expression cloning of a cocaine- and antidepressant-sensitive human noradrenaline transporter*. Nature, 1991. **350**(6316): p. 350-4.
 102. Boubaker, A. and A. Bischof Delaloye, *Nuclear medicine procedures and neuroblastoma in childhood. Their value in the diagnosis, staging and assessment of response to therapy*. Q J Nucl Med, 2003. **47**(1): p. 31-40.
 103. Ilias, I. and K. Pacak, *Diagnosis and management of tumors of the adrenal medulla*. Horm Metab Res, 2005. **37**(12): p. 717-21.
 104. Troncone, L. and V. Rufini, *131I-MIBG therapy of neural crest tumours (review)*. Anticancer Res, 1997. **17**(3B): p. 1823-31.
 105. Kang, T.I., P. Brophy, M. Hickeson, S. Heyman, A.E. Evans, M. Charron, and J.M. Maris, *Targeted radiotherapy with submyeloablative doses of 131I-MIBG is effective for disease palliation in highly refractory neuroblastoma*. J Pediatr Hematol Oncol, 2003. **25**(10): p. 769-73.
 106. Castellani, M.R., A. Chiti, E. Seregini, and E. Bombardieri, *Role of 131I-metaiodobenzylguanidine (MIBG) in the treatment of neuroendocrine tumours. Experience of the National Cancer Institute of Milan*. Q J Nucl Med, 2000. **44**(1): p. 77-87.
 107. Garaventa, A., O. Bellagamba, M.S. Lo Piccolo, C. Milanaccio, E. Lanino, L. Bertolazzi, G.P. Villavecchia, M. Cabria, G. Scopinaro, F. Claudiani, and B. De Bernardi, *131I-metaiodobenzylguanidine (131I-MIBG) therapy for residual neuroblastoma: a mono-institutional experience with 43 patients*. Br J Cancer, 1999. **81**(8): p. 1378-84.
 108. Garaventa, A., P. Guerra, A. Arrighini, L. Bertolazzi, M. Bestagno, B. De Bernardi, E. Lanino, G.P. Villavecchia, and F. Claudiani, *Treatment of advanced neuroblastoma with I-131 meta-iodobenzylguanidine*. Cancer, 1991. **67**(4): p. 922-8.

109. Lashford, L.S., I.J. Lewis, S.L. Fielding, M.A. Flower, S. Meller, J.T. Kemshead, and D. Ackery, *Phase I/II study of iodine 131 metaiodobenzylguanidine in chemoresistant neuroblastoma: a United Kingdom Children's Cancer Study Group investigation*. *J Clin Oncol*, 1992. **10**(12): p. 1889-96.
110. Matthay, K.K., K. DeSantes, B. Hasegawa, J. Huberty, R.S. Hattner, A. Ablin, C.P. Reynolds, R.C. Seeger, V.K. Weinberg, and D. Price, *Phase I dose escalation of 131I-metaiodobenzylguanidine with autologous bone marrow support in refractory neuroblastoma*. *J Clin Oncol*, 1998. **16**(1): p. 229-36.
111. Moyes, J.S., J.W. Babich, R. Carter, S.T. Meller, M. Agrawal, and T.J. McElwain, *Quantitative study of radioiodinated metaiodobenzylguanidine uptake in children with neuroblastoma: correlation with tumor histopathology*. *J Nucl Med*, 1989. **30**(4): p. 474-80.
112. Mairs, R.J., *Neuroblastoma therapy using radiolabelled [131I]metaiodobenzylguanidine ([131I]MIBG) in combination with other agents*. *Eur J Cancer*, 1999. **35**(8): p. 1171-3.
113. Smets, L.A., M. Janssen, M. Rutgers, K. Ritzen, and C. Buttenhuis, *Pharmacokinetics and intracellular distribution of the tumor-targeted radiopharmaceutical m-iodo-benzylguanidine in SK-N-SH neuroblastoma and PC-12 pheochromocytoma cells*. *Int J Cancer*, 1991. **48**(4): p. 609-15.
114. Montaldo, P.G., L. Raffaghello, F. Guarnaccia, V. Pistoia, A. Garaventa, and M. Ponzoni, *Increase of metaiodobenzylguanidine uptake and intracellular half-life during differentiation of human neuroblastoma cells*. *Int J Cancer*, 1996. **67**(1): p. 95-100.
115. Armour, A., S.H. Cunningham, M.N. Gaze, T.E. Wheldon, and R.J. Mairs, *The effect of cisplatin pretreatment on the accumulation of MIBG by neuroblastoma cells in vitro*. *Br J Cancer*, 1997. **75**(4): p. 470-6.
116. Meco, D., A. Lasorella, A. Riccardi, T. Servidei, R. Mastrangelo, and R. Riccardi, *Influence of cisplatin and doxorubicin on 125I-metaiodobenzylguanidine uptake in human neuroblastoma cell lines*. *Eur J Cancer*, 1999. **35**(8): p. 1227-34.
117. Greider, C.W., *Telomere length regulation*. *Annu Rev Biochem*, 1996. **65**: p. 337-65.
118. Harley, C.B., A.B. Futcher, and C.W. Greider, *Telomeres shorten during ageing of human fibroblasts*. *Nature*, 1990. **345**(6274): p. 458-60.
119. Hastie, N.D., M. Dempster, M.G. Dunlop, A.M. Thompson, D.K. Green, and R.C. Allshire, *Telomere reduction in human colorectal carcinoma and with ageing*. *Nature*, 1990. **346**(6287): p. 866-8.
120. Kim, N.W., M.A. Piatyszek, K.R. Prowse, C.B. Harley, M.D. West, P.L. Ho, G.M. Coviello, W.E. Wright, S.L. Weinrich, and J.W. Shay, *Specific association of human telomerase activity with immortal cells and cancer*. *Science*, 1994. **266**(5193): p. 2011-5.
121. Broccoli, D., J.W. Young, and T. de Lange, *Telomerase activity in normal and malignant hematopoietic cells*. *Proc Natl Acad Sci U S A*, 1995. **92**(20): p. 9082-6.
122. Harle-Bachor, C. and P. Boukamp, *Telomerase activity in the regenerative basal layer of the epidermis in human skin and in immortal and carcinoma-derived skin keratinocytes*. *Proc Natl Acad Sci U S A*, 1996. **93**(13): p. 6476-81.

123. Tahara, H., W. Yasui, E. Tahara, J. Fujimoto, K. Ito, K. Tamai, J. Nakayama, F. Ishikawa, E. Tahara, and T. Ide, *Immuno-histochemical detection of human telomerase catalytic component, hTERT, in human colorectal tumor and non-tumor tissue sections*. *Oncogene*, 1999. **18**(8): p. 1561-7.
124. Shay, J.W., Y. Zou, E. Hiyama, and W.E. Wright, *Telomerase and cancer*. *Hum Mol Genet*, 2001. **10**(7): p. 677-85.
125. Abdul-Ghani, R., P. Ohana, I. Matouk, S. Ayesh, B. Ayesh, M. Laster, O. Bibi, H. Giladi, K. Molnar-Kimber, M.A. Sughayer, N. de Groot, and A. Hochberg, *Use of transcriptional regulatory sequences of telomerase (hTER and hTERT) for selective killing of cancer cells*. *Mol Ther*, 2000. **2**(6): p. 539-44.
126. Hoare, S.F., L.A. Bryce, G.B. Wisman, S. Burns, J.J. Goings, A.G. van der Zee, and W.N. Keith, *Lack of telomerase RNA gene hTERC expression in alternative lengthening of telomeres cells is associated with methylation of the hTERC promoter*. *Cancer Res*, 2001. **61**(1): p. 27-32.
127. Zhao, J.Q., R.M. Glasspool, S.F. Hoare, A. Billsland, I. Szatmari, and W.N. Keith, *Activation of telomerase rna gene promoter activity by NF-Y, Sp1, and the retinoblastoma protein and repression by Sp3*. *Neoplasia*, 2000. **2**(6): p. 531-9.
128. Stanta, G., S. Bonin, B. Niccolini, A. Raccanelli, and F. Baralle, *Catalytic subunit of telomerase expression is related to RNA component expression*. *FEBS Lett*, 1999. **460**(2): p. 285-8.
129. Wisman, G.B., S. De Jong, G.J. Meersma, M.N. Helder, H. Hollema, E.G. de Vries, W.N. Keith, and A.G. van der Zee, *Telomerase in (pre)neoplastic cervical disease*. *Hum Pathol*, 2000. **31**(10): p. 1304-12.
130. Hiyama, E., K. Hiyama, T. Yokoyama, and J.W. Shay, *Immunohistochemical detection of telomerase (hTERT) protein in human cancer tissues and a subset of cells in normal tissues*. *Neoplasia*, 2001. **3**(1): p. 17-26.
131. Kolquist, K.A., L.W. Ellisen, C.M. Counter, M. Meyerson, L.K. Tan, R.A. Weinberg, D.A. Haber, and W.L. Gerald, *Expression of TERT in early premalignant lesions and a subset of cells in normal tissues*. *Nat Genet*, 1998. **19**(2): p. 182-6.
132. Majumdar, A.S., D.E. Hughes, S.P. Lichtsteiner, Z. Wang, J.S. Lebkowski, and A.P. Vasserot, *The telomerase reverse transcriptase promoter drives efficacious tumor suicide gene therapy while preventing hepatotoxicity encountered with constitutive promoters*. *Gene Ther*, 2001. **8**(7): p. 568-78.
133. Boyd, M., R.J. Mairs, S.C. Mairs, L. Wilson, A. Livingstone, S.H. Cunningham, M.M. Brown, M. Quigg, and W.N. Keith, *Expression in UVW glioma cells of the noradrenaline transporter gene, driven by the telomerase RNA promoter, induces active uptake of [131I]MIBG and clonogenic cell kill*. *Oncogene*, 2001. **20**(53): p. 7804-8.
134. el-Deiry, W.S., T. Tokino, V.E. Velculescu, D.B. Levy, R. Parsons, J.M. Trent, D. Lin, W.E. Mercer, K.W. Kinzler, and B. Vogelstein, *WAF1, a potential mediator of p53 tumor suppression*. *Cell*, 1993. **75**(4): p. 817-25.
135. Worthington, J., T. Robson, M. Murray, M. O'Rourke, G. Keilty, and D.G. Hirst, *Modification of vascular tone using iNOS under the control of a radiation-inducible promoter*. *Gene Ther*, 2000. **7**(13): p. 1126-31.

136. Vaidyanathan, G., H.S. Friedman, S.T. Keir, and M.R. Zalutsky, *Evaluation of meta-[211At]astatobenzylguanidine in an athymic mouse human neuroblastoma xenograft model*. Nucl Med Biol, 1996. **23**(6): p. 851-6.
137. Strickland, D.K., G. Vaidyanathan, and M.R. Zalutsky, *Cytotoxicity of alpha-particle-emitting m-[211At]astatobenzylguanidine on human neuroblastoma cells*. Cancer Res, 1994. **54**(20): p. 5414-9.
138. Pagnan, G., D.D. Stuart, F. Pastorino, L. Raffaghello, P.G. Montaldo, T.M. Allen, B. Calabretta, and M. Ponzoni, *Delivery of c-myc antisense oligodeoxynucleotides to human neuroblastoma cells via disialoganglioside GD(2)-targeted immunoliposomes: antitumor effects*. J Natl Cancer Inst, 2000. **92**(3): p. 253-61.
139. Pastorino, F., D. Stuart, M. Ponzoni, and T.M. Allen, *Targeted delivery of antisense oligonucleotides in cancer*. J Control Release, 2001. **74**(1-3): p. 69-75.
140. Stuart, D.D. and T.M. Allen, *Pharmacokinetics of pegylated liposomal asODNs*. Proc. Int. Symp. Control. Rel. Bioact. Mater, 1998. **25**: p. 366-367.
141. Stuart, D.D., G.Y. Kao, and T.M. Allen, *A novel, long-circulating, and functional liposomal formulation of antisense oligodeoxynucleotides targeted against MDR1*. Cancer Gene Ther, 2000. **7**(3): p. 466-75.
142. Ishida, O., K. Maruyama, K. Sasaki, and M. Iwatsuru, *Size-dependent extravasation and interstitial localization of polyethyleneglycol liposomes in solid tumor-bearing mice*. Int J Pharm, 1999. **190**(1): p. 49-56.
143. Huang, S.K., K. Hong, K.D. Lee, D. Papahadjopoulos, and D.S. Friend, *Light microscopic localization of silver-enhanced liposome-entrapped colloidal gold in mouse tissues*. Biochim Biophys Acta, 1991. **1069**(1): p. 117-21.
144. Yuan, F., M. Leunig, S.K. Huang, D.A. Berk, D. Papahadjopoulos, and R.K. Jain, *Microvascular permeability and interstitial penetration of sterically stabilized (stealth) liposomes in a human tumor xenograft*. Cancer Res, 1994. **54**(13): p. 3352-6.
145. Kanai, F., Y. Shiratori, Y. Yoshida, H. Wakimoto, H. Hamada, Y. Kanegae, I. Saito, H. Nakabayashi, T. Tamaoki, T. Tanaka, K.H. Lan, N. Kato, S. Shiina, and M. Omata, *Gene therapy for alpha-fetoprotein-producing human hepatoma cells by adenovirus-mediated transfer of the herpes simplex virus thymidine kinase gene*. Hepatology, 1996. **23**(6): p. 1359-68.
146. Cao, G., S. Kuriyama, J. Gao, M. Kikukawa, L. Cui, T. Nakatani, X. Zhang, H. Tsujinoue, X. Pan, H. Fukui, and Z. Qi, *Effective and safe gene therapy for colorectal carcinoma using the cytosine deaminase gene directed by the carcinoembryonic antigen promoter*. Gene Ther, 1999. **6**(1): p. 83-90.
147. Vernimmen, D., M. Gueders, S. Pisvin, P. Delvenne, and R. Winkler, *Different mechanisms are implicated in ERBB2 gene overexpression in breast and in other cancers*. Br J Cancer, 2003. **89**(5): p. 899-906.
148. Harris, J.D., A.A. Gutierrez, H.C. Hurst, K. Sikora, and N.R. Lemoine, *Gene therapy for cancer using tumour-specific prodrug activation*. Gene Ther, 1994. **1**(3): p. 170-5.
149. Sikora, K., J. Harris, H. Hurst, and N. Lemoine, *Therapeutic strategies using c-erbB-2 promoter-controlled drug activation*. Ann N Y Acad Sci, 1994. **716**: p. 115-24; discussion 124-5, 140-3.
150. Chen, L., D. Chen, Y. Manome, Y. Dong, H.A. Fine, and D.W. Kufe, *Breast cancer selective gene expression and therapy mediated by recombinant*

- adenoviruses containing the DF3/MUC1 promoter.* J Clin Invest, 1995. **96**(6): p. 2775-82.
151. Koeneman, K.S., C. Kao, S.C. Ko, L. Yang, Y. Wada, D.F. Kallmes, J.Y. Gillenwater, H.E. Zhou, L.W. Chung, and T.A. Gardner, *Osteocalcin-directed gene therapy for prostate-cancer bone metastasis.* World J Urol, 2000. **18**(2): p. 102-10.
 152. Chung, I., P.E. Schwartz, R.G. Crystal, G. Pizzorno, J. Leavitt, and A.B. Deisseroth, *Use of L-plastin promoter to develop an adenoviral system that confers transgene expression in ovarian cancer cells but not in normal mesothelial cells.* Cancer Gene Ther, 1999. **6**(2): p. 99-106.
 153. Muramatsu, T., *Midkine and pleiotrophin: two related proteins involved in development, survival, inflammation and tumorigenesis.* J Biochem (Tokyo), 2002. **132**(3): p. 359-71.
 154. Adachi, Y., P.N. Reynolds, M. Yamamoto, W.E. Grizzle, K. Overturf, S. Matsubara, T. Muramatsu, and D.T. Curiel, *Midkine promoter-based adenoviral vector gene delivery for pediatric solid tumors.* Cancer Res, 2000. **60**(16): p. 4305-10.
 155. Casado, E., J. Gomez-Navarro, M. Yamamoto, Y. Adachi, C.J. Coolidge, W.O. Arafat, S.D. Barker, M.H. Wang, P.J. Mahasreshti, A. Hemminki, M. Gonzalez-Baron, M.N. Barnes, T.B. Pustilnik, G.P. Siegal, R.D. Alvarez, and D.T. Curiel, *Strategies to accomplish targeted expression of transgenes in ovarian cancer for molecular therapeutic applications.* Clin Cancer Res, 2001. **7**(8): p. 2496-504.
 156. Wesseling, J.G., M. Yamamoto, Y. Adachi, P.J. Bosma, M. van Wijland, J.L. Blackwell, H. Li, P.N. Reynolds, I. Dmitriev, S.M. Vickers, K. Huibregtse, and D.T. Curiel, *Midkine and cyclooxygenase-2 promoters are promising for adenoviral vector gene delivery of pancreatic carcinoma.* Cancer Gene Ther, 2001. **8**(12): p. 990-6.
 157. Blackburn, E.H., *The end of the (DNA) line.* Nat Struct Biol, 2000. **7**(10): p. 847-50.
 158. Moyzis, R.K., J.M. Buckingham, L.S. Cram, M. Dani, L.L. Deaven, M.D. Jones, J. Meyne, R.L. Ratliff, and J.R. Wu, *A highly conserved repetitive DNA sequence, (TTAGGG)_n, present at the telomeres of human chromosomes.* Proc Natl Acad Sci U S A, 1988. **85**(18): p. 6622-6.
 159. Huffman, K.E., S.D. Levene, V.M. Tesmer, J.W. Shay, and W.E. Wright, *Telomere shortening is proportional to the size of the G-rich telomeric 3'-overhang.* J Biol Chem, 2000. **275**(26): p. 19719-22.
 160. Olovnikov, A.M., *A theory of marginotomy. The incomplete copying of template margin in enzymic synthesis of polynucleotides and biological significance of the phenomenon.* J Theor Biol, 1973. **41**(1): p. 181-90.
 161. Blackburn, E.H., *Telomerases.* Annu Rev Biochem, 1992. **61**: p. 113-29.
 162. Bryan, T.M. and T.R. Cech, *Telomerase and the maintenance of chromosome ends.* Curr Opin Cell Biol, 1999. **11**(3): p. 318-24.
 163. Greider, C.W. and E.H. Blackburn, *Identification of a specific telomere terminal transferase activity in Tetrahymena extracts.* Cell, 1985. **43**(2 Pt 1): p. 405-13.
 164. Lingner, J., T.R. Hughes, A. Shevchenko, M. Mann, V. Lundblad, and T.R. Cech, *Reverse transcriptase motifs in the catalytic subunit of telomerase.* Science, 1997. **276**(5312): p. 561-7.

165. Morin, G.B., *The human telomere terminal transferase enzyme is a ribonucleoprotein that synthesizes TTAGGG repeats.* Cell, 1989. **59**(3): p. 521-9.
166. Nakamura, T.M., G.B. Morin, K.B. Chapman, S.L. Weinrich, W.H. Andrews, J. Lingner, C.B. Harley, and T.R. Cech, *Telomerase catalytic subunit homologs from fission yeast and human.* Science, 1997. **277**(5328): p. 955-9.
167. Weinrich, S.L., R. Pruzan, L. Ma, M. Ouellette, V.M. Tesmer, S.E. Holt, A.G. Bodnar, S. Lichtsteiner, N.W. Kim, J.B. Trager, R.D. Taylor, R. Carlos, W.H. Andrews, W.E. Wright, J.W. Shay, C.B. Harley, and G.B. Morin, *Reconstitution of human telomerase with the template RNA component hTR and the catalytic protein subunit hTRT.* Nat Genet, 1997. **17**(4): p. 498-502.
168. Wright, W.E., M.A. Piatyszek, W.E. Rainey, W. Byrd, and J.W. Shay, *Telomerase activity in human germline and embryonic tissues and cells.* Dev Genet, 1996. **18**(2): p. 173-9.
169. Shay, J.W. and S. Bacchetti, *A survey of telomerase activity in human cancer.* Eur J Cancer, 1997. **33**(5): p. 787-91.
170. Feng, J., W.D. Funk, S.S. Wang, S.L. Weinrich, A.A. Avilion, C.P. Chiu, R.R. Adams, E. Chang, R.C. Allsopp, J. Yu, and et al., *The RNA component of human telomerase.* Science, 1995. **269**(5228): p. 1236-41.
171. Shay, J.W. and W.E. Wright, *Ageing and cancer: the telomere and telomerase connection.* Novartis Found Symp, 2001. **235**: p. 116-25; discussion 125-9, 146-9.
172. Koga, S., S. Hirohata, Y. Kondo, T. Komata, M. Takakura, M. Inoue, S. Kyo, and S. Kondo, *FADD gene therapy using the human telomerase catalytic subunit (hTERT) gene promoter to restrict induction of apoptosis to tumors in vitro and in vivo.* Anticancer Res, 2001. **21**(3B): p. 1937-43.
173. Komata, T., S. Koga, S. Hirohata, M. Takakura, I.M. Germano, M. Inoue, S. Kyo, S. Kondo, and Y. Kondo, *A novel treatment of human malignant gliomas in vitro and in vivo: FADD gene transfer under the control of the human telomerase reverse transcriptase gene promoter.* Int J Oncol, 2001. **19**(5): p. 1015-20.
174. Komata, T., Y. Kondo, T. Kanzawa, S. Hirohata, S. Koga, H. Sumiyoshi, S.M. Srinivasula, B.P. Barna, I.M. Germano, M. Takakura, M. Inoue, E.S. Ainemri, J.W. Shay, S. Kyo, and S. Kondo, *Treatment of malignant glioma cells with the transfer of constitutively active caspase-6 using the human telomerase catalytic subunit (human telomerase reverse transcriptase) gene promoter.* Cancer Res, 2001. **61**(15): p. 5796-802.
175. Gu, J., M. Andreeff, J.A. Roth, and B. Fang, *hTERT promoter induces tumor-specific Bax gene expression and cell killing in syngenic mouse tumor model and prevents systemic toxicity.* Gene Ther, 2002. **9**(1): p. 30-7.
176. Gu, J., S. Kagawa, M. Takakura, S. Kyo, M. Inoue, J.A. Roth, and B. Fang, *Tumor-specific transgene expression from the human telomerase reverse transcriptase promoter enables targeting of the therapeutic effects of the Bax gene to cancers.* Cancer Res, 2000. **60**(19): p. 5359-64.
177. Plumb, J.A., A. Bilisland, R. Kakani, J. Zhao, R.M. Glasspool, R.J. Knox, T.R. Evans, and W.N. Keith, *Telomerase-specific suicide gene therapy vectors expressing bacterial nitroreductase sensitize human cancer cells to the pro-drug CB1954.* Oncogene, 2001. **20**(53): p. 7797-803.

178. Boyd, M., R.J. Mairs, W.N. Keith, S.C. Ross, P. Welsh, G. Akabani, J. Owens, G. Vaidyanathan, R. Carruthers, J. Dorrens, and M.R. Zalutsky, *An efficient targeted radiotherapy/gene therapy strategy utilising human telomerase promoters and radioastatine and harnessing radiation-mediated bystander effects*. *J Gene Med*, 2004. **6**(8): p. 937-47.
179. Fullerton, N.E., R.J. Mairs, D. Kirk, W.N. Keith, R. Carruthers, A.G. McCluskey, M. Brown, L. Wilson, and M. Boyd, *Application of targeted radiotherapy/gene therapy to bladder cancer cell lines*. *Eur Urol*, 2005. **47**(2): p. 250-6.
180. Fullerton, N.E., M. Boyd, R.J. Mairs, W.N. Keith, O. Alderwish, M.M. Brown, A. Livingstone, and D. Kirk, *Combining a targeted radiotherapy and gene therapy approach for adenocarcinoma of prostate*. *Prostate Cancer Prostatic Dis*, 2004. **7**(4): p. 355-63.
181. Hunter, D.H., and Zhu, X., *Polymer-Supported Radiopharmaceuticals: [¹³¹I]MIBG and [¹²³I]MIBG*. *Journal of Labelled Compounds and Radiopharmaceuticals*, 1999. **42**: p. 653-661.
182. Boyd, M., *Preclinical evaluation of no-carrier-added [¹³¹I]meta-iodobenzyl guanidine, for the treatment of tumours transfected with the noradrenaline transporter gene*. *Lett Drug Des Disc*, 2004. **1**: p. 50-57.
183. Zalutsky, M.R., P.K. Garg, H.S. Friedman, and D.D. Bigner, *Labeling monoclonal antibodies and F(ab')₂ fragments with the alpha-particle-emitting nuclide astatine-211: preservation of immunoreactivity and in vivo localizing capacity*. *Proc Natl Acad Sci U S A*, 1989. **86**(18): p. 7149-53.
184. Vaidyanathan, G. and M.R. Zalutsky, *1-(m-[²¹¹At]astatobenzyl)guanidine: synthesis via astatate demetalation and preliminary in vitro and in vivo evaluation*. *Bioconjug Chem*, 1992. **3**(6): p. 499-503.
185. Biedler, J.L., S. Roffler-Tarlov, M. Schachner, and L.S. Freedman, *Multiple neurotransmitter synthesis by human neuroblastoma cell lines and clones*. *Cancer Res*, 1978. **38**(11 Pt 1): p. 3751-7.
186. Iavarone, A., A. Lasorella, T. Servidei, R. Riccardi, and R. Mastrangelo, *Uptake and storage of m-iodobenzylguanidine are frequent neuronal functions of human neuroblastoma cell lines*. *Cancer Res*, 1993. **53**(2): p. 304-9.
187. Boyd, M., S.H. Cunningham, M.M. Brown, R.J. Mairs, and T.E. Wheldon, *Noradrenaline transporter gene transfer for radiation cell kill by ¹³¹I meta-iodobenzylguanidine*. *Gene Ther*, 1999. **6**(6): p. 1147-52.
188. Boyd, M., R.J. Mairs, S.H. Cunningham, S.C. Mairs, A. McCluskey, A. Livingstone, K. Stevenson, M.M. Brown, L. Wilson, S. Carlin, and T.E. Wheldon, *A gene therapy/targeted radiotherapy strategy for radiation cell kill by [¹³¹I]meta-iodobenzylguanidine*. *J Gene Med*, 2001. **3**(2): p. 165-72.
189. Zhao, J.Q., S.F. Hoare, R. McFarlane, S. Muir, E.K. Parkinson, D.M. Black, and W.N. Keith, *Cloning and characterization of human and mouse telomerase RNA gene promoter sequences*. *Oncogene*, 1998. **16**(10): p. 1345-50.
190. Takakura, M., S. Kyo, T. Kanaya, H. Hirano, J. Takeda, M. Yutsudo, and M. Inoue, *Cloning of human telomerase catalytic subunit (hTERT) gene promoter and identification of proximal core promoter sequences essential for transcriptional activation in immortalized and cancer cells*. *Cancer Res*, 1999. **59**(3): p. 551-7.

191. Gil, M.E. and T.L. Coetzer, *Real-time quantitative RT-PCR for human telomere elongation reverse transcriptase in chronic myeloid leukemia*. *Leuk Res*, 2004. **28**(9): p. 969-72.
192. Boyd, M., S.C. Mairs, K. Stevenson, A. Livingstone, A.M. Clark, S.C. Ross, and R.J. Mairs, *Transfectant mosaic spheroids: a new model for evaluation of tumour cell killing in targeted radiotherapy and experimental gene therapy*. *J Gene Med*, 2002. **4**(5): p. 567-76.
193. Collas, P., *Modulation of plasmid DNA methylation and expression in zebrafish embryos*. *Nucleic Acids Res*, 1998. **26**(19): p. 4454-61.
194. Grassi, G., P. Maccaroni, R. Meyer, H. Kaiser, E. D'Ambrosio, E. Pascale, M. Grassi, A. Kuhn, P. Di Nardo, R. Kandolf, and J.H. Kupper, *Inhibitors of DNA methylation and histone deacetylation activate cytomegalovirus promoter-controlled reporter gene expression in human glioblastoma cell line U87*. *Carcinogenesis*, 2003. **24**(10): p. 1625-35.
195. Prosch, S., J. Stein, K. Staak, C. Liebenthal, H.D. Volk, and D.H. Kruger, *Inactivation of the very strong HCMV immediate early promoter by DNA CpG methylation in vitro*. *Biol Chem Hoppe Seyler*, 1996. **377**(3): p. 195-201.
196. Nicol Keith, W., T.R. Jeffrey Evans, and R.M. Glasspool, *Telomerase and cancer: time to move from a promising target to a clinical reality*. *J Pathol*, 2001. **195**(4): p. 404-14.
197. Urquidi, V., D. Tarin, and S. Goodison, *Role of telomerase in cell senescence and oncogenesis*. *Annu Rev Med*, 2000. **51**: p. 65-79.
198. Melissourgos, N., N.G. Kastrinakis, I. Davilas, P. Foukas, A. Farnakis, and M. Lykourinas, *Detection of human telomerase reverse transcriptase mRNA in urine of patients with bladder cancer: evaluation of an emerging tumor marker*. *Urology*, 2003. **62**(2): p. 362-7.
199. Juttermann, R., E. Li, and R. Jaenisch, *Toxicity of 5-aza-2'-deoxycytidine to mammalian cells is mediated primarily by covalent trapping of DNA methyltransferase rather than DNA demethylation*. *Proc Natl Acad Sci U S A*, 1994. **91**(25): p. 11797-801.
200. Wheldon, T.E., J.A. O'Donoghue, A. Barrett, and A.S. Michalowski, *The curability of tumours of differing size by targeted radiotherapy using 131I or 90Y*. *Radiother Oncol*, 1991. **21**(2): p. 91-9.
201. Gaze, M.N., R.J. Mairs, S.M. Boyack, T.E. Wheldon, and A. Barrett, *131I-meta-iodobenzylguanidine therapy in neuroblastoma spheroids of different sizes*. *Br J Cancer*, 1992. **66**(6): p. 1048-52.
202. Allen, B.J., *Targeted alpha therapy: evidence for potential efficacy of alpha-immunoconjugates in the management of micrometastatic cancer*. *Australas Radiol*, 1999. **43**(4): p. 480-6.
203. Imam, S.K., *Advancements in cancer therapy with alpha-emitters: a review*. *Int J Radiat Oncol Biol Phys*, 2001. **51**(1): p. 271-8.
204. Zalutsky, M.R. and G. Vaidyanathan, *Astatine-211-labeled radiotherapeutics: an emerging approach to targeted alpha-particle radiotherapy*. *Curr Pharm Des*, 2000. **6**(14): p. 1433-55.
205. Jurcic, J.G., S.M. Larson, G. Sgouros, M.R. McDevitt, R.D. Finn, C.R. Divgi, A.M. Ballangrud, K.A. Hamacher, D. Ma, J.L. Humm, M.W. Brechbiel, R. Molinet, and D.A. Scheinberg, *Targeted alpha particle immunotherapy for myeloid leukemia*. *Blood*, 2002. **100**(4): p. 1233-9.

206. Boyd, M., H.S. Spinning, and R.J. Mairs, *Radiation and gene therapy: rays of hope for the new millennium?* *Curr Gene Ther*, 2003. **3**(4): p. 319-39.
207. Djordjevic, B., *Bystander effects: a concept in need of clarification.* *Bioessays*, 2000. **22**(3): p. 286-90.
208. Belyakov, O.V., A.M. Malcolmson, M. Folkard, K.M. Prise, and B.D. Michael, *Direct evidence for a bystander effect of ionizing radiation in primary human fibroblasts.* *Br J Cancer*, 2001. **84**(5): p. 674-9.
209. Hallahan, D.E., H.J. Mauceri, L.P. Seung, E.J. Dunphy, J.D. Wayne, N.N. Hanna, A. Toledano, S. Hellman, D.W. Kufe, and R.R. Weichselbaum, *Spatial and temporal control of gene therapy using ionizing radiation.* *Nat Med*, 1995. **1**(8): p. 786-91.
210. Hallahan, D.E., V.P. Sukhatme, M.L. Sherman, S. Virudachalam, D. Kufe, and R.R. Weichselbaum, *Protein kinase C mediates x-ray inducibility of nuclear signal transducers EGR1 and JUN.* *Proc Natl Acad Sci U S A*, 1991. **88**(6): p. 2156-60.
211. Datta, R., E. Rubin, V. Sukhatme, S. Qureshi, D. Hallahan, R.R. Weichselbaum, and D.W. Kufe, *Ionizing radiation activates transcription of the EGR1 gene via CArG elements.* *Proc Natl Acad Sci U S A*, 1992. **89**(21): p. 10149-53.
212. Datta, R., N. Taneja, V.P. Sukhatme, S.A. Qureshi, R. Weichselbaum, and D.W. Kufe, *Reactive oxygen intermediates target CC(A/T)6GG sequences to mediate activation of the early growth response 1 transcription factor gene by ionizing radiation.* *Proc Natl Acad Sci U S A*, 1993. **90**(6): p. 2419-22.
213. Joki, T., M. Nakamura, and T. Ohno, *Activation of the radiosensitive EGR-1 promoter induces expression of the herpes simplex virus thymidine kinase gene and sensitivity of human glioma cells to ganciclovir.* *Hum Gene Ther*, 1995. **6**(12): p. 1507-13.
214. Kawashita, Y., A. Ohtsuru, Y. Kaneda, Y. Nagayama, Y. Kawazoe, S. Eguchi, H. Kuroda, H. Fujioka, M. Ito, T. Kanematsu, and S. Yamashita, *Regression of hepatocellular carcinoma in vitro and in vivo by radiosensitizing suicide gene therapy under the inducible and spatial control of radiation.* *Hum Gene Ther*, 1999. **10**(9): p. 1509-19.
215. Marples, B., S.D. Scott, J.H. Hendry, M.J. Embleton, L.S. Lashford, and G.P. Margison, *Development of synthetic promoters for radiation-mediated gene therapy.* *Gene Ther*, 2000. **7**(6): p. 511-7.
216. Mauceri, H.J., N.N. Hanna, J.D. Wayne, D.E. Hallahan, S. Heilman, and R.R. Weichselbaum, *Tumor necrosis factor alpha (TNF-alpha) gene therapy targeted by ionizing radiation selectively damages tumor vasculature.* *Cancer Res*, 1996. **56**(19): p. 4311-4.
217. Meyer, R.G., J.H. Kupper, R. Kandolf, and H.P. Rodemann, *Early growth response-1 gene (Egr-1) promoter induction by ionizing radiation in U87 malignant glioma cells in vitro.* *Eur J Biochem*, 2002. **269**(1): p. 337-46.
218. Manome, Y., T. Kunieda, P.Y. Wen, T. Koga, D.W. Kufe, and T. Ohno, *Transgene expression in malignant glioma using a replication-defective adenoviral vector containing the Egr-1 promoter: activation by ionizing radiation or uptake of radioactive iododeoxyuridine.* *Hum Gene Ther*, 1998. **9**(10): p. 1409-17.

219. Anton, M., I.E. Gomma, T. von Lukowicz, M. Molls, B. Gansbacher, and F. Wurschmidt, *Optimization of radiation controlled gene expression by adenoviral vectors in vitro*. *Cancer Gene Ther*, 2005. **12**(7): p. 640-6.
220. Nuyts, S., L. Van Mellaert, J. Theys, W. Landuyt, E. Bosmans, J. Anne, and P. Lambin, *Radio-responsive recA promoter significantly increases TNFalpha production in recombinant clostridia after 2 Gy irradiation*. *Gene Ther*, 2001. **8**(15): p. 1197-201.
221. Ueda, T., N. Akiyama, H. Sai, N. Oya, M. Noda, M. Hiraoka, and S. Kizaka-Kondoh, *c-IAP2 is induced by ionizing radiation through NF-kappaB binding sites*. *FEBS Lett*, 2001. **491**(1-2): p. 40-4.
222. Gartel, A.L., M.S. Serfas, and A.L. Tyner, *p21--negative regulator of the cell cycle*. *Proc Soc Exp Biol Med*, 1996. **213**(2): p. 138-49.
223. Brugarolas, J., K. Moberg, S.D. Boyd, Y. Taya, T. Jacks, and J.A. Lees, *Inhibition of cyclin-dependent kinase 2 by p21 is necessary for retinoblastoma protein-mediated G1 arrest after gamma-irradiation*. *Proc Natl Acad Sci U S A*, 1999. **96**(3): p. 1002-7.
224. Gu, Y., C.W. Turck, and D.O. Morgan, *Inhibition of CDK2 activity in vivo by an associated 20K regulatory subunit*. *Nature*, 1993. **366**(6456): p. 707-10.
225. Biankin, A.V., J.G. Kench, A.L. Morey, C.S. Lee, S.A. Biankin, D.R. Head, T.B. Hugh, S.M. Henshall, and R.L. Sutherland, *Overexpression of p21(WAF1/CIP1) is an early event in the development of pancreatic intraepithelial neoplasia*. *Cancer Res*, 2001. **61**(24): p. 8830-7.
226. Clasen, S., W.A. Schulz, C.D. Gerharz, M.O. Grimm, F. Christoph, and B.J. Schmitz-Drager, *Frequent and heterogeneous expression of cyclin-dependent kinase inhibitor WAF1/p21 protein and mRNA in urothelial carcinoma*. *Br J Cancer*, 1998. **77**(4): p. 515-21.
227. Codegioni, A.M., M.I. Nicoletti, G. Buraggi, G. Valoti, R. Giavazzi, M. D'Incalci, F. Landoni, A. Maneo, and M. Broggin, *Molecular characterisation of a panel of human ovarian carcinoma xenografts*. *Eur J Cancer*, 1998. **34**(9): p. 1432-8.
228. O'Hanlon, D.M., M. Kiely, M. MacConmara, R. Al-Azzawi, Y. Connolly, M. Jeffers, and F.B. Keane, *An immunohistochemical study of p21 and p53 expression in primary node-positive breast carcinoma*. *Eur J Surg Oncol*, 2002. **28**(2): p. 103-7.
229. Schwerer, M.J., A. Sailer, K. Kraft, K. Baczako, and H. Maier, *Patterns of p21(waf1/cip1) expression in non-papillomatous nasal mucosa, endophytic sinonasal papillomas, and associated carcinomas*. *J Clin Pathol*, 2001. **54**(11): p. 871-6.
230. Sourvinos, G. and D.A. Spandidos, *Decreased BRCA1 expression levels may arrest the cell cycle through activation of p53 checkpoint in human sporadic breast tumors*. *Biochem Biophys Res Commun*, 1998. **245**(1): p. 75-80.
231. Wasylyk, C., R. Salvi, M. Argentini, C. Dureuil, I. Delumeau, J. Abecassis, L. Debussche, and B. Wasylyk, *p53 mediated death of cells overexpressing MDM2 by an inhibitor of MDM2 interaction with p53*. *Oncogene*, 1999. **18**(11): p. 1921-34.
232. Yook, J.I. and J. Kim, *Expression of p21WAF1/CIP1 is unrelated to p53 tumour suppressor gene status in oral squamous cell carcinomas*. *Oral Oncol*, 1998. **34**(3): p. 198-203.

233. Vidal, M.J., F. Loganzo, Jr., A.R. de Oliveira, N.K. Hayward, and A.P. Albino, *Mutations and defective expression of the WAF1 p21 tumour-suppressor gene in malignant melanomas*. *Melanoma Res*, 1995. **5**(4): p. 243-50.
234. Karjalainen, J.M., M.J. Eskelinen, J.K. Kellokoski, M. Reinikainen, E.M. Alhava, and V.M. Kosma, *p21(WAF1/CIP1) expression in stage I cutaneous malignant melanoma: its relationship with p53, cell proliferation and survival*. *Br J Cancer*, 1999. **79**(5-6): p. 895-902.
235. Worthington, J., H.O. McCarthy, E. Barrett, C. Adams, T. Robson, and D.G. Hirst, *Use of the radiation-inducible WAF1 promoter to drive iNOS gene therapy as a novel anti-cancer treatment*. *J Gene Med*, 2004. **6**(6): p. 673-80.
236. Worthington, J., T. Robson, M. O'Keeffe, and D.G. Hirst, *Tumour cell radiosensitization using constitutive (CMV) and radiation inducible (WAF1) promoters to drive the iNOS gene: a novel suicide gene therapy*. *Gene Ther*, 2002. **9**(4): p. 263-9.
237. Sgouros, G., *Dosimetry of internal emitters*. *J Nucl Med*, 2005. **46 Suppl 1**: p. 18S-27S.
238. Ross, R.A., B.A. Spengler, and J.L. Biedler, *Coordinate morphological and biochemical interconversion of human neuroblastoma cells*. *J Natl Cancer Inst*, 1983. **71**(4): p. 741-7.
239. Bunz, F., A. Dutriaux, C. Lengauer, T. Waldman, S. Zhou, J.P. Brown, J.M. Sedivy, K.W. Kinzler, and B. Vogelstein, *Requirement for p53 and p21 to sustain G2 arrest after DNA damage*. *Science*, 1998. **282**(5393): p. 1497-501.
240. Mairs, R.J., M.N. Gaze, and A. Barrett, *The uptake and retention of metaiodobenzyl guanidine by the neuroblastoma cell line NB1-G*. *Br J Cancer*, 1991. **64**(2): p. 293-5.
241. Rodriguez-Lopez, A.M., D. Xenaki, T.O. Eden, J.A. Hickman, and C.M. Chresta, *MDM2 mediated nuclear exclusion of p53 attenuates etoposide-induced apoptosis in neuroblastoma cells*. *Mol Pharmacol*, 2001. **59**(1): p. 135-43.
242. Tweddle, D.A., A.J. Malcolm, N. Bown, A.D. Pearson, and J. Lunec, *Evidence for the development of p53 mutations after cytotoxic therapy in a neuroblastoma cell line*. *Cancer Res*, 2001. **61**(1): p. 8-13.
243. Chiarugi, V., L. Magnelli, M. Cinelli, and G. Basi, *Apoptosis and the cell cycle*. *Cell Mol Biol Res*, 1994. **40**(7-8): p. 603-12.
244. Chadwick, K.H. and H.P. Leenhouts, *The Molecular Theory of Radiation Biology*. 1981, Berlin, Heidelberg and New York: Springer
245. Akudugu, J.M., J.P. Slabbert, A. Serafin, and L. Bohm, *Frequency of radiation-induced micronuclei in neuronal cells does not correlate with clonogenic survival*. *Radiat Res*, 2000. **153**(1): p. 62-7.
246. Seitz, G., H.B. Stegmann, H.H. Jager, H.M. Schlude, H. Wolburg, V.A. Roginsky, D. Niethammer, and G. Bruchelt, *Neuroblastoma cells expressing the noradrenaline transporter are destroyed more selectively by 6-fluorodopamine than by 6-hydroxydopamine*. *J Neurochem*, 2000. **75**(2): p. 511-20.
247. Voute, P.A., C.A. Hoefnagel, J. de Kraker, R. Valdes Olmos, D.J. Bakker, and A.J. van de Kleij, *Results of treatment with 131 I-*

- metaiodobenzylguanidine (131 I-MIBG) in patients with neuroblastoma. Future prospects of zeto therapy.* Prog Clin Biol Res, 1991. **366**: p. 439-45.
248. Brown, J.M., *Exploiting the hypoxic cancer cell: mechanisms and therapeutic strategies.* Mol Med Today, 2000. **6**(4): p. 157-62.
249. Matthay, K.K., M.C. O'Leary, N.K. Ramsay, J. Villablanca, C.P. Reynolds, J.B. Atkinson, G.M. Haase, D.O. Stram, and R.C. Seeger, *Role of myeloablative therapy in improved outcome for high risk neuroblastoma: review of recent Children's Cancer Group results.* Eur J Cancer, 1995. **31A**(4): p. 572-5.
250. Stram, D.O., K.K. Matthay, M. O'Leary, C.P. Reynolds, G.M. Haase, J.B. Atkinson, G.M. Brodeur, and R.C. Seeger, *Consolidation chemoradiotherapy and autologous bone marrow transplantation versus continued chemotherapy for metastatic neuroblastoma: a report of two concurrent Children's Cancer Group studies.* J Clin Oncol, 1996. **14**(9): p. 2417-26.
251. Reynolds, C.P., R.C. Seeger, D.D. Vo, A.T. Black, J. Wells, and J. Ugelstad, *Model system for removing neuroblastoma cells from bone marrow using monoclonal antibodies and magnetic immunobeads.* Cancer Res, 1986. **46**(11): p. 5882-6.
252. Handgretinger, R., J. Greil, U. Schurmann, P. Lang, O. Gonzalez-Ramella, I. Schmidt, R. Fuhrer, D. Niethammer, and T. Klingebiel, *Positive selection and transplantation of peripheral CD34+ progenitor cells: feasibility and purging efficacy in pediatric patients with neuroblastoma.* J Hematother, 1997. **6**(3): p. 235-42.
253. Donovan, J., J. Temel, A. Zuckerman, J. Gribben, J. Fang, G. Pierson, A. Ross, L. Diller, and S.A. Grupp, *CD34 selection as a stem cell purging strategy for neuroblastoma: preclinical and clinical studies.* Med Pediatr Oncol, 2000. **35**(6): p. 677-82.
254. Grupp, S.A., J.W. Stern, N. Bunin, C. Nancarrow, A.A. Ross, M. Mogul, R. Adams, H.E. Grier, J.B. Gorlin, R. Shamberger, K. Marcus, D. Neuberg, H.J. Weinstein, and L. Diller, *Tandem high-dose therapy in rapid sequence for children with high-risk neuroblastoma.* J Clin Oncol, 2000. **18**(13): p. 2567-75.
255. Kanold, J., K. Yakouben, A. Tchirkov, A.S. Carret, J.P. Vannier, E. LeGall, P. Bordigoni, and F. Demeocq, *Long-term results of CD34(+) cell transplantation in children with neuroblastoma.* Med Pediatr Oncol, 2000. **35**(1): p. 1-7.
256. Lode, H.N., R. Handgretinger, U. Schuermann, G. Seitz, T. Klingebiel, D. Niethammer, and J. Beck, *Detection of neuroblastoma cells in CD34+ selected peripheral stem cells using a combination of tyrosine hydroxylase nested RT-PCR and anti-ganglioside GD2 immunocytochemistry.* Eur J Cancer, 1997. **33**(12): p. 2024-30.
257. Mata, S., M. Urbina, E. Manzano, T. Ortiz, and L. Lima, *Noradrenaline transporter and its turnover rate are decreased in blood lymphocytes of patients with major depression.* J Neuroimmunol, 2005. **170**(1-2): p. 134-40.
258. Hashimoto, T., K. Koizumi, T. Nishina, and K. Abe, *Clinical usefulness of iodine-123-MIBG scintigraphy for patients with neuroblastoma detected by a mass screening survey.* Ann Nucl Med, 2003. **17**(8): p. 633-40.
259. Montaldo, P.G., R. Carbone, M. Ponzoni, and P. Cornaglia-Ferraris, *gamma-Interferon increases metaiodobenzylguanidine incorporation and*

- retention in human neuroblastoma cells. Cancer Res, 1992. 52(18): p. 4960-4.*
260. el-Deiry, W.S., J.W. Harper, P.M. O'Connor, V.E. Velculescu, C.E. Canman, J. Jackman, J.A. Pietenpol, M. Burrell, D.E. Hill, Y. Wang, and et al., *WAF1/CIP1 is induced in p53-mediated G1 arrest and apoptosis. Cancer Res, 1994. 54(5): p. 1169-74.*
 261. Meyer, J., P. Wiedemann, O. Okladnova, M. Bruss, T. Staab, G. Stober, P. Riederer, H. Bonisch, and K.P. Lesch, *Cloning and functional characterization of the human norepinephrine transporter gene promoter. J Neural Transm, 1998. 105(10-12): p. 1341-50.*
 262. Apparsundaram, S., A. Galli, L.J. DeFelice, H.C. Hartzell, and R.D. Blakely, *Acute regulation of norepinephrine transport: I. protein kinase C-linked muscarinic receptors influence transport capacity and transporter density in SK-N-SH cells. J Pharmacol Exp Ther, 1998. 287(2): p. 733-43.*
 263. Apparsundaram, S., S. Schroeter, E. Giovanetti, and R.D. Blakely, *Acute regulation of norepinephrine transport: II. PKC-modulated surface expression of human norepinephrine transporter proteins. J Pharmacol Exp Ther, 1998. 287(2): p. 744-51.*
 264. Bonisch, H., R. Hammermann, and M. Bruss, *Role of protein kinase C and second messengers in regulation of the norepinephrine transporter. Adv Pharmacol, 1998. 42: p. 183-6.*
 265. Jayanthi, L.D., D.J. Samuvel, and S. Ramamoorthy, *Regulated internalization and phosphorylation of the native norepinephrine transporter in response to phorbol esters. Evidence for localization in lipid rafts and lipid raft-mediated internalization. J Biol Chem, 2004. 279(18): p. 19315-26.*
 266. Bauman, A.L., S. Apparsundaram, S. Ramamoorthy, B.E. Wadzinski, R.A. Vaughan, and R.D. Blakely, *Cocaine and antidepressant-sensitive biogenic amine transporters exist in regulated complexes with protein phosphatase 2A. J Neurosci, 2000. 20(20): p. 7571-8.*
 267. Wolff, J.A., R.W. Malone, P. Williams, W. Chong, G. Acsadi, A. Jani, and P.L. Felgner, *Direct gene transfer into mouse muscle in vivo. Science, 1990. 247(4949 Pt 1): p. 1465-8.*
 268. Vile, R.G. and I.R. Hart, *Use of tissue-specific expression of the herpes simplex virus thymidine kinase gene to inhibit growth of established murine melanomas following direct intratumoral injection of DNA. Cancer research, 1993. 53(17): p. 3860-4.*
 269. Yang, J.P. and L. Huang, *Direct gene transfer to mouse melanoma by intratumor injection of free DNA. Gene therapy, 1996. 3(6): p. 542-8.*
 270. Thomas, C.E., A. Ehrhardt, and M.A. Kay, *Progress and problems with the use of viral vectors for gene therapy. Nat Rev Genet, 2003. 4(5): p. 346-58.*
 271. Lundstrom, K., *Latest development in viral vectors for gene therapy. Trends Biotechnol, 2003. 21(3): p. 117-22.*
 272. Anderson, W.F., *Prospects for human gene therapy. Science, 1984. 226(4673): p. 401-9.*
 273. *Worldwide database of gene therapy clinical trials [online]. Available from URL <http://www.wiley.co.uk/genmed/clinical/>. Journal of Gene Medicine.*
 274. Kordower, J.H., M.E. Emborg, J. Bloch, S.Y. Ma, Y. Chu, L. Leventhal, J. McBride, E.Y. Chen, S. Palfi, B.Z. Roitberg, W.D. Brown, J.E. Holden, R. Pyzalski, M.D. Taylor, P. Carvey, Z. Ling, D. Trono, P. Hantraye, N. Deglon, and P. Aebischer, *Neurodegeneration prevented by lentiviral vector delivery*

- of GDNF in primate models of Parkinson's disease. *Science*, 2000. **290**(5492): p. 767-73.
275. Pawliuk, R., K.A. Westerman, M.E. Fabry, E. Payen, R. Tighe, E.E. Bouhassira, S.A. Acharya, J. Ellis, I.M. London, C.J. Eaves, R.K. Humphries, Y. Beuzard, R.L. Nagel, and P. Leboulch, *Correction of sickle cell disease in transgenic mouse models by gene therapy*. *Science*, 2001. **294**(5550): p. 2368-71.
 276. Kang, Y., L. Xie, D.T. Tran, C.S. Stein, M. Hickey, B.L. Davidson, and P.B. McCray, Jr., *Persistent expression of factor VIII in vivo following nonprimate lentiviral gene transfer*. *Blood*, 2005. **106**(5): p. 1552-8.
 277. Gerdes, C.A., M.G. Castro, and P.R. Lowenstein, *Strong promoters are the key to highly efficient, noninflammatory and noncytotoxic adenoviral-mediated transgene delivery into the brain in vivo*. *Mol Ther*, 2000. **2**(4): p. 330-8.
 278. Buller, R.E., I.B. Runnebaum, B.Y. Karlan, J.A. Horowitz, M. Shahin, T. Buekers, S. Petrauskas, R. Kreienberg, D. Slamon, and M. Pegram, *A phase I/II trial of rAd/p53 (SCH 58500) gene replacement in recurrent ovarian cancer*. *Cancer Gene Ther*, 2002. **9**(7): p. 553-66.
 279. Chevez-Barrios, P., M. Chintagumpala, W. Mieler, E. Paysse, M. Boniuk, C. Kozinetz, M.Y. Hurwitz, and R.L. Hurwitz, *Response of retinoblastoma with vitreous tumor seeding to adenovirus-mediated delivery of thymidine kinase followed by ganciclovir*. *J Clin Oncol*, 2005. **23**(31): p. 7927-35.
 280. Dummer, R., J.C. Hassel, F. Fellenberg, S. Eichmuller, T. Maier, P. Slos, B. Acres, P. Bleuzen, V. Bataille, P. Squiban, G. Burg, and M. Urosevic, *Adenovirus-mediated intralesional interferon-gamma gene transfer induces tumor regressions in cutaneous lymphomas*. *Blood*, 2004. **104**(6): p. 1631-8.
 281. Galanis, E., S.H. Okuno, A.G. Nascimento, B.D. Lewis, R.A. Lee, A.M. Oliveira, J.A. Sloan, P. Atherton, J.H. Edmonson, C. Erlichman, B. Randlev, Q. Wang, S. Freeman, and J. Rubin, *Phase I-II trial of ONYX-015 in combination with MAP chemotherapy in patients with advanced sarcomas*. *Gene Ther*, 2005. **12**(5): p. 437-45.
 282. Herman, J.R., H.L. Adler, E. Aguilar-Cordova, A. Rojas-Martinez, S. Woo, T.L. Timme, T.M. Wheeler, T.C. Thompson, and P.T. Scardino, *In situ gene therapy for adenocarcinoma of the prostate: a phase I clinical trial*. *Hum Gene Ther*, 1999. **10**(7): p. 1239-49.
 283. Khuri, F.R., J. Nemunaitis, I. Ganly, J. Arseneau, I.F. Tannock, L. Romel, M. Gore, J. Ironside, R.H. MacDougall, C. Heise, B. Randlev, A.M. Gillenwater, P. Bruso, S.B. Kaye, W.K. Hong, and D.H. Kirn, *a controlled trial of intratumoral ONYX-015, a selectively-replicating adenovirus, in combination with cisplatin and 5-fluorouracil in patients with recurrent head and neck cancer*. *Nat Med*, 2000. **6**(8): p. 879-85.
 284. Nemunaitis, J., F. Khuri, I. Ganly, J. Arseneau, M. Posner, E. Vokes, J. Kuhn, T. McCarty, S. Landers, A. Blackburn, L. Romel, B. Randlev, S. Kaye, and D. Kirn, *Phase II trial of intratumoral administration of ONYX-015, a replication-selective adenovirus, in patients with refractory head and neck cancer*. *J Clin Oncol*, 2001. **19**(2): p. 289-98.
 285. Sandmair, A.M., S. Loimas, P. Puranen, A. Immonen, M. Kossila, M. Puranen, H. Hurskainen, K. Tynnela, M. Turunen, R. Vanninen, P. Lehtolainen, L. Paljarvi, R. Johansson, M. Vapalahti, and S. Yla-Herttuala,

- Thymidine kinase gene therapy for human malignant glioma, using replication-deficient retroviruses or adenoviruses.* Hum Gene Ther, 2000. **11**(16): p. 2197-205.
286. Schuler, M., R. Herrmann, J.L. De Greve, A.K. Stewart, U. Gatzemeier, D.J. Stewart, L. Laufman, R. Gralla, J. Kuball, R. Buhl, C.P. Heussel, F. Kommos, A.P. Perruchoud, F.A. Shepherd, M.A. Fritz, J.A. Horowitz, C. Huber, and C. Rochlitz, *Adenovirus-mediated wild-type p53 gene transfer in patients receiving chemotherapy for advanced non-small-cell lung cancer: results of a multicenter phase II study.* J Clin Oncol, 2001. **19**(6): p. 1750-8.
287. Swisher, S.G., J.A. Roth, J. Nemunaitis, D.D. Lawrence, B.L. Kemp, C.H. Carrasco, D.G. Connors, A.K. El-Naggar, F. Fossella, B.S. Glisson, W.K. Hong, F.R. Khuri, J.M. Kurie, J.J. Lee, J.S. Lee, M. Mack, J.A. Merritt, D.M. Nguyen, J.C. Nesbitt, R. Perez-Soler, K.M. Pisters, J.B. Putnam, Jr., W.R. Richli, M. Savin, D.S. Schrupp, D.M. Shin, A. Shulkin, G.L. Walsh, J. Wait, D. Weill, and M.K. Waugh, *Adenovirus-mediated p53 gene transfer in advanced non-small-cell lung cancer.* J Natl Cancer Inst, 1999. **91**(9): p. 763-71.
288. Tursz, T., A.L. Cesne, P. Baldeyrou, E. Gautier, P. Opolon, C. Schatz, A. Pavirani, M. Courtney, D. Lamy, T. Ragot, P. Saulnier, A. Andreumont, R. Monier, M. Perricaudet, and T. Le Chevalier, *Phase I study of a recombinant adenovirus-mediated gene transfer in lung cancer patients.* J Natl Cancer Inst, 1996. **88**(24): p. 1857-63.
289. Blacklow, N.R., M.D. Hoggan, A.Z. Kapikian, J.B. Austin, and W.P. Rowe, *Epidemiology of adenovirus-associated virus infection in a nursery population.* Am J Epidemiol, 1968. **88**(3): p. 368-78.
290. Flotte, T.R., S.A. Afione, C. Conrad, S.A. McGrath, R. Solow, H. Oka, P.L. Zeitlin, W.B. Guggino, and B.J. Carter, *Stable in vivo expression of the cystic fibrosis transmembrane conductance regulator with an adeno-associated virus vector.* Proc Natl Acad Sci U S A, 1993. **90**(22): p. 10613-7.
291. Conrad, C.K., S.S. Allen, S.A. Afione, T.C. Reynolds, S.E. Beck, M. Fee-Maki, X. Barraza-Ortiz, R. Adams, F.B. Askin, B.J. Carter, W.B. Guggino, and T.R. Flotte, *Safety of single-dose administration of an adeno-associated virus (AAV)-CFTR vector in the primate lung.* Gene Ther, 1996. **3**(8): p. 658-68.
292. Halbert, C.L., T.A. Standaert, C.B. Wilson, and A.D. Miller, *Successful readministration of adeno-associated virus vectors to the mouse lung requires transient immunosuppression during the initial exposure.* J Virol, 1998. **72**(12): p. 9795-805.
293. Snyder, R.O., C.H. Miao, G.A. Patijn, S.K. Spratt, O. Danos, D. Nagy, A.M. Gown, B. Winther, L. Meuse, L.K. Cohen, A.R. Thompson, and M.A. Kay, *Persistent and therapeutic concentrations of human factor IX in mice after hepatic gene transfer of recombinant AAV vectors.* Nat Genet, 1997. **16**(3): p. 270-6.
294. Halbert, C.L., I.E. Alexander, G.M. Wolgamot, and A.D. Miller, *Adeno-associated virus vectors transduce primary cells much less efficiently than immortalized cells.* J Virol, 1995. **69**(3): p. 1473-9.
295. Russell, D.W., A.D. Miller, and I.E. Alexander, *Adeno-associated virus vectors preferentially transduce cells in S phase.* Proc Natl Acad Sci U S A, 1994. **91**(19): p. 8915-9.

296. Kay, M.A., C.S. Manno, M.V. Ragni, P.J. Larson, L.B. Couto, A. McClelland, B. Glader, A.J. Chew, S.J. Tai, R.W. Herzog, V. Arruda, F. Johnson, C. Scallan, E. Skarsgard, A.W. Flake, and K.A. High, *Evidence for gene transfer and expression of factor IX in haemophilia B patients treated with an AAV vector*. *Nat Genet*, 2000. **24**(3): p. 257-61.
297. Epstein, A.L., P. Marconi, R. Argnani, and R. Manservigi, *HSV-1-derived recombinant and amplicon vectors for gene transfer and gene therapy*. *Curr Gene Ther*, 2005. **5**(5): p. 445-58.
298. Latchman, D.S., *Gene delivery and gene therapy with herpes simplex virus-based vectors*. *Gene*, 2001. **264**(1): p. 1-9.
299. Furlan, R., P.L. Poliani, P.C. Marconi, A. Bergami, F. Ruffini, L. Adorini, J.C. Glorioso, G. Comi, and G. Martino, *Central nervous system gene therapy with interleukin-4 inhibits progression of ongoing relapsing-remitting autoimmune encephalomyelitis in Biozzi AB/H mice*. *Gene Ther*, 2001. **8**(1): p. 13-9.
300. Poliani, P.L., H. Brok, R. Furlan, F. Ruffini, A. Bergami, G. Desina, P.C. Marconi, M. Rovaris, A. Uccelli, J.C. Glorioso, G. Penna, L. Adorini, G. Comi, B. t Hart, and G. Martino, *Delivery to the central nervous system of a nonreplicative herpes simplex type 1 vector engineered with the interleukin 4 gene protects rhesus monkeys from hyperacute autoimmune encephalomyelitis*. *Hum Gene Ther*, 2001. **12**(8): p. 905-20.
301. Ruffini, F., R. Furlan, P.L. Poliani, E. Brambilla, P.C. Marconi, A. Bergami, G. Desina, J.C. Glorioso, G. Comi, and G. Martino, *Fibroblast growth factor-II gene therapy reverts the clinical course and the pathological signs of chronic experimental autoimmune encephalomyelitis in C57BL/6 mice*. *Gene Ther*, 2001. **8**(16): p. 1207-13.
302. Hellums, E.K., J.M. Markert, J.N. Parker, B. He, B. Perbal, B. Roizman, R.J. Whitley, C.P. Langford, S. Bharara, and G.Y. Gillespie, *Increased efficacy of an interleukin-12-secreting herpes simplex virus in a syngeneic intracranial murine glioma model*. *Neuro-oncol*, 2005. **7**(3): p. 213-24.
303. Parker, J.N., S. Meleth, K.B. Hughes, G.Y. Gillespie, R.J. Whitley, and J.M. Markert, *Enhanced inhibition of syngeneic murine tumors by combinatorial therapy with genetically engineered HSV-1 expressing CCL2 and IL-12*. *Cancer Gene Ther*, 2005. **12**(4): p. 359-68.
304. Goins, W.F., K.A. Lee, J.D. Cavalcoli, M.E. O'Malley, S.T. DeKosky, D.J. Fink, and J.C. Glorioso, *Herpes simplex virus type 1 vector-mediated expression of nerve growth factor protects dorsal root ganglion neurons from peroxide toxicity*. *J Virol*, 1999. **73**(1): p. 519-32.
305. Goins, W.F., N. Yoshimura, M.W. Phelan, T. Yokoyama, M.O. Fraser, H. Ozawa, N.J. Bennett, W.C. de Groat, J.C. Glorioso, and M.B. Chancellor, *Herpes simplex virus mediated nerve growth factor expression in bladder and afferent neurons: potential treatment for diabetic bladder dysfunction*. *J Urol*, 2001. **165**(5): p. 1748-54.
306. Goss, J.R., M. Mata, W.F. Goins, H.H. Wu, J.C. Glorioso, and D.J. Fink, *Antinociceptive effect of a genomic herpes simplex virus-based vector expressing human proenkephalin in rat dorsal root ganglion*. *Gene Ther*, 2001. **8**(7): p. 551-6.
307. Wilson, S.P., D.C. Yeomans, M.A. Bender, Y. Lu, W.F. Goins, and J.C. Glorioso, *Antihyperalgesic effects of infection with a preproenkephalin-encoding herpes virus*. *Proc Natl Acad Sci U S A*, 1999. **96**(6): p. 3211-6.

308. Kirn, D., R.L. Martuza, and J. Zwiebel, *Replication-selective virotherapy for cancer: Biological principles, risk management and future directions*. *Nat Med*, 2001. **7**(7): p. 781-7.
309. Martuza, R.L., A. Malick, J.M. Markert, K.L. Ruffner, and D.M. Coen, *Experimental therapy of human glioma by means of a genetically engineered virus mutant*. *Science*, 1991. **252**(5007): p. 854-6.
310. Dimitriadis, G.J., *Entrapment of plasmid DNA in liposomes*. *Nucleic Acids Res*, 1979. **6**(8): p. 2697-705.
311. Mukherjee, A.B., S. Orloff, J.D. Butler, T. Triche, P. Lalley, and J.D. Schulman, *Entrapment of metaphase chromosomes into phospholipid vesicles (lipochromosomes): carrier potential in gene transfer*. *Proc Natl Acad Sci U S A*, 1978. **75**(3): p. 1361-5.
312. Wreschner, D.H., G. Gregoriadis, D.B. Gunner, and R.R. Dourmashkin, *Entrapment of mRNA and rRNA into large monolamellar liposomes derived from hybrid small monolamellar liposomes*. *Biochem Soc Trans*, 1978. **6**(5): p. 930-3.
313. Dimitriadis, G.J., *Cellular uptake of ribonucleic acids entrapped into liposomes*. *Cell Biol Int Rep*, 1979. **3**(6): p. 543-9.
314. Fraley, R., R.M. Straubinger, G. Rule, E.L. Springer, and D. Papahadjopoulos, *Liposome-mediated delivery of deoxyribonucleic acid to cells: enhanced efficiency of delivery related to lipid composition and incubation conditions*. *Biochemistry*, 1981. **20**(24): p. 6978-87.
315. Nicolau, C., A. Le Pape, P. Soriano, F. Fargette, and M.F. Juhel, *In vivo expression of rat insulin after intravenous administration of the liposome-entrapped gene for rat insulin I*. *Proc Natl Acad Sci U S A*, 1983. **80**(4): p. 1068-72.
316. Wilson, T., D. Papahadjopoulos, and R. Taber, *The introduction of poliovirus RNA into cells via lipid vesicles (liposomes)*. *Cell*, 1979. **17**(1): p. 77-84.
317. Lavigne, C., Y. Lunardi-Iskandar, B. Lebleu, and A.R. Thierry, *Cationic liposomes/lipids for oligonucleotide delivery: application to the inhibition of tumorigenicity of Kaposi's sarcoma by vascular endothelial growth factor antisense oligodeoxynucleotides*. *Methods Enzymol*, 2004. **387**: p. 189-210.
318. Bartsch, M., A.H. Weeke-Klump, D.K. Meijer, G.L. Scherphof, and J.A. Kamps, *Cell-specific targeting of lipid-based carriers for ODN and DNA*. *J Liposome Res*, 2005. **15**(1-2): p. 59-92.
319. Felgner, P.L., T.R. Gadek, M. Holm, R. Roman, H.W. Chan, M. Wenz, J.P. Northrop, G.M. Ringold, and M. Danielsen, *Lipofection: a highly efficient, lipid-mediated DNA-transfection procedure*. *Proc Natl Acad Sci U S A*, 1987. **84**(21): p. 7413-7.
320. Felgner, P.L. and G.M. Ringold, *Cationic liposome-mediated transfection*. *Nature*, 1989. **337**(6205): p. 387-8.
321. Bennett, C.F., M.Y. Chiang, H. Chan, J.E. Shoemaker, and C.K. Mirabelli, *Cationic lipids enhance cellular uptake and activity of phosphorothioate antisense oligonucleotides*. *Mol Pharmacol*, 1992. **41**(6): p. 1023-33.
322. Gao, X. and L. Huang, *Cytoplasmic expression of a reporter gene by co-delivery of T7 RNA polymerase and T7 promoter sequence with cationic liposomes*. *Nucleic Acids Res*, 1993. **21**(12): p. 2867-72.

323. Lappalainen, K., A. Urtti, I. Jaaskelainen, K. Syrjanen, and S. Syrjanen, *Cationic liposomes mediated delivery of antisense oligonucleotides targeted to HPV 16 E7 mRNA in CaSki cells*. *Antiviral Res*, 1994. **23**(2): p. 119-30.
324. Shi, F., A. Nomden, V. Oberle, J.B. Engberts, and D. Hoekstra, *Efficient cationic lipid-mediated delivery of antisense oligonucleotides into eukaryotic cells: down-regulation of the corticotropin-releasing factor receptor*. *Nucleic Acids Res*, 2001. **29**(10): p. 2079-87.
325. Lewis, J.G., K.Y. Lin, A. Kothavale, W.M. Flanagan, M.D. Matteucci, R.B. DePrince, R.A. Mook, Jr., R.W. Hendren, and R.W. Wagner, *A serum-resistant cytofectin for cellular delivery of antisense oligodeoxynucleotides and plasmid DNA*. *Proc Natl Acad Sci U S A*, 1996. **93**(8): p. 3176-81.
326. Wang, C.Y. and L. Huang, *pH-sensitive immunoliposomes mediate target-cell-specific delivery and controlled expression of a foreign gene in mouse*. *Proc Natl Acad Sci U S A*, 1987. **84**(22): p. 7851-5.
327. Hafez, I.M., S. Ansell, and P.R. Cullis, *Tunable pH-sensitive liposomes composed of mixtures of cationic and anionic lipids*. *Biophys J*, 2000. **79**(3): p. 1438-46.
328. Hillery, A., *Heat-sensitive liposomes for tumour targeting*. *Drug Discov Today*, 2001. **6**(5): p. 224-225.
329. Sullivan, S.M. and L. Huang, *Enhanced delivery to target cells by heat-sensitive immunoliposomes*. *Proc Natl Acad Sci U S A*, 1986. **83**(16): p. 6117-21.
330. Litzinger, D.C., J.M. Brown, I. Wala, S.A. Kaufman, G.Y. Van, C.L. Farrell, and D. Collins, *Fate of cationic liposomes and their complex with oligonucleotide in vivo*. *Biochim Biophys Acta*, 1996. **1281**(2): p. 139-49.
331. Cullis, P.R., A. Chonn, and S.C. Semple, *Interactions of liposomes and lipid-based carrier systems with blood proteins: Relation to clearance behaviour in vivo*. *Adv Drug Deliv Rev*, 1998. **32**(1-2): p. 3-17.
332. Gabizon, A., R. Catane, B. Uziely, B. Kaufman, T. Safra, R. Cohen, F. Martin, A. Huang, and Y. Barenholz, *Prolonged circulation time and enhanced accumulation in malignant exudates of doxorubicin encapsulated in polyethylene-glycol coated liposomes*. *Cancer Res*, 1994. **54**(4): p. 987-92.
333. Papahadjopoulos, D., T.M. Allen, A. Gabizon, E. Mayhew, K. Matthey, S.K. Huang, K.D. Lee, M.C. Woodle, D.D. Lasic, C. Redemann, and et al., *Sterically stabilized liposomes: improvements in pharmacokinetics and antitumor therapeutic efficacy*. *Proc Natl Acad Sci U S A*, 1991. **88**(24): p. 11460-4.
334. Senior, J., C. Delgado, D. Fisher, C. Tilcock, and G. Gregoriadis, *Influence of surface hydrophilicity of liposomes on their interaction with plasma protein and clearance from the circulation: studies with poly(ethylene glycol)-coated vesicles*. *Biochim Biophys Acta*, 1991. **1062**(1): p. 77-82.
335. Gabizon, A. and D. Papahadjopoulos, *Liposome formulations with prolonged circulation time in blood and enhanced uptake by tumors*. *Proc Natl Acad Sci U S A*, 1988. **85**(18): p. 6949-53.
336. Li, S., A.R. Khokhar, R. Perez-Soler, and L. Huang, *Improved antitumor activity of cis-Bis-neodecanoato-trans-R,R-1,2-diaminocyclohexaneplatinum (II) entrapped in long-circulating liposomes*. *Oncol Res*, 1995. **7**(12): p. 611-7.

337. Muggia, F.M., J.D. Hainsworth, S. Jeffers, P. Miller, S. Groshen, M. Tan, L. Roman, B. Uziely, L. Muderspach, A. Garcia, A. Burnett, F.A. Greco, C.P. Morrow, L.J. Paradiso, and L.J. Liang, *Phase II study of liposomal doxorubicin in refractory ovarian cancer: antitumor activity and toxicity modification by liposomal encapsulation*. J Clin Oncol, 1997. **15**(3): p. 987-93.
338. Lee, R.J. and P.S. Low, *Folate-targeted liposomes for drug delivery*. J Liposome Res, 1997. **7**(4): p. 455-66.
339. Ishii, Y., Y. Aramaki, T. Hara, S. Tsuchiya, and T. Fuwa, *Preparation of EGF labeled liposomes and their uptake by hepatocytes*. Biochem Biophys Res Commun, 1989. **160**(2): p. 732-6.
340. Oku, N., Y. Tokudome, C. Koike, N. Nishikawa, H. Mori, I. Saiki, and S. Okada, *Liposomal Arg-Gly-Asp analogs effectively inhibit metastatic B16 melanoma colonization in murine lungs*. Life Sci, 1996. **58**(24): p. 2263-70.
341. Willis, M.C., B.D. Collins, T. Zhang, L.S. Green, D.P. Sebesta, C. Bell, E. Kellogg, S.C. Gill, A. Magallanez, S. Knauer, R.A. Bendele, P.S. Gill, and N. Janjic, *Liposome-anchored vascular endothelial growth factor aptamers*. Bioconjug Chem, 1998. **9**(5): p. 573-82.
342. Torchilin, V.P., B.A. Khaw, V.N. Smirnov, and E. Haber, *Preservation of antimyosin antibody activity after covalent coupling to liposomes*. Biochem Biophys Res Commun, 1979. **89**(4): p. 1114-9.
343. Barbet, J., P. Machy, and L.D. Leserman, *Monoclonal antibody covalently coupled to liposomes: specific targeting to cells*. J Supramol Struct Cell Biochem, 1981. **16**(3): p. 243-58.
344. Heath, T.D., B.A. Macher, and D. Papahadjopoulos, *Covalent attachment of immunoglobulins to liposomes via glycosphingolipids*. Biochim Biophys Acta, 1981. **640**(1): p. 66-81.
345. Huang, A., L. Huang, and S.J. Kennel, *Monoclonal antibody covalently coupled with fatty acid. A reagent for in vitro liposome targeting*. J Biol Chem, 1980. **255**(17): p. 8015-8.
346. Huang, A., S.J. Kennel, and L. Huang, *Interactions of immunoliposomes with target cells*. J Biol Chem, 1983. **258**(22): p. 14034-40.
347. Martin, F.J., W.L. Hubbell, and D. Papahadjopoulos, *Immunospecific targeting of liposomes to cells: a novel and efficient method for covalent attachment of Fab' fragments via disulfide bonds*. Biochemistry, 1981. **20**(14): p. 4229-38.
348. Martin, F.J. and D. Papahadjopoulos, *Irreversible coupling of immunoglobulin fragments to preformed vesicles. An improved method for liposome targeting*. J Biol Chem, 1982. **257**(1): p. 286-8.
349. Hernandez-Caselles, T., J. Villalain, and J.C. Gomez-Fernandez, *Influence of liposome charge and composition on their interaction with human blood serum proteins*. Mol Cell Biochem, 1993. **120**(2): p. 119-26.
350. Jones, M.N. and A.R. Nicholas, *The effect of blood serum on the size and stability of phospholipid liposomes*. Biochim Biophys Acta, 1991. **1065**(2): p. 145-52.
351. Schenkman, S., P.S. Araujo, R. Dijkman, F.H. Quina, and H. Chaimovich, *Effects of temperature and lipid composition on the serum albumin-induced aggregation and fusion of small unilamellar vesicles*. Biochim Biophys Acta, 1981. **649**(3): p. 633-47.

352. Matzku, S., H. Krempel, H.P. Weckenmann, V. Schirmacher, H. Sinn, and H. Stricker, *Tumour targeting with antibody-coupled liposomes: failure to achieve accumulation in xenografts and spontaneous liver metastases*. *Cancer Immunol Immunother*, 1990. **31**(5): p. 285-91.
353. Aragnol, D. and L.D. Leserman, *Immune clearance of liposomes inhibited by an anti-Fc receptor antibody in vivo*. *Proc Natl Acad Sci U S A*, 1986. **83**(8): p. 2699-703.
354. Betageri, G.V., C.D. Black, J. Szebeni, L.M. Wahl, and J.N. Weinstein, *Fc-receptor-mediated targeting of antibody-bearing liposomes containing dideoxycytidine triphosphate to human monocyte/macrophages*. *J Pharm Pharmacol*, 1993. **45**(1): p. 48-53.
355. Derksen, J.T., H.W. Morselt, and G.L. Scherphof, *Uptake and processing of immunoglobulin-coated liposomes by subpopulations of rat liver macrophages*. *Biochim Biophys Acta*, 1988. **971**(2): p. 127-36.
356. Dijkstra, J., M. van Galen, and G. Scherphof, *Influence of liposome charge on the association of liposomes with Kupffer cells in vitro. Effects of divalent cations and competition with latex particles*. *Biochim Biophys Acta*, 1985. **813**(2): p. 287-97.
357. Allen, T.M., E. Brandeis, C.B. Hansen, G.Y. Kao, and S. Zalipsky, *A new strategy for attachment of antibodies to sterically stabilized liposomes resulting in efficient targeting to cancer cells*. *Biochim Biophys Acta*, 1995. **1237**(2): p. 99-108.
358. Blume, G., G. Cevc, M.D. Crommelin, I.A. Bakker-Woudenberg, C. Klufft, and G. Storm, *Specific targeting with poly(ethylene glycol)-modified liposomes: coupling of homing devices to the ends of the polymeric chains combines effective target binding with long circulation times*. *Biochim Biophys Acta*, 1993. **1149**(1): p. 180-4.
359. Maruyama, K., T. Takizawa, T. Yuda, S.J. Kennel, L. Huang, and M. Iwatsuru, *Targetability of novel immunoliposomes modified with amphipathic poly(ethylene glycol)s conjugated at their distal terminals to monoclonal antibodies*. *Biochim Biophys Acta*, 1995. **1234**(1): p. 74-80.
360. Stuart, D.D. and T.M. Allen, *A new liposomal formulation for antisense oligodeoxynucleotides with small size, high incorporation efficiency and good stability*. *Biochim Biophys Acta*, 2000. **1463**(2): p. 219-29.
361. Brignole, C., G. Pagnan, D. Marimpietri, E. Cosimo, T.M. Allen, M. Ponzoni, and F. Pastorino, *Targeted delivery system for antisense oligonucleotides: a novel experimental strategy for neuroblastoma treatment*. *Cancer Lett*, 2003. **197**(1-2): p. 231-5.
362. Pastorino, F., C. Brignole, D. Marimpietri, G. Pagnan, A. Morando, D. Ribatti, S.C. Semple, C. Gambini, T.M. Allen, and M. Ponzoni, *Targeted liposomal c-myc antisense oligodeoxynucleotides induce apoptosis and inhibit tumor growth and metastases in human melanoma models*. *Clin Cancer Res*, 2003. **9**(12): p. 4595-605.
363. Honsik, C.J., G. Jung, and R.A. Reisfeld, *Lymphokine-activated killer cells targeted by monoclonal antibodies to the disialogangliosides GD2 and GD3 specifically lyse human tumor cells of neuroectodermal origin*. *Proc Natl Acad Sci U S A*, 1986. **83**(20): p. 7893-7.
364. Tumilowicz, J.J., W.W. Nichols, J.J. Cholon, and A.E. Greene, *Definition of a continuous human cell line derived from neuroblastoma*. *Cancer Res*, 1970. **30**(8): p. 2110-8.

365. Longo, L., H. Christiansen, N.M. Christiansen, P. Cornaglia-Ferraris, and F. Lampert, *N-myc amplification at chromosome band 1p32 in neuroblastoma cells as investigated by in situ hybridization*. J Cancer Res Clin Oncol, 1988. **114**(6): p. 636-40.
366. Kirpotin, D., J.W. Park, K. Hong, S. Zalipsky, W.L. Li, P. Carter, C.C. Benz, and D. Papahadjopoulos, *Sterically stabilized anti-HER2 immunoliposomes: design and targeting to human breast cancer cells in vitro*. Biochemistry, 1997. **36**(1): p. 66-75.
367. Pagnan, G., P.G. Montaldo, F. Pastorino, L. Raffaghello, M. Kirchmeier, T.M. Allen, and M. Ponzoni, *GD2-mediated melanoma cell targeting and cytotoxicity of liposome-entrapped fenretinide*. Int J Cancer, 1999. **81**(2): p. 268-74.
368. Hama, S., H. Akita, R. Ito, H. Mizuguchi, T. Hayakawa, and H. Harashima, *Quantitative comparison of intracellular trafficking and nuclear transcription between adenoviral and lipoplex systems*. Mol Ther, 2006. **13**(4): p. 786-94.
369. Oku, N. and Y. Namba, *Long-circulating liposomes*. Crit Rev Ther Drug Carrier Syst, 1994. **11**(4): p. 231-70.
370. Hettmer, S., S. Ladisch, and K. Kaucic, *Low complex ganglioside expression characterizes human neuroblastoma cell lines*. Cancer Lett, 2005. **225**(1): p. 141-9.
371. Zabner, J., A.J. Fasbender, T. Moninger, K.A. Poellinger, and M.J. Welsh, *Cellular and molecular barriers to gene transfer by a cationic lipid*. J Biol Chem, 1995. **270**(32): p. 18997-9007.
372. Wargalla, U.C. and R.A. Reisfeld, *Rate of internalization of an immunotoxin correlates with cytotoxic activity against human tumor cells*. Proc Natl Acad Sci U S A, 1989. **86**(13): p. 5146-50.
373. Varga, C.M., N.C. Tedford, M. Thomas, A.M. Klibanov, L.G. Griffith, and D.A. Lauffenburger, *Quantitative comparison of polyethylenimine formulations and adenoviral vectors in terms of intracellular gene delivery processes*. Gene Ther, 2005. **12**(13): p. 1023-32.
374. Colin, M., M. Maurice, G. Trugnan, M. Kornprobst, R.P. Harbottle, A. Knight, R.G. Cooper, A.D. Miller, J. Capeau, C. Coutelle, and M.C. Brahimi-Horn, *Cell delivery, intracellular trafficking and expression of an integrin-mediated gene transfer vector in tracheal epithelial cells*. Gene Ther, 2000. **7**(2): p. 139-52.
375. Zelphati, O. and F.C. Szoka, Jr., *Mechanism of oligonucleotide release from cationic liposomes*. Proc Natl Acad Sci U S A, 1996. **93**(21): p. 11493-8.
376. Budker, V., V. Gurevich, J.E. Hagstrom, F. Bortzov, and J.A. Wolff, *pH-sensitive, cationic liposomes: a new synthetic virus-like vector*. Nat Biotechnol, 1996. **14**(6): p. 760-4.
377. Choi, J.S., J.A. MacKay, and F.C. Szoka, Jr., *Low-pH-sensitive PEG-stabilized plasmid-lipid nanoparticles: preparation and characterization*. Bioconjug Chem, 2003. **14**(2): p. 420-9.
378. Mok, K.W., A.M. Lam, and P.R. Cullis, *Stabilized plasmid-lipid particles: factors influencing plasmid entrapment and transfection properties*. Biochim Biophys Acta, 1999. **1419**(2): p. 137-50.
379. Shi, F., L. Wasungu, A. Nomden, M.C. Stuart, E. Polushkin, J.B. Engberts, and D. Hoekstra, *Interference of poly(ethylene glycol)-lipid analogues with cationic-lipid-mediated delivery of oligonucleotides; role of lipid*

- exchangeability and non-lamellar transitions*. *Biochem J*, 2002. **366**(Pt 1): p. 333-41.
380. Boussif, O., F. Lezoualc'h, M.A. Zanta, M.D. Mergny, D. Scherman, B. Demeneix, and J.P. Behr, *A versatile vector for gene and oligonucleotide transfer into cells in culture and in vivo: polyethylenimine*. *Proc Natl Acad Sci U S A*, 1995. **92**(16): p. 7297-301.
381. Godbey, W.T., K.K. Wu, and A.G. Mikos, *Poly(ethylenimine) and its role in gene delivery*. *J Control Release*, 1999. **60**(2-3): p. 149-60.
382. Gao, X. and L. Huang, *Potential of cationic liposome-mediated gene delivery by polycations*. *Biochemistry*, 1996. **35**(3): p. 1027-36.
383. Fujii, G., *To fuse or not to fuse: the effects of electrostatic interactions, hydrophobic forces, and structural amphiphilicity on protein-mediated membrane destabilization*. *Adv Drug Deliv Rev*, 1999. **38**(3): p. 257-277.
384. Nir, S., F. Nicol, and F.C. Szoka, Jr., *Surface aggregation and membrane penetration by peptides: relation to pore formation and fusion*. *Mol Membr Biol*, 1999. **16**(1): p. 95-101.
385. Oren, Z., J. Ramesh, D. Avrahami, N. Suryaprakash, Y. Shai, and R. Jelinek, *Structures and mode of membrane interaction of a short alpha helical lytic peptide and its diastereomer determined by NMR, FTIR, and fluorescence spectroscopy*. *Eur J Biochem*, 2002. **269**(16): p. 3869-80.
386. Mastrobattista, E., G.A. Koning, L. van Bloois, A.C. Filipe, W. Jiskoot, and G. Storm, *Functional characterization of an endosome-disruptive peptide and its application in cytosolic delivery of immunoliposome-entrapped proteins*. *J Biol Chem*, 2002. **277**(30): p. 27135-43.
387. Van Rossenberg, S.M., K.M. Sliedregt-Bol, N.J. Meeuwenoord, T.J. Van Berkel, J.H. Van Boom, G.A. Van Der Marel, and E.A. Biessen, *Targeted lysosome disruptive elements for improvement of parenchymal liver cell-specific gene delivery*. *J Biol Chem*, 2002. **277**(48): p. 45803-10.
388. Kakudo, T., S. Chaki, S. Futaki, I. Nakase, K. Akaji, T. Kawakami, K. Maruyama, H. Kamiya, and H. Harashima, *Transferrin-modified liposomes equipped with a pH-sensitive fusogenic peptide: an artificial viral-like delivery system*. *Biochemistry*, 2004. **43**(19): p. 5618-28.
389. Li, W., F. Nicol, and F.C. Szoka, Jr., *GALA: a designed synthetic pH-responsive amphipathic peptide with applications in drug and gene delivery*. *Adv Drug Deliv Rev*, 2004. **56**(7): p. 967-85.
390. Simoes, S., V. Slepishkin, P. Pires, R. Gaspar, M.P. de Lima, and N. Duzgunes, *Mechanisms of gene transfer mediated by lipoplexes associated with targeting ligands or pH-sensitive peptides*. *Gene Ther*, 1999. **6**(11): p. 1798-807.
391. de Souza, D.L., B. Frisch, G. Duportail, and F. Schuber, *Membrane-active properties of alpha-MSH analogs: aggregation and fusion of liposomes triggered by surface-conjugated peptides*. *Biochim Biophys Acta*, 2002. **1558**(2): p. 222-37.
392. Ulvatne, H., H.H. Haukland, O. Olsvik, and L.H. Vorland, *Lactoferricin B causes depolarization of the cytoplasmic membrane of Escherichia coli ATCC 25922 and fusion of negatively charged liposomes*. *FEBS Lett*, 2001. **492**(1-2): p. 62-5.
393. Vogel, H.J., D.J. Schibli, W. Jing, E.M. Lohmeier-Vogel, R.F. Epand, and R.M. Epand, *Towards a structure-function analysis of bovine lactoferricin*

- and related tryptophan- and arginine-containing peptides. *Biochem Cell Biol*, 2002. **80**(1): p. 49-63.
394. Capecchi, M.R., *High efficiency transformation by direct microinjection of DNA into cultured mammalian cells*. *Cell*, 1980. **22**(2 Pt 2): p. 479-88.
395. Graessmann, M., J. Menne, M. Liebler, I. Graeber, and A. Graessmann, *Helper activity for gene expression, a novel function of the SV40 enhancer*. *Nucleic Acids Res*, 1989. **17**(16): p. 6603-12.
396. Mirzayans, R., R.A. Aubin, and M.C. Paterson, *Differential expression and stability of foreign genes introduced into human fibroblasts by nuclear versus cytoplasmic microinjection*. *Mutat Res*, 1992. **281**(2): p. 115-22.
397. Labat-Moleur, F., A.M. Steffan, C. Brisson, H. Perron, O. Feugeas, P. Furstenberger, F. Oberling, E. Brambilla, and J.P. Behr, *An electron microscopy study into the mechanism of gene transfer with lipopolyamines*. *Gene Ther*, 1996. **3**(11): p. 1010-7.
398. Dean, D.A., B.S. Dean, S. Muller, and L.C. Smith, *Sequence requirements for plasmid nuclear import*. *Exp Cell Res*, 1999. **253**(2): p. 713-22.
399. Brunner, S., T. Sauer, S. Carotta, M. Cotten, M. Saltik, and E. Wagner, *Cell cycle dependence of gene transfer by lipoplex, polyplex and recombinant adenovirus*. *Gene Ther*, 2000. **7**(5): p. 401-7.
400. Escriou, V., M. Carriere, F. Bussone, P. Wils, and D. Scherman, *Critical assessment of the nuclear import of plasmid during cationic lipid-mediated gene transfer*. *J Gene Med*, 2001. **3**(2): p. 179-87.
401. Ludtke, J.J., M.G. Sebestyen, and J.A. Wolff, *The effect of cell division on the cellular dynamics of microinjected DNA and dextran*. *Mol Ther*, 2002. **5**(5 Pt 1): p. 579-88.
402. Lechardeur, D., K.J. Sohn, M. Haardt, P.B. Joshi, M. Monck, R.W. Graham, B. Beatty, J. Squire, H. O'Brodovich, and G.L. Lukacs, *Metabolic instability of plasmid DNA in the cytosol: a potential barrier to gene transfer*. *Gene Ther*, 1999. **6**(4): p. 482-97.
403. Pollard, H., G. Toumaniantz, J.L. Amos, H. Avet-Loiseau, G. Guihard, J.P. Behr, and D. Escande, *Ca²⁺-sensitive cytosolic nucleases prevent efficient delivery to the nucleus of injected plasmids*. *J Gene Med*, 2001. **3**(2): p. 153-64.
404. Aronsohn, A.I. and J.A. Hughes, *Nuclear localization signal peptides enhance cationic liposome-mediated gene therapy*. *J Drug Target*, 1998. **5**(3): p. 163-9.
405. Chan, C.K. and D.A. Jans, *Enhancement of polylysine-mediated transferrin infection by nuclear localization sequences: polylysine does not function as a nuclear localization sequence*. *Hum Gene Ther*, 1999. **10**(10): p. 1695-702.
406. Collas, P. and P. Alestrom, *Rapid targeting of plasmid DNA to zebrafish embryo nuclei by the nuclear localization signal of SV40 T antigen*. *Mol Mar Biol Biotechnol*, 1997. **6**(1): p. 48-58.
407. Kaneda, Y., K. Iwai, and T. Uchida, *Increased expression of DNA cointroduced with nuclear protein in adult rat liver*. *Science*, 1989. **243**(4889): p. 375-8.
408. Subramanian, A., P. Ranganathan, and S.L. Diamond, *Nuclear targeting peptide scaffolds for lipofection of nondividing mammalian cells*. *Nat Biotechnol*, 1999. **17**(9): p. 873-7.

409. Chan, C.K. and D.A. Jans, *Enhancement of MSH receptor- and GAL4-mediated gene transfer by switching the nuclear import pathway*. *Gene Ther*, 2001. **8**(2): p. 166-71.
410. Hagstrom, J.E., J.J. Ludtke, M.C. Bassik, M.G. Sebestyen, S.A. Adam, and J.A. Wolff, *Nuclear import of DNA in digitonin-permeabilized cells*. *J Cell Sci*, 1997. **110** (Pt 18): p. 2323-31.
411. Ludtke, J.J., G. Zhang, M.G. Sebestyen, and J.A. Wolff, *A nuclear localization signal can enhance both the nuclear transport and expression of 1 kb DNA*. *J Cell Sci*, 1999. **112** (Pt 12): p. 2033-41.
412. van der Aa, M., G. Koning, J. van der Gugten, C. d'Oliveira, R. Oosting, W.E. Hennink, and D.J. Crommelin, *Covalent attachment of an NLS-peptide to linear dna does not enhance transfection efficiency of cationic polymer based gene delivery systems*. *J Control Release*, 2005. **101**(1-3): p. 395-7.
413. Branden, L.J., A.J. Mohamed, and C.I. Smith, *A peptide nucleic acid-nuclear localization signal fusion that mediates nuclear transport of DNA*. *Nat Biotechnol*, 1999. **17**(8): p. 784-7.
414. Neves, C., G. Byk, D. Scherman, and P. Wils, *Coupling of a targeting peptide to plasmid DNA by covalent triple helix formation*. *FEBS Lett*, 1999. **453**(1-2): p. 41-5.
415. Zanta, M.A., P. Belguise-Valladier, and J.P. Behr, *Gene delivery: a single nuclear localization signal peptide is sufficient to carry DNA to the cell nucleus*. *Proc Natl Acad Sci U S A*, 1999. **96**(1): p. 91-6.
416. Branden, L.J., B. Christensson, and C.I. Smith, *In vivo nuclear delivery of oligonucleotides via hybridizing bifunctional peptides*. *Gene Ther*, 2001. **8**(1): p. 84-7.
417. Morris, M.C., L. Chaloin, M. Choob, J. Archdeacon, F. Heitz, and G. Divita, *Combination of a new generation of PNAs with a peptide-based carrier enables efficient targeting of cell cycle progression*. *Gene Ther*, 2004. **11**(9): p. 757-64.
418. Tsutsui, J., K. Kadomatsu, S. Matsubara, A. Nakagawara, M. Hamanoue, S. Takao, H. Shimazu, Y. Ohi, and T. Muramatsu, *A new family of heparin-binding growth/differentiation factors: increased midkine expression in Wilms' tumor and other human carcinomas*. *Cancer Res*, 1993. **53**(6): p. 1281-5.
419. Nakagawara, A., J. Milbrandt, T. Muramatsu, T.F. Deuel, H. Zhao, A. Cnaan, and G.M. Brodeur, *Differential expression of pleiotrophin and midkine in advanced neuroblastomas*. *Cancer Res*, 1995. **55**(8): p. 1792-7.
420. Muramatsu, H., H. Shirahama, S. Yonezawa, H. Maruta, and T. Muramatsu, *Midkine, a retinoic acid-inducible growth/differentiation factor: immunochemical evidence for the function and distribution*. *Dev Biol*, 1993. **159**(2): p. 392-402.
421. Adachi, Y., P.N. Reynolds, M. Yamamoto, M. Wang, K. Takayama, S. Matsubara, T. Muramatsu, and D.T. Curiel, *A midkine promoter-based conditionally replicative adenovirus for treatment of pediatric solid tumors and bone marrow tumor purging*. *Cancer Res*, 2001. **61**(21): p. 7882-8.
422. Iyengar, R.V., C.A. Pawlik, E.J. Krull, D.A. Phelps, R.A. Burger, L.C. Harris, P.M. Potter, and M.K. Danks, *Use of a modified ornithine decarboxylase promoter to achieve efficient c-MYC- or N-MYC-regulated protein expression*. *Cancer Res*, 2001. **61**(7): p. 3045-52.

423. Pawlik, C.A., R.V. Iyengar, E.J. Krull, S.E. Mason, R. Khanna, L.C. Harris, P.M. Potter, M.K. Danks, and S.M. Guichard, *Use of the ornithine decarboxylase promoter to achieve N-MYC-mediated overexpression of a rabbit carboxylesterase to sensitize neuroblastoma cells to CPT-11*. *Mol Ther*, 2000. **1**(5 Pt 1): p. 457-63.
424. Narita, M., R. Bahar, M. Hatano, M.M. Kang, T. Tokuhisa, S. Goto, H. Saisho, S. Sakiyama, and M. Tagawa, *Tissue-specific expression of a suicide gene for selective killing of neuroblastoma cells using a promoter region of the NCX gene*. *Cancer Gene Ther*, 2001. **8**(12): p. 997-1002.
425. Coker, G.T., 3rd, L. Vinnedge, and K.L. O'Malley, *Characterization of rat and human tyrosine hydroxylase genes: functional expression of both promoters in neuronal and non-neuronal cell types*. *Biochem Biophys Res Commun*, 1988. **157**(3): p. 1341-7.
426. Steffens, S., A. Sandquist, S. Frank, U. Fischer, C. Lex, N.G. Rainov, and C.M. Kramm, *A neuroblastoma-selective suicide gene therapy approach using the tyrosine hydroxylase promoter*. *Pediatr Res*, 2004. **56**(2): p. 268-77.
427. Bilisland, A.E., C.J. Anderson, A.J. Fletcher-Monaghan, F. McGregor, T.R. Evans, I. Ganly, R.J. Knox, J.A. Plumb, and W.N. Keith, *Selective ablation of human cancer cells by telomerase-specific adenoviral suicide gene therapy vectors expressing bacterial nitroreductase*. *Oncogene*, 2003. **22**(3): p. 370-80.
428. Kim, E., J.H. Kim, H.Y. Shin, H. Lee, J.M. Yang, J. Kim, J.H. Sohn, H. Kim, and C.O. Yun, *Ad-mTERT-delta19, a conditional replication-competent adenovirus driven by the human telomerase promoter, selectively replicates in and elicits cytopathic effect in a cancer cell-specific manner*. *Hum Gene Ther*, 2003. **14**(15): p. 1415-28.
429. Gu, J., L. Zhang, X. Huang, T. Lin, M. Yin, K. Xu, L. Ji, J.A. Roth, and B. Fang, *A novel single tetracycline-regulative adenoviral vector for tumor-specific Bax gene expression and cell killing in vitro and in vivo*. *Oncogene*, 2002. **21**(31): p. 4757-64.
430. Sternberg, N., B. Sauer, R. Hoess, and K. Abremski, *Bacteriophage P1 cre gene and its regulatory region. Evidence for multiple promoters and for regulation by DNA methylation*. *J Mol Biol*, 1986. **187**(2): p. 197-212.
431. Hoess, R., K. Abremski, S. Irwin, M. Kendall, and A. Mack, *DNA specificity of the Cre recombinase resides in the 25 kDa carboxyl domain of the protein*. *J Mol Biol*, 1990. **216**(4): p. 873-82.
432. Ghosh, K. and G.D. Van Duyne, *Cre-loxP biochemistry*. *Methods*, 2002. **28**(3): p. 374-83.
433. Sauer, B., *Inducible gene targeting in mice using the Cre/lox system*. *Methods*, 1998. **14**(4): p. 381-92.
434. Lin, X., A.H. Fischer, K.Y. Ryu, J.Y. Cho, T.J. Sferra, R.T. Kloos, E.L. Mazzaferri, and S.M. Jhiang, *Application of the Cre/loxP system to enhance thyroid-targeted expression of sodium/iodide symporter*. *J Clin Endocrinol Metab*, 2004. **89**(5): p. 2344-50.
435. Nagayama, Y., E. Nishihara, M. Iitaka, H. Namba, S. Yamashita, and M. Niwa, *Enhanced efficacy of transcriptionally targeted suicide gene/prodrug therapy for thyroid carcinoma with the Cre-loxP system*. *Cancer Res*, 1999. **59**(13): p. 3049-52.

436. Takikawa, H., K. Mafune, H. Hamada, D.M. Nettelbeck, R. Muller, M. Makuuchi, and M. Kaminishi, *An advanced strategy of enhanced specific gene expression for hepatocellular carcinoma*. *Int J Oncol*, 2003. **22**(5): p. 1051-6.
437. Ueda, K., M. Iwahashi, M. Nakamori, M. Nakamura, I. Matsuura, H. Yamaue, and H. Tanimura, *Carcinoembryonic antigen-specific suicide gene therapy of cytosine deaminase/5-fluorocytosine enhanced by the cre/loxP system in the orthotopic gastric carcinoma model*. *Cancer Res*, 2001. **61**(16): p. 6158-62.
438. Yoshimura, I., S. Ikegami, S. Suzuki, T. Tadakuma, and M. Hayakawa, *Adenovirus mediated prostate specific enzyme prodrug gene therapy using prostate specific antigen promoter enhanced by the Cre-loxP system*. *J Urol*, 2002. **168**(6): p. 2659-64.
439. Takahashi, T., Y. Namiki, and T. Ohno, *Induction of the suicide HSV-TK gene by activation of the Egr-1 promoter with radioisotopes*. *Hum Gene Ther*, 1997. **8**(7): p. 827-33.
440. Nuyts, S., L. Van Mellaert, J. Theys, W. Landuyt, P. Lambin, and J. Anne, *The use of radiation-induced bacterial promoters in anaerobic conditions: a means to control gene expression in clostridium-mediated therapy for cancer*. *Radiat Res*, 2001. **155**(5): p. 716-23.
441. Scott, S.D., M.C. Joiner, and B. Marples, *Optimizing radiation-responsive gene promoters for radiogenetic cancer therapy*. *Gene Ther*, 2002. **9**(20): p. 1396-402.
442. Scott, S.D., B. Marples, J.H. Hendry, L.S. Lashford, M.J. Embleton, R.D. Hunter, A. Howell, and G.P. Margison, *A radiation-controlled molecular switch for use in gene therapy of cancer*. *Gene Ther*, 2000. **7**(13): p. 1121-5.
443. Wheldon, T.E., *Radiation physics and genetic targeting: new directions for radiotherapy. The Douglas Lea Lecture 1999*. *Phys Med Biol*, 2000. **45**(7): p. R77-95.
444. Kassis, A.I., F. Fayad, B.M. Kinsey, K.S. Sastry, R.A. Taube, and S.J. Adelstein, *Radiotoxicity of 125I in mammalian cells*. *Radiat Res*, 1987. **111**(2): p. 305-18.
445. Gaze, M.N., I.M. Huxham, R.J. Mairs, and A. Barrett, *Intracellular localization of metaiodobenzyl guanidine in human neuroblastoma cells by electron spectroscopic imaging*. *Int J Cancer*, 1991. **47**(6): p. 875-80.
446. Little, J.B., E.I. Azzam, S.M. de Toledo, and H. Nagasawa, *Bystander effects: intercellular transmission of radiation damage signals*. *Radiat Prot Dosimetry*, 2002. **99**(1-4): p. 159-62.
447. Mothersill, C. and C. Seymour, *Medium from irradiated human epithelial cells but not human fibroblasts reduces the clonogenic survival of unirradiated cells*. *Int J Radiat Biol*, 1997. **71**(4): p. 421-7.
448. Mothersill, C. and C. Seymour, *Radiation-induced bystander effects: past history and future directions*. *Radiat Res*, 2001. **155**(6): p. 759-67.
449. Mothersill, C. and C.B. Seymour, *Cell-cell contact during gamma irradiation is not required to induce a bystander effect in normal human keratinocytes: evidence for release during irradiation of a signal controlling survival into the medium*. *Radiat Res*, 1998. **149**(3): p. 256-62.

450. Mothersill, C.E., M.J. Moriarty, and C.B. Seymour, *Radiotherapy and the potential exploitation of bystander effects*. Int J Radiat Oncol Biol Phys, 2004. **58**(2): p. 575-9.
451. Nagasawa, H. and J.B. Little, *Induction of sister chromatid exchanges by extremely low doses of alpha-particles*. Cancer Res, 1992. **52**(22): p. 6394-6.
452. Prise, K.M., M. Folkard, and B.D. Michael, *Bystander responses induced by low LET radiation*. Oncogene, 2003. **22**(45): p. 7043-9.
453. Zhou, H., G. Randers-Pehrson, C.A. Waldren, D. Vannais, E.J. Hall, and T.K. Hei, *Induction of a bystander mutagenic effect of alpha particles in mammalian cells*. Proc Natl Acad Sci U S A, 2000. **97**(5): p. 2099-104.
454. Young, L.S., P.F. Searle, D. Onion, and V. Mautner, *Viral gene therapy strategies: from basic science to clinical application*. J Pathol, 2006. **208**(2): p. 299-318.
455. Pastorino, F., *Anti-GD₂ immunoliposomes: a suitable system for the specific delivery of antisense oligonucleotides against oncogenes to neuroectodermal tumour cells*. Res. Adv. in Cancer, 2001. **1**: p. 23-37.